UNIVERSITÀ
DEGLI STUDI
DI PADOVA

Sede Amministrativa: Università degli Studi di Padova

Dipartimento di Biologia

SCUOLA DI DOTTORATO DI RICERCA IN: BIOCHIMICA E BIOTECNOLOGIE
INDIRIZZO: BIOTECNOLOGIE
CICLO XXIII

FUNCTIONAL CHARACTERIZATION OF POTASSIUM CHANNELS IN THE CYANOBACTERIUM *SYNECHOCYSTIS* SP. PCC 6803

Direttore della Scuola : Ch.mo Prof. Giuseppe Zanotti
Coordinatore d'indirizzo: Ch.mo Prof. Giorgio Valle
Supervisore: Dott.ssa Elisabetta Bergantino

Dottoranda: Vanessa Checchetto

TABLE OF CONTENTS

ORGANIZATION OF THE THESIS _____ *I*

RIASSUNTO _____ *1*

SUMMARY _____ *5*

INTRODUCTION _____ *9*

1. Cyanobacteria _____ *11*

1.1 The structure of cyanobacteria cells _____ **12**

1.2 Taxonomy of cyanobacteria _____ **13**

1.3 *Synechocystis* sp. PCC 6803 _____ **14**

1.4 The importance of cyanobacteria and their biotechnological applications __ **15**

1.5 The endosymbiotic theory _____ **15**

2. Photosynthesis _____ *20*

2.1 Photosynthesis in plants and cyanobacteria _____ **21**

2.2 The Photosynthetic pigments _____ **24**

2.2.1 Chlorophylls _____ 24

2.2.2 Carotenoids _____ 25

2.2.3 The phycobiliproteins _____ 27

2.3 Photosystems _____ **28**

2.4 Photosynthesis steps _____ **29**

3. Ion transport systems _____ *31*

3.1 Carrier proteins _____ **32**

3.2 Ion channels _____ **32**

3.3 Potassium transport _____ **33**

3.3.1 Structure of K^+ channels _____ 36

3.3.2 Selectivity filter and gating _____ 37

3.4 The patch clamp technique _____ **38**

References _____ *40*

CHAPTER 1

Zanetti, M., Teardo,E., La Rocca, N., Zulkifli, L., Checchetto, V., Shijuku,T., Sato,Y., Giacometti G.M., Uozumi N., Bergatino E. and Szabò I. (2010). A novel potassium channel in photosynthetic cyanobacteria. PLoS ONE Volume 5 | Issue 4 | e10118

Checchetto V, Segalla A, La Rocca N, Giacometti G.M., Bergantino E., Szabò I. A prokaryotic thylakoid potassium channel is required for efficient photosynthesis in cyanobacteria (Manuscript in preparation)

CHAPTER 2

Checchetto V, Formentin E. Giacometti G.M., Szabò I, Bergantino E. Cloning, expression and functional characterization of a Ca^{2+}-dependent potassium channel from *Synechocystis* sp. PCC 6803 (Manuscript in preparation)

Checchetto V, Giacometti G.M., Szabò I, Bergantino E. Expression in *E.coli* of a putative calcium dependent potassium channel of the cyanobacterium *Synechocystis* sp. PCC6803 (Proceeding in progress)

CHAPTER 3

Akai M., Kiyoshi Onai K., Morishita M., Y.' Yukutake, Hiroyuki, Mino H., Shijuku T., Matsumoto H., Maruyama H., Arai F., Checchetto V., Szabò I., Miyake H, Itoh S., Suematsu M., Hazama A., Yasui M., Ishiura M', Uozumi N. Plasma membrane aquaporin AqpZ is involved in cell volume regulation and sensitivity to osmotic stress in *Synechocystis* sp. PCC 6803 (Manuscript in preparation)

De Marchi U., Checchetto V., Zanetti M., Teardo E., Soccio M., Formentin E., Giacometti G. M., Pastore D., Zoratti M.and Szabò I. (2010). ATP-Sensitive Cation-channel in Wheat (*Triticum durum* Desf.): Identification and Characterization of a Plant Mitochondrial Channel by Patch-clamp. Cell Physiol Biochem;26:975-982

ORGANIZATION OF THE THESIS

My research is part of a project concerning potassium (K^+) channels in prokaryotes and plants, conducted in the laboratories where I had my Ph.D. experience. My thesis developed along different lines. For this reason it comprises distinct sections. In the introduction section I describe the main aspects of cyanobacterial morphology and photosynthesis, as well as of ion transport systems including potassium channels. The general introduction is followed by chapters corresponding to single research lines. This organization has been favoured over a more traditional style to facilitate reading. Some chapters correspond to published papers, the other parts are written as manuscripts in preparation but are not submitted for publication yet. .

RIASSUNTO

Prima del Pre-Paleozoico, l'atmosfera terrestre aveva una composizione diversa rispetto a quella quella di oggi, infatti, gli organismi non erano in grado di vivere in condizioni aerobiche. L'avvento dei cianobatteri ha portato rilevanti innovazioni, infatti, questi a differenza di altri batteri fototrofi esistenti a quel tempo, presentavano molecole di clorofilla e complessi proteici che permisero di utilizzare l'acqua come donatore di elettroni per la produzione dell'ossigeno. Questa modificazione ha permesso, lungo milioni di anni, di ottenere l'attuale atmosfera. Tutti questi cambiamenti portarono ad una inevitabile evoluzione biochimica e metabolica degli organismi. Nel Proterozoico o agli inizi del Cambriano, i cianobatteri iniziarono a risiedere all'interno di alcune cellule eucariotiche. Secondo la teoria endosimbiotica, i cloroplasti evolsero da un piccolo cianobatterio primitivo presente all'interno delle cellule eucariotiche. Oggi, i cianobatteri si trovano in diversi ambienti terrestri, da oceani ad acque dolce, in terre artiche, in deserti ed in sorgenti termali.

La nostra attenzione è focalizzata sul cianobatterio *Synechocystis* sp. PCC 6803. Questo ceppo è stato isolato per la prima volta da una sorgente di acqua dolce in California e ora è considerato un buon organismo modello per studi scientifici. È spontaneamente trasformabile, è in grado di integrare DNA estraneo nel suo genoma attraverso ricombinazione omologa (consentendo la sostituzione mirata dei geni) e può crescere in assenza di fotosintesi se viene fornita un'adeguata fonte di carbonio, come il glucosio. Inoltre è il primo organismo fotosintetico per il quale il genoma è stato sequenziato (Kaneko *et al.*, 1996).

Nel proteoma di *Synechocystis* sono stati identificati diversi putativi canali ionici (Kuo *et al.*, 2005). Tuttavia, nessuno di essi è stato caratterizzato da un punto di vista funzionale e il loro ruolo fisiologico rimane ancora sconosciuto. I canali ionici sono proteine di membrana che controllano il passaggio degli ioni attraverso esse. Queste proteine, in tutti i procarioti e gli eucarioti, permettono la corretta distribuzione ionica necessaria per le funzioni cellulari. Le caratteristiche base dei canali sono la selettività ed il gating, la prima è la proprietà che controlla il tipo di ioni che attraversa la membrana, la seconda è il processo di apertura e chiusura del percorso degli ioni. In realtà il passaggio attraverso il poro è regolato da un *gate*, che può essere aperto o chiuso da segnali chimici, meccanici o elettrici (Hille, 2001).

Il potassio (K^+) è il catione più abbondante negli organismi viventi e svolge un ruolo cruciale per la sopravvivenza e lo sviluppo delle cellule, regolando l'attività enzimatica e il potenziale

di membrana. Questo è uno dei motivi per i quali i canali del potassio sono una delle classi di canali più studiate. Il campo dei canali del potassio procariotici ha subito un rapido sviluppo negli ultimi anni grazie all'applicazione di una combinazione di tecniche di bioinformatica e biologia molecolare, affiancate a studi di elettrofisiologia e studi strutturali. La comprensione della loro struttura e del meccanismo di conduzione degli ioni permette di ottenere ulteriori informazioni sulla funzione dei canali di potassio in generale.

Uno *screening* bioinformatico del proteoma di *Synechocystis* sp. PCC 6803 ha individuato due proteine putative su cui abbiamo concentrato la nostra attenzione. La prima è stata chiamata SynK e mostra omologia di sequenza con KvAP (un canale del potassio voltaggio di *A. pernix*) (Jiang *et al.*, 2003). La seconda, SynCaK, mostra omologia di sequenza con MthK, un canale del potassio Ca^{2+}-dipendente di *M. thermoautotrophicum* (Jiang *et al.*, 2002). Il nostro obiettivo era quello di capire se effettivamente queste proteine funzionano come canali ionici e di comprendere il loro ruolo nella fisiologia dei cianobatteri.

Le caratteristiche e la funzione di queste proteine sono state studiate attraverso un approccio integrato comprendente tecniche di biologia molecolare, biochimica, elettrofisiologia e microscopia.

Il gene *SynK* (ORF slr0498) è stato inizialmente identificato nel genoma di *Synechocystis* sp. PCC 6803 utilizzando la sequenza amminoacidica del filtro di selettività (TMTTVGYGD) come sequenza *query*. Questa proteina di funzione sconosciuta mostra sei segmenti transmembrana (S1-S6) ed una regione del poro tra le eliche S5 e S6. Prima di iniziare il mio Dottorato, *SynK* è stato clonato ed espresso in cellule di mammifero (*Chinese Hamster ovary*, CHO) in fusione con la EGFP (una proteina fluorescente). Una successiva analisi western-blotting ha dimostrato che la proteina di fusione è correttamente espressa. Studi di microscopia confocale hanno dimostrato la sua localizzazione nella membrana di cellule CHO e l'analisi *patch-clamp* ha rivelato un'attività di canale *outwardly rectifying* selettivo per il potassio. Inoltre, è stata dimostrata per SynK, in frazioni di membrana isolate da cianobatteri, mediante microscopia elettronica (attraverso la tecnica dell'*immunogold*) e tecniche di western blot, una doppia localizzazione nella plasmamembrana e nelle membrane tilacoidi.

Durante il mio Dottorato, è stata eseguita la costruzione di due diversi mutanti del canale SynK. Il primo mutante corrisponde alla proteina con una mutazione puntiforme nel filtro di selettività del poro (mutazione Y181A) e utilizzato per l'espressione in cellule CHO. In base alla letteratura, questa proteina mutante perde la sua attività di canale del potassio. Inoltre, è stato prodotto un ceppo mutante *knock-out* (ΔSynK) in *Synechocystis*. La sua analisi funzionale ha permesso di capire il ruolo fisiologico di SynK nei cianobatteri.

Al fine di caratterizzare la funzione della proteina SynK, abbiamo inizialmente verificato, attraverso western blot, che il ceppo mutante effettivamente non esprimesse la proteina. Mentre per valutare il ruolo fisiologico della proteina SynK, abbiamo confrontato la crescita del ceppo *wild-type* (WT) e mutante in diverse condizioni. La caratterizzazione del fenotipo mutante è stata studiata confrontando l'attività fotosintetica nel WT e nel mutante.

Utilizzando un approccio simile abbiamo identificato nel genoma di *Synechocystis* sp. PCC 6803 una seconda proteina classificata come putativo canale del potassio (ORF sll0993) che mostra omologia di sequenza con MthK, un canale del potassio calcio dipendente di *Methanobacterium thermoautophicum*. Attraverso l'utilizzo di vari programmi di predizione strutturale, abbiamo analizzato la sequenza primaria della proteina tradotta e abbiamo osservato che questa (che abbiamo chiamato SynCaK), come MthK, contiene due segmenti transmembrana, un filtro di selettività tipico dei canali del K^+, con sostituzioni conservative, e un dominio di regolazione della conduttanza del potassio (*RCK domain*).

Anche in questo caso, abbiamo clonato ed espresso la proteina in fusione con EGFP in cellule CHO e studiato la loro attività tramite *patch clamp*. Inoltre, al fine di studiare il ruolo di SynCaK nella fisiologia dei cianobatteri abbiamo prodotto un mutante *knock-out* per SynCaK. Per ottenere ulteriori informazioni sull'attività del canale, abbiamo espresso e iniziato la purificazione della proteina in un altro sistema eterologo, *E. coli*. Le proteine canale-ricombinanti sono spesso studiate mediante la loro integrazione in doppi strati artificiali (Ruta *et al.*, 2003).

Durante il mio Dottorato, ho anche continuato il lavoro iniziato durante la mia tesi di laurea in Biotecnologie Industriali sullo studio dei canali ionici nei mitocondri delle *Graminaceae*. Tecniche classiche di bioenergetica hanno rivelato attività compatibili con la presenza di un canale di potassio nei mitocondri di grano duro, ma lo studio dei canali nei mitocondri di sistemi vegetali è un campo ancora inesplorato nel mondo. A tal fine, è stato iniziato uno studio attraverso l'utilizzo parallelo di diverse tecniche, che hanno consentito una caratterizzazione più completa delle attività dei canali presenti nei mitocondri di grano. In particolare, sono stati seguiti due approcci. In primo luogo, studi biochimici sui mitocondri isolati, attraverso l'uso di SDS-PAGE e immunoblotting, che hanno permesso la valutazione del campione utilizzato in termini di arricchimento e di purezza (dati del tutto assenti in letteratura fino ad oggi). In secondo luogo, sono state definite preparazioni di mitocondri da radici di grano duro adatte per studi elettrofisiologici. In particolare, per la prima volta è stata applicata la tecnica di *patch clamp* su mitocondri vegetali.

Infine, ho svolto una collaborazione con il laboratorio del Professor Nobuyuki Uozumi presso la Tohoku University in Giappone. Questo gruppo ha ottenuto un mutante per l'acquaporina di *Synechocystis*. Le acquaporine sono proteine di membrana incorporate nelle membrane cellulari che regolano il flusso dell'acqua. Ho contribuito alla caratterizzazione del *mutant-less acquaporin* attraverso esperimenti di misura dell'attività fotosintetica. In particolare, sono stati eseguiti diversi esperimenti di evoluzione di ossigeno che dimostrano che l'efficienza fotosintetica è più alta nel mutante rispetto al WT quando gli organismi vengono incubati in un mezzo iperosmotico. Il passo successivo sarà quello di chiarire esattamente come uno stress iperosmotico e l'assenza di acquaporina sono correlati con la fotosintesi e quindi il meccanismo sottostante.

SUMMARY

Before Pre-Paleozoic, the Earth's atmosphere had a composition different from today; in fact the organisms are not able to live in aerobic condition. The advent of cyanobacteria brought significant innovations, in fact, these bacteria unlike other phototrophs existing at that time, had chlorophyll molecules and protein complexes that allowed the use of water as electron donor to produce oxygen gas. This innovation developed over millions of years to get the current atmosphere. All these changes led to an inevitable biochemical and metabolic evolution of organisms. In Proterozoic or in early Cambrian, cyanobacteria began to reside within certain eukaryote cells. According to the endosymbionthic theory, chloroplasts evolved from a small primitive cyanobacterium settled within eukaryotic cells. Today, cyanobacteria are found throughout the Earth's environment, from oceans to fresh water and soil in the arctic areas, deserts and hot springs.

Our attention is focused on cyanobacterium *Synechocystis* sp. PCC 6803. This strain was isolated for the first time from fresh water in California and now is considered a good model for scientific studies. It is spontaneously transformable, is able to integrate foreign DNA into its genome by homologous recombination (allowing targeted gene replacement) and can grow in the absence of photosynthesis if a suitable fixed-carbon source such as glucose is provided. Moreover it is the first photosynthetic organism for which the complete genome was sequenced (Kaneko *et al.*, 1996).

In the proteome of *Synechocystis* several putative ion channels can be identified (Kuo *et al.*, 2005). However, none of them have been characterized from the functional point of view and their physiological role is still unknown. Ion channels are ubiquitous membrane proteins that control the passage of ions through biological membranes. These proteins, in all prokaryotes and eukaryotes, allow the correct ion distribution necessary to cellular functions. The basic features of the channels are selectivity and gating, the first is the property that controls the kind of ion that flows across the membrane and the second is the process of opening and closing the ion pathway. In fact the passage through the pore is governed by a "gate," which may be opened or closed by chemical, mechanical or electrical signals (Hille, 2001).

Potassium (K^+) is the most abundant cation in organisms and plays a crucial role in the survival and development of cells, by regulating enzyme activity and tuning membrane potential. This is one of the reasons for which potassium channels are one of the most studied

among classes of channels. The field of prokaryotic potassium channels underwent a rapid development over the past years thanks to the application of a combination of bioinformatics and molecular biology, beside electrophysiology and structural studies. Understanding of their structure and actual mechanism of ion conduction allow to obtain more information about the function of potassium channels in general.

A bioinformatic screening of *Synechocystis* sp. PCC 6803 proteome identified two putative proteins on which we focused our attention. The first one was named SynK and it displays sequence homology with KvAP (a voltage gated potassium channel of *A. pernix*) (Jiang *et al.*, 2003). The second one, SynCaK, displays sequence homology to MthK, a Ca^{2+}-dependent potassium channel from *M. thermoautotrophicum* (Jiang *et al.*, 2002). Our goal was to understand whether they actually function as ion channels and to reveal their roles in the physiology of cyanobacteria.

The characteristics and function of these proteins were studied through an integrated approach involving molecular biology techniques, biochemistry, electrophysiology and microscopy.

SynK (ORF slr 0498) was initially identified in the genome of *Synechocystis* sp. PCC 6803 using the selectivity filter amino acid sequence (TMTTVGYGD) as a query sequence. This protein of unknown function shows six membrane spanning segments (S1-S6) and a pore region between S5 and S6 helixes. Before starting my Ph.D, *SynK* gene has been cloned and expressed in mammalian cells (Chinese Hamster Ovary, CHO) in fusion with EGFP (a fluorescent protein). Subsequent Western-blotting analysis showed that the fusion protein was correctly expressed. Confocal microscopy studies demonstrated its membrane localization and patch-clamp analysis revealed an activity of voltage-gated outwardly rectifying potassium selective channel in CHO cells. In addition, the double location of SynK in plasma and thylakoid membrane of cyanobacteria was shown by immunogold electron microscopy and Western blot on isolated membrane fractions.

During my P.h.D, I performed the construction of two different mutants of SynK channel. The first SynK mutant, corresponding to the protein with a single amminoacid mutation in the selectivity filter of the pore (mutation Y181A), was used for expression in CHO cells. In accordance to the literature, this mutant protein loses its potassium channel activity. I also produced a ΔSynK *Synechocystis* mutant strain. Its functional analysis allowed to understand the physiological role of SynK in cyanobacteria.

In order to characterize the function of the SynK protein, we initially verified that the deletion mutant did not express Synk, using Western blot technique. To evaluate the physiological role of the SynK protein, we initially compared growth of the wild type (WT) and mutant strain in

different conditions. Characterization of the mutant phenotype was investigated by comparing photosynthetic activity in WT and mutant strains.

Using a similar approach we have identified in the genome of *Synechocystis* sp. PCC 6803 a second protein classified as a putative potassium channel (ORF *sll*0993) that displays sequence homology with MthK, a calcium dependent potassium channel from the archeon *Methanobacterium thermoautophicum*. Using several structural prediction programs, we analyzed the primary sequence of the protein translated from sll0993 and we observed that this protein (that we called SynCaK), like MthK, is predicted to contain two membrane spanning segments, a recognizable K^+ channel signature sequence, with only conservative substitutions, and a regulatory sequence for K^+ conductance (RCK).

Also in the case of sll0993, we cloned and expressed the protein in fusion with GFP in CHO cells and studied their activity by patch clamp. Moreover, in order to study the role of SynCaK in cyanobacteria physiology we produced a SynCaK-deficient *Synechocystis* mutant.

To gain further information about the activity of the channel, we have expressed and started the purification of the protein in another heterologous system, E. *coli*. Purified recombinant channel proteins are often studied by incorporating them into an artificial planar bilayer system (Ruta *et al*., 2003).

During my Ph.D, I also continued the work begun during my thesis in Biotecnology on the study of ion channels in mitochondria of *Graminaceae*. Classical bioenergetics techniques reveal activities compatible with the presence of a potassium channel in durum wheat mitochondria, but the study of channels in mitochondria of plant systems is a still unexplored field in the world. To this end, we started a study through the parallel use of different techniques, which allowed a more complete characterization of the activity of channels present in wheat mitochondria. In particular, we followed two approaches. First, biochemical studies on isolated mitochondria, through the use of SDS-PAGE and immunoblotting, allowed the evaluation of the sample used in terms of enrichment and purity (data completely absent in the literature to date). Second, preparations of mitochondria from roots of durum wheat were suitable for electrophysiological studies in particular patch clamp technique, applied for the first time on plant mitochondria.

Finally, I was involved in collaboration with the laboratory of Professor Nobuyuki Uozumi at Tohoku University in Japan. This group obtained a mutant for *Synechocystis* aquaporin. Aquaporins are membrane proteins embedded in the cell membrane that regulate the flow of water. I contributed to the characterization of the acquaporin-less mutant by performing experiments measuring photosynthetic activity. In particular, we performed several

experiments of oxygen evolution demonstrating that the photosyntetic efficiency is higher in the mutant with respect to the WT when the organisms are incubated in hyperosmotic medium. The next step is to clarify how exactly a hyperosmotic stress and the absence of aquaporin are correlated with the photosynthesis and what is the underlying mechanism.

~ INTRODUCTION ~

1. CYANOBACTERIA

Geobiological evidence indicates that life arose at least 3500 million years ago, but the question of when oxygenic photosynthesis evolved is still unanswered. Cyanobacteria are among the earliest life forms on earth, emerging at least 2500 million years ago, and have been involved in the formation of the earth's atmosphere. This event dramatically changed the life forms on Earth and promoted an explosion of biodiversity up to now the production of oxygen by cyanobacterial photosynthesis contributes to keeping the balance of our atmosphere.

Cyanobacteria are oxygenic photosynthetic gram negative bacteria, formerly known as "blue green algae", they have no relationship to any of the various eukayotic algae. The term algae, in fact, is commonly referred to any aquatic organisms capable of photosynthesis but this is a misleading name, for the reason that algae are eukaryotic organisms, not prokaryotes like Cyanobacteria.

Cyanobacteria get their name from the bluish pigment phycocyanin (Greek: κυανός (kyanós)=blue), which they use to capture light for photosynthesis. Nevertheless, not all cyanobacteria are blue: they can be red or pink from the pigment phycoerythrin. The Red Sea gets its name from occasional blooms of a reddish species of *Oscillatoria* and African flamingos get their pink colour from eating *Spirulina* (source: http://www.ucmp.berkeley.edu/bacteria/cyanolh.htm).

A feature of cyanobacteria is their adaptability to very different ecological niche, for this reason they display an ability to synthesize structurally and functionally diverse natural products. Due to this enormous biodiversity among cyanobacteria, until now only a small proportion of cyanobacterial species and their natural products have been identified.

All cyanobacteria are unicellular, some species may grow in colonies or filaments, often surrounded by a gelatinous or mucilaginous sheath (Figure 1). Today, they are present in freshwater lakes and oceans, as well as they survive also in very hostile environments such as deserts, hot and acidic springs, and even in the arctic ice.

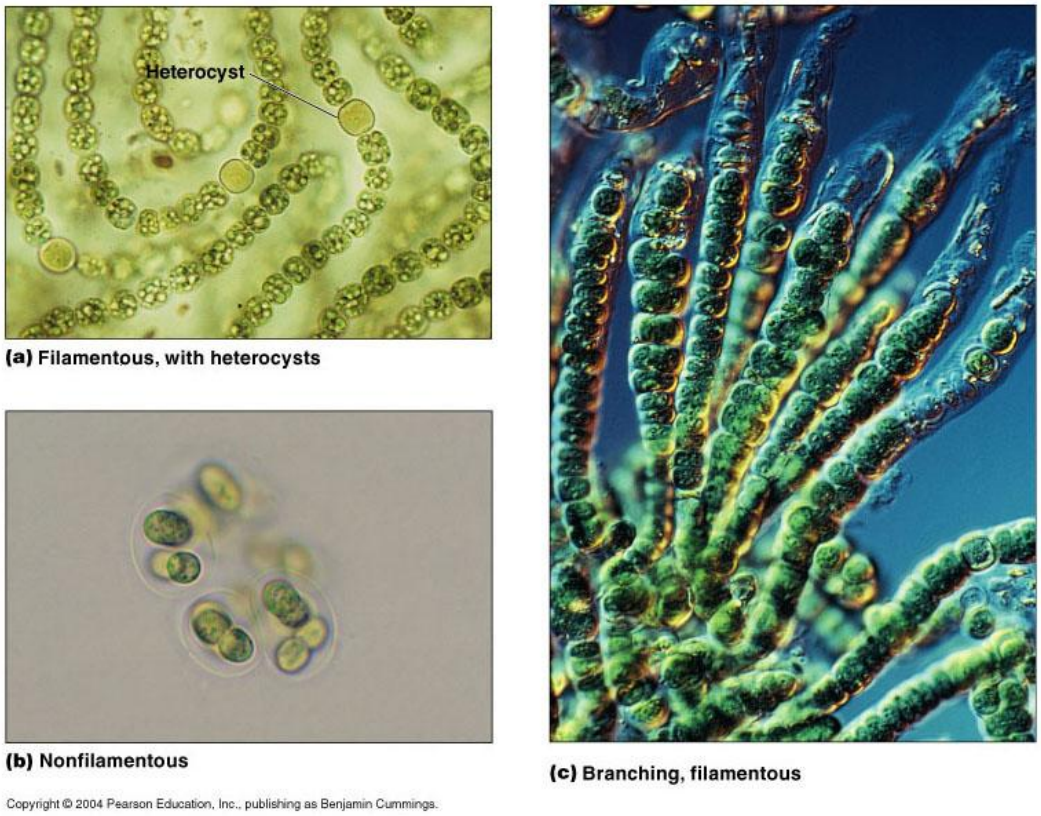

Figure 1: Growth of cyanobacteria. Cyanobacteria are unicellular organism that can grow in filaments (a,c) or in colonies (b).(Tortora *et al*., 1986).

1.1 The structure of cyanobacteria cells

Cyanobacteria are Gram-negative prokaryotic organisms that have considerable morphological diversification and size. The cyanobacteria cells did not contain cellular organelles typical of eukaryotic cells, however, they are considered more complex that other bacteria since they have an internal membrane system.

Cells are surrounded by a cytoplasmic membrane and a multilayered cell wall composed of an inner layer of peptidoglycan and an outer layer of lipo-polysaccharide (Hoiczyk & Hansel, 2000). In addition to these layers external mucilaginous mass, which is a key feature for the colonization and survival of the organism may be present. This layer allows the adhesion to the substrate, working like water supply, since it soak in water and slowly releases it helping to overcome adverse periods, hindering predation and cellular association so the cells biofilm formation (or felt). This layer is often variously pigmented and it has different functions, including the protection by high radiation, especially ultraviolet light (UV) (Van den Hoek *et al*., 1995).

In the cytoplasm there are present 70S ribosomes and DNA, which is located at the center of the cell in a defined area called nucleoplasm (Pupillo *et al*., 2003; Van den Hoek *et al*., 1995).

Sometimes there are also vesicles that regulate gas flotation of cells and a series of granules located between the thylakoids. These granules contain reserve substances such as cyanophycin, a polymer consisting of arginine and aspartic acid, which represents a reserve of nitrogen, granules of glycogen and poly-β-hydroxybutyrate, representing carbon stocks (Flores & Herrero, 2004) and granules of polyphosphate, reserves of phosphate (Figure 2). The accumulation of cyanophycean starch, a glucan very similar to glycogen and to amylopectin of higher plants, is very important (Fuhs, 1973; Meeuse, 1962). Finally, in the cytoplasm there are also carboxysomes, polyhedral bodies that contain carbonic anhydrase enzyme Rubisco (ribulose-1,5-bisphosphate carboxylase/oxygenase) and are involved in the assimilation of inorganic carbon. Many cyanobacteria are able to fix atmospheric nitrogen, for this reason they have the enzyme nitrogenase, usually inactivated by oxygen. Therefore, cyanobacteria have evolved a number of strategies to allow the activity of this enzyme.

Cyanobacteria reproduce themselves by vegetative and asexual methods. Vegetative reproduction occurs by fission or fragmentation or by the formation of hormogonia, i.e. short chains of cells, or by producing akinetic, cell-rich material reserves that allow their survival in a state of dormancy under unfavorable conditions (Van den Hoek *et al.*, 1995). Unicellular forms exhibit fission while filamentous multicellular forms exhibit fragmentation.

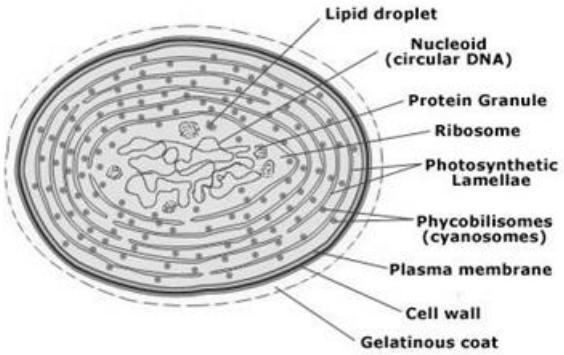

Figure 2: Structure of a cyanobacteria cell

1.2 Taxonomy of cyanobacteria

For many years, the taxonomy of cyanobacteria has been an object of a dispute in the scientific community and has been changed several times in response to information gradually acquired using different methods of investigation (Van den Hoek *et al.*, 1995; Whitton & Potts, 2002). Now, the cyanobacteria are divided into five orders based on morphological

features, as proposed in the system of Anagnostidis and Komárek (1988): Chroococcales, Oscillatoriales, Nostocales, Stigonematales and Pleurocapsales.

The members of Chroococales are unicellular and usually aggregated in colonies. In Pleurocapsales, the cells form internal spores called baeocytes. In Oscillatorialles, the cells do not form specialized cells (akinets and heterocysts) whereas in Nostocalles and Stigonematalles the cells have the ability to develop heterocysts in certain conditions.

1.3 *Synechocystis* sp. PCC 6803

The strain 6803 was first isolated from fresh water in California and deposited in the Pasteur Culture Collection (PCC). It is considered a good model for scientific studies because: it was recognized to be spontaneuosly transformable, it is able to integrate foreign DNA into its genome by homologous recombination (allowing targeted gene replacement) and it can grow in the absence of photosynthesis if a suitable fixed-carbon source such as glucose is provided. The unicellular cyanobacterium Synechocystis sp. PCC 6803 was the third prokaryote and the first photosynthetic organism whose genome was completely sequenced (Kaneko *et al.*, 1996). About 3500 genes encoding for proteins are recognized. In a first time the scientists started an in silico analysis and the function of the proteins was analyzed comparing the encoding sequences to proteins from other organisms using the algorithm BLAST (http://www.ncbi.nlm.nih.gov/BLAST). Half of the Synechocystis proteins resulted correlated with known functions whereas the other half are classified proteins of unknown function (Figure 3).

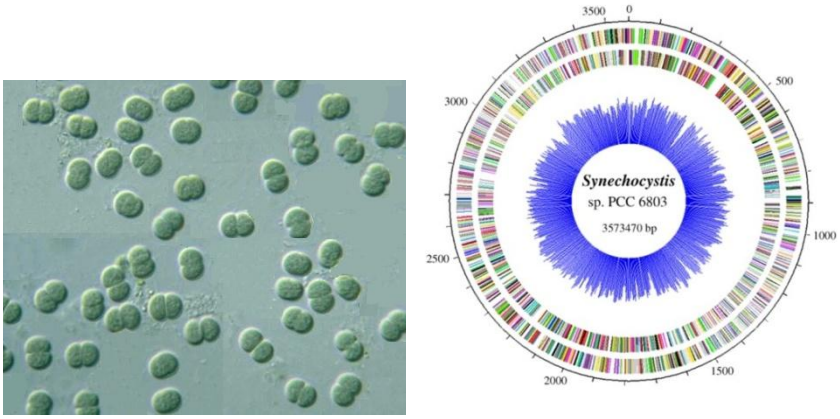

Figure 3: *Synechocystis* sp. PCC 6803: a) microscopy image of Synechocystis sp.6803, b) Genome Map of Synechocystis sp. PCC 6803 (Reference:http://www.kazusa.or.jp/cyano/Synechocystis/map/click/cmap.html).

1.4 The importance of cyanobacteria and their biotechnological applications

Cyanobacteria are interesting for different reasons: they form symbiotic relationship with many plants (especially legumes) and many fungi (forming complex symbiotic organisms known as lichens), they have circadian rhythms, they exhibit gliding mobility, and they can differentiate into specialized cell types called heterocysts.

First of all, they are very important for the growth of plants, in fact they are able to convert atmospheric nitrogen into an organic form such as nitrate or ammonia, molecules that normally plants sponge up from the soil through the roots. Along with algae, cyanobacteria are being considered as an alternative energy source. In addition, in the last few years, cyanobacteria have been recognized as a potent source for numerous natural molecules including anticancer, antimicrobial and hypertension lowering activities. It can be assumed that these organisms hold an attractive source for the pharmaceutical industry (Herrero *et al.*, 2008). However, some species of cyanobacteria produce also neurotoxins, hepatotoxins, cytotoxins and endotoxins that are hazardous to animals and humans. Finally, they are considered an ideal model system for studying fundamental processes such as photosynthesis.

1.5 The endosymbiotic theory

Plastids are major organelles found in the cells of plants and algae. They are divided into several types depending on morphology and function. For example, chloroplasts are the principal actors in photosynthesis, leucoplasts are implicated in the synthesis of monoterpene, amyloplasts are involved in starch storage and chromoplasts are concerned in the pigment synthesis and storage. One plastid can change into another type of plastid. Plastids have their genome, own specific genes, ribosomes, RNAs and are able to produce a part of the proteins required for their function. They contain photosynthetic proteins and pigments that determine the colour of cells. It is generally accepted that plastids are originated from endosymbiotic cyanobacteria.

The endosymbiontic theory describes the evolution of life on Earth or rather the transition from prokaryotic to eukaryotic cell. Initially the Earth's atmosphere did not contain oxygen; this was present only in the liquid state, bound to hydrogen in water molecules. The first life forms were prokaryotes, whose metabolism was anaerobic. Oxygen gas was generated by the first prokaryotes able to perform the photosynthesis: cyanobacteria. The presence of these new organisms changed radically the atmosphere making it "breathable".

The other prokaryotes adapted themselves to new conditions, taking advantage of the reactivity of atmospheric oxygen to produce energy from the demolition of organic substances: this development led to the start of aerobic metabolism, which proved more profitable and more efficient than anaerobic.

According to the latest theories, the actual eukaryotic cell is the result of two combined events:

- the formation of internal membrane systems (except chloroplasts and mitochondria) from folding inside the cell membrane. This process would rise to the Golgi apparatus, the nucleus membrane, the granular and smooth endoplasmic reticulum;
- the formation of mitochondria and chloroplasts.

According to the endosymbiontic model, chloroplasts and mitochondria would evolved from small prokaryotes settled within larger cells. The ancestors of mitochondria were aerobic heterotrophic prokaryotes (Proteobacteria), which could free up large amounts of energy by using cellular respiration. Chloroplasts, however, would have originated from cyanobacteria incorporated by primitive eukaryotic cells (Figure 4).

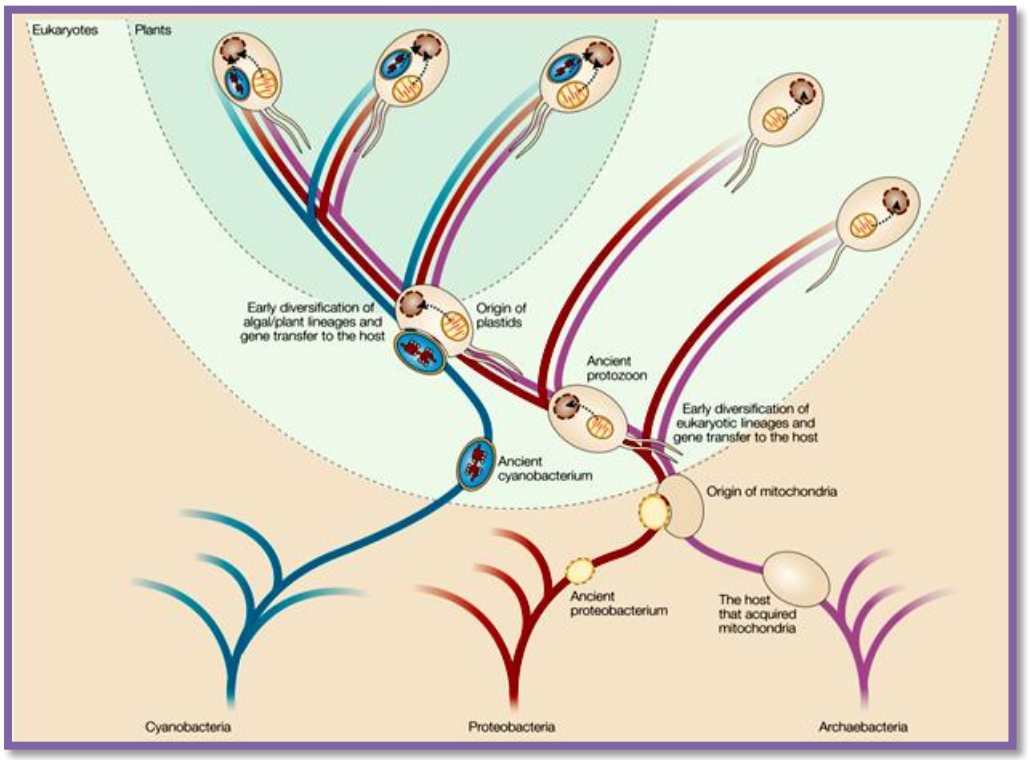

Figure 4: Endosymbiontic evolution and the tree of genomes: The origin of Eukaryotes possibly occurred in the process of endosymbiosis. Both mitochondria and chloroplasts have characteristics of bacteria, including their own DNA and bacterial ribosomes (Timmis *et al*., 2004)

The established symbiosis was beneficial for all actors: the incorporated cell became dependent on host cell for the supply of organic and inorganic molecules, while the host cell had an available continue reserve of food (produced by photosynthetic cells) and more energy (produced in the form of ATP). The endosymbiontic theory, as suggested by Mereschkowsky in 1905, was supported by Ris & Singh in 1960 and then popularized by Margulis in 1981.

Strong phylogenetic, structural, and biochemical analyses have now confirmed that a single symbiotic association between a cyanobacterium and a mitochondria-containing eukaryote between 1.2 and 1.5 Ga ago led to the birth of primary plastids of algae, plants, and glaucophytes (Dyall *et al*., 2004). Genomic organization of several plastid RNA and protein confirm a common origin (Keeling, 2004). The type of cyanobacteria that gave rise to plastids is still being investigated.

According to the model now accepted a heterotrophic eukaryotic would phagocyte without digestion a cyanobacterium. The two cells gradually integrated themselves, the cyanobacterium lost many of its genes and transferred others genes in the host cell nucleus, making the organelle that today we know (Gray, 1999). Plastids originated directly from this event are called primary plastids: these organelles are formed by two membranes probably corresponding to the inner and outer membrane of the cyanobacterium (Jarvis & Soll, 2001). The first photosynthetic cells derived from this first event of endosymbiosis: in particular, red algae, green algae (hence higher plants) and glaucophytes (unicellular algae). Secondary endosymbiosis occurs when the product of primary endosymbiosis is itself engulfed and retained by another free living eukaryote. Secondary endosymbiosis has occurred several times and has given rise to extremely diverse groups of algae and other eukaryotes. Two independent "secondary endosymbiosis", regarding the green algae, have produced Euglenids Chlorarachniophytes, while a single event in the secondary endosymbiosis of red algae gave rise to all Cromoalveolate (Figure 5).

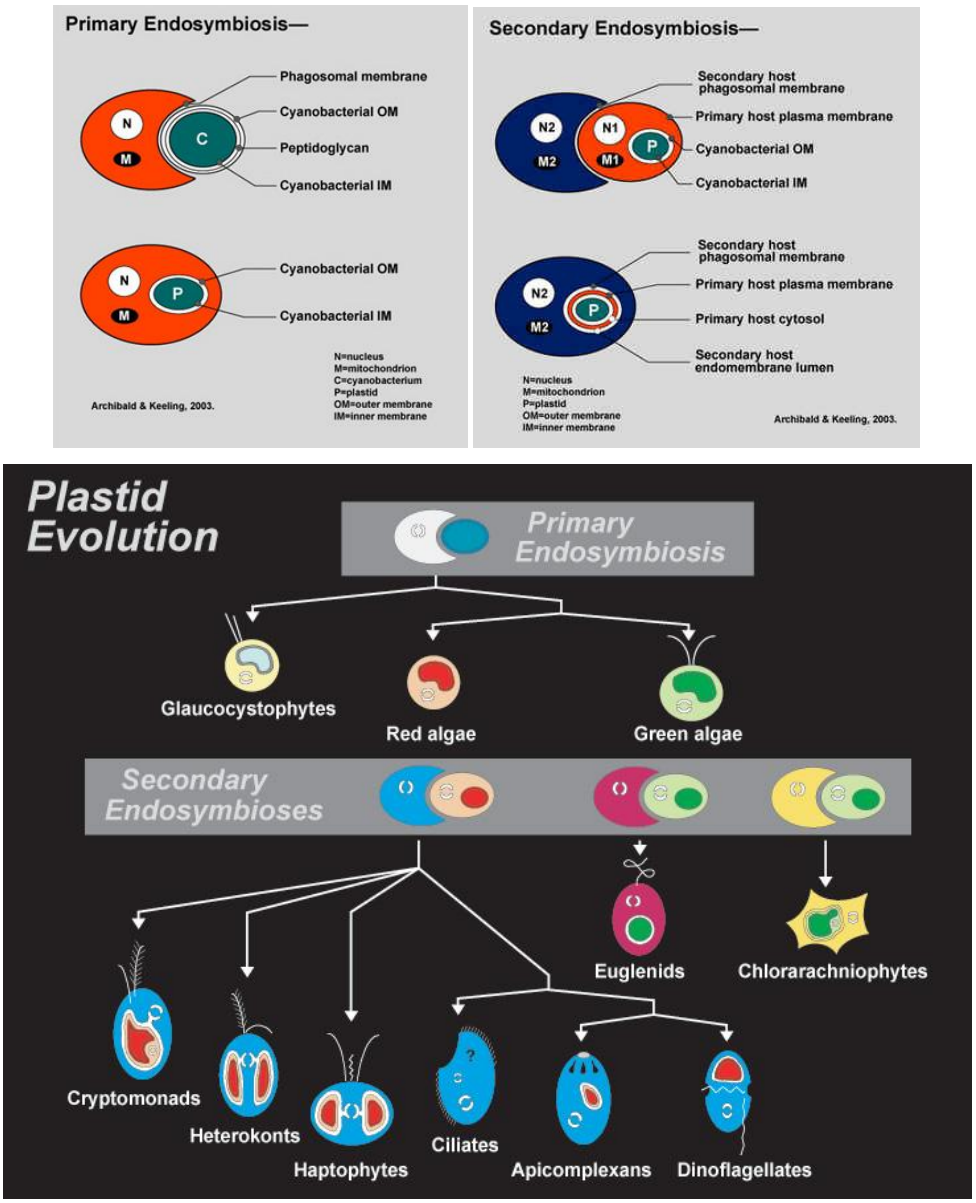

Figure 5: Primary and secondary endosymbyosis. The illustration shows the origin and the distribution of plastids through primary and secondary endosymbiosis (Keeling, 2004) .

The process that transformed the cyanobacterium symbiont in the current plastids involved two important phenomena: the legacy of some processes and components and the emergence of entirely new structures. The legacy includes the photosynthesis, 70S ribosomes, the protein responsible for the division and, in some primitive plastid, the peptidoglycan wall. New facilities include part of machinery of import of proteins, which allows the import of plastid proteins encoded in the nucleus. The actual chloroplast genome encodes 100-200 proteins, demonstrating that it suffered a marked reduction during the endosymbiosis. Cyanobacteria, in fact, encode for thousands proteins. Although it is accepted that the transfer of genes to the nucleus has occurred during the evolution of plastid, the extent of the transfer has only

recently been estimated. For example, the genome of *Arabidopsis thaliana* encodes 24,990 proteins; 800 to 2000 of them came from cyanobacteria (Martin *et al*., 2002). A recent study showed that the extent of the transfer is greater: the proteins derived from the cyanobacterium were 4.500 (18% of the genome) (Martin *et al*., 2002) (The Arabidopsis Genome Iniative, 2000). These proteins also belong to various classes and many are located in different compartments of the chloroplast (Martin *et al*., 2002).

2. PHOTOSYNTHESIS

Photosynthesis (from the Greek φώτο-[photo-], "light," and σύνθεσις [synthesis], "putting together", "construction") is the process consisting in the conversion of the light energy to useful forms (Figure 6). Photosynthesis occurs in algae, in plants and in many species of bacteria.

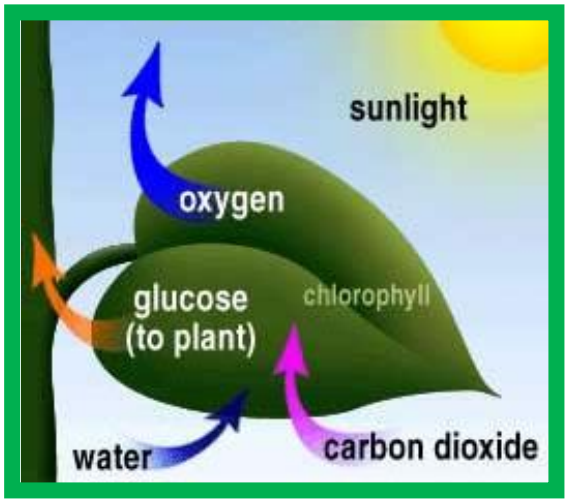

Figure 6: Photosynthesis. Photosynthesis converts light energy into the chemical energy of sugars and other organic compounds. This process consists of a series of chemical reactions that require carbon dioxide and water and store chemical energy in the form of sugar.

Plants capture only one thousandth of the sunlight that falls on the Earth. Yet, without this process all life would come to a halt.

In 1969, Rabinowitch and Govindjee wrote: "*A living organism is like a running clock. If it is not wound up, it will sooner or later run out of energy and stop. If the clock of life on earth would be left to run down without rewinding, it would take less than one hundred years for all life on the planet to approach its end. First green plants would die from starvation. Humans and other animals who feed on plants would follow. And finally, bacteria and fungi feeding on*

dead animal and plant tissues would exhaust their food and die too" (http://www.life.illinois.edu/govindjee/textzsch.htm).

2.1 Photosynthesis in plants and cyanobacteria

Photosynthesis is a redox process in which electromagnetic energy is converted into chemical energy and carbon dioxide into an organic compound. Photosynthesis can be divided into two phases: a photochemical light period and a chemical dark phase. The first phase is the transformation of electromagnetic energy (into adenosine triphosphate ATP) and the reduction of $NADP^+$ to NADPH. This phase involves the release of various secondary products (in plants and cyanobacteria is gaseous oxygen O_2). During the dark period, ATP and NADPH provide energy and reducing power required for CO_2 reduction.

In nature, there are two types of photosynthesis: anoxygenic and oxygenic. Anoxygenic photosynthesis is led by green sulfur bacteria, purple bacteria and Heliobacteria and requires reduced forms of sulfur (H_2S), molecular hydrogen or other organic compounds (Pupillo *et al.*, 2003).

The overall reaction can be described as follows:

$$CO_2 + H_2O \rightarrow O_2 + (CH_2O)$$

water is oxidized to oxygen and carbon dioxide is reduced to carbohydrates.

In plants, photosynthesis takes place in specialized cellular organelles called chloroplasts.

The chloroplast (Figure 7) is made up of 3 types of membranes:

1. an outer membrane which is thought to be freely permeable,
2. an inner membrane which contains integral membrane proteins that regulate the passage in and out of the chloroplast (e.g. small molecules like sugars and proteins synthesized in the cytoplasm of the cell but used within the chloroplast),
3. a system of thylakoid membranes that enclose a lumen similar to cytosol of the cells. This third membrane forms a series of flattened disk-shaped sacs called thylakoids. Individual thylakoids communicate with each other and form stacks of thylakoids called grana.

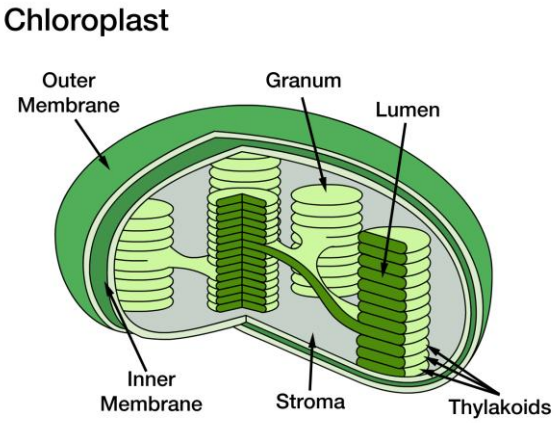

Figure 7: A chloroplast. The ellipsoid-shaped chloroplast is enclosed in a double membrane and the area in between the two layers is called the intermembrane space.. The outer layer of the double membrane is much more permeable than the inner layer, which features a number of embedded membrane transport proteins Thylakoids are a phospholipid bilayer membrane-bound compartment. A granum is a stack of thylakoids folded on top of one another. The stroma is the fluid space within the chloroplast. The lumen is the fluid filled space within a thylakoid.

The thylakoid system is a very important evolutionary acquisition of organisms performing oxygenic photosynthesis; it is the site of location of their photosynthetic machinery. The development of thylakoids strongly correlates with the occurrence of oxygenic photosynthesis, and almost all organisms performing this process possess this specialized membrane system. Whereas the nature of the photosynthetic reaction and the principal architecture of the thylakoid membrane are now reasonably well understood, many aspects of the evolution and progression of thylakoid biogenesis remain elusive.

The thylakoid membrane system of cyanobacteria, as well as of many algae, is built up of long lamellae that enclose an aqueous compartment, the lumen. Their architecture allows the chloroplast to significantly increase the surface utilized for the photosynthetic process and thereby to achieve a more efficient exploitation of light energy. Moreover, the thylakoid system compartmentalization and flexibility allow a better quality regulation.

There are four major protein complexes embedded into the thylakoid membrane: photosystem I and II (PSI and PSII, respectively) with their antenna proteins, the cytochrome b_6f complex and the ATP synthase (Figure 8). They include a variety of co-factors and pigments, and require multiple assembly steps. Moreover, the photosynthetic complexes are not equally distributed along the thylakoid membrane but have preferential locations. PSI and ATP synthase are more abundant in stroma lamellae while PSII and LHCII are predominantly found inside the grana stacks (Andersson and Anderson, 1980). The cytochrome b6f complex

is most likely equally distributed (Albertsson, 2001; Allen and Forsberg, 2001), although there is no general agreement on this question (Vallon *et al.*, 1991; Van Roon *et al.*, 2000).

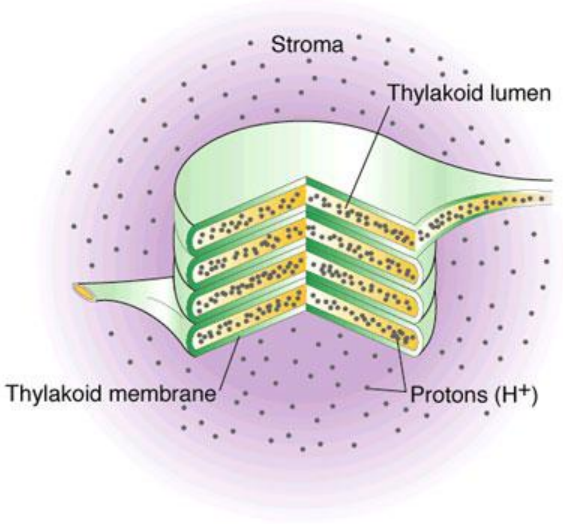

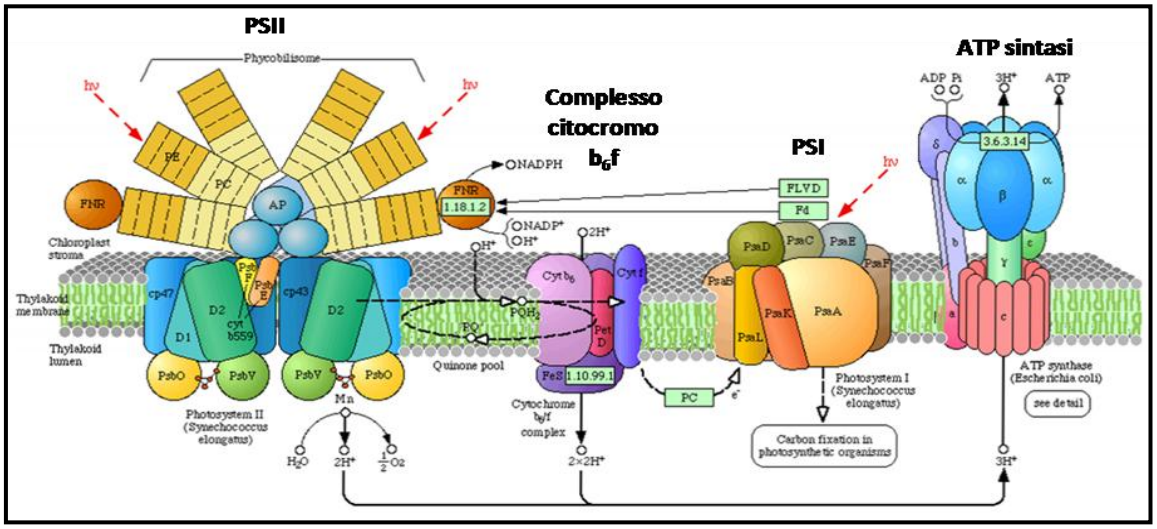

Figure 8: Thylakoid structure: Thylakoid cartoon (Copyright ©2002 Thomson Learning, Inc), and diagram of the thylakoid membrane showing electron transfer through a number of electron carriers. The enzyme coupling proton movement to ATP synthesis is also shown (ATP synthase) (Campbell, Reece, & Simon, 2008).

Thylakoids have also a peculiar lipid composition, which is similar in cyanobacteria and higher plants (Dilley *et al.*, 2001; Kelly & Dörmann, 2004). Their main components are unsaturated galactolipids, namely monogalactosyl diacylglycerol (MGDG), which makes up more than 50% of the total thylakoid lipids, and digalactosyl diacylglycerol DGDG (about 25%). Additionally, the thylakoids contain phosphatidylglycerol and sulfoquinovosyl diacylglycerol together with other minor components.

2.2 The Photosynthetic pigments

Biological pigments are usually non-covalently attached to proteins that form pigment-protein complexes which are organized as the photosynthetic unit (PSU).

The protein molecules impose an appropriate molecular geometry on the photosynthetic pigments, binding them close together with respect to one another for efficient transfer of energy. In order to ensure the conversion of light energy into chemical energy, during the photosynthetic process, the presence of ubiquitous pigments such as chlorophyll and carotenoids is required. In particular, in cyanobacteria, the chlorophyll a, the carotenoids β-carotene and zeaxanthin, and a specific class of pigments called phycobiliproteins (found only in cyanobacteria, Red algae and Criptoficee) are present.

2.2.1 Chlorophylls

The chlorophyll pigments are metal-porphyrins belonging to the tetrapyrrole family. They are characterized by a cyclic tetrapyrrole ring with a coordinated atom of Mg^{2+} in the center, and a long side chain formed by an acyclic diterpene alcohol, the phytol (Kirk *et al.*, 1967).

In eukaryotic organisms, there are two types of chlorophylls: chlorophyll a and chlorophyll b, which differ for the presence of a methyl group or an aldehyde group at the C3 of the second tetrapyrrole ring (Beale, 1999), whereas in cyanobacteria only the chlorophyll *a* is found (Figure 9).

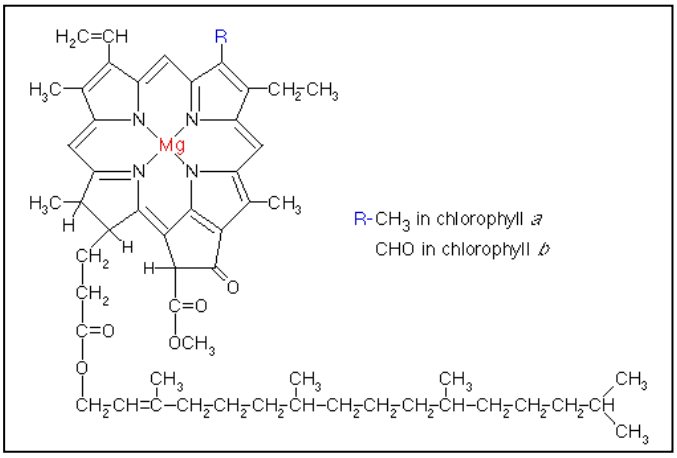

Figure 9: Structure of *chlorophyll a* and *chlorophyll b*. A magnesium atom is held in a porphyrin ring, chlorophyll a and chlorophyll b diverge for the presence of a methyl group or an aldehyde group at the C3 of the second tetrapyrrole ring.

Chlorophylls absorb light in the red (550-700 nm) and blue visible region (< 480 nm) and release fluoresce in the red spectrum at wavelengths slightly greater than the wavelengths of absorption (Figure 10).

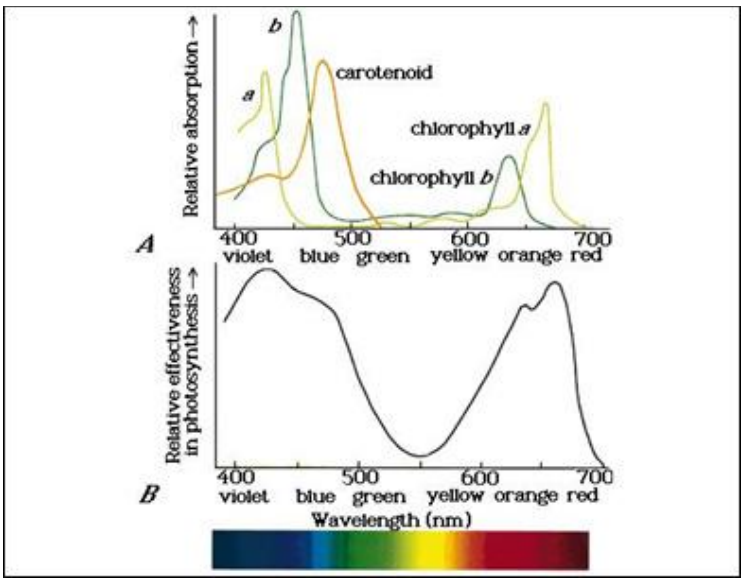

Figure 10: The absorption spectrum of chlorophyll a, chlorophyll b and carotenoid, and the spectrum of action of photosynthesis. The chlorophyll absorbs short wavelengths up to 400 nm, here photosynthetic activity is low, the maximum absorption for photosynthesis is at 425 nm. The photosynthetic activity shows a peak between 650 and 680 nm.

2.2.2 Carotenoids

Carotenoids are isoprenoid compounds formed by 40 carbon atoms, characterized by a linear central portion (with double bonds) and two cyclized ends. They are divided in two classes: hydrocarbon carotenes, present mainly in the reaction centers, and xanthophylls, which contain oxygen atoms, mainly located in the antenna complex (Raven *et al.*, 1984) (Figure 11). In eukaryota the β-carotene and the xanthophylls lutein, zeaxanthin, violaxanthin and neoxantin are the major pigments (Young *et al*,, 1997). Carotenes are colored yellow-orange while xanthophylls are orange-red.

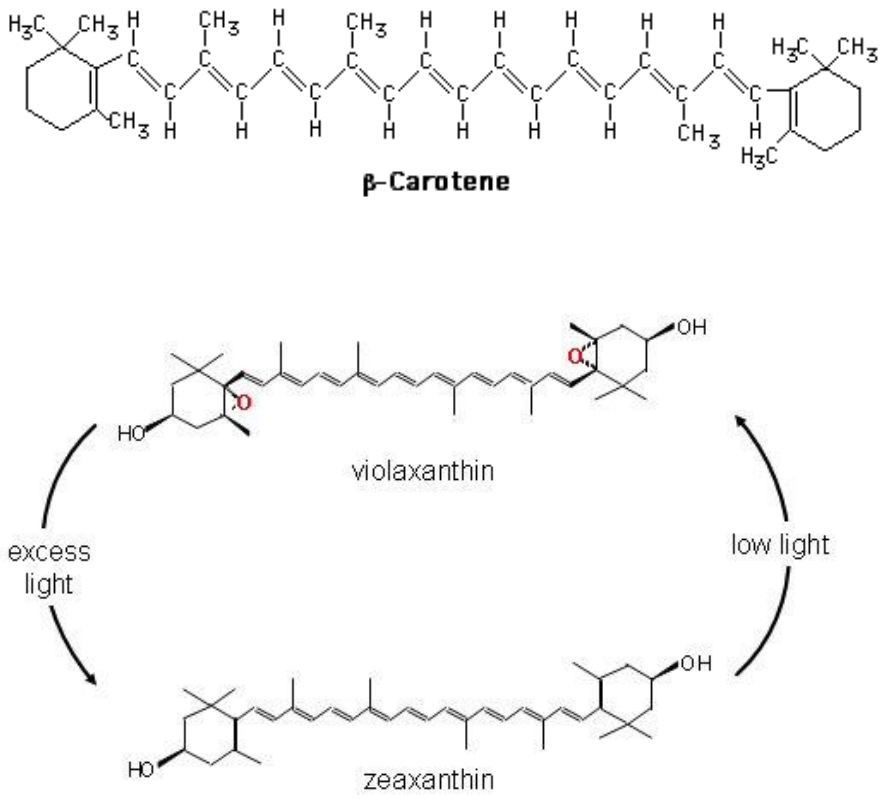

Figure 11: Types of carotenoids. Carotenoids as β-carotene consist only of carbon and hydrogen; other carotenoids, as zeaxanthin and violaxanthin contain also oxygen

Although, also in cyanobacteria, β-carotene and zeaxanthin are the mainly carotenoids, in many species echinenone, mixoxantofill, oscilloxantin, β-cryptoxanthin are also found (Pupillo *et al*., 2003).

Carotenoids absorb light between 390 and 530 nm, region of purple-blue. They are important as antenna pigments, as well as for protection of the photosynthetic pigments from photo-oxidation damage. In fact, they are able to de-energize both chlorophyll triplet (3Chl *) and singlet oxygen, both harmful, and dissipate the excitation energy captured as heat.

In eukaryota, carotenoids play an additional protective function; they are able to reduce the amount of light energy in the reaction center of PSII, dissipating it as heat (thermal dissipation). This process is conducted by the xanthophylls in the "cycle of violaxanthin". In case of exceeding radiant energy, violaxanthin is de-epoxidated in anteraxanthin and then to zeaxanthin (Hirschberg, 2001). These forms are able to absorb light energy, which is then dissipated as heat (Huner *et al*., 1998).

Some papers have recently shown that carotenoids, in stress conditions such as a high intensity light or high temperature, may play a structural role in stabilizing and protecting the

lipid phase thylakoids membranes (Havaux, 1998). Both these processes are not present in cyanobacteria, which lack violaxanthin. Probably, they are able to defend themselves from excess of light energy by implementing the mechanism of state transitions. In photosynthecic organisms the distribution of excitation between PSII and PSI can be altered by changing the association of light harvesting complexes with photosystems, as a rapid response to variations in illumination conditions. These variations are called 1-state 2 transitions. The biochemical mechanism of state transitions in cyanobacteria is not known, but it is likely to be significantly different from that in green plants. Energy transfer and mutant studies have shown that phycobilisomes in cyanobacteria can transfer energy directly to PSI as well as to PSII (Mullineaux, 1994; Rakhimberdieva *et al.*, 2001). State transitions change the relative energy transfer from phycobilisomes to PSI and PSII, and also the distribution of chlorophyll-absorbed energy (Thor *et al.*, 1998).

2.2.3 The phycobiliproteins

There are important accessory pigments present only in cyanobacteria, red algae and Criptomonadi, which serve as the primary light-harvesting antennae for PSII. The phycobiliproteins are characterized by a chromophore, defined bilin, which is linked to a cysteine residue of the apoprotein (Figure 12). During the photosynthetic process they work as antenna pigments.

They are divided in three groups:

1. Phycoerythrin: red (maximum absorption 545-570 nm);
2. Phycocyanin: blue (maximum absorption 620 nm);
3. Allophycocyanin: blue-purple (maximum absorption 650-670 nm).

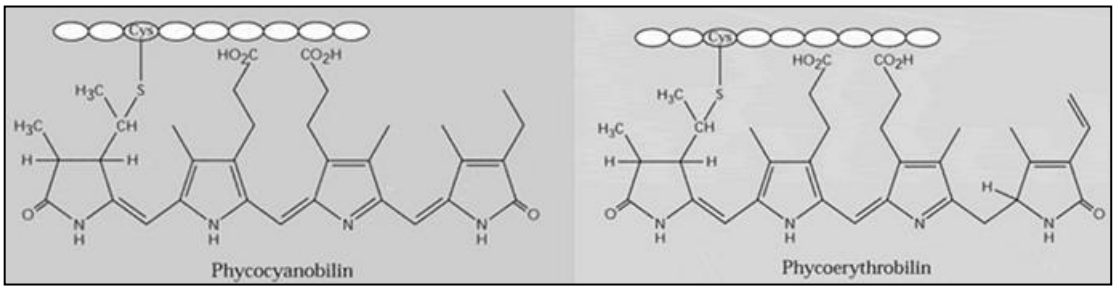

Figure 12: Molecular structures of phycobiliproteins

The phycobiliproteins are composed of two subunits (α and β) that may be associated in form of trimers $(\alpha, \beta)_3$ and hexamers $(\alpha, \beta)_6$, to form disk-shaped units.

Phycobilisomes are constructed from two main structural elements: a core substructure and peripheral rods that are arranged in a hemidiscoidal fashion around that core. The core of most hemidiscoidal phycobilisomes is composed of three cylindrical subassemblies. The peripheral rods radiate from the lateral surfaces of the core substructure which are not in contact with the thylakoid membrane (Figure 13). The assembly of phycobilisomes is possible thank to the presence of smaller 'linker polypeptides,' most of which do not bear chromophores, which interact with phycocyanin and phycoerythrin maintaining the aggregation and the stacking in the peripheral region of the phycobilisomes (Tandeau de Marsac and Cohen-Bazire, 1977).

Absorbed light energy is transferred by very rapid, radiation-less downhill energy transfer from phycoerythrin or phycoerythrocyanin (if present) to C-phycocyanin and then to allophycocyanin species that act as the final energy transmitters from the phycobilisome to the PSII or (partially) PSI reaction centers.

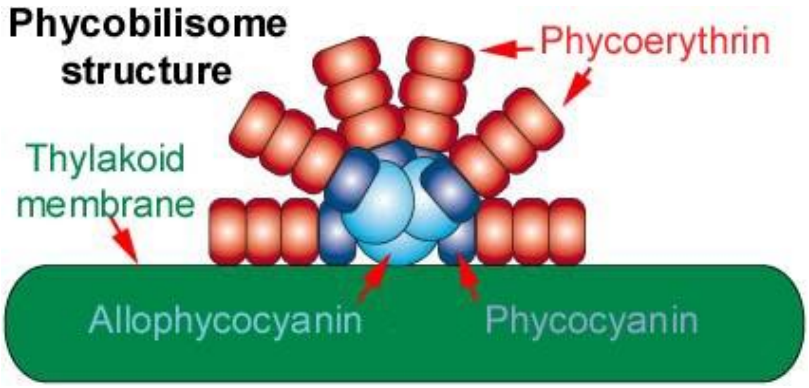

Figure 13: Structure of phycobilisome (www.botany.hawaii.edu**)**

2.3 Photosystems

The thylakoidal membranes of cyanobacteria are structurally and functionally similar to the chloroplasts of higher plants. Photosystems consist of two distinct components that cooperate: the reaction center consists of hydrophobic membrane proteins and photochemically active chlorophylls, and the antenna, which collects radiant energy and transmits it to the center of response. In cyanobacteria, as in plants, photosynthesis is carried out by multiprotein complexes PSII and PSI. Photosystem II (PSII) is a large homodimeric protein–cofactor

complex located in the photosynthetic thylakoid membrane that acts as light-driven water:plastoquinone oxidoreductase. Cyanobacterial PSII includes a reaction center, called "Type II" or "quinone", an internal antenna and an external antenna. The reaction center is a dimer of proteins, D1 and D2, which binds a pair of molecules of chlorophyll a photochemically active (P680).

Also a cytochrome b, defined cyt b559, and two plastochinons: Q_A (which is the partner of the photochemically active chlorophyll in photochemical reaction) and the Q_B are part of the reaction center. Associated with the center of reaction on the luminal side, there is the complex evolving oxygen (OEC), where photolysis of water takes place. Outside the reaction center, deeply embedded in the membrane, there is an internal antenna consisting of two-pigment complex protein, called CP43 and CP47, containing chlorophyll a molecules. Finally, in the stromal side of the membrane, outside of PSII, the antenna is located, constituted by the phycobilisomes.

The cyanobacterial PSII differs from that of plants primarily for the antenna that consists of the phycobilisomes (Figure 8). The composition of phycobilisomes varies greatly among different species of cyanobacteria.

PSI is an integral membrane protein complex that normally functions to transfer electrons from the soluble electron carrier plastocyanin (Pc) to the soluble electron carrier ferredoxin (Fd). Under certain environmental conditions in some cyanobacteria and algae, alternative electron donors and acceptors, such as cytochrome c6 and flavodoxin, can function in place of PC and Fd. In terms of functional activity PSI is unique in generating highly reducing species that are capable of reducing $NADP^+$ in an energetically favourable reaction. The PSI reductants are the strongest produced in any biological system.

Unlike PSII, the cyanobacterial PSI lacks an external antenna. The PSI consists of a heterodimer (PsaA / PsaB) to which hundreds of molecules of chlorophyll are linked basically acting as the the antenna of the photosystem (Xu *et al.*, 2001). In addition to the heterodimer, accessory proteins are also part of PSI, however nothing is known about their precise function (Xu *et al.*, 2001).

2.4 Photosynthesis steps

Photosynthesis in plants and cyanobacteria produces both ATP and NADPH and occurs in two phases: the light phase that is light-dependent and the dark phase or phase of carbon fixation that is independent from light.

The oxygen atoms of two water molecules bind to a cluster of manganese atoms in a water-splitting enzyme that enables electrons to be removed one at a time to fill the holes created by light in chlorophyll molecules in the reaction center. As soon as four electrons have been removed from the two water molecules, O_2 is released. The core of the reaction center in PSII produces strong electron donors in the form of reduced quinone molecules in the membrane. The quinones pass their electrons to an H^+ pump called the cytochrome *b_6-f complex*. The complex pumps H^+ into the thylakoid space across the thylakoid membrane and the resulting electrochemical gradient drives the synthesis of ATP by an ATP synthase. The final electron acceptor in this electron-transport chain is the PSI. Each electron that enters is boosted to a very high energy level that allows it to be passed to the iron-sulfur center in ferredoxin and then to $NADP^+$ to generate NADPH).

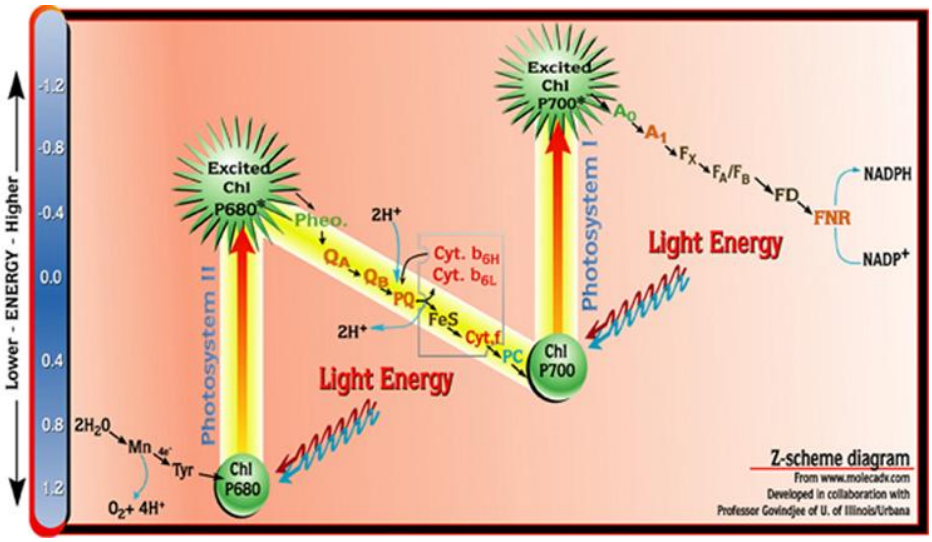

Figure 14: Z-scheme. This particular diagram was developed by Wilbert Veit and Govindjee, in 2000 Abbreviations used are (from left to the right of the diagram): Mn for a manganese complex containing 4 Mn atoms, bound to Photosystem II (PSII) reaction center; Tyr for a particular tyrosine in PSII; O_2 for oxygen; H^+ for protons; P680 for the reaction center chlorophyll (Chl) in PSII: it is the primary electron donor of PSII; Excited (Chl) P680 for P680* that has the energy of the photon of light; Pheo for pheophytin molecule (the primary electron acceptor of PSII; it is like a chlorophyll a molecule where magnesium (in its center) has been replaced by two "H"s); Q_A for a plastoquinone molecule tightly bound to PSII; Q_B for another plastoquinone molecule that is loosely bound to PSII; FeS for Rieske Iron Sulfur protein;Cyt. F for Cytochrome f; $Cytb_6$ (L and H) for Cytochrome b_6 (of Low and High Energy); PC for copper protein plastocyanin; P700 for the reaction center chlorophyll (Chl;actually a dimer, i.e., two molecules together) of PSI; it is the primary electron donor of PSI; Excited (Chl) P700 for P700* that has the energy of the photon of light; Ao for a special chlorophyll a molecule (primary electron acceptor of PSI); A_1 for a phylloquinone (Vitamin K) molecule; F_X, F_A, and F_B are three separate Iron Sulfur Centers; FD for ferredoxin; and FNR for Ferredoxin NADP oxido Reductase (FNR). Three major protein complexes are involved in running the "Z" scheme: (1) Photosystem II; (2) Cytochrome bf complex (containing Cytb6; FeS; and Cytf) and (3) Photosystem I. The diagram does not show where and how ATP is made. (http://www.life.illinois.edu/govindjee/ZSchemeG.html).

3. ION TRANSPORT SYSTEMS

The plasma membrane is a selectively permeable barrier that allows the separation and the exchange of materials between the inner and the outer of the cells. In fact, a continuous exchange of nutrients (e.g. sugar and aa), the elimination of toxic substances (e.g. CO_2) and the regulation of ions' cellular concentration (e.g. K^+, Na^{2+}; Cl^-) for the survey and the correct cellular growth is necessary

Non-ionic solutes and small molecules pass across membrane by simple diffusion, while ions and big polar molecules need specific transport membrane proteins. Various transport system were described in the literature; in general they are complexes consisting of integral membrane proteins and cytosolic components. Transport proteins can be divided in two main categories: carrier proteins and channel proteins. Carrier proteins are responsible for the passive and the active transport, whereas channel proteins are responsible only for passive transport (Figure 15).

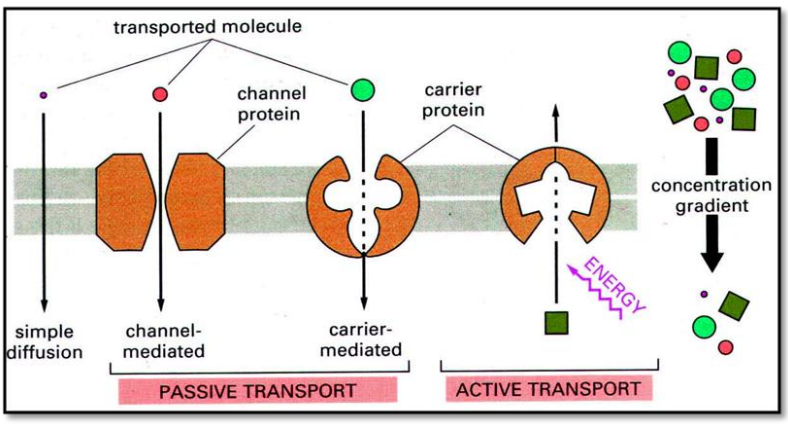

Figure 15: Passive and active transport. Carrier proteins are involved in the passive and in the active transport, whereas channel proteins are only involved in the passive transport. (Alberts *et al.*, 2002)

3.1 Carrier proteins

The carriers bind solutes and allow their movement from one side to the other side of phospholipidic bilayer by facilitated diffusion and active transport. Each carrier protein recognizes only one substance or one group of substances. The substrate binds the carrier molecule at the binding site, with a certain binding affinity, and then it is translocated in the other side of the membrane where it is finally released according to its binding affinity. All steps are reversible.

The carriers can work in both directions (transport in and out of the cells). They can transport a single type of molecule (mechanism called uniport) or can combine the movements of two inorganic ions, an inorganic ion and a organic molecule or two organic molecules. If the transport of solutes is in the same direction the movement is named symport, if it is in oppositive directions it is called antiport (Figure 16).

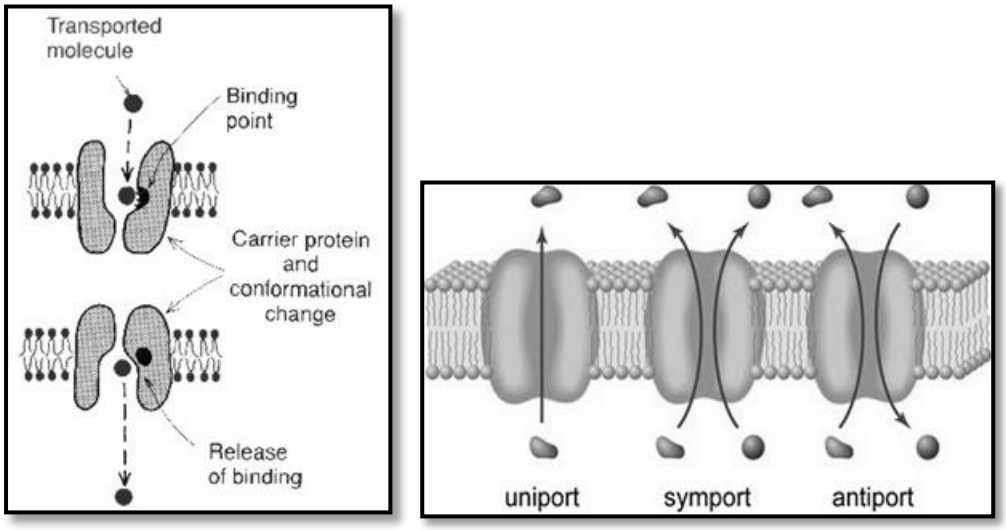

Figure 16: Carrier transport and diagram comparing uniport, symport, and antiport. Uniports simply move solutes from one side to another. Cotransport systems work by simultaneously sending two solutes across the lipid bilayer. There are two types of cotransport systems: symport, in which the solutes move in the same direction, or antiport, in which they are sent in opposite directions.

3.2 Ion channels

Ion channels are transmembrane proteins that create ion-selective pores in the membranes and allow the passive transport of ions in and out of cells. They are present in every forms of life, such as viruses, prokaryotes, animals and plants and they are usually categorized on the basis of the preferable ion: e.g. K^+, Na^+, Ca^{2+} and Cl^- channels.

The passage of ions through the channels is determined by the compatibility of ion size with the pore size and the presence of electronic charges localized on the internal wall of the channel. Ions are polar particles that in aqueous solution are enveloped by a wrapping of water called hydration shell; for this reason every ion displays a dehydrated ray (due only to ion) and hydrated ray (due to ion and water molecules). For example, the hydration shell of a K^+ or Na^+ ion contains six water molecules. The diameters of dehydrated Na^+ and K^+ ions are 0.98Å and 1.33Å, respectively. The effective diameter of hydrated ion is larger in Na^+ than in K^+ (Table 1**)**

ION	DEHYDRATED RAY (Å)	HYDRATED RAY (Å)
Na^+	0.98	2.91
K^+	1.33	1.88
NH_4^+	1.45	1.89
Cl^-	1.80	1.92

Table 1: Dehydrated and hydrated ray of some ions (Taglietti & Casella, 1997)

The channels' selectivity is correlated to charges placed in the pore: the positive charges drive back cations and the channel results more selective for anion, conversely, the negative charges repulse anions and the channel is more selective for cations. Channels are very selective proteins but an ion channel perfectly selective for one specific ion does not exist.
Channels display gates that control the activation/deactivation of the protein. The gating, the mechanism of opening and closing of the pore, is an important feature. In general a channel presents three different phases: open, close and inactive states. In the open state the passage of ions is allowed while it is blocked in the other states. Ion channel proteins open and close their pores in response to various stimuli. The nature of stimulus permits to classify the channels in different category:

1. mechanically-gated channels: activated by mechanic stress;
2. voltage-gated channels: activated by change of membrane potential;
3. ligand-gated channels: activated by an extracellular or intracellular ligand.

3.3 Potassium transport

K^+ is the most abundant ion in cytoplasm of biological systems. The cytosolic K^+ concentration ranges between 50 and 250 mM in plants and fungi, 300 and 500 mM in

bacteria and up to 1 M in bacteria grown in hyperosmotic media. Unlike most other cations, the accumulation of K^+ does not interfere with the structure and reactions of macromolecules such as DNAs, RNAs and proteins in aqueous solution.

The force that moves the ions through membrane proteins is the combination of electrical transmembrane potential and ion concentration gradient across the membrane. The combination of these two effects is called electrochemical gradient. The electrochemical gradient of K^+ across the membrane that can be expressed as:

$$\Delta\mu K^+ = F\Delta\Psi^+ RT \ln [K^+]_{in}/[K^+]_{out}$$

where $\Delta\Psi$ is the membrane potential, F is Faraday's costant, R is the gas constant, T is the temperature in degrees Kelvin and $[K^+]$ the concentration of K^+ in and out.

It can be expressed also as driving voltage (expressed in mV):

$$\Delta\mu K^+/F = \Delta\Psi^+ 58 \log [K^+]_{in}/[K^+]_{out}$$

Usually $[K^+]_{in}$ is higher than $[K^+]_{out}$ and consequently cytoplasm are electrically negative.

K^+ plays a crucial role in a series of basic mechanisms. For example, in animals it is involved in muscular contraction, in plants is implicated in cell elongation, stomata movements, regulation of gas exchanges, and the transduction of various signals (Clarkson & Hanson, 1980; Véry & Sentenac, 2002; Zimmermann & Sentenac, 1999).

Bacteria, fungi and plants have two specific families of K^+ transporters: Trk/Ktr/HKT (transpoter K^+ in fungi and bacteria, K^+ transporter in bacteria and High-affinity K^+ transporter in plants) and HAK/Kup/KT (high-affinity K^+ uptake in fungi and in plants, K^+ uptake in bacteria and K^+ transporter in plants) families. For example E. *coli* presents three K^+ uptake systems, Trk, Kdp and Kup, and two K^+ efflux system, KefB and KefC, that resemble Na^+/H^+ and K^+/H^+ antiport (Epstein, 2003).

In *Synechocystis* three types of K^+ transports are identified: Ktr, Kdp and K^+ channels (Figure 17). Several analyses reveal that Ktr is composed of tree subunits KtrA, KtrB and KtrE and that it is regulated by an ATPase and by an Na^+/H^+ antiporter (Berry *et al.*, 2003; Matsuda *et al.*, 2004). Another K^+ uptake system present in *Synechocystis* is KtrAB, encoded by ORF sll0493 for the A subunit and by srl1509, the potassium translocation subunit B. It transports K^+ by Na^+/K^+ symport, utilizing sodium motive force (Berry *et al.*, 2003)

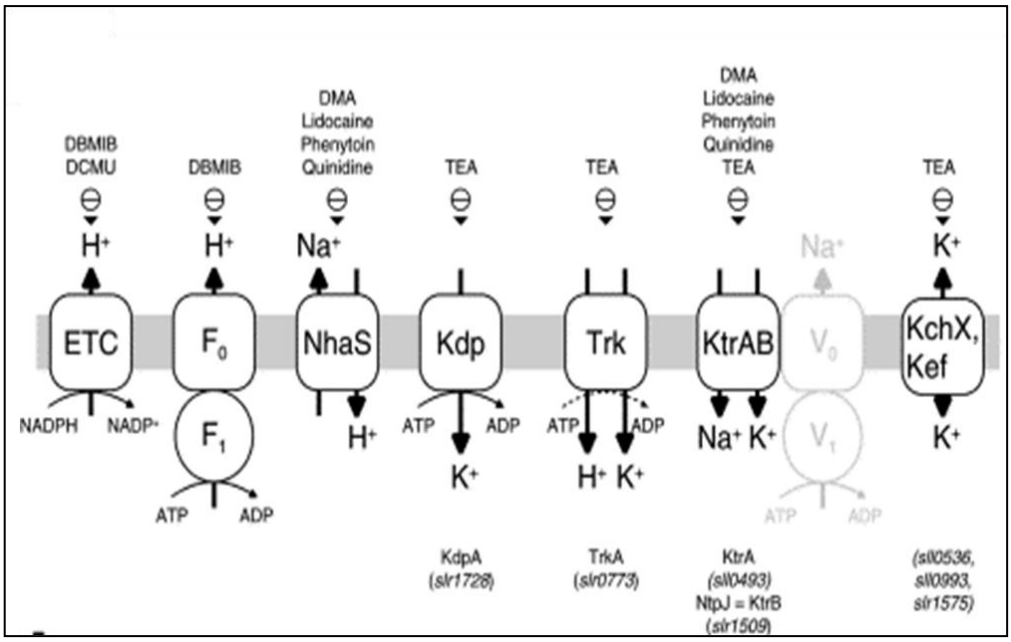

Figure 17: K^+ transports in *Synechocystis*: Genes and proteins implicated in potassium uptake in *Synechocystis* 6803, with possible sites of inhibitor action (Berry *et al*., 2003)

Potassium channels are found in viruses, Bacteria, Archea and Eukarya but initially they were studied only in the animal kingdom and in particular into the nervous system. Hence, the 2003 Nobel Prize in Chemistry was awarded for the study of structure and mechanism of a bacteria K^+ channel. Most of the knowledge about their tetrameric architecture and function was gained from studies on the bacterial channels, KcsA from *Streptomyces lividans* (Doyle *et al*., 1998), MthK from *Methanobacterium thermoautotrophicum* (Jiang *et al*., 2002) and KvAP from *Aeropyrum pernix* (Jiang *et al*., 2003) (Figure 18).

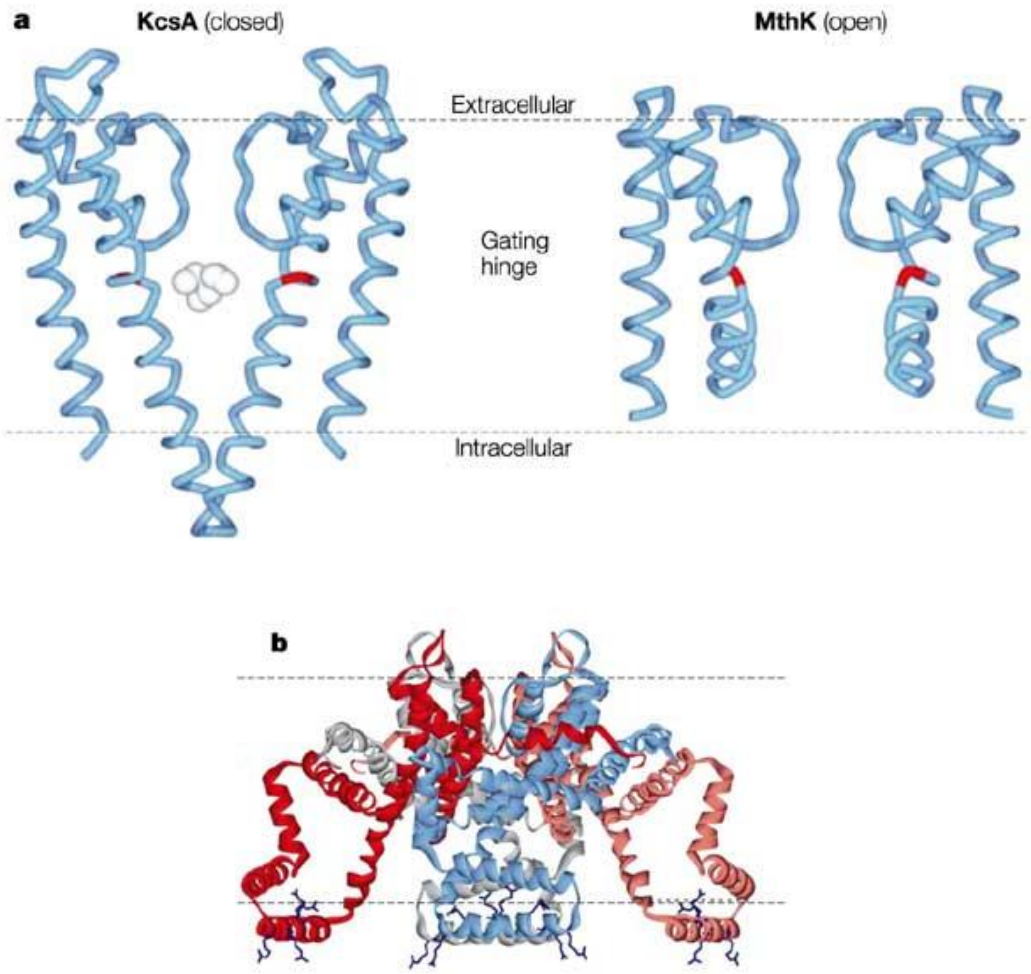

Figure 18: Tetrameric architecture of bacteria channels. a) KcsA and MthK channels. The red residue in both channels (G99 in KcsA and G83 in MthK) is a glycine residue that has been proposed to serve as a gating hinge. b) View of the tetrameric structure of KvAP (Swart, 2004).

3.3.1 Structure of K^+ channels

K^+ channels are tetrameric proteins composed by principal subunits, called α-subunit or pore-forming subunit, and auxiliary subunits, named β and γ, that serve to deploy or to regulate the main α-subunit. The smaller α-subunit consists of two transmembrane α helices TM1 and TM2 (TM helical, transmembrane segment).

Kvc, a 94 ammino acids protein encoded by *Paramecium busaria* chlorella virus 1 (PBCV-1), is the smallest known protein to form a functional potassium ion channel (Plugge *et al.*, 2000) and basically corresponds to the "pore module" of potassium channels (TM1-P-TM2, where P indicates the pore of channel). TM1-P-TM2 without additional domain is the minimal structure to have a protein that works as channel; this configuration allows permeation,

filtration and gating. TM1-P-TM2 is present also in prokaryotic and eukaryotic inward rectifying channels (Kir). Through evolution, the 2 TM channel likely duplicated to form 4 TM channels and this phenomenon permitted the formation of a heterodimer (α-α').

In eukaryotic systems, α-subunits in an S1-S2-S3-S4-S5-P-S6 (S, transmembrane segment) arrangement are also identified. These kinds of channels are usually called Shaker channels, named due to a mutant of *Drosophila melanogaste*r, which corresponded to the first cloned potassium channel (Tempel *et al.*, 1987). These proteins are composed of four identical subunits, and each polypeptide presents a short intra-cytoplasmatic domain (c.a. 60 aa), an hydrophobic core composed by 6 TM and a long C-terminal region. The S5-P-S6 remembers the TM1-P-TM2 core of the 2 TM channels while a variety of experiments suggest that S4 helix works as voltage sensor and that it contains positive ammino acids, in particular arginines and lysines.

Other rare forms have been discovered in unicellular eukaryotes, e.g. ciliates and fungi, these channels display 8 TM (S1-S2-S3-S4-S5-P-S6-S7-P-S8) or 12 TM motives (S1-S2-S3-S4-S5-P1-S6-S7-S8-S9-S10-S11-P2-S12) (Ketchum *et al*, 1995; Zhou *et al*, 1995).

3.3.2 Selectivity filter and gating

The selectivity filter is present in all channels and is an aa sequence that determines wich ions can pass through the pore. It is located at the narrowest part of the pore. The crystal structure of KcsA at the resolution of 2 Amstrong (Å) elucidated the permeation process in K^+ channels: it showed that the filter is 12 Å long and has more or less 2,5 Å diameter (Choe, 2002). K^+ ions are attracted by negative charges of the selectivity filter and accumulate near the pore. The oxygen atoms surrogate water for the dehydrated K^+ ions (1,3 Å). This oxygen lined checkpoint is repeated five times every 3.0 Å along the filter (Choe, 2002).

The three-dimensional image of the selectivity filter, revealed by X-ray crystallography, is the work of several years of study by Prof. Roderic Mackinonn (Rockfeller University). Normally potassium ions are surrounded by eight water molecules. In order to pass through the selectivity filter, each potassium ion has to shed these water molecules. The oxygen atoms of the filter region surround each potassium ion and perfectly replace the normal layer of water molecules. To compensate for the energetic cost of dehydration, the carbonyl oxygen atoms come into very close contact with the ion. K^+ ions are moved along the pore and once out of the filter, they are again surrounded by water molecules. Other ions have different radius size with respect to K^+, and cannot pass through the pore. For example, sodium ions are slightly

smaller and they fail the interaction with oxygen atoms present in the filter. Other ions do not fit in the filter precisely so that the energetic cost and gains are not well balanced. Since the K^+ filter mimics precisely the hydration sphere of K^+ ion, there is little cost for a K^+ ion to enter or exit the filter but a substantial cost for cations of different diameter.

The K^+ filter is usually marked by the consensus GYGD amino acid sequence, but a replacement D to E is found in many species of cyanobacteria, in some species of proteobacteria and in few species of other phyla. Another change is found in the thermophilic *Thermotoga maritima* where a glycine is mutated in a serine (GYS). Mutant analyses suggested that mutation of these residues cause loss of K^+ selectivity (Kuo *et al*., 2003).

3.4 The patch clamp technique

Various electrophysiological techniques can be used for the study of ion channels. I describe only the patch clamp technique given that it was used for my work. The patch clamp technique permits a real time analysis of the current flowing through a single ion channel located in cell or organelle membranes. This technique was introduced, for the first time, in 1976 by Erwin Neher and Bert Sakmann, who won the Nobel Prize in Physiology and Medicine in 1991. The patch clamp is based on Ohm equation that allows to measure current intensity in the presence of a difference of potential:

$$V=Re \cdot I$$

where I = current intensity, Re= system resistance (due to the membrane) and V= potential.

This technique uses glass pipettes (2-3 µm of diameter) containing a salt solution, resembling the internal milieu of the cells, where an electrode is present. The pipette acts as a fluid bridge between a cell and the transducing electrode. When a little suction is applied to the pipette there is the generation of a tight sealing (Giga Ohm sealing) of the membrane against the pipette. The measured current is captured by a differential amplificator that convert the current in tension and we can observe a value of potential difference that is proportional to recorded current.

Usually pipettes are pulled and fire-polished by Pipette Microforge to reduce the pipette capacitance by coating the tampered shank of the pipette up to a few micrometers. Frequently, the patch clamp setup comprises also a microscope to a resolution that offer the viewing of the access to the cell by a patch pipette.

Figure 19 illustrate the most used configurations for the patch clamp technique: cell-attached, whole cell, inside-out, outside-out and perforated patch. In the cell-attached patch the pipette is attached to a membrane and the operator applied a little suction. It allows single channel recording. From cell-attached configuration is possible obtain the whole cell configuration. In this configuration another little suction is applied and this causes the rupture of the patch of the membrane exposing the whole cell to the pipette solution. The inside-out and outside-out are excised patch techniques, because the patch is removed from the cell. Outside-out configuration is due to pulling the pipette from whole cell. Alternatively, inside out configuration results from pulling the pipette away from cell in the cell -attached mode.

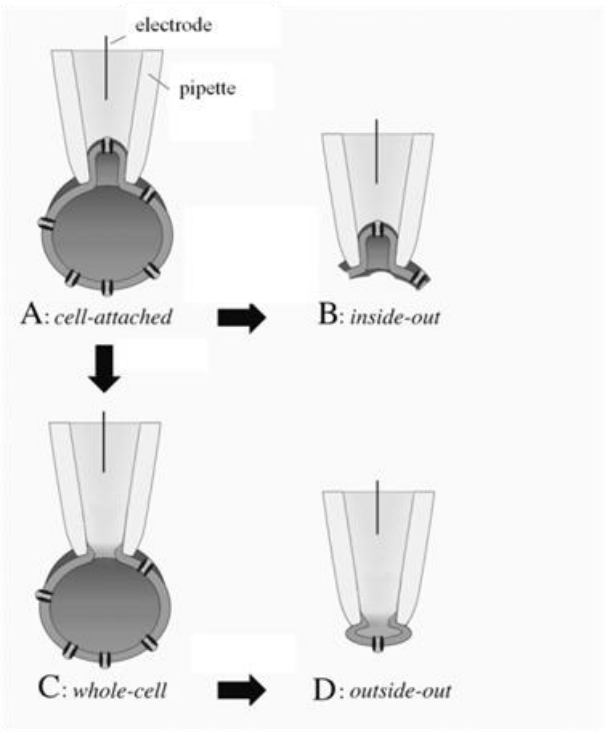

Figure 19: Patch clamp configuartions: a) cell-attached, b) inside-out configuration, c) whole-cell configuration and d) outside-out configuration.

REFERENCES

Alberts, B., Johnson, A., Lewis, J., Raff, M., Roberts, K., & Walter, P. Molecular biology of the cell. 2002. *New York: Garland Science,*

Albertsson P.A. (2001) A quantitative model of the domain structure of the photosynthetic membrane. Trends Plant Sci (6) 349–354

Allen JF, Forsberg J (2001) Molecular recognition in thylakoid structure and function. Trends Plant Sci 6: 317–326

Anagnostidis, K., & Komárek, J. (1988). Modern approach to the classification system of cyanophytes. 3-oscillatoriales. *Algological Studies, 50*, 327-472.

Andersson, B. and Anderson, J.M.(1980) Lateral heterogeneity in the distribution of chlorophyll-protein complexes of the thylakoid membranes of spinach chloroplasts. Biochim Biophys Acta (593), 427–440

Beale, S. I. (1999). Enzymes of chlorophyll biosynthesis. *Photosynthesis Research, 60*(1), 43-73.

Berry, S., Esper, B., Karandashova, I., Teuber, M., Elanskaya, I., Rögner, M., *et al*. (2003). Potassium uptake in the unicellular cyanobacterium synechocystis sp. strain PCC 6803 mainly depends on a ktr-like system encoded by slr1509 (ntpJ). *FEBS Letters, 548*(1-3), 53-58.

Campbell, N. A., Reece, J. B., & Simon, E. J. (2008). *L'essenziale di biologia* Pearson Paravia Bruno Mondad.

Choe, S. (2002). Potassium channel structures. *Nature Reviews Neuroscience, 3*(2), 115-121.

Clarkson, D. T., & Hanson, J. B. (1980). The mineral nutrition of higher plants. *Annual Review of Plant Physiology, 31*(1), 239-298.

Dilley, R. A., Nishiyama, Y., Gombos, Z., & Murata, N. (2001). Bioenergetic responses of synechocystis 6803 fatty acid desaturase mutants at low temperatures. *Journal of Bioenergetics and Biomembranes, 33*(2), 135-141.

Doyle, D. A., Cabral, J. M., Pfuetzner, R. A., Kuo, A., Gulbis, J. M., Cohen, S. L., *et al*. (1998). The structure of the potassium channel: Molecular basis of K conduction and selectivity. *Science, 280*(5360), 69.

Dyall, S. D., Brown, M. T., & Johnson, P. J. (2004). Ancient invasions: From endosymbionts to organelles. *Science, 304*(5668), 253.

Epstein, W. (2003). The roles and regulation of potassium in bacteria. *Progress in Nucleic Acid Research and Molecular Biology, 75*, 293-320.

Flores, E., & Herrero, A. (2004). Assimilatory nitrogen metabolism and its regulation. *The Molecular Biology of Cyanobacteria,* , 487-517.

Fuhs, G. W. (1973). Cytochemical examination of blue-green algae.

Gray, M. W. (1999). Evolution of organellar genomes. *Current Opinion in Genetics & Development, 9*(6), 678-687.

Havaux, M. (1998). Carotenoids as membrane stabilizers in chloroplasts. *Trends in Plant Science, 3*(4), 147-151.

Herrero, A., Flores, E., & Flores, F. G. (2008). *The cyanobacteria: Molecular biology, genomics, and evolution* Caister Academic Pr.

Hille, B. (2001). Ion channels of excitable membranes.

Hirschberg, J. (2001). Carotenoid biosynthesis in flowering plants. *Current Opinion in Plant Biology, 4*(3), 210-218.

Hoiczyk, E., & Hansel, A. (2000). Cyanobacterial cell walls: News from an unusual prokaryotic envelope. *Journal of Bacteriology, 182*(5), 1191-1199.

Huner, N., Öquist, G., & Sarhan, F. (1998). Energy balance and acclimation to light and cold. *Trends in Plant Science, 3*(6), 224-230.

Jarvis, P., & Soll, J. (2001). Toc, tic, and chloroplast protein import. *Biochimica Et Biophysica Acta (BBA)-Molecular Cell Research, 1541*(1-2), 64-79.

Jiang, Y., Lee, A., Chen, J., Cadene, M., Chait, B. T., & MacKinnon, R. (2002). The open pore conformation of potassium channels. *Nature, 417*(6888), 523-526.

Jiang, Y. X., Lee, A., Chen, J. Y., Ruta, V., Cadene, M., Chait, B. T., *et al*. (2003). X-ray structure of a voltage-dependent K+ channel. *Nature, 423*(6935), 33-41.

Kaneko, T., Sato, S., Kotani, H., Tanaka, A., Asamizu, E., Nakamura, Y., *et al*. (1996). Sequence analysis of the genome of the unicellular cyanobacterium synechocystis sp. strain PCC6803. II. sequence determination of the entire genome and assignment of potential protein-coding regions. *DNA Res, 3*(3), 109-36.

Keeling, P. (2004). A brief history of plastids and their hosts. *Protist, 155*(1), 3-8.

Kelly, A. A., & Dörmann, P. (2004). Green light for galactolipid trafficking. *Current Opinion in Plant Biology, 7*(3), 262-269.

Ketchum, K. A., Joiner, W. J., Sellers, A. J., Kaczmarek, L. K., & Goldstein, S. A. N. (1995). A new family of outwardly rectifying potassium channel proteins with two pore domains in tandem.

Kirk, J. T. O., Tilney-Bassett, R. A. E., Emerson, R., Kennedy, D., Park, R. B., Beadle, G. W., *et al*. (1967). *The plastids: Their chemistry, structure, growth and inheritance* WH Freeman London and SanFrancisco.

Kuo, M. M. C., Saimi, Y., & Kung, C. (2003). Gain-of-function mutations indicate that escherichia coli kch forms a functional K conduit in vivo. *The EMBO Journal, 22*(16), 4049-4058.

Kuo, M. M. C., Haynes, W. J., Loukin, S. H., Kung, C., & Saimi, Y. (2005). Prokaryotic K+ channels: From crystal structures to diversity. *FEMS Microbiology Reviews, 29*(5), 961-985.

Margulis, L. (1981). *Symbiosis in cell evolution: Life and its environment on the early earth* WH Freeman San Francisco.

Martin, W., Rujan, T., Richly, E., Hansen, A., Cornelsen, S., Lins, T., *et al*. (2002). Evolutionary analysis of arabidopsis, cyanobacterial, and chloroplast genomes reveals plastid phylogeny and thousands of cyanobacterial genes in the nucleus. *Proceedings of the National Academy of Sciences of the United States of America, 99*(19), 12246.

Matsuda, N., Kobayashi, H., Katoh, H., Ogawa, T., Futatsugi, L., Nakamura, T., *et al*. (2004). Na -dependent K uptake ktr system from the cyanobacterium synechocystis sp. PCC 6803 and its role in the early phases of cell adaptation to hyperosmotic shock. *Journal of Biological Chemistry, 279*(52), 54952.

Meeuse, B. J. D. (1962). Storage products. *Physiology and Biochemistry of Algae,* , 289-313.

Mereschkowsky, C. (1905). Über natur und ursprung der chromatophoren im pflanzenreiche. *Biol Centralbl, 25*, 593-604.

Mullineaux, C. W. (1994). Excitation energy transfer from phycobilisomes to photosystem I in a cyanobacterial mutant lacking photosystem II. *Biochimica Et Biophysica Acta (BBA)-Bioenergetics, 1184*(1), 71-77.

Plugge, B., Gazzarrini, S., Nelson, M., Cerana, R., Van Etten, J. L., Derst, C., *et al*. (2000). A potassium channel protein encoded by chlorella virus PBCV-1. *Science, 287*(5458), 1641.

Pupillo, P., Cervone, F., Cresti, M., & Rascio, N. (2003). *Biologia vegetale* Zanichelli.

Rakhimberdieva, M. G., Boichenko, V. A., Karapetyan, N. V., & Stadnichuk, I. N. (2001). Interaction of phycobilisomes with photosystem II dimers and photosystem I monomers and trimers in the cyanobacterium spirulina platensis†. *Biochemistry, 40*(51), 15780-15788.

Raven, P. H., Evert, R. F., Eichhorn, S. E., & Aliotta, G. (1984). *Biologia delle piante* Zanichelli Bologna.

Ris, H., & Singh, R. (1961). Electron microscope studies on blue-green algae. *The Journal of Biophysical and Biochemical Cytology, 9*(1), 63.

Ruta, V., Jiang, Y. X., Lee, A., Chen, J. Y., & MacKinnon, R. (2003). Functional analysis of an archaebacterial voltage-dependent K+ channel. *Nature, 422*(6928), 180-185.

Swartz K. J. (2004). Towards a structural view of gating in potassium channels. *Nature Reviews Neuroscience* (**5)**,905-916

Taglietti, V., & Casella, C. (1997). *Elementi di fisiologia e biofisica della cellula* La goliardica pavese.

Tempel, B. L., Papazian, D. M., Schwarz, T. L., Jan, Y. N., & Jan, L. Y. (1987). Sequence of a probable potassium channel component encoded at shaker locus ofDrosophila. *Science (Wash.DC), 237*, 770-775.

Tandeau de Marsac, N. T., Cohen-Bazire, G. (1977). Molecular composition of cyanobacterial phycobilisomes. Proc. NatL Acad. Sci. USA 74: 1635-39

Thor, J. J., Mullineaux, C. W., Matthijs, H. C. P., & Hellingwerf, K. J. (1998). Light harvesting and state transitions in cyanobacteria. *Botanica Acta, 111*, 430-443.

Timmis, J. N., Ayliffe, M. A., Huang, C. Y., & Martin, W. (2004). Endosymbiotic gene transfer: Organelle genomes forge eukaryotic chromosomes. *Nature Reviews Genetics, 5*(2), 123-135.

Tortora, G. J., Funke, B. R., & Case, C. L. (1986). *Microbiology: An introduction* Benjamin-Cummings Publishing Company.

Vallon, O., Bulte, L., Dainese, P., Olive, J., Bassi, R., Wollman, F.A. (1991) Lateral redistribution of cytochrome b6/f complexes along thylakoid membranes upon state transitions. Proc Natl Acad Sci USA, 88, 8262-8266

Van den Hoek, C., Mann, D. G., & Jahns, H. J. (1995). *Algae:(an introduction to phycology)*

Van Roon, H., van Breemen, J.F.L., de Weerd, F.L., Dekker, J.P., Boekema, E.J. (2000) Solubilization of green plant thylakoid membranes with n-dodecyl-α,D-maltoside. Implications for the structural organization of the Photosystem II, Photosystem I, ATP synthase and cytochrome b(6)f complexes, Photosynth. Res., 64, 155–166

Véry, A. A., & Sentenac, H. (2002). Cation channels in the arabidopsis plasma membrane. *Trends in Plant Science, 7*(4), 168-175.

Whitton, B., & Potts, M. (2002). Introduction to the cyanobacteria. *The Ecology of Cyanobacteria, ,* 1-11.

Xu, W., Tang, H., Wang, Y., & Chitnis, P. R. (2001). Proteins of the cyanobacterial photosystem I. *Biochimica Et Biophysica Acta (BBA)-Bioenergetics, 1507*(1-3), 32-40.

Young, A. J., Phillip, D., Ruban, A., Horton, P., & Frank, H. (1997). The xanthophyll cycle and carotenoid-mediated dissipation of excess excitation energy in photosynthesis. *Pure and Applied Chemistry, 69*(10), 2125-2130.

Zhou, X. L., Vaillant, B., Loukin, S. H., Kung, C., & Saimi, Y. (1995). YKC1 encodes the depolarization-activated K channel in the plasma membrane of yeast. *FEBS Letters, 373*(2), 170-176.

Zimmermann, S., & Sentenac, H. (1999). Plant ion channels: From molecular structures to physiological functions. *Current Opinion in Plant Biology, 2*(6), 477-482.

~ CHAPTER 1 ~

OPEN ACCESS Freely available online

PLoS one

A Novel Potassium Channel in Photosynthetic Cyanobacteria

Manuela Zanetti[1], Enrico Teardo[1], Nicoletta La Rocca[1], Lalu Zulkifli[2], Vanessa Checchetto[1], Toshiaki Shijuku[2], Yuki Sato[2], Giorgio Mario Giacometti[1], Noboyuki Uozumi[2], Elisabetta Bergantino[1]*, Ildikò Szabò[1]*

1 Department of Biology, University of Padova, Padova, Italy, **2** Department of Biomolecular Engineering, Graduate School of Engineering, Tohoku University, Sendai, Japan

Abstract

Elucidation of the structure-function relationship of a small number of prokaryotic ion channels characterized so far greatly contributed to our knowledge on basic mechanisms of ion conduction. We identified a new potassium channel (SynK) in the genome of the cyanobacterium *Synechocystis* sp. PCC6803, a photosynthetic model organism. SynK, when expressed in a K^+-uptake-system deficient *E.coli* strain, was able to recover growth of these organisms. The protein functions as a potassium selective ion channel when expressed in Chinese Hamster Ovary cells. The location of SynK in cyanobacteria in both thylakoid and plasmamembranes was revealed by immunogold electron microscopy and Western blotting of isolated membrane fractions. SynK seems to be conserved during evolution, giving rise to a TPK (two-pore K^+ channel) family member which is shown here to be located in the thylakoid membrane of *Arabidopsis*. Our work characterizes a novel cyanobacterial potassium channel and indicates the molecular nature of the first higher plant thylakoid cation channel, opening the way to functional studies.

Citation: Zanetti M, Teardo E, La Rocca N, Zulkifli L, Checchetto V, et al. (2010) A Novel Potassium Channel in Photosynthetic Cyanobacteria. PLoS ONE 5(4): e10118. doi:10.1371/journal.pone.0010118

Editor: Hany A. El-Shemy, Cairo University, Egypt

Received November 16, 2009; **Accepted** March 12, 2010; **Published** April 12, 2010

Copyright: © 2010 Zanetti et al. This is an open-access article distributed under the terms of the Creative Commons Attribution License, which permits unrestricted use, distribution, and reproduction in any medium, provided the original author and source are credited.

Funding: The European Molecular Biology Organization (Young Investigator Program grant to I.S.), the Italian Ministry for University and Research (MIUR) (to I.S.) and the University of Padova (to E.B. and I.S.) are acknowledged for financial support. This work was also supported by grant FISR from MIUR to G.M.G. This work was also supported by grants-in-aid for scientific research (17078005, 19380058 and 20-08103 to N.U.) from MEXT and JSPS. The funders had no role in study design, data collection and analysis, decision to publish, or preparation of the manuscript.

Competing Interests: The authors have declared that no competing interests exist.

* E-mail: elisabetta.bergantino@unipd.it (EB); ildi@civ.bio.unipd.it (IS)

Introduction

Cyanobacteria, the first organisms capable of performing oxygenic photosynthesis during evolution, still today give major contribution to the maintenance of the biosphere [1]. The unicellular photoheterotrophic transformable cyanobacterium *Synechocystis* sp. PCC6803, characterized by an intracellular thylakoid membrane, where both photosynthesis and respiration take place, is the first photosynthetic organism for which the complete genome sequence has been published [2].

In vitro or *in vivo* function is not known for any of the putative potassium channels identified in the genomes of over ten species of cyanobacteria [3,4]. The only cyanobacterial ion channels characterized up to now are the prokaryotic glutamate receptor GluR0 [5] and the ligand-gated channel GLIC [6]. In general, the physiological role of bacterial channels is still largely unknown, except for bacterial chloride channel ClC [7], mechanosensitive channels [8] and *H. pylori* HpKchA, a putative potassium channel [9]. Potassium is the major intracellular cation in bacteria [10]. However, membrane potential adjustment rather than K^+ uptake has been hypothesized to be the major function of K^+ channels in prokaryotes, although direct proof is still missing [3]. In *Synechocystis* a Ktr-like system encoded by *slr1509*, rather than a *bona fide* channel, seems to be the main responsible for potassium uptake [4,11].

In higher plant thylakoids several potassium-conducting cation channel activities have been described [12–15]. Furthermore, a putative potassium channel protein has been found in thylakoids of spinach [16]. Unfortunately, the molecular identity of the protein(s) responsible for these activities is unknown, as is the nature of the putative channel protein.

In the present study we characterized a novel cyanobacterial potassium channel. Furthermore, our work identifies its homolog in higher plants from molecular point of view and indicates its localization in the thylakoid membrane.

Results

Bioinformatic analysis of SynK putative potassium channel

We identified in the genome of *Synechocystis* sp. PCC 6803, a hypothetical protein of unknown function (*slr 0498*) by homology search using the highly conserved selectivity filter [17,18] amino acid sequence (T-X-G-[Y-F-L]-G-D) as a query sequence. SynK was predicted to harbour six membrane-spanning segments (S1–S6) and a pore region between helices S5 and S6 (Figure 1A). The aminoacid sequence of two other well-characterized prokaryotic 6 TM potassium channels, KvAP [19] and KvLm [20], is also shown for comparison. Although sequence homology between SynK, KvAP and KvLm is not high, some residues known to be

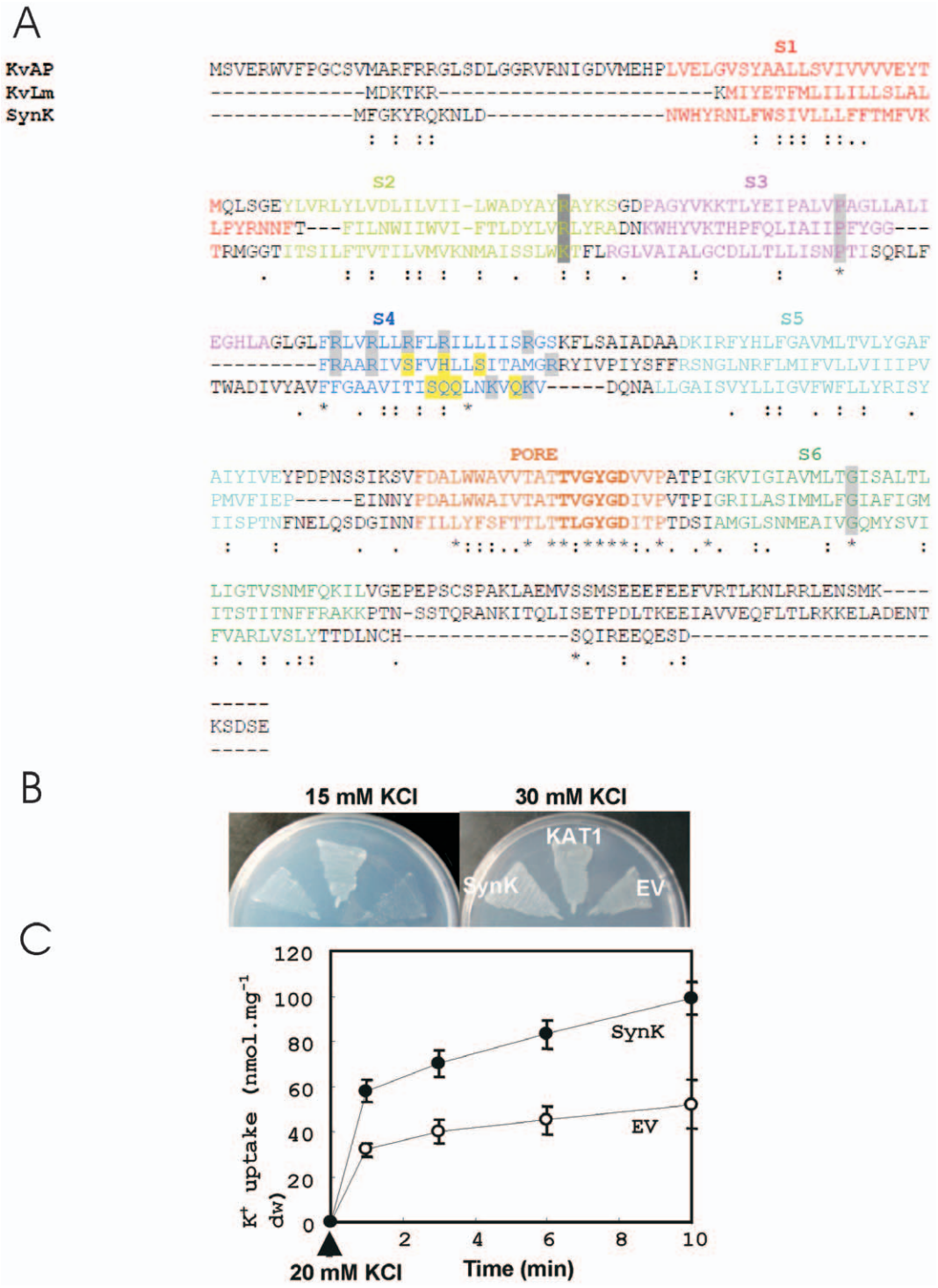

Figure 1. SynK protein permits potassium flux, as revelaed by its expression in K^+-uptake deficient *E. coli* strain LB2003. A) SynK (*Synechocystis sp*. PCC 6803; gi:16331771) is characterized by selectivity filter sequence (bold characters) in pore region (brown characters) and by six predicted transmembrane segments (S1–S6 represented by different colours). ClustalW (1.83) alignments of SynK sequence with KvAP from *Aeropyrum pernix* (gi:14601099) and KvLm from *Listeria monocytogenes* (gi:16411529), two depolarization-activated prokaryotic potassium channels, is shown. ''*'' - identical residues in all aligned sequences; '':''–conserved and ''.'' - semi-conserved substitutions. Definition of S1–S6 segments in latter proteins is shown according to [19] and [20], in different colours. In SynK S1–S6 segments were defined according to secondary structure predictions (Porter, SPLIT4, TMHMM2 algorithms) and adjusted taking into account delimitation of α-helices as inferred from crystal structure of KvAP (according to [20]). Conserved residues, functional in Kv gating, are shaded grey. Please note the presence of some of the highly conserved residues in the sensor sequence of Kv channels, such as K63 in S2 and P86 in S3 in SynK. Polar residues (S and Q) in S4 are shaded yellow. **B**) Complementation growth test of *E. coli* LB2003 cells by *SynK*. *E. coli* LB2003 was transformed with plasmid harbouring pPAB404-*SynK* or empty vector. KAT1, an *Arabidopsis* K channel, was also included as a positive control. Transformants were grown on media supplemented with different concentration of KCl. **C**) Potassium uptake by K^+-depleted *E.coli* containing *SynK* or empty vector. Net K^+ uptake by *SynK*-expressing *E. coli* LB2003 cells and control cells harbouring empty vector were measured at 20 mM KCl. Data are averages ±SD of results from four independent experiments.
doi:10.1371/journal.pone.0010118.g001

important for channel gating are also conserved in SynK (Figure 1A). Positive charges present in the S4 helix of KvAP determine voltage-dependent gating [19]. KvLm has only two positive charges in S4, but shows strong voltage-dependence [20]. SynK does not display evenly spaced positive charges in the predicted S4 segment, nor does it contain regulatory domains. On the basis of bioinformatic analysis, SynK may be classified as a "core-only", six-TM, putative potassium channel protein (see also ref.3). The closest homologues of SynK are found in other cyanobacteria species (Figure S1).

SynK forms functional, potassium-conducting protein, when expressed in a K^+-uptake-system deficient *E.coli* strain

An *E.coli* K^+ uptake–deficient mutant has been successfully used to study potassium transport activity of transporter systems from plants [21] as well as from *Synechocystis* [22]. Here we cloned the *Synechocystis SynK* gene into the *E. coli* strain LB2003, carrying mutations in genes encoding the three major K^+ uptake systems, Kdp, Trk, and Kup [23]. Thus, LB2003 does not grow at K^+ concentrations $\leq$10 mM, due to negligible K^+ uptake activity at potassium concentrations in the low millimolar range. Complementation test on solid media shows that *SynK*-expressing *E. coli* LB2003 cells grew well on a medium supplemented with 15 mM KCl, whereas *E. coli* cells harbouring empty vector did not (Figure 1B). Time course uptake experiment shows that K^+ influx by *SynK*-expressing cells was higher compared to that of cells containing empty vector (Figure 1C). Net potassium uptake measurements by K^+-depleted *E. coli* cells in the presence of 10 to 80 mM KCl revealed V_{max} values of 553 and 460 nmol min^{-1} g^{-1} dry weight for *SynK*-expressing cells and for the control cells, respectively (Figure S2). These data suggest that SynK may mediate K^+ uptake when expressed in *E. coli*.

Expression of SynK in CHO cells gives rise to potassium-conducting current

Additional functional characterization was performed in a mammalian cell system, given that SynK did not express in oocytes (Uozumi et al, unpublished). No electrophysiological studies have been performed on any cyanobacterial membrane until now. However, cloned prokaryotic channels have previously been shown to function in both heterologous expression systems e.g. [5,6,20,24] and in artificial lipid bilayers e.g. [19,25].

The sequence of SynK was isolated from the *Synechocystis* genome by PCR and a SynK-EGFP (enhanced green fluorescent protein at C-terminus) fusion protein was expressed in CHO (Chinese hamster ovary) cells. Mammalian HEK and CHO cells do not have significant endogenous potassium current, and are suitable for the expression of prokaryotic and even the viral channel Kcv e.g. [5,26]. Green fluorescence of SynK-GFP was clearly associated with the plasma membrane (PM) (Figure 2A and Figure S3). Immunoblotting with anti-GFP antibody as well as by a specific anti-SynK antibody (Figure S4) revealed the presence of a product with the expected molecular weight of the fusion protein (for SynK and SynK-EGFP fusion proteins predicted MWs are 26445 and 53979 Da, respectively) (Figure 2B). However, lower MW products, corresponding to either EGFP alone (28 kDa), to SynK alone (27 kDa) or to degradation products of the fusion protein, were also observed and may account for the fluorescent signal observable in the cytosol of some cells (Figure S3 and not shown). Western blot of separated membrane and soluble fractions from transfected cells showed the presence of the 54 kDa fusion protein exclusively in the former one indicating that the correctly translated product is inserted into the membrane (Figure 2C). The same protein was also recognized by another antibody which was developed against the common selectivity filter sequence of potassium channels (anti-KPORE, Figure S5 for details), confirming that anti-SynK recognizes a potassium channel protein.

Transfected CHO cells were identified by green fluorescence and analyzed by patch clamping in whole-cell configuration. SynK gave rise to an outwardly rectifying current (Figure 3A and B) (n = 32). Cells either left untransfected or transfected with control plasmids never displayed such a current (Figure 3C) (n = 40). The SynK current had an instantaneous and a slowly activating component (Figure 3A), the latter having an activation voltage of +67 mV as determined from the Boltzman fit of the G/G_{max} curve (Figure 3D). SynK activity was selective for cations as indicated by the fact that it was observed in the presence of potassium gluconate (Figure 3F, and not shown). Tail current analysis revealed a reversal potential (E_{rev}) of -21 ± 4 mV (n = 4) which is consistent with potassium selectivity (the predicted E_{rev} for a perfectly selective channel in our ionic conditions is -23 mV) (Figure 3E). Furthermore, SynK was blocked by 15 mM cesium (Figure 3F) and could not be observed with solutions containing tetraethylammonium chloride (n = 10, not shown), a general potassium channel blocker [17]. To further prove that the activity observed was due to SynK, we also transfected CHO cells with SynK bearing a single point mutation in the selectivity filter GYGD (in the mutant tyrosine 181 was changed to alanine). K^+ channels with GAGD sequence are known to be expressed, but are unable to conduct a current e.g. [27]. The mutant SynK was efficiently expressed and targeted to PM in CHO cells (Figure S3) but did not give rise to current (n = 6) (not shown). These data indicate that SynK does form a potassium selective channel.

SynK is located to both thylakoid and plasmamembrane in cyanobacteria

Determination of the subcellular localization of a protein is an important step toward understanding its function. To address this point, we obtained a polyclonal antibody against a recombinant protein expressed in *E.coli*, comprising the first 144 amino acids but not the pore region (Figure S4). The antibody recognized a band with the predicted molecular weight of 26 kDa (Figure 4A) with an efficiency comparable to that of the commercially available anti-ATP-ase antibody (Figure S6). Under certain solubilization conditions, known to permit visualization of SDS-resistant multimeric forms of prokaryotic potassium channels e.g. [28], bands with apparent molecular weights of 26, 52, 76 and 110 kDa were detected (Figure 4A). These values match the predicted masses for the monomeric (26445 Da) and multimeric forms of SynK, and point to a tetrameric organization. The use of anti-KPORE antibody further confirmed that anti-SynK recognized a potassium channel in cyanobacteria. To investigate the location of SynK protein, cytoplasmic and thylakoid membranes were isolated. Control blots performed with antibodies against marker proteins of the various fractions (Figure 4B) indicated that the cross-contamination in our preparation is low. At equal loaded protein quantity of plasmamembrane (PM), soluble (SOL), thylakoid (THYL) and outer membrane (OM) fractions, both anti-SynK and anti-KPORE antibodies recognized a 26 kDa band in the PM fraction as well as a 26 kDa band and a 24.5 kDa band in the thylakoid fraction (Figure 4C). These proteins are integral membrane proteins as they are resistant to alkaline extraction (not shown). Immunogold electron microscopy confirmed localization of the channel in the thylakoid and in the

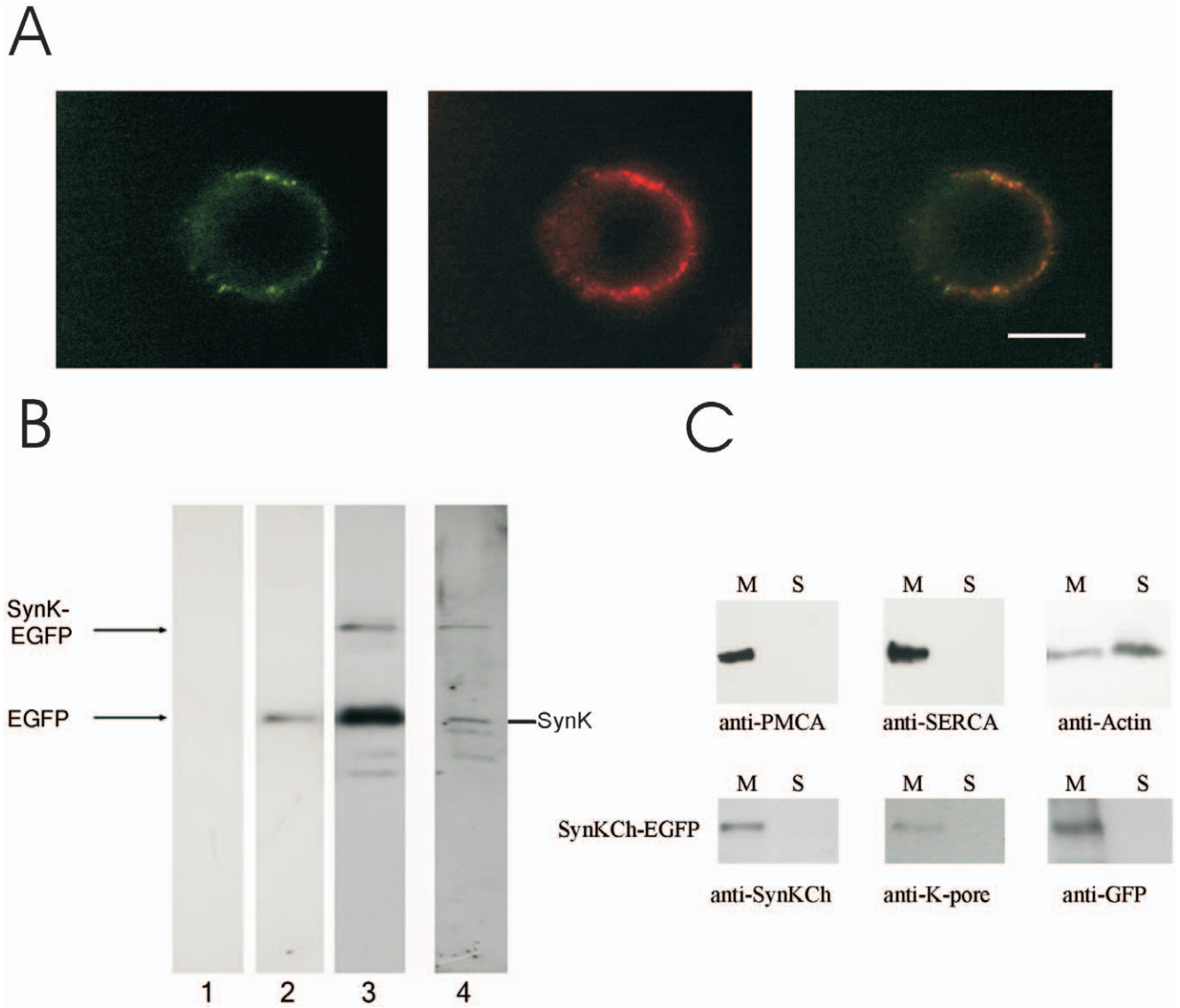

Figure 2. Expression of SynK in Chinese Hamster Ovary cells. A) SynK-EGFP fusion protein expression in CHO cell plasma membrane, revealed by fluorescence microscopy. Fusion protein (left image) and PM-specific Vybrant DiI dye (central image) co-located as indicated by overlapping image (right). Representative images are shown. Bars: 10 μm. Unequal distribution of Vybrant DiI may be due to preferential concentration of dye in rafts or to rapid vesicular uptake. **B**) SynK-EGFP is expressed with predicted molecular weight in CHO cells. Untransfected cells (lane 1) and CHO cells transfected with pEGFP-N1 (lane 2) or pSynK-EGFP (lanes 3, 4) were lysed 72 h after transfection, and 50 μg (lanes 1, 2, 4) or 100 μg (lanes 3) total proteins were loaded. Membranes were developed with anti-GFP (lanes 1–3) or anti-SynK (lane 4) primary antibodies. Arrows: positions of EGFP (28 kDa), SynK (27 kDa) and SynK-EGFP (54 kDa) proteins. **C**) SynK fusion protein is revealed in membraneous fraction. The purity of soluble and membrane fractions obtained from transfected CHO cells was checked by antibodies against marker proteins of the plasmamembrane (PMCA) (140 kDa), endoplasmatic reticulum (SERCA) (110 kDa) and cytosol (actin) (42 kDa) (upper panels). Actin is found also in the membraneous fraction because it is in part associated to organelles and cytoskeletron. SynK-EGFP fusion protein is present in the membraneous fraction (lower panels). Equal volumes of pellet and supernatant fractions, obtained as described in the Material and Method section, were loaded on SDS-PAGE (25 μl for samples developed with anti-SynK and anti-KPORE and 15 μl for those developed with anti-GFP antibody).
doi:10.1371/journal.pone.0010118.g002

plasmamembrane (Figure 4D). As a positive control we used a specific antibody against CP43 protein of Photosystem II (Figure 4E), known to be located exclusively in the thylakoid membrane [29] and as negative control we used gold-coupled secondary IgG (Figure S7). Please note that the position of the anti-CP43-coupled gold particles with respect to the thylakoid membrane (white membraneous structure) is comparable to that obtained with anti-SynK antibody.

A homolog of SynK is present in the thylakoid membrane of *Arabidopsis*

The closest homolog of SynK in *Arabidopsis* is TPK3 (Score: 41,2; expect value: 3e-08, 36% identity, 51% positivities; Figure S8), which has a consensus prediction for localization in chloroplasts (http://aramemnon.botanik.uni-koeln.de/). TPK5 also shows some sequence similarity to SynK, and has a very strong predicted targeting for chloroplast according to several

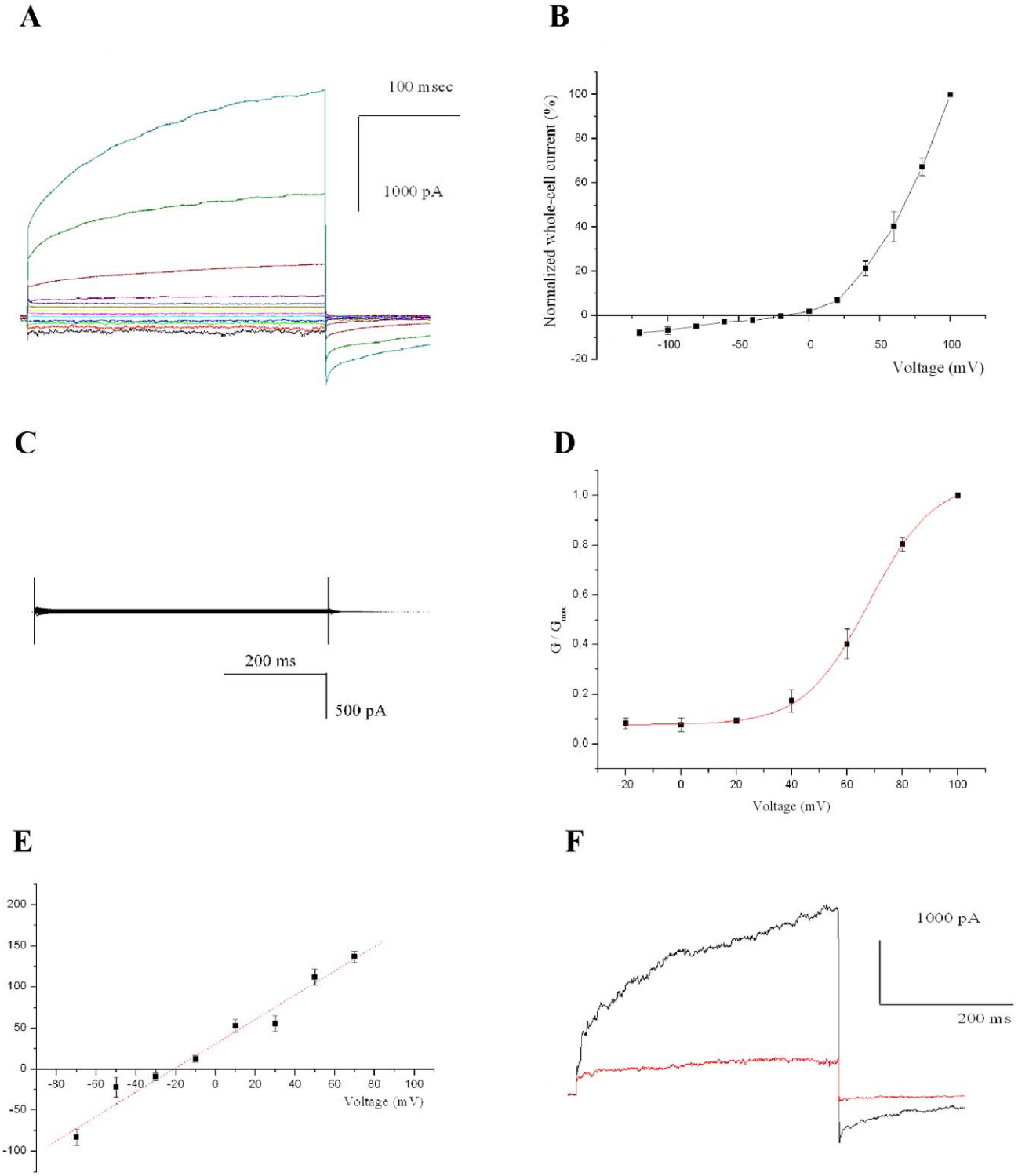

Figure 3. SynK functions as a potassium channel in CHO cells. A) Representative whole-cell currents in a pSynK-EGFP-transfected fluorescent cell, elicited by application of voltage steps of 300 ms duration, from −140 to + 100 mV in 20-mV steps, from a holding potential of −50 mV. Pulses were applied every 45 seconds, allowing complete deactivation of the channel. Different colours refer to different applied voltages. **B**) Current-voltage relationship. Peak currents normalized to current measured at +100 mV (n = 6, SEM values are reported). **C**) as in A), but from a control, pEGFP-N1-transfected cell. **D**) Boltzman fit of G/G_{max} (n = 6). **E**) Determination of selectivity from tail currents, elicited by stepping voltage for 400 ms to +60 mV, followed by application of −100 to + 100 mV in 20-mV voltage steps for 400 ms. Tail currents are reported as function of voltage. Reversal potential is −21±4 mV (n = 4). In A) to E) bath and pipette solutions contained 150 mM NaCl, 70 mM KCl and 134 mM KCl, respectively. **F**) Current recorded in K^+-gluconate solution at +100 mV, before (black) and after (red) addition of 15 mM Cs^+ to bath. Results are representative of 4 experiments.

doi:10.1371/journal.pone.0010118.g003

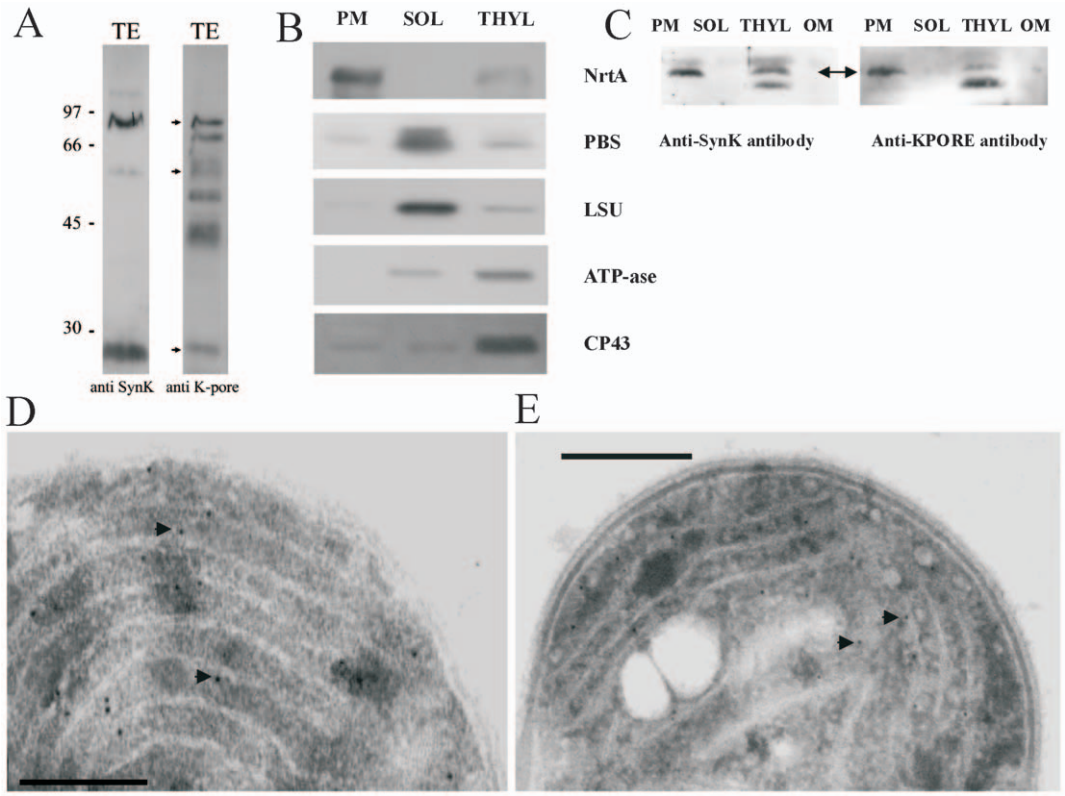

Figure 4. Localization of SynK in *Synechocystis*. A) Whole-cell cyanobacterial lysates containing 0.1 μg chlorophyll/lane were loaded on SDS-PAGE without urea and blotted with anti-SynK (1:2500 dilution) (lane 1) and anti-KPORE (1:10000) (lane 2) polyclonal antibodies. Apparent MWs of monomer, SDS-resistant dimer trimer and tetramer forms correspond to 26, 52, 76 and ca. 110 kDa. The anti-KPORE antibody, as expected, given the predicted presence of various potassium channels in this organism, recognized other proteins as well (lane 2). **B**) Plasmamembrane (PM), soluble (SOL) and thylakoid membrane (THYL) fractions were isolated from *Synechocystis*. The resulting fractions were checked for purity by using antibodies against markers of the plasmamembrane (NrtA), of the soluble fraction (PBS: allophycocyanin; LSU: large subunit of Rubisco) and of Thylakoid (ATP-ase and CP43). Cross-contamination to small extenct can be observed. 20 μg of proteins/lane. **C**) The obtained fractions were assayed for SynK content by using anti-SynK (left panel) and anti-KPORE (right panel) antibodies. 20 μg of proteins loaded/lane. The apparent MWs of the observed bands are 26 kDa (arrow) in the PM fraction and 26 and 24.5 kDa in the THYL fraction. **D**) Anti-SynK antibody used for immunogold electron microscopy confirms location of SynK protein in thylakoids (white membraneous structures). Arrows emphasize some of the gold particles. Bar: 200 nm. **E**) As control, anti-CP43 was used. Bar: 500 nm.
doi:10.1371/journal.pone.0010118.g004

algorithms. Although electrophysiological and biochemical evidence suggest the presence of potassium-conducting channel(s) in higher plant thylakoid membrane, the molecular nature of this(ese) protein(s) is unknown. Given that the SynK antibody was developed against the first 144 amino acids of the protein, i.e. a region comprising stretches of amino acid sequences which are conserved also in TPK5 and TPK3, we predicted that *a priori*, the anti-SynK antibody might recognize both proteins in *Arabidopsis* thylakoids, if these proteins were located in that membrane system. Anti-SynK antibody revealed a protein with an apparent MW of 54 kDa in thylakoids isolated from *Arabidopsis* (Figure 5A). Membrane proteins often display a migration resulting in different MW from that predicted. Since an MW of 54 kDa is somewhat higher than that predicted for TPK5 and TPK3 (46,3 and 48,7 kDa, respectively), we developed a monoclonal antibody (3A8) against a region conserved in *Arabidopsis* TPK3/5 but not in other members of the TPK family. 3A8 gave visible reaction already with 100 ng of the immunogenic peptide in dot blot (not shown). The 54 kDa band was recognized by both anti-SynK and 3A8 (Figure 5A) and also by other two monoclonal antibodies developed against the same peptide and by anti-KPORE (not shown). The specificity of the recognition by 3A8 is indicated by the significant decrease of the intensity of the band when the antibody was pre-incubated with its immunogenic peptide prior to blot development (Figure 5B). The identified protein is an integral membrane protein (Figure S9). Furthermore, the 54 kDa protein, pulled down by anti-SynK antibody from *Arabidopsis* thylakoid, was recognized by the monoclonal anti-TPK3/5 antibody (Figure 5C). To further prove the nature of the 54 kDa band, we performed Western blots on thylakoids isolated from TPK5-knock-out *Arabidopsis* mutant (Figure 5D). The intensity of the 54 kDa band was not significantly altered in the thylakoid membrane isolated from the knock-out plant with respect to that observed in WT thylakoids. Given that in the TPK5-knock-out plants transcripts of TPK5 were absent (not shown), the 54 kDa band in the mutant plant was attributed to TPK3. Therefore we checked for the presence of this band in plants with a t-DNA insertion in the TPK3-encoding gene. t-DNA insertion mutants are only available in the UTR or in the promoter regions for TPK3. UTR (untranslated regions) may affect efficiency of translation and the lifetime of transcripts. The transcript level of TPK3 was slightly reduced in the UTR-insertion mutant with respect to that found in wild-type (not shown). In thylakoids isolated from these plants there was a decrease of the intensity of the 54 kDa band, but complete disappearance could not be observed, being compatible with the presence of a reduced amount of TPK3. Given that most

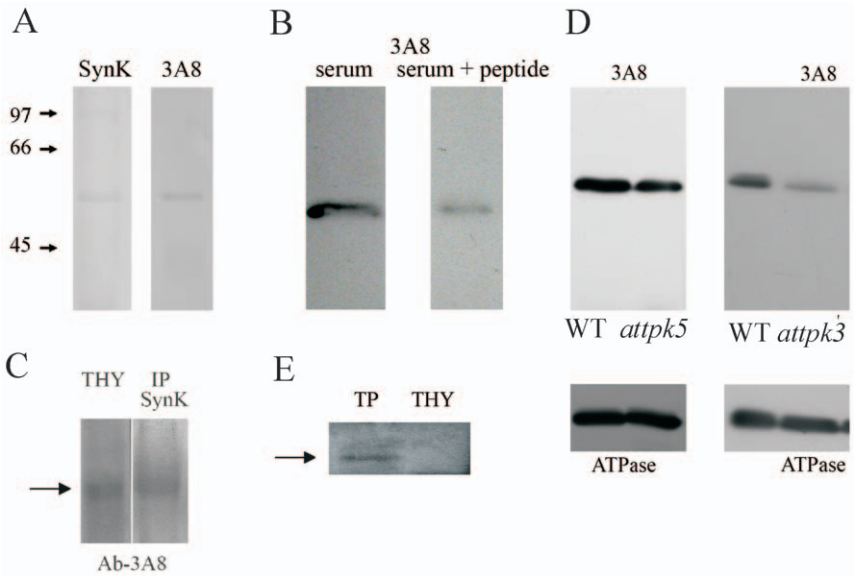

Figure 5. SynK homolog TPK3 is located in the thylakoid membrane of *Arabidopsis*. **A**) SynK and the monoclonal antibody 3A8 against TPK3/5 recognize the same, 54 kDa band in *Arabidopsis* wild-type thylakoids (proteins corresponding to 30 μg chorophyll were loaded). **B**) Intensity of the 54 kDa band decreased when the antibody was preincubated with 300 μM immunogenic peptide. The two lanes (30 μg Chl/lane) are from the same blot and were processed together. **C**) Thylakoids isolated from WT *Arabidopsis* plants were immunoprecipitated with anti-SynK antibody and blotted with 3A8 monoclonal antibody. **D**) Thylakoids (30 μg Chl/lane) isolated from wild type and TPK5-knock-out (left panel) and TPK3-knock-down (right panel) plants were loaded and assayed with the monoclonal antibody. The same membranes were stripped and reblotted with anti-ATP-ase to check for equal loading. **E**) Tonoplast and thylakoid fractions (20 μg of total protein of each) were loaded and developed with anti-TIP1.1 antibody (TIP1.1 is indicated by arrow at 28 kDa). In A, C and E nitrocellulose membranes and the BCIP/NBT (Sigma) development system, while in B and D PVDF membrane and ECL system was used.
doi:10.1371/journal.pone.0010118.g005

TPK channels, including TPK1, have been proposed to be located in the membrane around the vacuole, i.e. in tonoplast in plant cells [30], we checked for contamination of our thylakoid preparation by tonoplast. In Figure 5E the anti-TIP1.1 antibody raised against an aquaporin located to tonoplast [31], recognized a 28 kDa band in isolated tonoplasts, but not in thylakoids. As a further control, the localization of TPK1 in *Arabidopsis* cells was assayed by using a specific anti-TPK1 monoclonal antibody. Western blot analysis of vacuolar and thylakoid fractions revealed the presence of a 51 kDa band only in vacuoles isolated from WT but not in those obtained from TPK1 knock-out plants, confirming tonoplast location of TPK1 and indicating that TPK proteins might migrate with a higher than predicted MW (Figure S10).

Discussion

In the present work we report cloning and functional characterization of a novel potassium channel of cyanobacteria. The SynK protein, identified as putative potassium channel by bioinformatics, was shown to mediate potassium transport when expressed in *E.coli* LB2003 and gave rise to potassium-selective current when studied in Chinese Hamster Ovary cells. Specific anti-SynK antibody localized the channel protein both in thylakoid and in plasmamembrane in *Synechocystis* cyanobacteria. SynK is thus the first potassium channel identified in the thylakoid membrane from molecular point of view. Furthermore, SynK seems to be the ancestor of a TPK family member in *Arabidopsis*, which we show to be located in thylakoids of higher plants.

SynK is shown here to function as potassium-conducting channel when expressed in heterologous systems (Figures 1–3), although structural determinants of voltage sensitivity in SynK and factors determining the instantaneous component remain to be clarified. Data of Figure 4 indicate SynK to be located in both plasma and thylakoid membranes in *Synechocystis*. Recently, we have identified another ion-conducting pathway, a sodium/proton antiporter, in the thylakoid membrane of the same organism [32]. Dual localization of several proteins and ion channels have been described in eukaryotic systems e.g. [33–35]. The targeting mechanisms are not well known in cyanobacteria, but according to one model, proteins may be initially targeted to either membrane and sorted afterwards, possibly by vesicle transport [29]. Recently, the Tat protein transport system was described to function in both membrane systems [36]. In the thylakoid membrane fraction the anti-SynK antibody detected two bands, one with a slightly lower MW than that predicted (Figure 4C). Whether this lower MW band corresponds to a mature form of the thylakoid-targeted protein or to a partially degraded protein remains to be determined.

Chloroplasts are descendents of an ancestral endosymbiont of cyanobacterial origin e.g. [37,38]. Nuclear genes coding for chloroplast proteins involved in photosynthesis and organelle biogenesis have been identified. A recent work identified other nuclear-encoded chloroplast proteins of endosymbiont origin by using functional orthogenomics [35]. Our data suggest that SynK may be an ancestor of TPK3 which is a member of the two-pore potassium channel family in *Arabidopsis* [39]. When BLAST analysis is performed, TPK3 is the closest homolog of SynK in the whole *Arabidopsis* genome and *vice versa*, according to Aramemnon. The evolutionary origin of eukaryotic tandem-pore channels is still elusive but according to one hypothesis, 6TM prokaryotic PNBD-less potassium channels (like SynK) might have given origin to TPK channels [40]. A conserved pore region feature (presence of YF residues) in both SynK and plant TPK

channels further point to an evolutionary link between the two proteins (Figure S11).

Our findings indicate the presence of TPK3 protein in the thylakoid membrane (Figure 5). Independently of whether SynK is the precursor of TPK3 or not, this is the first thylakoid-located cation channel identified from molecular point of view in higher plants (in addition to proton-conducting F_0/F_1 ATP-ase). Given that the electrophysiological activity of TPK3 has not been described up to now, it is difficult to predict which of the previously described electrophysiological activities [12–15] can be assigned to TPK3 protein. In any case, the thylakoid localization of this protein opens the way to functional characterization of this still putative channel. Despite a consensus prediction for chloroplast localization of TPK1, TPK2 TPK5 and TPK3 (see Aramemnon site), these proteins have previously been shown to be targeted to the vacuolar membrane of protoplasts from *Arabidopsis* cultured cells that transiently expressed AtTPK in fusion with GFP or YFP under the control of the cauliflower mosaic virus (CaMV) 35S promoter [30]. Interestingly, AtTPK3 fusion protein accumulated also in additional, non-identified internal membranes when using this system (Figure 2b of ref. 30). We would like to point out that we detect AtTPK3, shown to exhibit high transcript level [30], in thylakoids obtained from genetically non-manipulated *Arabidopsis* plants, by using a specific monoclonal antibody. Thus, observation of the protein in thylakoids due to possible overexpression-induced mistargeting can be excluded. Our results do not exclude localization of TPK3 in other membranes as well, nor they exclude the presence of other channels as well in thylakoids. SynK and TPK3 might be involved counterbalancing cation fluxes from the lumen towards the stroma during photosynthesis, which would permit dissipation of the transmembrane potential but not that of the pH gradient [12,15,41]. Presuming the same orientation of SynK in the CHO plasma membrane and in thylakoids, at positive voltages of the thylakoid (proposed to reach +70 mV on the lumenal side during proton flux into the lumen [42]) SynK could permit the quick exit of potassium from the lumen. Direct genetic proof in favour of the "counterbalance" hypothesis is still missing, due also to the fact that cation channels have not been identified from a molecular point of view neither in cyanobacterial thylakoid nor in that of higher plants.

In summary, we report the molecular identification of two thylakoid-located potassium channels, SynK in cyanobacteria and TPK3 in *Arabidopsis*. SynK represents the first cyanobacterial core-only type potassium channel, and seems to be the anchestor of TPK3 of the two-pore potassium channel family. Our results open the way for understanding the physiological roles of these thylakoid channels and for determining their role, if any, in the regulation of photosynthesis.

Materials and Methods

Strains and growth conditions are described in supplementary Text S1. Expression of SynK in *E.coli* and measurement of K^+ uptake was performed according to [21] and [43]. Expression of SynK in CHO cells was performed according to [44]. DNA constructs and transformation of *Synechocystis* sp. PCC 6803 as well as plant growth, genotyping and transcript analysis of *Arabidopsis* are detailed in the suplementary material. Thylakoids from plants were isolated as described [45]. Membrane fractionations of CHO cells, cyanobacteria and *Arabidopsis* were performed according to [46], [47] and [48], respectively. Immunoprecipitation, electron microscopy and immunogold labelling were performed according to [49] and [50], respectively. Patch clamp analysis is according to [34,44] and is detailed in supplementary Text S1.

Supporting Information

Text S1
Found at: doi:10.1371/journal.pone.0010118.s001 (0.04 MB DOC)

Figure S1 Closest homologues of SynK are found in cyanobacteria. A) The closest homologues of SynK (Syn, *Synechocystis* sp. PCC 6803; gi:16331771) are found in other cyanobacteria species. Sequence alignment (ClustalW (1.83) algorithm) of SynK, of a hypothetical protein (Lyng, *Lyngbya* sp. PCC 8106; gi:119457762) and K^+ channel pore region (Croco, *Crocosphaera watsonii* WH 8501; gi:46119130). "*" - identical residues in all aligned sequences; ":" - conserved and "." - semi-conserved substitutions. BLAST analysis revealed E values (number of hits expected to be found by chance) of 2×10–24 and 4×10–19 and positivity over length of aligned sequence of 55% (223 amino acids) and 56% (207) when compared SynK with *Lyngbya* and *Crocosphaera watsonii* proteins, respectively. Typical selectivity filter for potassium is in green. Glycine in S6, important for gating is in yellow.
Found at: doi:10.1371/journal.pone.0010118.s002 (0.02 MB DOC)

Figure S2 Potassium uptake by K^+-depleted *E.coli* containing SynK or empty vector. Net potassium uptake measurements by K^+-depleted *E. coli* cells in the presence of 10 to 80 mM KCl revealed Vmax values of 553 and 460 nmol min^{-1} g^{-1} dry weight for SynK-expressing cells and for the control cells, respectively Lineweaver-Burk plot of K^+ uptake data obtained from four independent experiments is shown.
Found at: doi:10.1371/journal.pone.0010118.s003 (0.02 MB PDF)

Figure S3 Expression of SynK and SynK mutant in Chinese Hamster Ovary cells. SynK-EGFP WT and mutant (non-conducting mutant with GAGD instead of GYGD in the pore region) fusion protein expression in CHO cell plasma membrane was revealed by confocal microscopy. Images with GFP fusion proteins (left images) and FM4-64 dye (central images) and merged signals (right images) are shown for WT SynK-GFP (upper panels) and mutant SynK-GFP (lower panels). Graphics shown beside the merged images represent profile plots of GFP (green) and FM4-64 (red) fluorescence intensity as a function of the distance for a particular region of interest (ROI), from inside the cell (in) to outside (out). Peaks falling in the same region correspond to co-localization.
Found at: doi:10.1371/journal.pone.0010118.s004 (0.48 MB PDF)

Figure S4 Anti-SynK antibody recognizes recombinant and native SynK. Recombinant protein (144 N-terminal amino acids of SynK fused with a 6 His-tag at C-terminus) was expressed in *E. coli* and purified as described in Materials and Methods. Protein was purified as a 30-kDa dimer (see lane 2). 30-kDa protein, recognized by anti-His antibody (not shown), was used for antibody production. Pre-immune antiserum did not recognize either purified 30 kDa protein (lane 3) or proteins in cyanobacteria whole-cell lysate (lane 4); serum from immunized rabbit clearly reacted with the recombinant protein (lane 5) and recognized SynK of 26 kDa in whole-cell lysate (in cells containing 0.1 μg chlorophyll) even at 1:5000 dilution (lane 6).
Found at: doi:10.1371/journal.pone.0010118.s005 (0.16 MB DOC)

Figure S5 Anti-KPORE antibody recognizes other potassium channels. Anti-KPORE antibody was used at 1:10000 dilution on whole-cell lysate of Jurkat lymphocytes, known to express Kv1.3

channel with apparent MW of 65 kDa (Magic Marks loaded on lane 1). Same bands were recognized by anti-KPORE (lane 2) and by a specific antibody against Kv1.3 (1:200) (lane 3) in SDS-PAGE with 6 M urea. 50 μg total proteins were loaded. Anti-KPORE antibody also recognized purified GST-Kv1.3 protein (lane 4, 10 μg loaded, predicted MW 87 kDa) (production of GST-Kv1.3 is described in Gulbins et al, Biochim. Biophys. Acta, in press). Anti-KPORE antibody also recognized KCa3.1 in HCT116 colon cancer cell line (not shown), and monomeric as well as multimeric forms of the purified Kcv viral potassium channel (not shown) and of purified KvAP (kindly provided by P.Facci, not shown).
Found at: doi:10.1371/journal.pone.0010118.s006 (0.07 MB DOC)

Figure S6 Anti-SynK antibody efficiently recognizes SynK in whole-cell lysate of cyanobacteria. Cells corresponding to the O.D. (at 730 nm) shown on the figure were solubilized in SB and loaded on SDS-PAGE. The blot was first developed with anti-SynK antibody and after re-stripping with anti-ATP-ase antibody (Agrisera). Efficiency of anti-Synk and anti-ATP-ase antibodies is comparable.
Found at: doi:10.1371/journal.pone.0010118.s007 (3.76 MB PDF)

Figure S7 Secondary antibody does not label cyanobacteria in immunogold electron microscopy. As control, only secondary IgG was used. Bar: 500 nm.
Found at: doi:10.1371/journal.pone.0010118.s008 (0.05 MB PDF)

Figure S8 Sequence homology between cyanobacterial SynK and *Arabidopsis* TPK3 (At4g18160). Aminoacid sequence alignments obtained by T-COFFEE algorithm. "*" - identical residues in all aligned sequences; ":" - conserved, "." - semi-conserved substitutions.
Found at: doi:10.1371/journal.pone.0010118.s009 (0.21 MB PDF)

Figure S9 The 54 kDa protein is an integral membrane protein. Thylakoids (100 mg total proteins) were subjected to alkaline extraction (0.2 M Na2CO3 for 30 minutes), pelleted and both pellet and supernatants were loaded. The 54 kDa band is not present in the supernatant fraction indicating that it is an integral membrane protein. Blots were developed with the indicated antibodies.
Found at: doi:10.1371/journal.pone.0010118.s010 (0.10 MB PDF)

Figure S10 TPK1 locates to tonoplast in *Arabidopsis*. A specific monclonal antibody was used to reveal location of TPK1 in WT and atkco1 plants. Cells were fractionated and loaded on continuous sucrose gradient. Fractions positive for tonoplast TIP1 (VAC) or for thylakoid membrane D2 (THYL) were loaded. TPK1 is visible only in the vacuolar fraction of WT cells (at 50 kDa). An aspecific recognition is seen at approx. 35 kDa in thylakoids in both WT and mutant organisms.
Found at: doi:10.1371/journal.pone.0010118.s011 (0.06 MB PDF)

Figure S11 Pore region and YF residues are highly conserved between SynK and TPK channels of *Arabidopsis*. Voltage-gated Kv and KCNQ channels are characterized by a conserved pore region feature, namely, the presence of two tryptophans in tandem (W67 and W68 in KcsA) (Minor DL (2001) Potassium channels: life in the post-structural world. Current Opinion in Structural Biology, 11: 408–414). In plant shaker-like inward rectifier channels, the second tryptophan is highly conserved and the first is replaced by a tyrosine. These same positions are strongly conserved within other families of potassium channels, however, as different residues. Animal Kir channels harbour LF or SF residues in the same position (Minor 2001). Instead, in animal two-pore channels, in viral Kcv as well as in all plant two-pore channels the same positions are occupied by tyrosine and phenylalanine (YF). SynK has the same YF aminoacids in the corresponding position, further suggesting that SynK might have given origin to two-pore channels during evolution. Interestingly, GORK and SKOR outwardly rectifying voltage-dependent channels, also harbour YF residues in the corresponding position but, in contrast to TPK3, do not show significant homology with SynK. Aminoacid sequence alignments obtained by T-COFFEE algorithm. "*" - identical residues in all aligned sequences; ":" - conserved, "." - semi-conserved substitutions. YF residues, typical of Kcv, animal and plant two-pore potassium channels are indicated. At4g01840: TPK5; Atg1g02510: TPK4; At4g18160: TPK3; At5g46370: TPK2; At5g55630: TPK1.
Found at: doi:10.1371/journal.pone.0010118.s012 (0.03 MB PDF)

Acknowledgments

The authors are grateful to Drs. M. Zoratti, A. Moroni, F. Tombola, A. Accardi and F. Rigoni for useful discussions. They thank very much Drs. A. Costa and E. Formentin for the confocal microscopy analysis. They thank G. Zambolin for help with construction of the patch clamp set-up and G. Walton for revision of the English text.

Author Contributions

Conceived and designed the experiments: MZ ET GMG IS. Performed the experiments: MZ ET NLR LZ VC TS YS IS. Analyzed the data: MZ ET NLR LZ VC TS YS GMG NU EB IS. Wrote the paper: NU EB IS.

References

1. Herrero A, Flores E (2008) The cyanobacteria: molecular biology, genetics and evolution. Caister Academic Press.
2. Kaneko T, Sato S, Kotani H, Tanaka A, Asamizu E, et al. (1996) Sequence analysis of the genome of the unicellular cyanobacterium *Synechocystis sp.* strain PCC6803. II. Sequence determination of the entire genome and assignment of potential protein-coding regions. DNA Res 3: 109–136.
3. Kuo M-M-C, Haynes W-J, Loukin S-H, Kung C, Saimi Y (2005) Prokaryotic K^+ channels: from crystal structures to diversity. FEMS Microbiology Reviews 29: 961–985.
4. Matsuda N, Uozumi N (2006) Ktr-mediated potassium transport, a major pathway for potassium uptake, is coupled to a proton gradient across the membrane in *Synechocystis sp. PCC 6803*. Biosci Biotechnol Biochem 70: 273–275.
5. Chen G-Q, Ciu C, Mayer M-L, Gouaux E (1999) Functional characterization of a potassium-selective prokaryotic glutamate receptor. Nature 402: 817–821.
6. Bocquet N, Prado de Carvalho L, Cartaud J, Neyton J, Le Poupon C, et al. (2007) A prokaryotic proton-gated ion channel from the nicotinic acetylcholine receptor family. Nature 445: 116–119.
7. Iyer R, Iverson T-M, Accardi A, Miller C (2002) A biological role for prokaryotic ClC chloride channels. Nature 419: 715–718.
8. Martinac B (2004) Mechanosensitive ion channels: molecules of mechanotransduction. Journal of Cell Science 117: 2449–2460.
9. Stingl K, Brandt S, Uhlemann EM, Schmid R, Altendorf K, et al. (2007) Channel-mediated potassium uptake in *Helicobacter pylori* is essential for gastric colonization. EMBO J 26: 232–241.
10. Epstein W (2003) The roles and regulation of potassium in bacteria. Prog Nucleic Acid Res Mol Biol 75: 293–320.
11. Berry S, Esper B, Karandashova I, Teuber M, Elanskaya I, et al. (2003) Potassium uptake in the unicellular cyanobacterium *Synechocystis sp.* Strain PCC6803 mainly depends on a Ktr-like system encoded by slr1509 (ntpJ). FEBS Lett 548: 53–58.
12. Tester M, Blatt MR (1989) Direct measurement of K^+ channels in thylakoid membranes by incorporation of vesicles into planar lipid bilayers. Plant Physiol 91: 249–252.
13. Enz C, Steinkamp T, Wagner R (1993) Ion channels in the thylakoid membrane (a patch clamp study). Biochim Biophys Acta 1143: 67–76.
14. Pottosin II, Schonknecht G (1996) Ion channel permeable for divalent and monovalent cations in native spinach thylakoid membranes. J Membr Biol 152: 223–233.

15. Hinnah SC, Wagner R (1998) Thylakoid membranes contain a high-conductance channel. Eur J Biochem 253: 606–613.
16. Fang Z, Mi F, Berkowitz G (1995) Molecular and physiological analysis of a thylakoid K^+ channel protein. Plant Physiol 108: 1725–1734.
17. Hille B (2003) Chapter 5. In Ion channels of excitable membranes Sinauer Ed. Sundreland, USA, Third edition.
18. Jan L-Y, Jan Y-N (1997) Cloned potassium channels from eukaryotes and prokaryotes. Annu Rev Neurosci 20: 91–123.
19. Ruta V, Jiang Y, Lee A, Chen J, MacKinnon R (2003) Functional analysis of an archaebacterial voltage-dependent K^+ channel. Nature 422: 180–184.
20. Santos J-S, Lundby A, Zazueta C, Montal M (2006) Molecular template for a voltage sensor in a novel K^+ channel. Identification and functional characterization of KvLm, a voltage-gated K^+ channel from *Listeria monocytogenes*. J Gen Physiol 128: 283–300.
21. Uozumi N (2001) Escherichia coli as an expression system for K^+ transport systems from plants. Am J Physiol Cell Physiol 281: C733–C739.
22. Matsuda N, Kobayashi H, Katoh H, Ogawa T, Futatsugi L, et al. (2004) Na^+-dependent K^+ uptake Ktr system from the cyanobacterium *Synechocystis sp*. PCC 6803 and its role in the early phases of cell adaptation to hyperosmotic shock. J Biological Chemistry 279: 54952–54962.
23. Stumpe S, Bakker E-P (1997) Requirement of a large K^+-uptake capacity and of extracytoplasmic protease activity for protamine resistance of *Escherichia coli*. Arch Microbiol 167: 126–136.
24. Kuo M-M-C, Saimi Y, Kung C, Choe S (2007) Patch clamp and phenotypic analyses of a prokaryotic cyclic nucleotide-gated K^+ channel using *Escherichia coli* as a host. J Biol Chem 282: 24294–24301.
25. Schrempf H, Schmidt O, Kümmerlen R, Hinnah S, Müller D, et al. (1995) A prokaryotic potassium ion channel with two predicted transmembrane segments from *Streptomyces lividans*. EMBO J 14: 5170–5178.
26. Gazzarrini S, Severino M, Lombardi M, Morandi M, DiFrancesco D, et al. (2003) The viral potassium channel Kcv: structural and functional features. FEBS Letters 552: 12–16.
27. Heginbotham L, Lu Z, Abramson T, MacKinnon R (1994) Mutations in the K^+ channel signature sequence. Biophysical Journal 66: 1061–1067.
28. Cortes D-M, Perozo E (1997) Structural dynamics of the *Streptomyces lividans* K^+ channel (SKC1): oligomeric stoichiometry and stability. Biochemistry 36: 10343–10352.
29. Zak E, Norling B, Maitra R, Huang F, Andersson B, et al. (2001) The initial steps of biogenesis of cyanobacterial photosystems occur in plasma membranes. Proc Natl Acad Sci USA 98: 13443–13448.
30. Voelker C, Schmidt D, Mueller-Roeber B, Czempinski K (2006) Members of the *Arabidopsis* AtTPK/KCO family form homomeric vacuolar channels in planta. Plant J 48: 296–306.
31. Ma S, Quist T-M, Ulanov A, Joly R, Bohnert H-J (2004) Loss of TIP1;1 aquaporin in *Arabidopsis* leads to cell and plant death. Plant J 40: 845–59.
32. Tsunekawa K, Shijuku T, Hayashimoto M, Kojima Y, Onai K, et al. (2009) Identification and Characterization of the Na^+/H^+ Antiporter Nhas3 from the Thylakoid Membrane of *Synechocystis* sp. PCC 6803. J Biol Chem 284: 16513–21.
33. Karniely S, Pines O (2005) Single translation-dual destination. EMBO Reports 6: 420–425.
34. Szabo I, Bock J, Grassmé H, Soddemann M, Wilker B, et al. (2008) Mitochondrial potassium channel Kv1.3 mediates Bax-induced apoptosis in lymphocytes. Proc Natl Acad Sci USA 105: 14861–14866.
35. Ishikawa M, Fujiwara M, Sonoike K, Sato N (2009) Orthogenomics of photosynthetic organisms: bioinformatic and experimental analysis of chloroplast proteins of endosymbiont origin in *Arabidopsis* and their counterparts in *Synechocystis*. Plant Cell Physiol 50: 773–788.
36. Aldridge C, Spence E, Kirkilionis MA, Frigerio L, Robinson C (2008) Tat-dependent targeting of Rieske iron-sulphur proteins to both the plasma and thylakoid membranes in the cyanobacterium *Synechocystis* PCC6803. Mol Microbiol 70: 140–150.
37. Martin W, Rujan T, Richly E, Hansen A, Cornelsen S, et al. (2002) Evolutionary analysis of *Arabidopsis*, cyanobacterial, and chloroplast genomes reveals plastid phylogeny and thousands of cyanobacterial genes in the nucleus. Proc Natl Acad Sci USA 99: 12246–12251.
38. Sato N (2006) Origin and evolution of plastids: genomic view on the unification and diversity of plastids. In The Structure and Function of Plastids. Edited by Wise, R.R. and Hoober, J.K. pp. 75–102. Springer, Dordrecht.
39. Maser P, Thomine S, Schroeder JI, Ward JM, Hirschi K, et al. (2001) Phylogenetic relationships within cation transporter families of *Arabidopsis*. Plant Physiol 126: 1646–67.
40. Derst C, Karschin A (1998) Evolutionary link between prokaryotic and eukaryotic K^+ channels. J Exp Biol 201: 2791–2799.
41. Schonknecht G, Hedrich R, Junge W, Raschke K (1988) A voltage dependent chloride channel in the photosynthetic membrane of higher plant. Nature 336: 589–592.
42. Remis D, Bulychev AA, Kurella GA (1986) The electrical and chemical components of the proton motive force in chloroplasts as measured with capillary and pH-sensitive electrodes. Biochim Biophys Acta 852: 68–73.
43. Tholema N, Bakker EP, Suzuki A, Nakamura T (1999) Change to alanine of one out ot four selectivity filter glycines in KtrB causes a two magnitude decrease in the affinities for both K^+ and Na^+ of the Na^+ dependent K^+-uptake system KtrAB from Vibrio alginolyticus. FEBS Lett 450: 217–220.
44. Downey P, Szabò I, Ivashinika N, Negro A, Guzzo F, et al. (2000) KDC1, a Novel Carrot Root Hair K^+ Channel. Cloning, characterization and expression in mammalian cells. J Biological Chemistry 275: 39420–39426.
45. Bergantino E, Segalla A, Brunetta A, Teardo E, Rigoni F, et al. (2003) Light- and pH-dependent conformational change of the PsbS subunit of photosystem II. Proc Natl Acad Sci USA 100: 15265–15270.
46. Pulina MW, Rizzuto R, Brini M, Carafoli E (2006) Inhibitory interaction of the plasma membrane Na^+/Ca^{2+} exchangers with the 14-3-3 proteins. J Biol Chem 281: 19645–19654.
47. Bolter B, Soll J, Schulz A, Hinnah S, Wagner R (1998) Origin of a chloroplast protein importer. Proc Natl Acad Sci USA 95: 15831–15836.
48. Ishikawa F, Suga S, Uemura T, Sato MH, Maeshima M (2005) Novel type aquaporin SIPs are mainly localized to the ER membrane and show cell-specific expression in *Arabidopsis thaliana*. FEBS Lett 579: 5814–5820.
49. Teardo E, de Laureto PP, Bergantino E, Dalla Vecchia F, Rigoni F, et al. (2007) Evidences for interaction of PsbS with photosynthetic complexes in maize thylakoids. Biochim Biophys Acta Bioenergetics 1767: 703–11.
50. Rascio N, Cuccato F, Dalla Vecchia F, La Rocca N, Larcher W (1999) Structural and functional features of *Ranunculus trichophyllus Chaix*., a freshwater submerged macrophyte. Plant Cell Environ 22: 205–212.

Zanetti et al, Supplementary Material

Materials and Methods

Strains and growth conditions

The wild-type *Synechocystis* sp. glucose-tolerant strain PCC 6803 was grown at 30°C under white light (30 μmol of photons / m^2sec) and shaking in standard BG-11 medium, buffered at pH 8.0 with 10 mM HEPES (*N*-2-hydroxyethylpiperazine-*N'*-2-ethanesulfonic acid) and supplemented with 10 mM glucose for photoheteroptrophic growth. For cultures grown on plates, the BG11 medium was supplemented with 1.5% agar and 0.3% sodium thiosulfate.

Expression of SynK in E. coli defective in K^+ uptake system

Heat shock method was used for the transformation of *E. coli* strain LB2003 competent cells by pPAB404-*SynK*. For the complementation growth test, the cells of *E. coli* LB2003 containing the plasmids were plated on a synthetic solid medium containing 34 mM Na_2HPO_4, 17 mM NaH_2PO_4, 8 mM $(NH_4)_2SO_4$, 0.4 mM $MgSO_4$, 0.6 μM $FeSO_4$, and 2% glucose , in the presence of 0.25 mM IPTG, 40 μg/ml of ampicillin, and various concentration of KCl. The plates were then subjected to an overnight incubation at 30°C. K^+ uptake assay was essentially measured as described elsewhere [43] . *E. coli* LB2003 cells were cultured in a synthetic medium at 30°C. The cells were collected by centrifugation, resuspended in 120 mM Tris-HCl (pH 8.0) and 1 mM EDTA was added after the cell concentration was adjusted to an OD_{578} of 30. Subsequently, the cell suspension was shaken for 10 min at 37 °C, collected by centrifugation, and washed twice with 200 mM HEPES-NaOH (pH 7.5) and then resuspended in the same buffer. After shaking for 20 min at room temperature, the concentration of cells was adjusted to an OD_{578} of 3 with the same buffer. Ten minutes prior to the start of the K^+ uptake measurement, 10 mM glucose was added to the suspension. One ml of the cell suspension was taken at an indicated time and transferred into a tube containing 150 μl of silicon oil, and subsequently centrifugated at 12,000 rpm for 1 min. The potassium content of cell pellet was determined by flame photometry.

DNA Constructs and Transformation of Synechocystis sp. PCC 6803.

The forward K+E (5'-GAGCCAG**GAATTC**ATGTTTGGCAAATATCGAC-3') and reverse K+F (5'-ATGGGCTC**GGATCC**GATTCCTGTTCTTCC-3') primers, introducing restriction sites *EcoRI* and *BamHI* respectively, were used to generate a 725-bp PCR product including exactly the *slr 0498* open

reading frame (ORF). The *EcoRI-BamHI* fragment, subsequently obtained by restriction digestion, was then cloned into the same sites of plasmid pEGFP-N1 (Clontech) to give plasmid pEGFP-SynK. In the new plasmid, the entire insert was completely sequenced to verify that no undesired mutation had been inserted by Taq polymerase (Platinum® *Taq* DNA Polymerase High Fidelity, Invitrogen). For production of the SynK-EGFP fusion bearing mutation Y181A, two overlapping fragments were generated in separate PCR amplifications, corresponding to the 5' region (primers K+E and Y2Arev, 5'-TATGTCACCGGCGCCCAGGGTGG-3') and 3' region (primers Y2Afor, 5'-ACCCTGGGCGCCGGTGACATAAC-3', and K+F) of the *slr0498* ORF. These two fragments were purified from oligonucteotides, mixed and used as template in a third amplification with primers K+E and K+F. The resulting band was then processed as described above.

The forward NtK-Nco (5'-TTCGAAT**CCATGG**TTGGCAAATATCGACAG-3') and reverse Ntk-Xho (5'-ATAGGATATCCG**CTCGAG**TAAAAACCAAAAGAC-3') primers, introducing restriction sites *NcoI* and *XhoI* respectively, were used to generate a 432-bp fragment by PCR amplification of plasmid pEGFP-SynK and subsequent restriction digestion. Plasmid pET-NtK5 was constructed by cloning this fragment into vector pET28b (Novagen), cut by the same enzymes; the cloned insert was controlled by sequencing.

Plant growth, genotyping and transcript analysis

A. thaliana wt (Columbia-0) and mutant plants were grown under short day (10/14 hours light/dark) with 100 μmol photons m^{-2} s^{-1} light at 23/18°C in a controlled growth chamber. Mutant plants are T-DNA insertion lines from SALK collection: *attpk5* (SALK_123690C), *attpk3* (SALK_090886) and *attpk1* (SALK_131790C). Mutants were genotyped by PCR. After genomic DNA extraction by using standard protocol, PCR primers were used as follow: *attpk5*-specific, 5'-TCGCTGTTGTTTTCGTCTTG-3' and 5'-CAAAGGATCCCCCAAAAGAT-3'; *attpk3*-specific, 5'-CTCTTGGAAGGTGGCAGTGG-3' and 5'-GTTGGGGCAGGTTTGTTGTT-3'; *attpk1*-specific, 5'-CGTCATGCTGGATATTTTGG-3' and 5'-AGACGAAGGCACAAGCAAGT-3'; T-DNA-specific, 5'-CGATGGCCCACTACGTGAACCA-3' and 5'-TGGTTCACGTAGTGGGCCATCG-3'. Total RNA was extracted from 100 mg of powdered leaves using the TriZol reagent (Gibco, Germany). After treatment with RNase-free DNase I (Ambion Ltd, UK), first strand cDNA was synthesized starting from 5μg of total RNA using the PowerScript™ Reverse Transcriptase (Clontech, USA). The presence of the transcripts was assayed by PCR using primers located in the exons located before and after the intron.

Thylakoid membrane purification

Thylakoids were isolated as described [45]. Briefly, *Arabidopsis* leaves were homogenized in 0.33 M sorbitol, 50 mM Tricine (pH 7.8), 5 mM $MgCl_2$, and 10 mM NaCl. After filtering, the homogenate was centrifuged at 4,500 *g* for 2 min, and the pellet was resuspended in 50 mMTricine (pH 7.8), 5 mM $MgCl_2$, and 10 mM NaCl. After centrifugation at 4,500 *g* for 10 min, the resulting thylakoids were resuspended in 100 mM sorbitol, 50 mM Tricine (pH 7.8), 5 mM $MgCl_2$, and 10 mM NaCl.

Purification of His-tagged SynK antigen and production of antisera

The recombinant NtSynK-His protein (144 N-terminal amino acids of SynK fused with a 6 His-tag at the C-terminus) was expressed in *E. coli* strain BL21(DE3), transformed with plasmid pET-NtK5, by the addition of 0.7 mM IPTG (≈200 μg/liter of 2-h culture). The protein was purified from solubilized inclusion bodies by affinity purification on nitrilotriacetic acid resin (Qiagen) and subsequent electroelution of the corresponding band from SDS/12-17% PAGE with 6 M urea. The purified protein was used as antigen to immunize two rabbits by subcutaneous injections, with poly(A)-poly(U) as adjuvant and following standard immunization routes.

Cell culture, fluorescence and confocal microscopy.

Plasmid pEGFP-SynK was used to transfect CHO-K1 cells [44]. These were cultured at 37°C in a humidified atmosphere containing 5% CO_2 on glass coverslips in Dulbecco's essential medium (D-MEM) (GIBCO) containing 10% fetal bovine serum, 2 mM L-glutamine, 100 μg/ml streptomycin and 100 units/ml penicillin. 40%-confluent culture was transfected using Lipofectamine 2000 Reagent (Invitrogen). Following transfection, cells were cultured for 72 h at 37°C or at 30°C, in the presence of 1 mM Cs^+, in order to prevent K^+ ion imbalances. 1 mM Cs^+ was not toxic for these cells. GFP fluorescence was examined with a Leica DMR microscope. The fluorescence filters were set at excitation 480 nm and emission 510 nm.

CHO cells were labeled with Vybrant DiI cell-labeling solution (Molecular Probes). This highly lipophilic dye can be analyzed by fluorescence microscopy: excitation 550 nm and emission 565 nm. For fluorescence microscopy, cells were assayed 72 hours after transfection with 3,2 μg plasmid DNA. Incubation with 0.125 μl of Vybrant DiI of cells in a small Petri dish (1 ml of culturing medium) for 8 minutes was followed by washing the cells three times.

For confocal images, obtained by using Leica LCS-SP2 system (Leica Microsystems, Heidelberg, Germany), FM4-64 (Invitrogen) was used as plasmamembrane dye according to product instruction. Co-localization with GFP signal was analyzed by Leica LCS software (Profile Plot). Cells were assayed 48 hours following transfection.

Cell lysis, membrane fractionation, SDS-PAGE and immunoblot analysis.

CHO cells, transfected with plasmids pEGFP-N1 (1.5 μg plasmid for every 2 million cells) and pEGFP-SynK (3.2 μg plasmid per 2 million cells) were lysed with SDS-PAGE loading buffer (LB) (50 μl LB for 10^6 cells) in the presence of protease inhibitors. Total protein concentration was determined by the Bradford assay. For fractionation, transfected CHO cells (8 x 10^6 cells) were washed with PBS, then harvested in 10 mM Tris/HCl pH 8, 2 mM EDTA, 2 mM PMSF, 1 mM DTT. Cells were disrupted by three cycles of freeze and thaw at -200°C (liquid nitrogen)/37°C. The membrane fraction was sedimented at 11.000 g for 30 min at 4°C. Pellet (membrane fraction) was resuspended in 100 μL sample buffer. The supernatant (soluble fraction) was precipitated with four volumes of ice cold acetone: after centrifugation for 5 min at maximum speed, the corresponding pellet was resuspended in 100 μL of SB [46]. Proteins were resolved by SDS-PAGE and electroblotted to nitrocellulose or PVDF (polyvinyldifluoridene) membranes. The blots were probed with primary antibody raised against GFP (1:2500), SynK (1:1000), KPORE (1:5000), PMCA (1:1000), SERCA (1:2500) and actin (1:5000). Primary antibody was detected with the ECL detection system (Pierce).

For cyanobacteria, cells were directly lysed in LB and loaded on SDS-PAGE containing or lacking 6 M urea, as specified. Samples were either boiled or not, in order to visualize multimeric or monomeric forms. Quantification was made by measuring OD_{730} and chlorophyll concentrations of the cultures. Proteins were blotted onto PVDF and membranes were decorated with primary antibodies in the presence of 1 % milk. Membrane fractionation of *Synechocystis* was performed by slight modification of the procedure described in Bolter et al, 1998 [47] . The blots were probed with anti-SynK (1:1000), anti-NrtA (kind gift of Prof. Pakrasi) (1:5000), anti-Rubisco large subunit (1:10000), anti-CP43 (1:1000), anti-ATP-ase (Agrisera) (1:10000) and anti-allophycocyanin (kind gift of Prof. Barbato) (1:1000).

For *Arabidopsis* cell membrane fractionation was performed according to [48]. Immunoprecipitation was performed as described in [49].

Anti-K-PORE antibody was produced against the synthetic peptide TTMTTLGYGD (Sigma). 3A8 monoclonal antibody was raised against the synthetic peptide IYSFNRDHYSGIET (Monoclonal

Antibody Core Facility, EMBL). Anti-TIP1,1 (1:500) was a kind gift of Professor Raikhel. Anti-AtTPK1 antibody was raised against synthetic peptide DDVKIDEPPPHPSK (EMBL).

Patch clamp analysis.

Patch clamping experiments were performed in whole-cell patch configuration on control pEGFP-N1-transfected or pEGFP-SynK-transfected CHO cells [44]. Bath solution:150 mM NaCl, 70 mM KCl, 1 mM $MgCl_2$, 2 mM $CaCl_2$, 10 mM Hepes, pH 7.4 adjusted with NaOH. Pipette solution: 134 mM KCl, 2 mM $MgCl_2$, 10 mM $CaCl_2$, 10 mM K^+/EGTA, 10 mM Hepes, pH 7.35 adjusted with KOH, unless specified otherwise. In experiments with TEA^+, Na^+ and K^+ were replaced by TEA^+. In experiments with gluconate, bath: 180 mM Kgluconate, 5 mM KCl, 1 mM $MgCl_2$, 2 mM $CaCl_2$, 10 mM Hepes, pH 7.4; pipette: 114 mM Kgluconate, 2 mM $MgCl_2$, 10 mM $CaCl_2$, 10 mM EGTA, 10 mM Hepes, pH 7.35. Potentials were applied and currents were monitored by an EPC-7 amplifier. Pulse protocol was applied and data analysis was performed by the PCLAMP8 program set. For tail current determination leak current was subtracted. Pipette resistance was 2-5 megaOhm. Data were low pass-filtered with an eight-pole Bessel filter with a cut-off frequency of 1 kHz. Intracellular voltages are reported and outward currents are plotted upwards.

Electron microscopy and Immunogold labelling

Pellets of cyanobacteria were fixed overnight at 4°C in 3% glutaraldehyde in 0.1 M sodium cacodylate buffer (pH 6.9) and then processed for electron microscopy according to [50]. Ultrathin sections, cut with an ultramicrotome (Ultracut, Reichert-Jung), were post-stained with lead citrate and examined under a transmission electron microscope (TEM 300, Hitachi) operating at 75 kV. For immunogold labeling, *Synechocystis* cells were fixed for 2 h in 4% paraformaldehyde and 0.25% glutaraldehyde in 0.1 M phosphate buffer (pH 7.2), post-fixed for 1 h in 1% osmium tetroxide in the same buffer, dehydrated in ethanol, and embedded in London resin white. Ultrathin sections picked up on gold grids were deosmicated with sodium metaperiodate, washed with 0.01 M PBS (pH 7.2), incubated for 20 min on 1% BSA in PBS, and treated with rabbit primary polyclonal antibody against SynK. After washing with PBS, sections were incubated with colloidal gold (15 nm) conjugated with goat anti-rabbit IgG. Sections were then stained with uranyl acetate followed by lead citrate, and examined under the electron microscope. A control experiment was performed by eliminating the incubation of sections with the primary antibody (Figure S7).

A prokaryotic thylakoid potassium channel is required for efficient photosynthesis in cyanobacteria

Vanessa Checchetto, Anna Segalla, Nicoletta La Rocca, Giorgio Mario Giacometti, Elisabetta Bergantino, Ildikò Szabò

Department of Biology, University of Padova, viale G. Colombo 3.
Correspondence to: I.S. ildi civ.bio.unipd.it, E.B. elisabetta.bergantino unipd.it

Abstract— We have recently identified a new putative potassium channel (SynK) in the cyanobacterium *Synechocystis* sp. PCC 6803, a photoheterotrophic model organism for the study of photosynthesis. SynK was demonstrated to function as a potassium selective channel and to be located predominantly to the thylakoid membrane. In order to study its physiological role, a SynK-knock-out mutant was obtained and characterized. Fluorimetric experiments indicated that SynK-less cyanobacteria are unable to build up a proton gradient as efficiently as WT across the thylakoid membrane upon illumination. Accordingly, chlorophyll fluorescence measurements indicated a decreased photosynthetic efficiency in mutant cells grown at normal light intensity (50 µE m^{-2} s^{-1}). The lack of the channel did not cause an altered membrane organization, cell size and growth under photoheterotrophic conditions, but caused bleaching of the cells cultured at high light intensity (200 or 500 µE m^{-2} s^{-1}). Osmotic and salt stress response did not depend on SynK. These data shed light on the function of a prokaryotic potassium channel in the counterbalance flux and reports evidence for the first time on the requirement of a thylakoid ion channel for optimal photosynthesis by means of a genetic approach.

I. INTRODUCTION

The unicellular photoheterotrophic transformable cyanobacterium *Synechocystis* sp. PCC 6803 is the first photosynthetic organism for which the complete genome sequence is known. This prokaryote is characterized by an intracellular membrane system with thylakoids, where both photosynthesis and respiration take place. Cyanobacteria provide suitable model systems for studies of the effects of environmental stress on photosynthesis since these prokaryotes perform oxygenic photosynthesis using a photosynthetic apparatus similar to that found in chloroplasts of higher plants and algae. Moreover, cyanobacterial cells can easily be exposed directly to defined stress conditions in culture and they are able to acclimate to a wide range of environmental stresses. Cyanobacteria are considered to represent the progenitors of chloroplasts. *Synechocystis* has been widely used for genetic and biochemical studies of photosynthesis and various related metabolic processes.

Each of the over ten species of cyanobacteria whose genomes have been completely sequenced contains at least one gene predicted to encode a potassium channel. However, for none of these putative channels their *in vivo* function is known, and *in vitro* activity was proven only for one, SynK (Zanetti *et al.*, 2010). In general, while electrophysiological studies have been performed with success both on native bacterial membranes e.g. Szabò *et al.*, 1990) and on recombinant prokaryotic ion channels (e.g. Schrempf *et al.*, 1995), only very few studies addressed the physiological function of ion channels in prokaryotes.

Gain-of-function mutations indicate that in *E. coli* six transmembrane-containing Kch proteins conduct potassium *in vivo*. Overexpression of Kch inhibits growth at moderate external potassium concentrations (Epstein *et al.*, 2003). The only putative prokaryotic potassium channel for whose physiological function genetic evidence has recently been obtained is *Helicobacter pylori* HpKchA, of the two transmembrane RCK (regulation of K^+ conductance) domain family. HpKchA-mediated potassium uptake is essential for gastric colonization by *H. pylori*, which lacks known bacterial K^+ uptake systems (Stingl *et al.*, 2007). Concerning *Synechocystis*, a Ktr-like system encoded by *slr1509* seems to be the main responsible for potassium uptake in these organisms (Berry *et al.*, 2003).

In *Synechocystis*, several transporters of the plasmamembrane have been characterized from functional point of view, including a nitrate transporter (NrtABCD) (Omata *et al.*, 1989), iron transporter FutA (Koropatkin *et al.*, 2007), Calcium-proton exhanger (Waditee *et al.*, 2004), bicarbonate transporter CmpABCD (Omata *et al.*, 1999), sodium-proton antiporter NhaS (Inaba *et al.*, 2001) and a sodium-dependent potassium uptake system (Matsuda *et al.*, 2004). Furthermore, acquaporin was also found in the cytoplasmic membrane (Tchernov *et al.*, 2001). Much less is known about transporters located in the thylakoid membrane: to our knowledge, only NhaS3 has been

located to this membrane (Tsunekawa *et al.*, 2009). Concerning ion channels, the putative mechanosensitive channel MscL has been proposed to mediate calcium release upon plasmamembrane depolarization (Nazarenko *et al.*, 2003), and the recombinant form of the first prokaryotic glutamate receptor, GluR0 of *Synechocystis* has been characterized (Chen *et al.*, 1999).

In a recent study, we identified in the genome of *Synechocystis* sp. PCC 6803, SynK (slr0498), displaying the selectivity filter aminoacid sequence (TMTTVGYGD), typical of all known K^+ channels (Zanetti *et al.*, 2010). This sequence forms a structural element known as a selectivity filter, which prevents the passage of Na^+ ions but allows K^+ ions to pass across the membrane at rates approaching the diffusion limit. SynK was found to function as potassium-selective channel when expressed in mammalian cells. Furthermore SynK complemented K^+ uptake in a K^+transporter-deficient *E. coli* strain and its localization within cyanobacteria was determined. SynK represents the first thylakoid-located ion channel identified in cyanobacteria and is conserved in various photosynthetic cyanobacteria species.

During photosynthesis, a light-driven flux of protons from the stromal to the lumenal side of the thylakoid membrane occurs against the electrochemical gradient via the cytochrome b_6f complex. This process is expected to lead to the formation of a pH gradient, as well as to the development of a transmembrane electrical potential. Instead, transthylakoid $\Delta\mu H^+$ is mainly composed of ΔpH, although recent works indicate the contribution of the electric field to steady-state transthylakoid proton motive force, at least in certain conditions both in higher plants and eukaryotic algae (e.g. Cruz *et al.*, 2001). It has been proposed that in higher plants an initial transthylakoid electrical potential of around +70 mV (positive on the lumenal side) quickly reaches a steady state of around 15-30 mV (Remis *et al.*, 1986). It should be noted that, whereas other factors may also modulate SynK activity, at least in heterologous system, the channel is activated at positive voltages and $V_{1/2}$ is 67 mV (Zanetti *et al.*, 2010). Presuming the same orientation of SynK in the CHO plasma membrane and in thylakoids, at positive voltages SynK would permit the quick exit of potassium from the lumen. In higher plants, the decay from +70 to +15-30 mV is thought to be due either to the exit of counterbalancing cations from the lumen towards the stroma or to the entry of anions from the stroma (Schonknecht *et al.*, 1988), which would permit dissipation of the transmembrane potential but not that of the pH gradient. Magnesium (Barber *et al.*, 1974) and potassium (Tester and Blatt, 1989) have been proposed to act as dominant counterions. In higher plants, K^+ flux out of the thylakoid has been measured upon illumination (Dilley and Vernon, 1965; Chow *et al.*., 1976) and TEA^+, a potassium channel inhibitor has been shown to reduce photosynthetic efficiency on isolated thylakoids (Berkowitz *et al.*, 1995). However, direct genetic proof in favour of the "counterbalance" hypothesis is still missing, given also to the fact that gene(s) encoding for the thylakoid-located potassium channel(s) have not been identified for higher plants.

In cyanobacteria, potassium might be an efficient counter-ion as well, given its high concentration in the cytoplasm (around 200 mM) (Epstein, 2003).

In the present paper we provide evidence for the physiological role of the first *bona fide* potassium channel identified in cyanobacteria. We show that the thylakoid-located SynK is involved in the mediation of counterion flux during photosynthesis and thereby lack of the channel reduces photosynthetic activity. To our knowledge, this is the first report indicating the direct role of an ion channel in the regulation of photosynthesis by genetic means.

II. RESULTS

In order to understand the importance of SynK for cyanobacterial physiology, we constructed a mutant deficient in SynK. The *Synechocystis* PCC 6803 strain is spontaneously transformable and integrates foreign DNA into its genome (present in dozen of copies) by homologous recombination, thus allowing targeted gene replacement, avoiding thus random mutations/insertions.

ΔSynK was produced by inserting a kanamycin-resistance cassette into the *Synechocystis* genome, between nucleotide 209 (numbering from the A_1TG codon) and 566 of the *slr0498* open reading frame. The linear DNA fragment used to transform cyanobacteria was designed to produce large deletion of the ORF (from aminoacids 71 to 189, including the pore region), by double homologous recombination (Fig 1A). Its insertion in the correct position of the genomic DNA was verified by PCR (Fig. 1B). Complete segregation of the recombinant chromosomes, usually reached by means of three to six subcloning passages, could be obtained in the ΔSynK mutant strain after the 3rd subcloning (Fig. 1B) and the cells were able to grow on plates with 50 $\mu g\ ml^{-1}$ kanamycin. Figure 1C shows that both the SynK monomeric and the functionally active tetrameric form (102 kDa) of SynK were completely missing from the knock-out strain for SynK. We have observed the tetrameric form- it is well known that prokaryotic potassium channels tend to migrate as tetramers even in the presence of SDS in gel electrophoresis (Cortes and Perozo, 1997).

Given that the mutant strain is homoplasmic and, in accordance, it does not express the protein, it is suitable for the determination of the physiological role of the channel protein. As mentioned in the introduction, potassium fluxes seem to account for the lack of significant steady electrical membrane potential during light reaction of photosynthesis in higher plants. The lack of a potassium channel on illuminated thylakoids could restrict the K^+ efflux. Restriction of K^+ efflux in the light would lead to an increased membrane potential (the lumen becoming more positive) across the thylakoid concomitantly with light- induced proton pumping during photosynthesis.

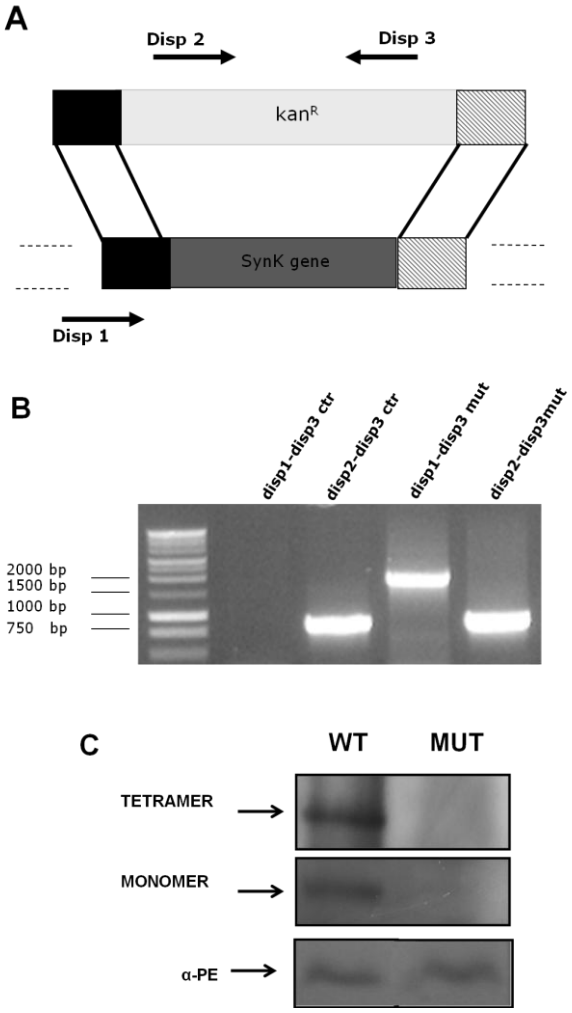

Figure 1. Construction of ΔSynK *Synechocystis* lacking SynK thylakoid-located potassium channel. A) Schematic diagram of the construction of knock-out. ΔSynK was obtained by inserting a kanamycin-resistance cassette into *Synechocystis* genome. Forward and reverse primers, introducing mutagenic sites, were used to generate the a PCR product containing the SynK gene in the central position and two flanking regions. The correct insertion was controlled by PCR using different primers: Disp2-Disp3 are primers that bind the Kanamycin cassette, while Disp1 binds in *Synechocystis* genome in a flanking region of the SynK gene. B) Confirmation of the correct insertion of Kanamycin-resistance gene in mutant by PCR with the specific primers. 1: Molecular mass markers. 2: Genomic DNA isolated from a cell used as positive control, corresponding to a WT strain containing a kanamycin resistance cassette in a non-coding region, amplified with disp1 and disp3. 3: Genomic DNA isolated from the same strain, amplified with disp2 and disp3. 4: Genomic DNA isolated from the ΔSynK mutant cells amplified with disp1 and disp3. 5: Genomic DNA isolated from the ΔSynK mutant cells amplified with disp2 and disp3. C) Western blot of whole cyanobacterial cells solubilised in the sampling buffer. WB was developed by anti-SynK antibody and recognized both the monomeric (around 30 kDa) and the tetrameric (around 100 kDa apparent MW) forms of the channel only in WT but not in the mutant cells. Cells were loaded based on equal O.D. WB was stripped and re-blotted with anti-phycoerythrin antibody (lower row).

In cyanobacteria we expect the same kind of behaviour given that under conditions where photosynthesis occurs, respiration seems negligible. Unfortunately, to our knowledge, no reliable methods are available for determination of the transmembrane electrical potential solely in thylakoids in cyanobacteria (Teuber *et al.*, 2001). However, given that the build-up of positive charge within the lumen would increase the electrical gradient against which proton pumping must occur, we can expect a decreased pH gradient formation in the mutant strain upon illumination.

To investigate this point, the fluorescent probe Acridine Orange (AO) was used to measure thylakoid membrane energization in intact cells grown at 50 µE $m^{-2}s^{-1}$, according to Teuber *et al.* (2001). Measurement with AO has been reported to show distinct kinetic phases: a fast decrease of fluorescence upon illumination, indicating lumen acidification, was followed by a fast increase when the illumination was turned off, indicating collapse of ΔpH across the thylakoid membrane. First we've proved that acridine orange uptake into intact cells took place with the same kinetics and to the same extent in WT and mutant cells kept in the dark (Fig. 2A). As mentioned above, if a lumenal positive membrane potential persisted because of lack of counterbalance ion movements, this should prevent protons from entering the lumen, and should thus compromise build-up of the proton gradient upon illumination. In accordance, lumen acidification in the mutant was not as efficient as in the WT organism (Fig. 2B). These results indicated the build-up of the pH gradient in the mutant as well as in the WT, although the equilibrium pH gradient, shown by the ΔF/F ratio at the steady state level, was 35 % higher in the WT with respect to the mutant. The ΔF/F ratio is 0,1726±0,0139 in the WT (n=27) versus 0,1276±0,01272 (n=22) (p=0,023) (Fig. 2B) in the mutant.

Pre-incubation of WT cells with saturating concentration (10 µM) of FCCP (carbonylcyanide-p-trifluoromethoxyphenylhydrazone) which acts as a protonophore and thus as an uncoupler, almost completely dissipated ΔpH (Fig. 2C). FCCP causes the thylakoid membrane to be freely permeable to protons, uncoupling electron transport from ATP synthesis. As protons are pumped into the lumen, they diffuse out through the synthetic proton channel. Under these conditions, neither an electrical gradient nor a ΔpH would develop in the light across the thylakoid membrane. However, when much lower concentration of FCCP (0,2 µM) was used, the collapse of ΔpH in illuminated samples (as followed by increase in the AO signal) was significantly greater in the mutant than in the WT organisms (Fig. 2D). This data indicates that in accordance with the hypothesis described above, the proton concentration in the lumen following illumination is lower (and therefore ΔpH can be dissipated easier) in the mutant cells with respect to WT. Nigericin (50 µM) and valinomycin (5 µM) were also used (not shown): nigericin is an ionophore which stimulates exchange of K^+ and H^+ between the two sides of the membrane, thereby abolishes ΔpH. Valinomycin equilibrate potassium concentrations on both sides of the membrane and thereby diminish the difference of electrical potential formed across the membrane. In preliminary trials we could however not observe a clear effect of valinomycin on ΔpH formation in the mutant strain (not shown). The effect of channel inhibition by Cs^+ or TEA^+, previously shown to inhibit heterologously expressed SynK (Zanetti *et al.*, 2010), on ΔpH across the thylakoid membrane in intact cells could not be investigated, since these ions do not permeate the bacterial cytoplasmic membrane.

Addition of TEACl (100 mM) and Cesium chloride (80 mM) to intact WT cells into the cuvette had no effect on the gradient formation (Fig. 2E), indicating that PM-located SynK (which has been shown to be blocked by 10 mM Cs^+ in patch clamp experiments) is not involved in the regulation of ΔpH formation across the thylakoid membrane. Channel modulators have been shown to exert various effects on PM-located channels in cyanobacteria, indicating that these drugs are able to cross the outer membrane, presumably through large porins (Pomati *et al.*, 2004). The back pressure on proton pumping occurring because of increased positive charge in the lumen would impose an increased restraint on electron transport (i.e. following the concept of "photosynthetic control" described by Edwards and Walker, 1984), resulting in an inhibition of O_2 evolution.

The photosynthetic rates of *Synechocystis* WT and mutant cells grown under 50 µE $m^{-2}s^{-1}$ light were determined by measuring oxygen evolution in the presence of HCO_3^-, which allows determination of the activity of the whole electron transfer chain. As shown in Figure 3A, O_2 evolution was significantly decreased by 35% in the mutant strain. To check whether reduced oxygen production correlated with decreased electron transport, we have measured ETR (relative electron transport rate) values obtained for the WT and mutant cells, grown at 50 µE m^{-2} s^{-1}, under various light intensities. At light intensities below 50 µE m^{-2} s^{-1} photosynthetically active radiation (PAR), there was no significant difference between the WT and the mutant strain in their ETR. The ETR values increased in the WT by increasing the light intensity to attain the maximal value at around 800 µE $m^{-2}s^{-1}$ and then slightly decreased at higher intensities (Figure 3B). In contrast, ETR values in the mutant decreased at light intensities above 500 µE m-2 s-1 to reach zero value at 1850 mE m-2 s-1, indicating that the mutant was more susceptible to high light than the WT. The result obtained in the mutant is in

accordance with the decreased ΔpH, since linear and cyclic electron transport are directly coupled to proton transduction.

Given that an inefficient proton pumping against the electrochemical gradient due to the lack of the potassium channel reduces electron transport and thus is expected to lead to reduced PQ pool formation, we've checked whether application of DBMIB (2,5-dibromo-3-methyl-6-isopropyl-p-benzoquinone), known to inhibit electron transport between PSI and PSII and thus reduce the PQ pool, induced the same kind of changes in ETR what we observed with the mutant. Figure 3C illustrates that this was indeed the case, suggesting that the lack of the channel may result indeed in a reduced PQ pool. The concentration of DBMIB (5 µM) used here has previously been shown to reduce the PQ pool in cyanobacteria (Hihara *et al.*, 2003).

In order to check whether the higher susceptibility of the mutant versus WT to high light had an impact on the PSII/PSI ratio, we compared the PSII/PSI ratio in these strains cultured at 50 µE m-2 s-1, by two independent methods. Figure 3D shows a decrease in the intensity of signals on Western blot of components of PSII (samples were loaded on the basis of chlorophyll concentration in cyanobacteria, Chl a is more abundant in PS I than in PS II (Chl *a* PSI:Chl *a* PSII >= 4), namely of D1, D2 reaction center proteins as well as of internal antennae CP43 and CP47 in the mutant with respect to WT thylakoids. This decrease in PSII/PSI ratio was further confirmed by fluorescence spectra at 77 K (Figure 3E). The excitonic connection between antenna pigments and reaction center cores was examined in a series of 77 K fluorescence emission spectral measurements. PBS excitation spectra (580 nm; reflecting mainly the energy transfer from PBS to PSI and PSII) and Chl excitation (i.e. 435 nm; induction of fluorescence emission of the photosystems directly) spectra are shown.

The peak at 665 nm indicate allophycocyanin emission. The peak at 685 nm contains contributions from the phycobilisome linker pigment and from the fluorescence of chlorophyll molecules associated with PSII. The peaks at 695 and 720 nm originate from the PSII-P680 (fluorescence of chlorophyll molecules specifically associated with CP47) and PSI-P700 reaction center core chlorophylls, respectively. While shape and position of the PBS peaks are similar in WT and SynK mutant (left panel), their relative intensities are higher in the mutant, suggesting a slightly diminished energy transfer from PBS to the reaction center in absence of the SynK protein, even though no net difference in the PBS content of these organisms could be observed (see Western blot of Fig. 3D). A quantitative linear relationship between PSI/PSII fluorescence and the molar ratio between the photosystems has been observed (Murakami *et al.*, 1997). Thereby, the ratio of the peak intensities at 685/695 nm relative to 725 nm provide a rough estimation on the PSII/PSI ratio. SynK deficiency results in a lower PSII/ PSI fluorescence (corresponding with molar) ratio (Fig. 3E, right panel). The same tendency was found by fluorescence induction measurements with variable fluorescence component (Fv) originating from PSII and minimal fluorescence (F_0) containing emissions also from PBS (Campbell *et al.*, 1998) and PSI. While WT samples show Fv/Fm ratios of 0.243 ± 0.027 (n=6 independent experiments), the corresponding value in SynK mutant is 0.120 ± 0.02 (n=6) (p=0.005), at equal chlorophyll concentrations. The slightly higher F_0 level in the mutant also contributes to the lower Fv/Fm ratio: F_0 in WT was 0.405 ±0.009 (n=6), while in the mutant it was 0.46±0.016 (n=6) (p>0.05). The lower Fv/Fm value in the mutant may also reflect a decreasing PSII/PSI ratio. Thus, in accordance with data of literature (e.g. Bernat *et al.* m 2009), lower PSII/PSI ratio involves lower linear electron transport activity.

To further characterize the chlorophyll fluorescence in the mutant strain, we determined the fast kinetics of the fluorescence rise upon onset of saturating light. As shown in Fig. 4A, the various rise phases, reflecting different electron transfer steps in PSII, are not altered in the mutant. State transition was also measured with pulse modulated fluorescence and repetitive application of saturation pulses for assessment of Fm and Fm' as described by Asada. The state transition in cyanobacteria is triggered in the same way as that in higher plants. State 1 is achieved by oxidation of intersystem electron carriers (usually by "excess" excitation of PSI). Reduction of intersystem electron carriers, most likely plastoquinone (Mullineaux and Allen, 1990), either by "excess" excitation of PSII or by a dark respiratory pathway, triggers the conversion to state 2. State 2 is characterized by a decrease in PSII variable fluorescence, a decrease in the PSII absorbance cross section, and an increase in the PSI absorbance cross section as compared with state 1 (Mullineaux, 1992).The dark-adapted cyanobacteria display a low Fm-level, characteristic of state 2.

The dark fluorescence yield F_0 is much higher than in green plants, due to strong overlapping of non-variable fluorescence from phycocyanin and presumably also from Chl *a* in PSI. When a low intensity of blue light, absorbed almost exclusively by PSI, is applied, maximal fluorescence Fm' rises to a high level, characteristic of state 1. Decline occurs when actinic illumination is turned off, and state 2 is approached again. There is no significant difference in the ability to undergo state transition between the WT and mutant organisms (Fig. 4B). The above results indicate an altered electron transfer rate and an altered PSII/PSI ratio in the mutant with respect to WT in the cells grown under 50 µE $m^{-2}s^{-1}$ light.

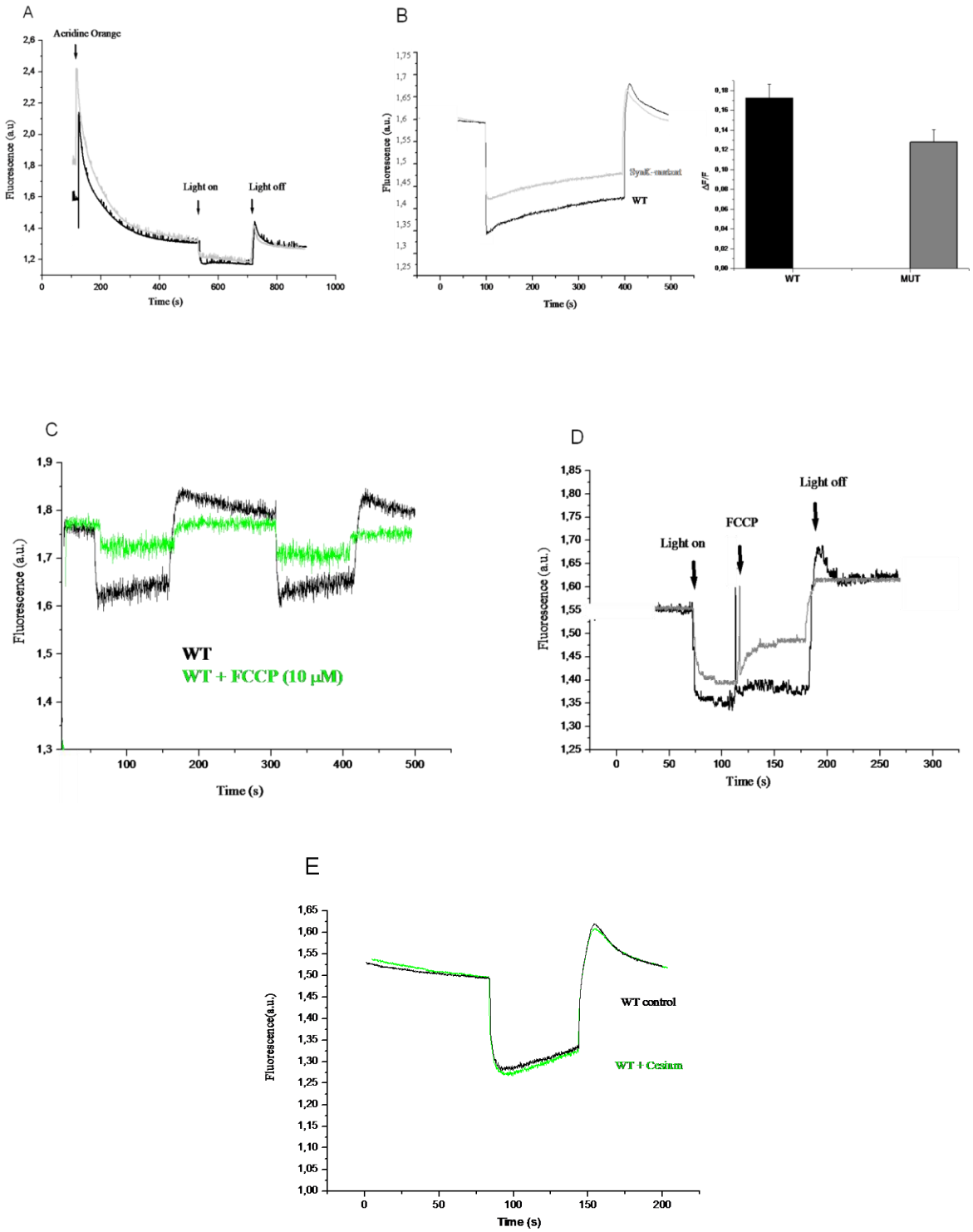

Figure 2: Formation of ΔpH across the thylakoid membrane is compromised in the SynK-less mutant cyanobacteria. A) Acridine Orange uptake takes place in both WT and mutant cells with similar kinetics. Cell cultures containing 10 µg/ml Chlorophyll were suspended in the assay medium and when indicated 5 µM Acridine Orange was added. Fluorescence was continuously monitored. Decrease in the fluorescence corresponds to uptake of the dye into the cells. B) Representative traces obtained from WT and mutant organisms. Downward deflection correspond to quenching of the AO fluorescence due to its protonation within the lumen following application of light, while upward deflection indicates dissipation of ΔpH when the light is switched off. Right panel shows ΔF/F values for WT (n=27) and mutant (n=22) cells. C) Addition of 10 µM FCCP prevents formation of proton gradient under illumination in WT cells, while addition of 0,2 µM FCCP under illumination induces partial proton gradient dissipation (D). The experiment was repeated 3 times. E) Addition of 80 mM Cesium Chloride did not alter proton gradient formation. Representative trace of 3 experiments giving similar results is shown.

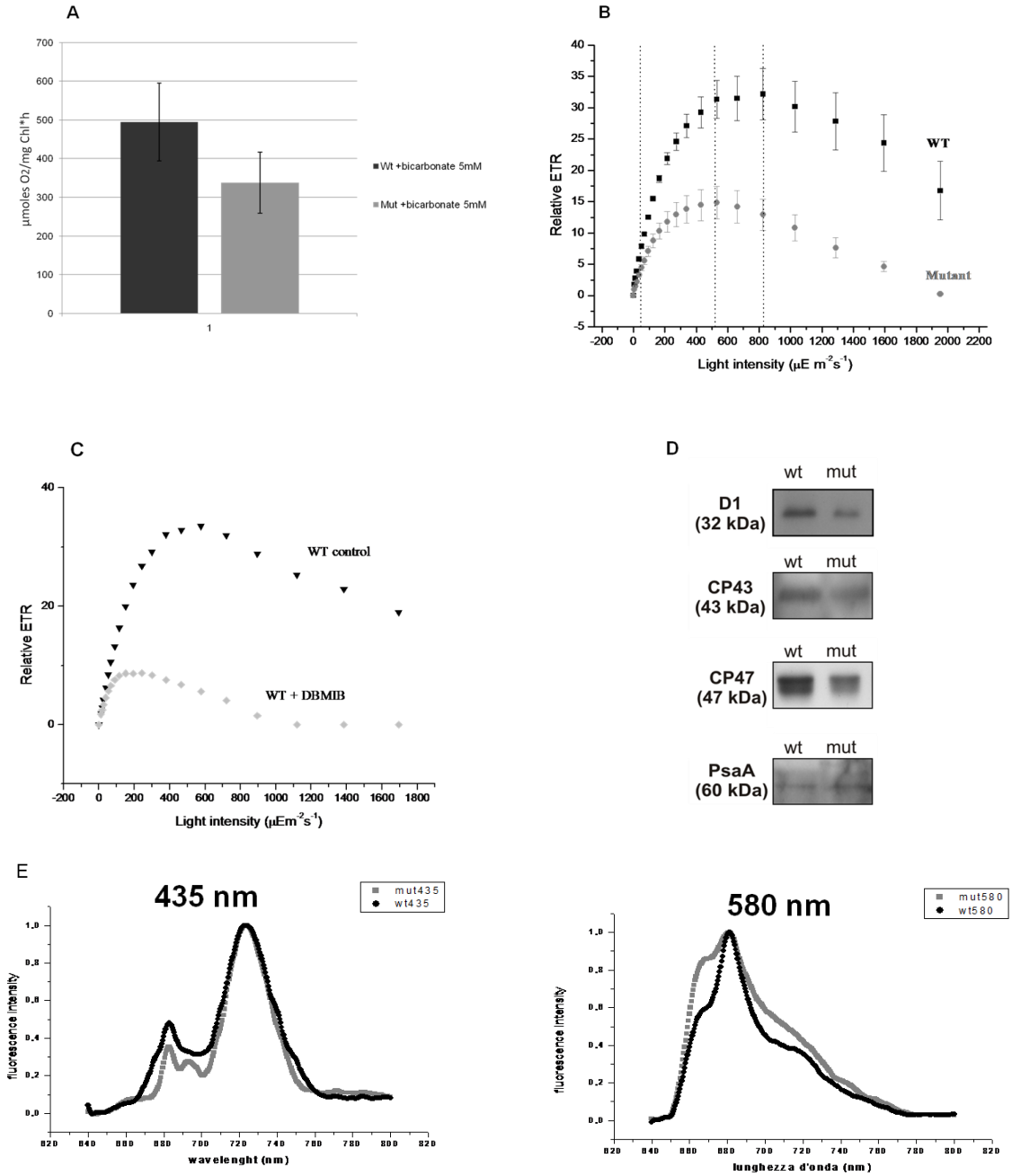

Figure 3. Lack of SynK potassium channel reduces overall photosynthetic activity. A) Oxygen evolution measurements of wt and mutant *Synechocystis* cells. Oxygen evolution was measured in the presence of 5mM $HCO3^-$ to measure the electron transfer throughout the entire photosynthetic electron transfer chain. Wild-type and mutant cells grown in BG-11 supplemented with 5 mM glucose under 50 µE $m^{-2}s^{-1}$ light condition for 48 were assayed. Error bars indicate the standard deviation of 9 independent experiments. The p value of t-test is < 0.05 (p = 6,28621 10-9). B) Relative electron transport rate (ETR) determined by chlorophyll fluorescence measurements at different light intensities (x scale) and calculated by using the DUAL-PAM program are reported for WT and mutant cells. Light intensities at which cells were grown, and at which maximal ETR values are obtained are shown with dashed lines. Shown are medium ±SD values (n= 7 different cultures for WT and n=8 different cultures for mutant). C) Representative ETR measurement: ETR was measured for WT cells in the absence and then in the presence of 5 µM DBMIB, known to induce reduction of the PQ pool by inhibition of the cytochrome b6f complex. The same effect was observed other 2 times. D) Western blot analysis of PSII and PSI subunit contents. Wild-type and mutant cells grown in BG-11 supplemented with 5 mM glucose under 50 µE $m^{-2}s^{-1}$ light condition for 48 h were assayed. The cells were completely broken using bead beater and proteins were separated on a 12% polyacrylamide gel, 6 M urea. Immunological detection of proteins of wild-type and ΔSynK cells with the following antibodies: anti-D1 (1:10000), anti-CP43 (1:1000), anti-CP47 (1:5000) and anti-PsaA (1:500). Equal amount of chlorophyll a were loaded in each lane: 0,1 µg for D1, 0,25 µg for CP43 and CP47 and 0,75 µg for PsaA. Western blots shown are representative of 4 experiments. E) Fluorescence emission spectra at 77 K of whole cells from *Synechocystis* sp. PCC 6803 wild type and SynK mutant strains. Spectra were recorded at the same concentration of chlorophyll a (5 µg/ml). The excitation wavelengths were 435 nm and 580 nm. Spectra were obtained 3 times, giving similar results.

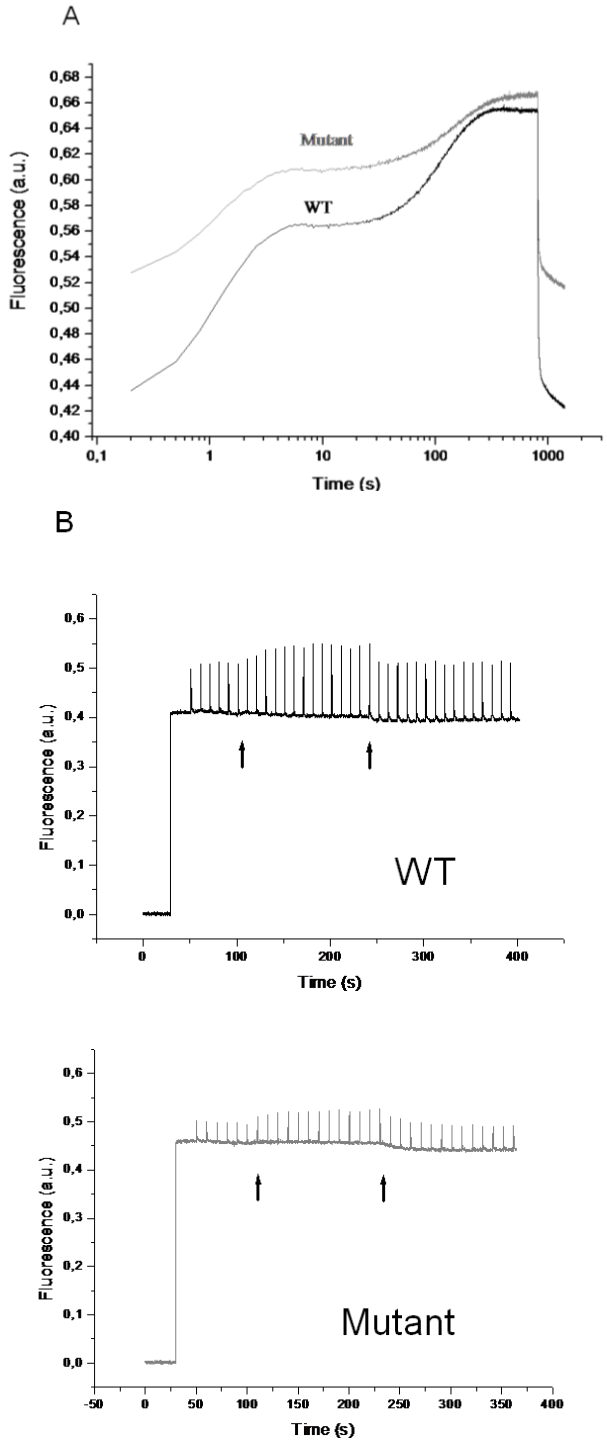

Figure 4. Mutant cells undergo state transition. A) Fast chlorophyll induction kinetics shown for WT and mutant. Curves are average of 20 measurements for each cell type. B) Cells were dark adapted for 10 minutes and typical changes of fluorescence yield in *Synechocystis* PCC 6803 related to light induced state changes were measured by pulse modulation fluorometry and the saturation pulse method. Dark-adapted cells in state 2 were illuminated by moderate PSI light (blue, 60/µmol quanta $m^{-2}s^{-1}$ peaking around 425 nm) to reach state 1. Consecutive darkening induced reversion to state 2.

In order to exclude that such a difference might be due to a direct effect of the mutation on PSII or PSI assembly, we performed ETR measurements also on the cells grown at very low, 5 µE m^{-2} s^{-1} light intensity. If the effect of the mutation on PSII/PSI ratio was due to and indirect, regulatory mechanism come into play when the cells are cultured at "stressing" light intensity,
lowering this parameter should *a priori* permit the mutants to behave as WT. As illustrated on Fig. 5A and 5B, this was indeed the case: both ETR and PSII protein levels were comparable in the mutant and WT, indicating that lack of SynK itself did not impact on photosystem assembly and function. Fv/Fm value was 0,36±0,04 (n=3) in the WT and 0,27±0,05 (n=3) ($p>0.05$) in the mutant. Thus, results of the experiments shown above suggest that thylakoid K^+ channel function is required for optimal photosynthetic capacity, especially when cells are grown at higher light intensities The lack of SynK however did not have any effect on the membrane organization in cyanobacteria, as assessed by transmission electron microscopy (TEM) (Fig. 6A). In the dark, where photosynthesis does not take place and cells produce ATP by respiration in the presence of an added carbon source (5 mM glucose), the mutant was able to grow as efficiently as the wild type, suggesting that SynK does not regulate respiration (Fig. 6B). Growth curves were comparable also in the case of culturing the cells in the presence of 0.5 M sorbitol to induce osmotic stress, and of 0.5 M NaCl, able to induce salt stress (Fig. 6C and D). In both cases no change in pigmentation occurred. These results indicate that SynK is likely not to be involved in the response of these organisms to salt and osmotic stresses. Under different light conditions, the cell volume did not change significantly (not shown) as determined by using fluorescence microscopy. Significant differences in growth between WT and mutant could not be observed either at 5 or 50 µ$Em^{-2}s^{-1}$ light intensity (not shown), but after 48 hours we detected a slight but significant decrease in the chlorophyll content of the cells cultured at 50 µ$Em^{-2}s^{-1}$. At equal O.D. measured at 730 nm, mutants had 9,8% less chlorophyll content with respect to WT organisms. Viceversa, at equal chlorophyll concentration (0,01 µg/ml Chl), cell number was 11,99 x 10^6 +/-92 (n=6) in WT, while 15,63 x 10^6+/-17 (n=7) cells/µg Chl in the mutant cell culture, as determined by flow cytometer analysis. At higher light intensity (200 µ$Em^{-2}s^{-1}$), there was no significant difference in growth between WT and the mutant, in the absence of glucose, i.e. in phototrophic conditions (not shown). However, after 7-10 days of culturing, we could reproducibly observe a visible bleaching of the mutant cultured at 200 or 500 µ$Em^{-2}s^{-1}$, while the WT culture

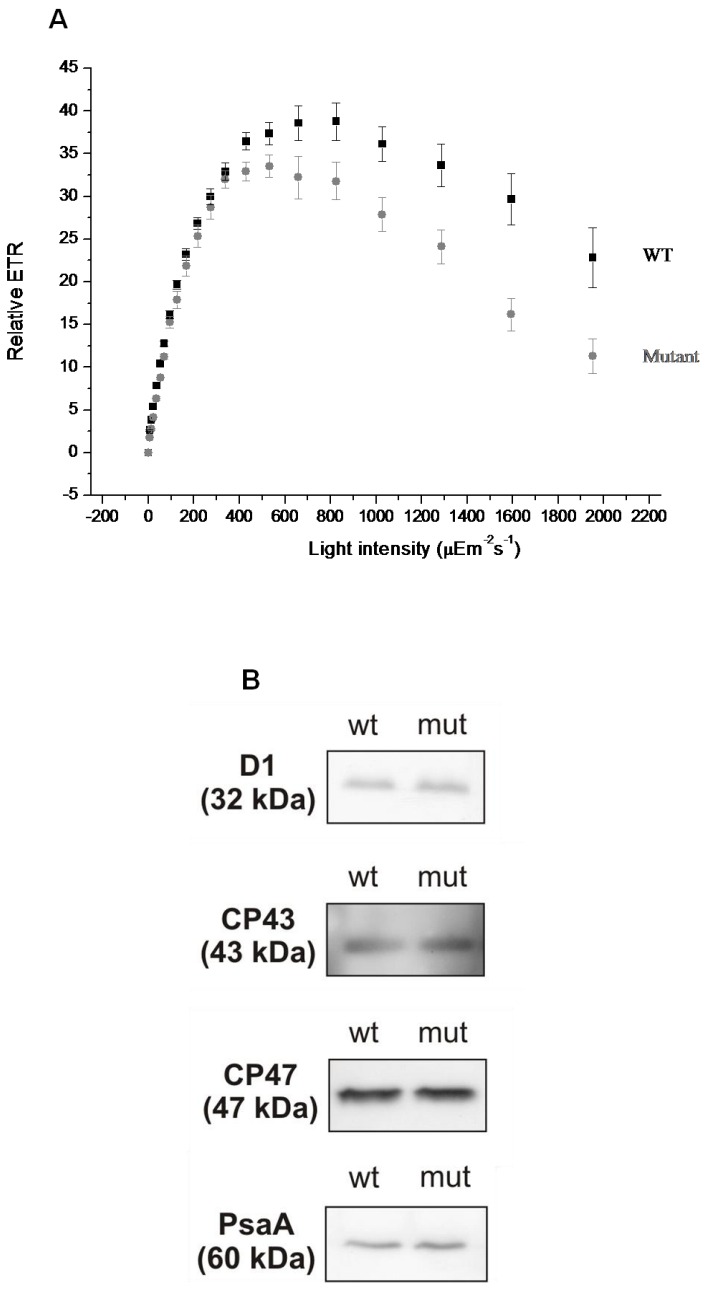

Figure 5. Mutant cells grown under low light intensity do not display and altered electron transport rate and a decrease in Photosystem II components. A) Experiments were performed as described for Figure 3B on cells grown at 5 µE m-2s-1 intensity. B) Western blot analysis of the PSII and PSI subunit contents in cells grown under low light condition. Wild-type and mutant cells grown in BG-11 supplemented with 5 mM glucose under 5 µE $m^{-2}s^{-1}$ light condition for 48 h. Experiment was performed as described in 3D.

maintained pigmentation (Fig. 6E). Please note that the measurement of O.D. does not give information about the pigment content of the cells. These results are in agreement with the higher susceptibility of the mutant versus WT toward high light intensity and are indicative of an oxidative stress in the mutant organisms cultured under light stress conditions.

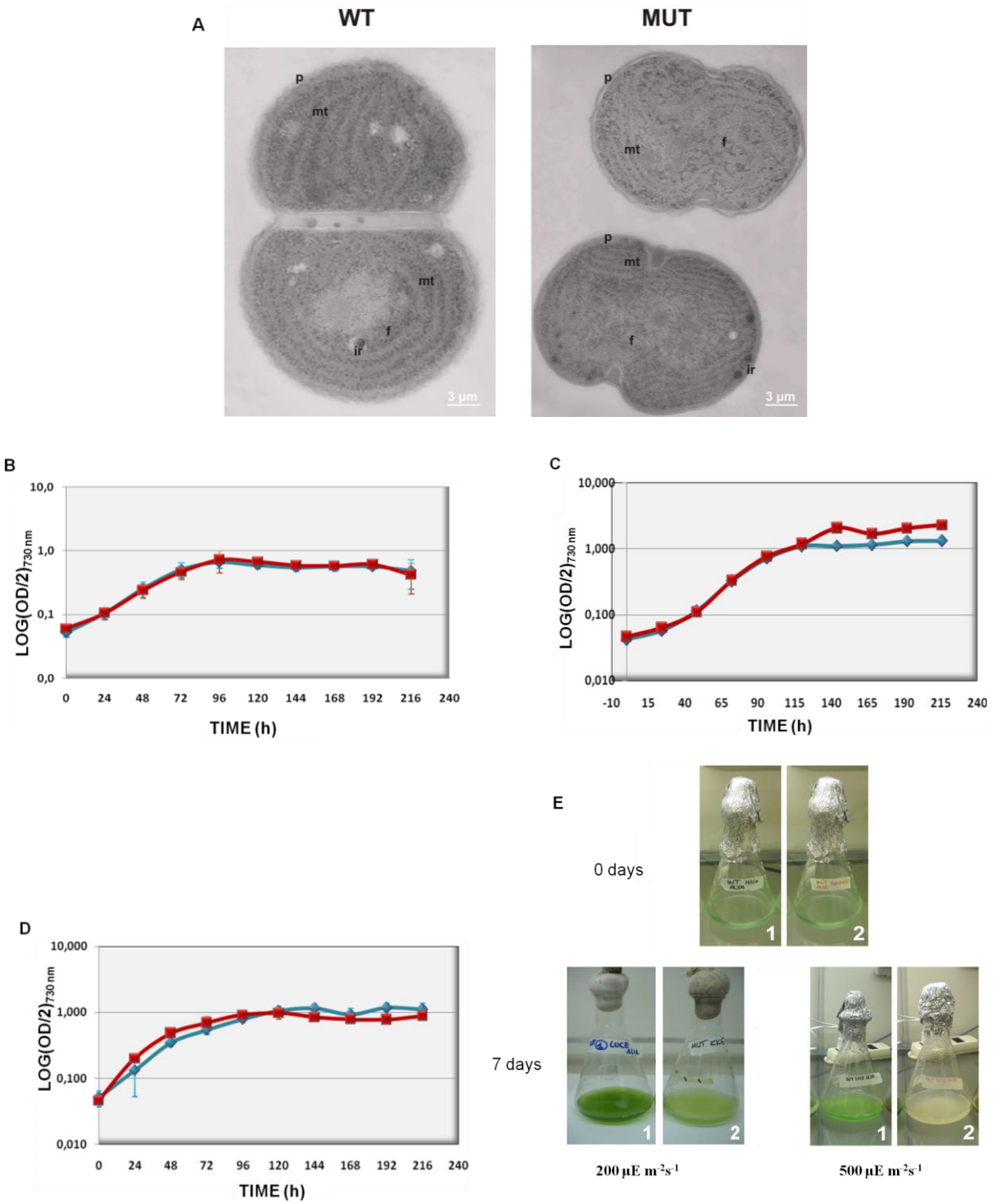

Figure 6. Mutant cells do not display altered membrane organization but are more photosensitive with respect to wild-type organisms. A) Transmission electron microscopy of Synechocystis sp. PCC 6803 cells. Wild-type and mutant cells grown in BG-11 supplemented with 5 mM glucose under 50 µE $m^{-2}s^{-1}$ light condition for 48 h. Scale bar = 3 µm, p= cellular wall, mt= thylakoidal membrane, f = phycobilisomes and ir = including reserve. B) Growth of wild-type (WT) and ΔSynK cells on liquid BG11 medium supplemented with 5 mM glucose in the dark. The measure of O.D. was performed using the plate reader Spectra Max 190 (Molecular Devices) using 300 µl of the culture. The measurements were conducted every 24 hours. Optical density at 0 time point was 0.1 (at 730 nm). C) Cells were grown in BG11 medium supplemented with 5 mM glucose and 0.5 M sorbitol, and O.D. was determined as above. D) Cells were grown in BG11 medium supplemented with 5 mM and 0.5 M NaCl. E) Comparison of growth profile of Synechocystis wild type and ΔSynK. Cells growing in liquid culture under different light conditions, 200 and 500 µE $m^{-2}s^{-1}$, are shown. Cells were grown with an initial optical density of 0.1 (at 730 nm) and culturing was continued for 7 days. For each growth curve medium value ±SD are shown (n=3-5). Bleaching was reproducibly observed in 6 independent experiments.

III. DISCUSSION

The physiological role of potassium channels in prokaryotes is still largely unexplored. Here we show that SynK, a voltage-dependent potassium channel of *Synechocystis*, previously shown to be located in the thylakoid membrane in this organism, has a direct effect on photosynthesis. In particular, SynK is necessary for the efficient formation of the transthylakoid proton gradient and seems to be involved in the counterbalance ion flux. During photosynthesis, proton influx into the lumen is counterbalanced by exit of positive charges. Pharmacological experiments suggested that in higher plants the counterion might correspond to potassium and/or magnesium. Our results indicate that potassium flux via SynK importantly contributes to counterbalance, however does not account for all of the ion flux, at least in cyanobacterial thylakoids. The finding that the electron transfer rate is compromised in the mutant at normal but not low light intensity, and the mutant seems more susceptible to high light intensity with respect to the WT suggests that potassium flux via SynK comes into play especially at higher light intensities. According to the counterbalance hypothesis, lack of the efflux of positive charges from the lumen toward the stroma in chloroplasts or the cytoplasm in cyanobacteria, should lead to accumulation of positive charges and therefore of positive-inside electrical potential on the luminal side. As a consequence, influx of protons should become decreased, leading to impaired electron flux and impaired oxygen evolution. Our data show indeed a significantly reduced proton gradient formation across the thylakoid as well as an impaired electron transport rate and oxygen evolution in the SynK-less mutant, and thus are compatible with the above hypothesis. SynK thus is the first ion channel the function of which has a direct effect on photosynthesis. Importantly, ETR and PSII assembly are not altered in the mutant cultured at low light intensity, indicating that the mutation itself does not have an impact on the photosynthetic apparatus. This result also makes unlikely an indirect effect of the lack of the channel via regulation of osmotic strength, previously shown to affect photosynthesis.

Decreased electron flux should lead to a change in PSII photochemistry. Absorption of photons by pigments associated with PSII elevates them to an electronic excited state. These pigments return to the ground state primarily via three routes. Measurement of fluorescence from cells under a given condition can be used to gather real-time information on the status of the photosynthetic process. One such measurement is the determination of the ratio of variable fluorescence to maximal fluorescence (Fv/Fm), which is interpreted as a measure of maximal quantum efficiency of PSII photochemistry. We found a significant decrease in this parameter in the mutants grown under normal light intensity. When compared with the WT, a decreased rate of photosynthetic electron transfer correlated with a decrease of PSII activity in thylakoid membranes. In contrast, the content of PSI remained unchanged within the range of error in the mutant. This dynamic in the stoichiometry of photosynthetic membrane proteins is in agreement with observations that the amount of PSI in *Synechocystis* sp. PCC 6803 thylakoid membranes remains stable, whereas the amount of PSII varies according to the change of external parameters. Lack of the channel as well as DBMIB at the concentration used is expected to cause a dysfunction of the cytochrome *b6f* complex (the former in terms of proton pumping ability against a larger proton gradient in the mutant with respect to WT) which causes a highly reduced PQ pool, previously shown to result in a decrease of functional PSII population by Rogner and colleagues who described a cyanobacteria mutant lacking ssr2998, a protein associated with the cytochrome b6f complex and shown to regulate electron transport (Volkmer *et al.*, 2007) .

The reduced PSII activity and ETR observed in mutant cells at normal/high light intensities indicate an increased sensitivity of PSII to light stress in the mutant. When light perceived by photosynthetic organisms cannot be completely utilized for downstream processes, it leads to a redox imbalance and an excessive production of damaging reactive oxygen species (ROS). The recombination of Chl cation P_{680} with downstream electron transport cofactors pheophytin (Phe) or the primary stable electron acceptor plastoquinone Q_A can lead to the formation of triplet Chlorophyll states and ultimately to the formation of singlet oxygen, which in turn may damage the photosynthetic machinery. D1 protein of Photosystem II is degraded and replaced by a new copy every 5 h under low light growth conditions, and every 20 min under intense illumination in cyanobacteria, to guarantee the maintenance of a steady-state level of the D1 protein in PSII complexes. Due to the capacity of photosynthetic organisms to increase the turn-over rate of the D1 protein upon increasing light intensity, a decrease in the total amount of D1 protein occurs only upon prolonged and severe light stress, which results in impairment of the photosynthetic capacity, i.e., photoinhibition. In our case, photoinhibition and ROS accumulation likely occurs as indicated by the bleaching of the mutant culture after 7-10 days. Unfortunately, no technique for quantitative singlet oxygen and ROS determination in cyanobacterial cells has been described to our knowledge.

Recent studies of photoinhibition of PSII in cyanobacteria suggest that oxidative stress due to reactive oxygen species (ROS) inhibits the repair of PSII but does not stimulate the photodamage to PSII (Nishiyama *et al.*, 2001). ROS inhibit also the synthesis of the majority of the thylakoidal proteins. Thus, the decrease in PSII/PSI ratio we observe under normal light condition in the mutant which is more sensitive to light stress with respect the WT, may reflect an increased production of singlet oxygen which inhibits PSII repair and additionally, causes bleaching. In accordance with this hypothesis, we observed a slight decrease of chlorophyll content in the mutant already after 48 hs of culturing at normal light. Alternatively, the slight change in the PSII/PSI ratio in favour of PSI in the SynK mutant may reflect an adjustment of the ATP/NADPH ratio necessary for mutant growth under sub-optimal conditions. Acclimation of plants to sub-optimal, low light conditions, for example is known to involve reduction of the PSII/PSI ratio aiming at adjustment of the ATP/NADPH ratio through cyclic electron flow (Finazzi *et al.*. 1999). SynK does lead to impaired photosynthesis, but does not lead to significant decrease in optical density of the culture, suggesting that the lack of the channel does not fully compromise ATP production. Further work is needed to nail down the exact signalling mechanism leading from the decrease of counterbalance flux to the loss of pigmentation in the mutants.

While no information is available on regulation of photosynthesis by ion channels for cyanobacteria, in the case of higher plants mostly pharmacological experiments indicate involvement of potassium (Berkowitz *et al.*, 1995), calcium (Krieger, 1995) and chloride-selective channels (Segalla *et al.*, 2005) in the regulation of photosynthesis. Unfortunately only very few ion channels of the higher plant thylakoid have been identified from molecular point of view, hampering a systematic study of their physiological roles. We've recently identified TPK3 two-pore potassium channel, which seems to be related to SynK, in the thylakoid of *Arabidopsis* by using a specific monoclonal antibody (Zanetti *et al.*, 2010). The physiological role of TPK3 has still to be determined – homozygous mutants lacking TPK3 are not available in the seed banks to our knowledge. ClC^- also seems to be located in thylakoids (Marmagne *et al.*, 2007), although another study located it to the outer envelope membrane by proteomics (Teardo *et al.*, 2005). Plants lacking ClC-e did not display altered growth and showed a very subtle photosynthetic phenotype, furthermore the underlying mechanism has not been investigated (Marmagne *et al.*, 2007).

In summary, while the existence of ion channels in thylakoids is known for several decades, their molecular identity is still largely unclear. Identification of SynK in the cyanobacterial thylakoid allowed us to understand that the potassium flux across this channel contributes to the counterbalance and ensures maximally efficient photosynthesis. It has to be determined whether TPK3 plays a similar role in *Arabidopsis*. In higher plants however the high gene redundancy for potassium channels may hinder photosynthesis-related phenotype.

IV. MATERIALS AND METHODS

Strains and growth conditions

Synechocystis sp. PCC 6803 was maintained under photoheterotrophic growth conditions at 30°C under white light in BG-11 medium (17.65 Mm $NaNO_3$, 0.30 mM $MgSO_4 \cdot 7\ H_2O$, 0.25 mM $CaCl_2 \cdot 2H_2O$, 0.19 mM Na_2CO_3, 0.003 mM Na-EDTA, 0.029 mM citric acid, 0.030 mM Ammonio citrato ferrico, 46 µM H_3BO_3, 0.17 µM $Co(NO_3)_2 \cdot 6H_2O$, 0.32 µM $CuSO_4 \cdot 5H_2O$, 9.2 µM $MnCl_2 \cdot 4H_2O$, 1.6 µM $Na_2MoO_4 \cdot 2H_2O$, 0.77 µM $ZnSO_4 \cdot 7H_2O$, 0.17 µM $K_2HPO_4 \cdot 3H_2O$) supplemented with 10 mM TES/NaOH (pH 8.2), 0.3% $Na_2S_2O_3$-$5H_2O$, and 1.5% agar (separately autoclaved) or on liquid BG-11 medium. The heterotrophic conditions were characterized by the growth of bacteria in the presence of 5 mM or 30 mM D-glucose. Sugars were sterilized by filtration (filters with pore size 0.45 µm; Millipore Corp.) and were added to the culture media at the final concentrations indicated. Indeed, for the phototrophic conditions we used different illuminations: high, normal and low light regimes corresponded to 500, 50 and 5 µE m^{-2} s^{-1}, respectively. For dark condition, the flasks were wrapped with aluminum foil. In the mutant cultures, kanamycin was included in the medium at a final concentration of 50 µg/ml. For liquid cultures, the agar and thiosulfate were omitted and the cultures were continuously shaked.

Determination of chlorophyll concentration

Determination of chlorophyll concentrations in *Synechocystis* cells was carried out as described by Mac Kinney (1941). Briefly, chlorophyll was extracted by methanol and absorbance was measured at 666 nm.

Determination of protein concentration

The protein concentration was determined using the BCA method (Sigma), according to the standard procedure recommended by the manufacturer. We

read the absorbance at 562 nm. The protein concentration was determined from direct comparison with a calibration curve constructed using known concentrations of the protein albumin.

Sample preparation for electrophoresis and Western blotting

The wild type and mutant cultures were inoculated at optical density 0.1(λ=730nm) and grown for 48 hours at light intensities of 5 μE $m^{-2}s^{-1}$ (low light) and 50 μE $m^{-2}s^{-1}$ (normal light). The mechanical disruption of cells was performed by Bead Beater (GlenMills, USA). All steps were carried out at 4 °C in the dark to prevent the degradation of proteins. The bacterial cultures were centrifuged for 10 minutes at 12000 g. The supernatant was removed and the pellet was washed with 5 Mm Tris/HCl pH 8.0, 1 mM PMSF, 1 mM benzamidine and 1 mM caproic acid. Samples were again centrifuged at 12,000 g for 10 min. The supernatant was discarded and the new pellet resuspended in 20 mM Tris/HClpH 8.0, 600 mM sucrose, 1 mM PMSF, 1 mM benzamidine and 1 mM caproic acid. Then samples were incubated in 1/1 ratio with Glass Beads (Sigma G-1145), previously soaked in 20 mM Tris/HCl pH 8.0, 600 mM sucrose. The disruption of cells was confirmed by optical microscope analyses. After the sedimentation of the beads the supernatant was recollected and the chlorophyll and protein concentrations were determined and the samples were stored at -20 C.

SDS-polyacrylamid electrophoresis (SDS-PAGE) and Western-blotting

Protein samples were denatured in 10% SDS, 50% glycerol, 312.5 mM Tris/HCl pH 6.8, 15% β-mercaptoethanol and bromphenol blue. Denatured proteins were electrophoresed on polyacrylamide according to the method of Laemmli (1970). The proteins were electrophoretically transferred to nitrocellulose or PVDF membranes. The membranes were incubated for 1 h in blocking solution (10% skim milk powder in 100 mM Tris-HCl, pH 7.5, 150 mM NaCl) washed five times (100 mM Tris-HCl, pH 7.5, 150 mM NaCl; for 5 min each time) and then soaked for 2 h at room temperature in primary antibody diluted in blocking solution (without milk). After other washing, the membranes were incubated in agitation at room temperature with the secondary antibody. Primary antibody was detected by two different methods: a chemioluminescent and a colorimetric detection. For ECL reaction HRP-conjugated goat antirabbit antibody was used as secondary antibody and proteins were visualized with ECL (Pierce) In the second case we used a secondary antibody anti-rabbit alkaline phosphatase conjugate. The immunoreaction was visualized by incubation with 100 mM Tris-HCl, pH 9.5, 100mM NaCl, 5M MgCl2, 0.035% NBT (w/v), 0.0175% BCIP (w/v).

DNA Constructs and Transformation of ***Synechocystis* sp. PCC 6803**

The forward K+E (5'-GAGCCAGGAATTCATGTTT GGCAAATATCGAC-3') and reverse K+F (5'-ATGGGCTCGGATCCGATTCCTGTTCTTCC-3') primers, introducing restriction sites *EcoRI* and *BamHI* respectively, were used to generate a PCR product including exactly the slr 0498 open reading frame. The *EcoRI-BamHI* fragment, subsequently obtained by restriction digestion, was then cloned into the same sites of plasmid pEGFP-N1 (Clontech) to give plasmid pEGFP-SynK. In the new plasmid, the entire insert was completely sequenced to verify that no undesired mutation had been inserted by Taq polymerase (Platinum® Taq DNA Polymerase High Fidelity, Invitrogen).
The construct for mutagenesis of *Synechocystis* was produced as follows. A SpeI-BstXI fragment, corresponding to the central portion of the slr 0498 sequence and including the coding region for the pore, was deleted from plasmid pEGFP-SynK and substituted by a synthetic adaptor introducing a PstI restriction site. A kanamycin-resistance gene (kan^r), derived by PstI digestion from plasmid pUC4K (Pharmacia), was cloned into this site of the obtained pEGFP-SynK plasmid. The final construct was used to transform wild-type *Synechocystis* sp. PCC 6803.

Oxygen Evolution Measurements

Experiments were performed using a Clark electrode (Hansatech CBID) as described by Walker (1987). The wild type and mutant strains were grown (start optical density 0.1 at 730 nm) at a light intensity of 50 μmol photons m-2 s-1. The measures of oxygen evolution were performed after 48 hours (in exponential phase). Chlorophyll concentration was equal to 10 μg/mL in all of the experiments, and oxygen evolution was measured at 25 °C in the dark, followed by the application of light with an intensity of 2000 μE$m^{-2}s^{-1}$. The measurement is made in the presence of 5mM bicarbonate. The Fluorescence Induction Program (FIP) allowed the determination of the rate of oxygen evolution, expressed in V/s, by a linear fitting of the curves obtained under various conditions and the expression of it as μmol O_2/(mg Chl × h) by taking into account the chlorophyll concentration, the volume of the experimental mixture, the oxygen content of air-saturated water at 25 °C, and calibration of the oxygen electrode. Experiments were repeated at least nine times, and mean standard deviation (±SD) values are reported

in the figures. Independent unpaired *t* tests were performed, and significant differences ($p < 0.05$).

Low temperature (77K) fluorescence spectroscopy

Two-day-old cultures were harvested by centrifugation (5000×g for 10 min at 25°C) and resuspended in fresh BG-11 at a chlorophyll concentration of 2,5 µg/mL. The samples were diluted and transferred into glass capillaries, and instantly frozen in liquid nitrogen. The analysis was performed at 77 K using a spectrofluorimeter. The excitation wavelengths were 435 and 580 nm.

***Chlorophyll a* fluorescence measurement**

The Fv/Fm paremeter, that indicates the efficiency of excitation energy capture by open PSII reaction center, was measured at room temperature using a Dual-PAM-100 (Walz, Germany). Before measurement, cells were dark-adapted for 10 minutes. The non-actinic fluorescence-measuring light was switched on to obtain the initial fluorescence (Fo). We applied actinic light intensity increasing from 0 µE m^{-2} sec^{-1} to 2000 µE m^{-2} sec^{-1}. Maximal fluorescence (Fm) was measured using illumination with a pulse of red saturating light (10000 µE m^{-2} s^{-1}). Fv/Fm was calculated as (Fm−Fo)/Fm. Saturating pulses were given at intervals of 20 sec. The variable fluorescence (Fv) was calculated as (Fm - Fo), and the ratio Fv/Fm reflects the potential yield the photochemical reaction of PSII.

Measurement of ΔpH across thylakoids in cyanobacteria

Time-resolved measurements of fluorescence indicator Acridine Orange (AO) with *Synechocystis* 6803 cells at 30°C were performed according to Teuber *et al.*. (2001), with a PAM101/102/103 fluorimeter (Walz, Germany) with GFP filter set (excitation at 480 nm, cut-off < 505 nm; emission with long-pass filter 515 nm, cut-off 575 nm). To avoid a high background of phycobilisome or chlorophyll fluorescence, AO fluorescence was recorded below 575 nm. The cell suspension was supplemented with 50 mM Tricine (pH 8) and incubated with 5 µM indicator in the dark for 20 minutes before measurements. Actinic light was applied by fiber optic and was low enough to avoid actinic effects. Chlorophyll concentration was adjusted to 10 µg/ml. Although a simple relation between fluorescence quenching due to accumulation of protonated amines in the lumen and ΔpH across the thylakoid membrane has been proposed, this method only allows a semi-quantitative indication of pH changes in intact cyanobacteria. In general, the cytoplasmic pH increases by about 0.5 units, while the lumen pH decreases by the same amount when cells are illuminated at an external pH 8, as determined by other techniques.

Electron microscopy

Pellets of cyanobacteria were fixed overnight at 4°C in 3% glutaraldehyde in 0.1 M sodium cacodylate buffer (pH 6.9) and then processed for electron microscopy according to Rascio *et al.*. (1999). Ultrathin sections, cut with an ultramicrotome (Ultracut, Reichert-Jung), were post-stained with lead citrate and examined under a transmission electron microscope (TEM 300, Hitachi) operating at 75 kV.

V. REFERENCES

Barber J, Mills JB, Nicolson J (1974) Studies with cation specific ionophores show that within the intact chloroplast Mg^{2+} acts as the main exchange cation for H^+ pumping. FEBS Lett 49: 106–110

Bernát G, Waschewski N, Rögner M. (2009) Towards efficient hydrogen production: the impact of antenna size and external factors on electron transport dynamics in *Synechocystis* PCC 6803. Photosynth Res. 99:205-16.

Berry S, Esper B, Karandashova I, Teuber M, Elanskaya I, Rögner M, Hagemann M. (2003) Potassium uptake in the unicellular cyanobacterium *Synechocystis* sp. Strain PCC6803 mainly depends on a Ktr-like system encoded by slr1509 (ntpJ). FEBS Lett. 548: 53-58.

Biophys Acta 852: 68–73

Campbell D, Hurry V, Clarke AK, Gustafsson P, Oquist G. (1998) Chlorophyll fluorescence analysis of cyanobacterial photosynthesis and acclimation. Microbiol Mol Biol Rev. 62:667-83.

Chen G-Q, Ciu C, Mayer M-L, Gouaux E (1999) Functional characterization of a potassium-selective prokaryotic glutamate receptor. Nature, 402: 817-821.

Chow WS, Wagner G, Hope AB (1976) Light-dependent redistribution of ions in isolated spinach chloroplasts. Aust J Plant Physiol 3: 853-861

Cortes,D.M. and Perozo,E. (1997) Structural dynamics of the Streptomyces lividans K^+ channel (SKC1): oligomeric stoichiometry and stability. Biochemistry, 36, 10343-10352.

Cruz,J.A., Sacksteder,C.A., Kanazawa,A. and Kramer,D.M. (2001) Contribution of electric field (ΔΨ) to steady state transthylakoid proton motive force in vitro and in vivo. Control of pmf parsing into ΔΨ and ΔpH by ionic strength. Biochemistry, 40, 1226-1237.

Dilley RA, Vernon LP. (1965) Ion and water transport processes related to the light-dependent shrinkage of spinach chloroplasts. Arch Biochem Biophys. 111:365-75.

Edwards GE, Walker DA. (1984) Influence of glycerate on photosynthesis by wheat chloroplasts. Arch Biochem Biophys. 231:124-35.

Epstein W (2003) The roles and regulation of potassium in bacteria. Prog. Nucleic Acid Res. Mol. Biol. 75:293-320.

Epstein W. (2003) The roles and regulation of potassium in bacteria. Prog Nucleic Acid Res Mol Biol. 75:293-320.

Fang Z, Mi F, Berkowitz GA. (1995) Molecular and Physiological Analysis of a Thylakoid K+ Channel Protein. Plant Physiol. 108:1725-1734.

Finazzi G, Furia A, Barbagallo RP, Forti G. (1999) State transitions, cyclic and linear electron transport and photophosphorylation in Chlamydomonas reinhardtii. Biochim Biophys Acta. 1413:117-29.

Hihara,Y., Sonoike,K., Kanehisa,M. and Ikeuchi,M. (2003) DNA microarray analysis of redox-responsive genes in the genome of the cyanobacterium *Synechocystis* sp. strain PCC6803. J. of Bacteriology, 185, 1719-1725.

Inaba M, Sakamoto A, Murata N. (2001) Functional expression in Escherichia coli of low-affinity and high-affinity Na(+)(Li(+))/H(+) antiporters of *Synechocystis*. J Bacteriol. 183:1376-84.

Koropatkin N, Randich AM, Bhattacharyya-Pakrasi M, Pakrasi HB, Smith TJ. (2007) The structure of the iron-binding protein, FutA1, from *Synechocystis* 6803. J Biol Chem. 282:27468-77.

Krieger A. (1995) Effect of the Ca2+ channel activator CGP 28392 on reactivation of oxygen evolution of Ca(2+)-depleted photosystem II. FEBS Lett. 367:173-6.

Marmagne A, Vinauger-Douard M, Monachello D, de Longevialle AF, Charon C, Allot M, Rappaport F, Wollman FA, Barbier-Brygoo H, Ephritikhine G. (2007) Two members of the Arabidopsis CLC (chloride channel) family, AtCLCe and AtCLCf, are associated with thylakoid and Golgi membranes, respectively. J Exp Bot. 58:3385-93.

Matsuda N, Kobayashi H, Katoh H, Ogawa T, Futatsugi L, Nakamura T, Bakker EP, Uozumi N. (2004) Na+-dependent K+ uptake Ktr system from the cyanobacterium *Synechocystis* sp. PCC 6803 and its role in the early phases of cell adaptation to hyperosmotic shock. J Biol Chem. 279:54952-62.

Mullineaux, C.W. (1992). Excitation energy transfer from phycobilisomes to photosystem I in a cyanobacterium. Biochimica et Biophysica Acta 1100, 285–292.

Mullineaux, C.W., and Allen, J.F. (1990). State 1-state 2 transitions in the cyanobacterium Synechococcus 6301 are controlled by the redox state of electron carriers between photosystems I and II. Photosynthesis Research 23, 297–311.

Murakami A, Kim SJ, Fujita Y. (1997Changes in photosystem stoichiometry i) n response to environmental conditions for cell growth observed with the cyanophyte *Synechocystis* PCC 6714. Plant Cell Physiol. 38:392-7.

Nazarenko LV, Andreev IM, Lyukevich AA, Pisareva TV, Los DA. (2003) Calcium release from *Synechocystis* cells induced by depolarization of the plasma membrane: MscL as an outward Ca2+ channel. Microbiology. 149:1147-53.

Nishiyama Y, Yamamoto H, Allakhverdiev SI, Inaba M, Yokota A, Murata N. (2001) Oxidative stress inhibits the repair of photodamage to the photosynthetic machinery. EMBO J. 20:5587-94.

Omata T, Ohmori M, Arai N, Ogawa T. (1989) Genetically engineered mutant of the cyanobacterium Synechococcus PCC 7942 defective in nitrate transport. Proc Natl Acad Sci U S A. 86:6612-6.

Omata T, Price GD, Badger MR, Okamura M, Gohta S, Ogawa T. (1999) Identification of an ATP-binding cassette transporter involved in bicarbonate uptake in the cyanobacterium Synechococcus sp. strain PCC 7942. Proc Natl Acad Sci U S A. 96:13571-6.

Pomati F, Burns BP, Neilan BA. (2004) Use of Ion-Channel Modulating Agents to Study Cyanobacterial Na(+) - K(+) Fluxes. Biol Proced Online. 6:137-143.

Remis D, Bulychev AA, Kurella GA (1986) The electrical and chemical components of the proton motive force in chloroplasts as measured with capillary and pH-sensitive electrodes. Biochim

Schonknecht, G.; Hedrich, R.; Junge, W.; Raschke, K. A voltage dependent chloride channel in the photosynthetic membrane of higher plant. Nature 1988, 336, 589-592.

Schrempf H, Schmidt O, Kümmerlen R, Hinnah S, Müller D, Betzler M, Steinkamp T, Wagner R. (1995) A prokaryotic potassium ion channel with two predicted transmembrane segments from Streptomyces lividans. EMBO J., 14: 5170-5178.

Segalla A, Szabo I, Costantini P, Giacometti GM. (2005) Study of the effect of ion channel modulators on photosynthetic oxygen evolution. J Chem Inf Model. 45:1691-700.

Stingl K, Brandt S, Uhlemann EM, Schmid R, Altendorf K, Zeilinger C, Ecobichon C, Labigne A, Bakker EP, de Reuse H. (2007) Channel-mediated potassium uptake in Helicobacter pylori is essential for gastric colonization. EMBO J. 26: 232-241.

Szabò,I., Petronilli,V., Guerra,L. and Zoratti,M. (1990) Cooperative mechanosensitive ion channels in Escherichia coli. Biochem.Biophys.Res.Com. 171, 280-286

Tchernov D, Helman Y, Keren N, Luz B, Ohad I, Reinhold L, Ogawa T, Kaplan A. (2001) Passive entry of CO2 and its energy-dependent intracellular conversion to HCO3- in cyanobacteria are driven by a photosystem I-generated deltamuH+. J Biol Chem. 276:23450-5.

Teardo E, Frare E, Segalla A, De Marco V, Giacometti GM, Szabò I. (2005) Localization of a putative ClC chloride channel in spinach chloroplasts. 579:4991-6.

Tester,M. and Blatt,M.R. (1989) Direct measurement of K^+ channels in thylakoid membranes by incorporation of vesicles into planar lipid bilayers. Plant Physiol. 91, 249-252.

Teuber,M., Rogner,M. and Berry,S. (2001) Fluorescent probes for non-invasive bioenergetic studies of whole cyanobacterial cells. Biochim. Biophys. Acta, 1506, 31-46.

Tsunekawa K, Shijuku T, Hayashimoto M, Kojima Y, Onai K, Morishita M, Ishiura M, Kuroda T, Nakamura T, Kobayashi H, Sato M, Toyooka K, Matsuoka K, Omata T, Uozumi N. (2009) Identification and characterization of the Na+/H+ antiporter Nhas3 from the thylakoid membrane of *Synechocystis* sp. PCC 6803. J Biol Chem. 284:16513-21.

Volkmer T, Schneider D, Bernát G, Kirchhoff H, Wenk SO, Rögner M. (2007) Ssr2998 of *Synechocystis* sp. PCC 6803 is involved in regulation of cyanobacterial electron transport and associated with the cytochrome b6f complex. J Biol. Chem. 282:3730-7.

Waditee R, Hossain GS, Tanaka Y, Nakamura T, Shikata M, Takano J, Takabe T, Takabe T. (2004) Isolation and functional characterization of Ca2+/H+ antiporters from cyanobacteria. J Biol Chem. 279:4330-8.

Zanetti, M., Teardo,E., La Rocca, N., Zulkifli, L., Checchetto, V., Shijuku,T., Sato,Y., Giacometti,G.M., Uozumi,N., Bergatino,E. and Szabò,I. (2010). A novel potassium channel in photosynthetic cyanobacteria, PLOS One 5, e10118

~ CHAPTER 2 ~

Cloning, expression and functional characterization of a Ca^{2+}-dependent potassium channel from *Synechocystis* sp. PCC 6803

Vanessa Checchetto[1], Elide Formentin[1], Giorgio Mario Giacometti[1], Ildikò Szabò[1*] and Elisabetta Bergantino[1*]
1 Department of Biology, University of Padova, Padova, Italy
* E-mail: elisabetta.bergantino@unipd.it (EB); ildi@civ.bio.unipd.it (IS)

Abstract— *Synechocystis* sp. PCC 6803 is a unicellular photosynthetic prokaryote that can acclimatize to a wide range of environmental changes (Glatz *et al*., 1999). A bioinformatic screening of *Synechocystis* proteome identified a putative 2TM channel (SynCaK) that displays sequence homology to MthK, a Ca^{2+}-dependent potassium channel from *M. thermoautotrophicum*. To understand whether SynCaK works as ion channel, we cloned and expressed it in fusion with EGFP in mammalian Chinese hamster ovary cells and studied its activity by patch clamp. In cyanobacteria the location of SynCaK in plasmamembrane was revealed by Western blotting of isolated membrane fractions. In order to understand its function in cyanobacteria, a SynCaK-deficient mutant (ΔSynCaK) of *Synechocystis* sp. PCC 6803 has been obtained. Characterization of the mutant has not revealed a clear phenotype up to now under normal growth conditions and upon osmotic or salt stress.

I. INTRODUCTION

Cyanobacteria are prokaryotic plant-like photosynthetic organisms. They are considered the ancestors of plant chloroplasts. It is thought, in fact, that in Proteozoic or in the early Cambrian, cyanobacteria began to take up residence within certain eukaryote cells in an endosymbiontic process. Our attention is focused on the cyanobacterium *Synechocystis* sp. PCC 6803. It is considered a model organism in the field of photosynthesis and is the first photosynthetic organism for which the complete genome was sequenced (Kaneko *et al*., 1996).

Synechocystis sp. PCC 6803 is characterized by an intracellular membrane system, the thylakoids, where both photosynthesis and respiration take place; it can grow in the absence of photosynthesis if a suitable carbon source such as glucose is provided (Williams, 1988) and it is spontaneously transformable and is able to integrate foreign DNA into its genome by homologous recombination.

Channels are ubiquitous membrane proteins that control the passage of ions through the biological membranes. These proteins, present in viruses, prokaryotes and eukaryotes, allow a correct ion distribution necessary to cellular functions. The basic properties of the channels are selectivity and gating, the first being the process of ion flow across the membrane and the second the process of opening and closing the ion pathway (Hille, 2001). Potassium (K^+) is the most abundant cation in organisms and plays a crucial role in the survival and development of cells, by regulating enzyme activity and tuning electrochemical membrane potential.

The study of prokaryotic potassium channels underwent a rapid development over the past years thanks to the application of a combination of bioinformatics and molecular biology approaches. Understanding their structure and function would allow to gain more information about several processes in prokaryotic, but also in eukaryotic cells.

By means of a bioinformatic screening we identified in *Synechocystis* sp. PCC 6803 a protein classified as a putative potassium channel (NP_440478, encoded by the open reading frame *sll*0993). Until now, no experimental evidence about its function has been reported. To evaluate the SynCaK function we isolated the coding sequence by PCR from the *Synechocystis* genomic DNA, we produced a fusion protein SynCaK-EGFP that was expressed in Chinese hamster ovary cells and then we analyzed the protein function by patch-clamp. Furthermore a SynCaK-deficient mutant was obtained and partially characterized.

II. RESULTS AND DISCUSSION

Structural features of the SynCaK channel

A search in the non-redundant protein database at the National Center for Biotechnology Information, using the W-BLAST algorithm and the amino acid sequence (T-X-G-[Y-F]-G-[D-E]) as a query, revealed in *Synechocystis* sp. PCC 6803 a protein classified as a putative potassium channel (NP_440478). Until now, there is no experimental evidence about the function of this protein but sequence analyses underlines a sequence homology with MthK, a calcium dependent potassium channel from the archeon *Methanobacterium thermoautophicum* (Jiang *et al*., 2002). Using several

structural prediction programs, we performed an *in silico* analysis of the primary sequence and we observed that SynCaK, like MthK, contains two membrane spanning segments, a recognizable K^+ channel signature sequence, with only conservative substitutions, and a regulatory sequence for K^+ conductance (RCK) (Figure 1A, 1B). RCK domain is a binding motif observed in different prokaryotic and eukaryotic proteins, all containing an alternating βαβαβ Rossmann-fold structural arrangement (Bellamacina, 1996). For K^+ channels, RCK domains allow regulation by cytosolic ligands other than nucleotides. The RCK domain is homologous to the pair of domains that constitute TrkA, the intracellular component of the Trk system of prokaryotic K^+ transporters (Derst & Karschin, 1998; Durell *et al*., 1999; Parra-Lopez *et al*.,1994). The RCK domains present in *Synechocystis* TrkA contain the NAD binding glycine motif, GXGXXXG...D, indicating a particular ligand binding function (Bellamacina, 1996). The former includes a Rossmann motif, which may bind to NAD^+ or NADH, so mediating conformational switches. Since TrkA-N and TrkA-C are also present in the MthK channel, a similar domain organization for SynCaK is possible. The MthK RCK is a cytoplasmic regulatory domain and studies about crystal structure of the MthK channel revealed an octameric gating ring composed of eight intracellular ligand-binding RCK domains. Binding of Ca^{2+} by RCK regulates the gating ring conformation which in turn leads to the opening and closing of the channel.

Figure 1B shows the alignment of SynCaK with the aminoacid sequences of other potassium channels with two spanning membrane domains. The sequences were aligned using the Clustal W algorithm

A)

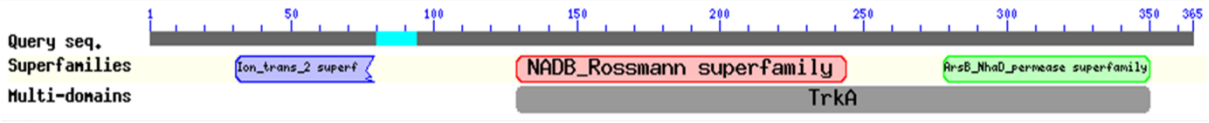

.

>gi|16329750|ref|NP_440478.1|
potassium channel [Synechocystis sp. PCC 6803]

MGLGSSSQENLLNLIDRQGRRLRQELMAGAITLAGLFVVGTAW
YRYVEDWTWLDAFYMTTI**TLATVGFGE**THPLSPASRLFT
ILLILMGLLTIGYMVNRFTEAFIQGYFQDSLRRRQEQKVIERL
ADHYILC**GYGRTG**QQIAFEFAVENIPFVVIDASPEVIIQA
KLRDYAVLQGDATLDEILLAAHIERAICIVSALSSDAENLYTV
LSAKTLNPKIRAIARASSEEAVQKLKRAGADEVVSPYITGGKR
LAAAALRPQVVSFVDGILTGADRSFYMEEFRIGAEDCPYIGQT
LREAQLRAQSGALILAIRRQDRKLIVGPMGDTHLLDADSLICL
GTVEQLRALNQLLCPLNPARVRLPKNHR

No.	N terminal	transmembrane region	C terminal	type	length
1	24	QELMAGAITLAGLFVVGTAWYRY	46	SECONDARY	23
2	75	SPASRLFTILLILMGLLTIGYMV	97	PRIMARY	23

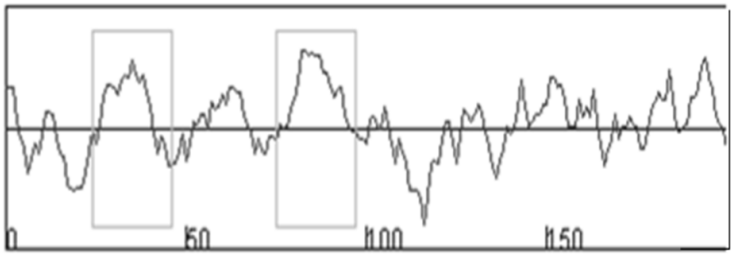

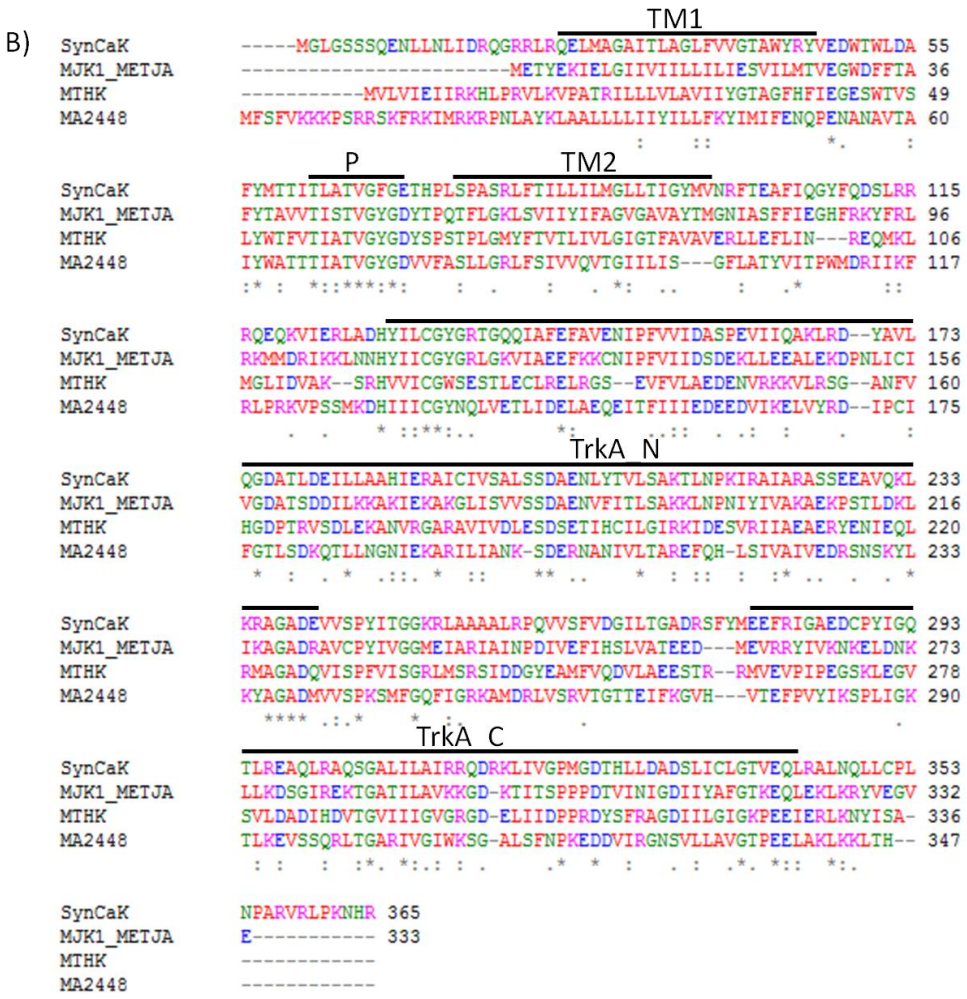

Figure 1: SynCaK primary structure. A) NP_440478 sequence: amino acid sequence of SynCaK. Red: typical selectivity filter of potassium channels (TXXTGFGE). Green: the NAD binding glycine motif. Hydropathy profile and amino acid sequence of two transmembrane helices. B) Clustal W alignment of SynCaK with the deduced amino acid sequences of other potassium channels with two transmembrane domains. Alignments of SynCaK sequence (accession number NP_440478) with potassium channel protein MJK1_METJA of *Methanocaldococcus jannaschii* (accession number Q57604), MthK channel of *Methanobacterium thermoautotrophicum* (accession number (O27564) and potassium channel protein of *Methanosarcina acetivorans C2A* (accession number NP_617354).

Identification of SynCaK channel in *Synechocystis* membranes

To determine the subcellular localization of SynCaK cytoplasmic and thylakoid membranes were isolated. We developed a specific polyclonal antibody against a specific sequence of 15 amino acids of the protein. In whole cyanobacteria cell extracts, the antibody recognized a band corresponding to the monomeric and tetrameric forms of SynCaK. Strongest recognition was observed of a 45 kDa band. The predicted MW of the monomer is: 40,51 kDa. To confirm that the recognitionwas specific, we performed also a competition assay (Figure 2A). While recognition of the tetrameric form as well as of two bands around the predicted MW (the one of 45 and the one of 40 kDa) seemed to be specific indeed, a band at about 42 kDa did not disappear, indicating the possibility of aspecific cross-reaction. Whether the 40 kDa is a partially degraded form of the 45 kDa protein, or, viceversa, the 45 kDa protein is a post-translationally modified form of the 40 kDa protein is unclear at present.

By Western blotting of an SDS-PAGE loaded with equal protein quantities of plasmamembrane (PM), soluble (SOL), thylakoid (THYL) fractions, the anti-SynCaK antibody recognized a strong 40 kDa band in the PM fraction (Figure 2B). We could also observe faint 40 kDa bands in THYL, whose intensities were consistent

with residual contamination from fraction purification. This was checked by using specific antibodies against markers for the plasmamembrane (NrtA), for the soluble fraction (PBS: allophycocyanin; LSU: large subunit of Rubisco) and for thylakoids (ATPase and CP43) (Figure 2C). In fact, a slight contamination of the thylakoid by PM can be observed. The protein in the soluble fraction recognized by our antibody might correspond to the 42 kDa aspecific band seen in whole cyanobacteria.

Expression of SynCaK in CHO and analysis of SynCaK-EGFP fusion protein localization.

Given that expression of SynCaK in *E.coli* was toxic for bacterial cells (data not shown), we decided to characterize the protein from its functional point of view by heterologous expression in mammalian cells followed by electrophysiological analysis. Such approach has been successfully applied by various groups for the study of prokaryotic and even viral channels. To verify the localization of the putative channel in the heterologous system, we constructed vectors for expression of the (wild-type and F68A mutant, see further) SynCaK genes in fusion with that coding for EGFP. This is a red-shifted variant of wild-type GFP which has been optimized for brighter fluorescence and higher expression in mammalian cells (excitation maximum = 488 nm;emission maximum = 507 nm). Genes were cloned to be expressed as fusions to the N-terminus of EGFP. At the same time, we produced a mutated form of SynCaK in the selectivity filter of the putative channel to be used as negative control for the electrophysiological experiments. The localization of both forms was studied in CHO cells. Once, transfected into mammalian cell, correct plasma membrane localization was a pre-requisite for the analysis of protein function by patch-clamp. We verified this condition by using a specific plasma membrane fluorescent dye (FM64). Figure 3 shows fluorescence microscopy analysis of CHO cells transfected with wild-type and mutant SynCaK-EGFP fusions, indicating that both forms reach at least in part the plasmamembrane.

Functional analysis.

Transfected CHO cells were analyzed by patch clamping in whole-cell configuration. While cells transfected with the control vector encoding only for EGFP did not display any current at different potentials (n=50) (Fig. 4B), SynCaK-transfected cells displayed an ion channel activity (Figure 4A) (n=14). The same experiment was performed also with the vector expressing the F68A SynCaK-EGFP fusion: in the latter, the introduced single point mutation changes a very conserved amino acid of the pore region, in general essential for potassium channel function

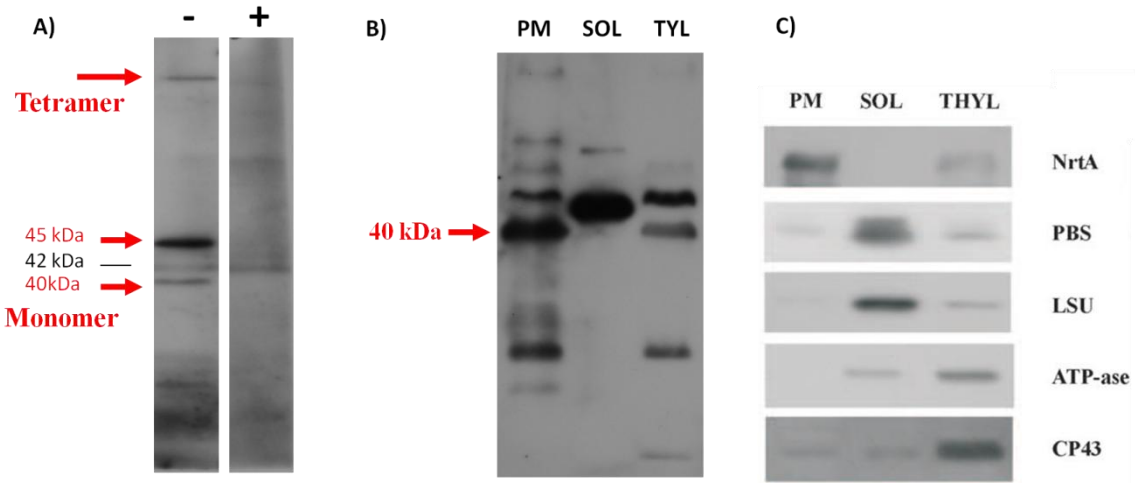

Figure 2: SynCaK localization: A) Left lane: in whole cyanobacteria the antibody recognizes the monomeric form(s (40 and 45 kDa) and the tetrameric form of the channel. Right lane: Competition assay performed in whole *Synechocystis* sp. PCC6803 cells. A membrane decorated using the antibody α-SynCaK incubated without peptide (lane -) and the membrane decorated using the antibody α-SynCaK incubated with peptide (lane +) and processed together are shown; B) Plasmamembrane (PM), soluble (SOL) and thylakoid membrane (THYL) fractions were isolated from *Synechocystis* (10 µg of proteins/lane). The membrane is decorated using Ab α-SynCaK at 1: 2500 dilution; C) The purity of fractions were checked by using antibodies against markers of the lasmamembrane (NrtA), of the soluble fraction (PBS: allophycocyanin; LSU: large subunit of Rubisco) and of Thylakoid (ATPase and CP43), 20 µg of proteins/lane.

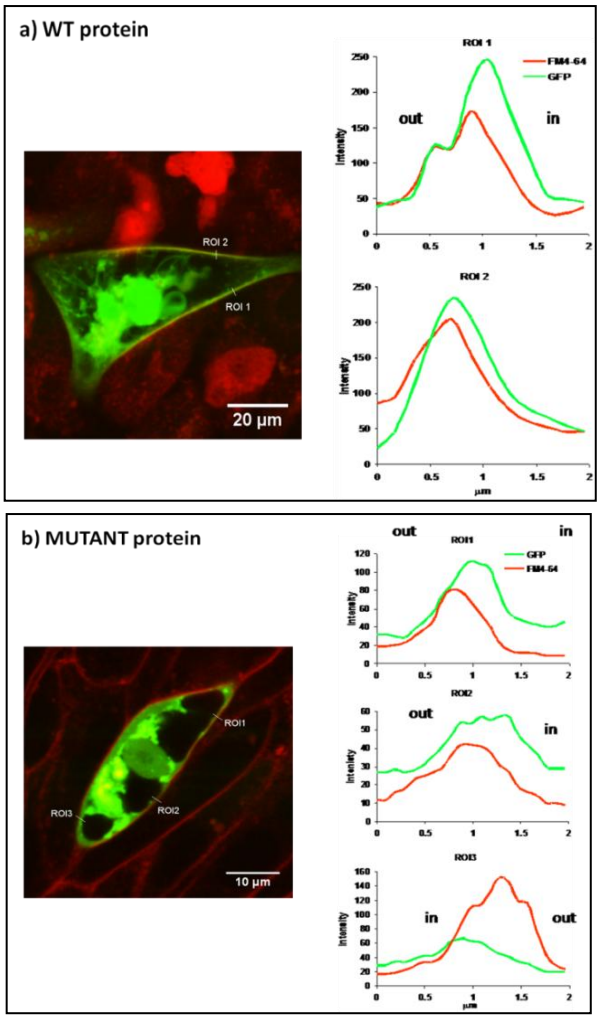

Figure 3: Expression of SynCaK in CHO cells. SynCaK-EGFP fusion expression in CHO cell plasma membrane as revealed by confocal microscopy. Co-localization of fusion proteins and plasma membrane-specific dye, FM-64 was observed. Overlapping is indicated by analysis of ROI (Region of interest). Images were analyzed using ImageJ (http://rsb.info.nih.gov/ij/index.html), in green EGFP and in red the PM dye. a) WT SynCaK protein, b) F68A SynCaK protein. Representative images are shown. Bars: 10 µm in WT image and 20 µm in MUTANT image.

In this latter case, transfected CHO did not display detectable currents (Figure 4C) (n=5). SynCaK activity was selective for cations, displaying a reversal potential of - 50 mV (n=3) while the predicted value for a perfectly selective potassium channel in our ionic conditions is -64 mV (data not shown).

To record single channel activity and to study the effect of cytoplasmic calcium on channel activity, we performed an analysis in the inside-out configuration. Control-transfected patches did not display any current in the presence of 2 mM calcium on the cytoplasmic side (Fig. 4D). In contrast, addition of 2 mM and 10 mM calcium to the bath (Fig. 4E and F) induced an increase of the open probability of the ion channel activity when working with SynCaK-expressing cells. These results suggest that calcium have direct effects on the opening and the activity of the channel, in accordance with the prediction that sll0993 might give rise to a calcium-activated potassium channel activity.

Disruption of the SynCaK gene in *Synechocystis*

Synechocystis PCC 6803 is capable to integrate exogenous DNA into its genome (present in a dozen of copies) by homologous recombination, thus allowing targeted gene replacement. Approximately four fifths of the 1098 nucleotide long ORF sll0993, encoding the SynCaK potassium channel, were substituted by a kanamycin resistance cassette (Figure 5A). Nine different knock-out mutants were recovered after ten rounds of subcloning and complete segregation was verified by PCR on purified genomic DNA. The figure shows that, according to PCR analyses, no wild-type DNA molecules were retained in the final clones.

The absence of the SynCaK protein in the mutant was evaluated also by Western-blotting (Figure 5B) confirming the lack of protein expression, even in the tetrameric form.

Study of physiological role of the SynCak

To evaluate the physiological role of the SynCaK protein, we initially compared growth of the wild type (WT) and mutant strain under different conditions. Until now, we observed the growth in presence of 0.5 M NaCl, 0.5 M Sorbitol, 0.01 M and 0.10 M $CaCl_2$, but we did not found a clear-cut condition of growth provoking significant differences between WT and mutant cell phenotypes so far. This part of the project is in progress (Figure 6).

III. SUMMARY

In the present work we've identified a calcium-dependent potassium channel in photosynthetic cyanobacteria. The sll0993 was cloned and expressed in CHO cells and proved to behave as a potassium-selective channel. Further electrophysiological experiments are required to better characterize the single channel activity of SynCaK and to determine the minimal calcium concentration needed to activate the channel. Given that very restricted information is available about the physiological role of ion channels in prokaryotes in general, it will be of utmost importance

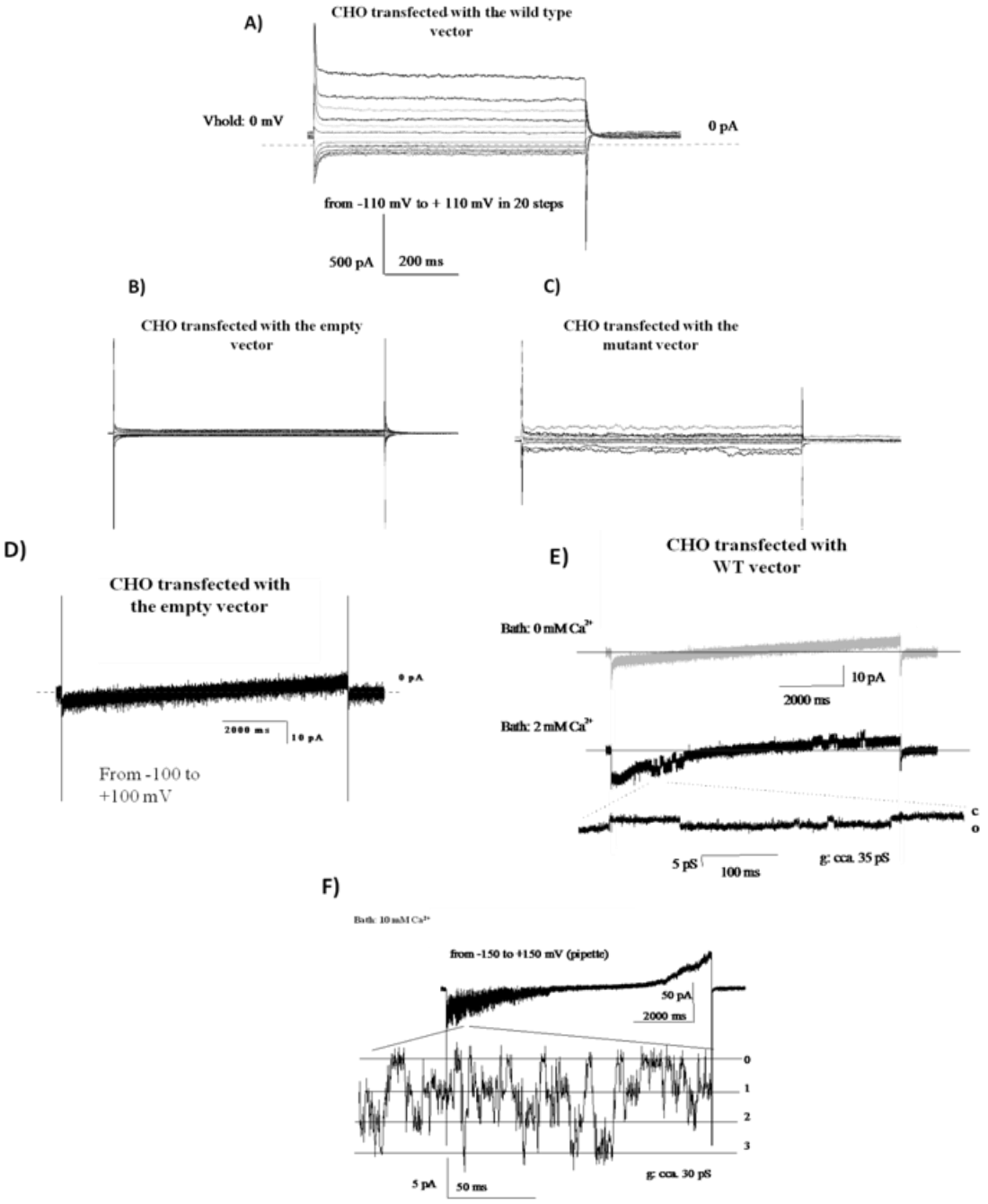

Figure 4 SynCaK functions as a potassium channel when expressed in CHO cells. A) Representative whole-cell currents in a pSynCaK-EGFP-transfected fluorescent cell, elicited by application of 20-mV steps voltage steps of 200 ms duration, from -110 to +110 mV. Patch pipette contained calcium. B) Representative whole-cell currents in a pEGFP-transfected fluorescent cell in the same conditions as in A). C) Representative whole-cell currents in a mutated F68A pSynCaK-EGFP-transfected fluorescent cell. In A) to C) , bath and pipette solutions contained 150 mM Na-gluconate, 5 mM KCl and 150 mM K-gluconate respectively. D) Inside-out configuration performed in pEGFP-transfected fluorescent cell: negative control in the presence of 2 mM Ca^{2+} in the bath. E) Representative single current trace in a pSynCaK-EGFP-transfected fluorescent cell, bath and pipette solutions contained 150 mM Na-gluconate and 150 mM K-gluconate respectively. When different concentration of calcium, i.e. 0, 2 and 10 mM $CaCl_2$,, were added to the bath solution (i.e. cytoplasmic side), an increase in the channels' open probability could be observed. Results are representative of 3 experiments.

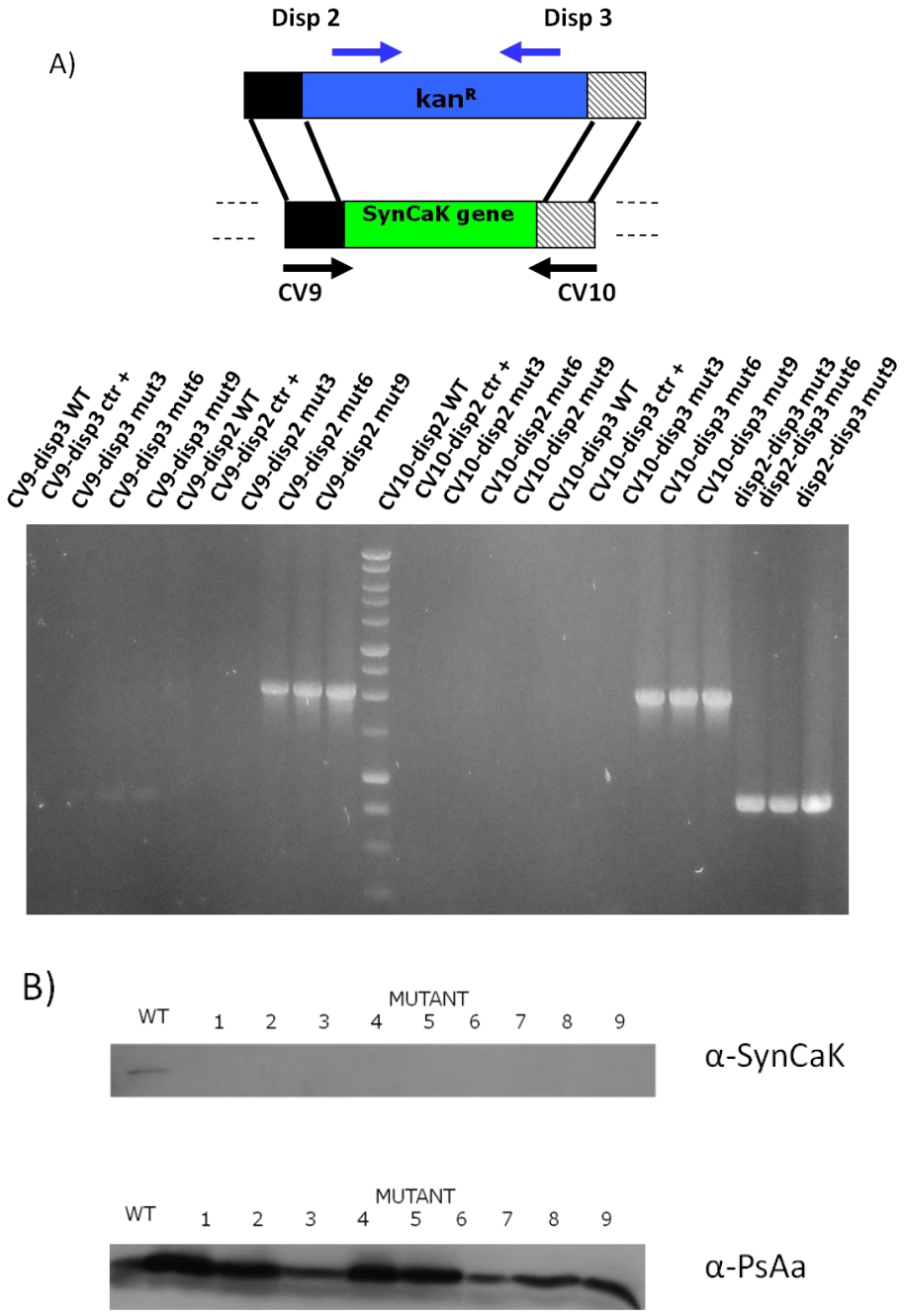

Figure 5: Construction of a SynCaK-deficient *Synechocystis* strain. A) Schematic diagram of construction of mutant organism. ΔSynK was obtained by inserting a kanamycin-resistance cassette into *Synechocystis* genome. Forward and reverse primers, introducing mutagenic sites, were used to generate a PCR product containing the SynCaK gene in the central position and two flanking regions. Wide portion of the *sll*0993 was substituted by a kanamycin-resistance cassette (see Experimental Procedures section for details). PCR analyses indicated no amplification of the WT gene and amplification of the kanamycin cassette in mutants (three representatives are shown). disp2-disp3 are primers that bind the Kanamycin cassette, while CV9 and CV10 bind in the *Synechocystis* genome. B) Western-blotting of protein extracts using the SynCaK antibody, showing no detection of SynCaK channel in mutant strains. The same membrane was treated using an antibody against PsaA, a protein of photosystem I, to test for equal loading.

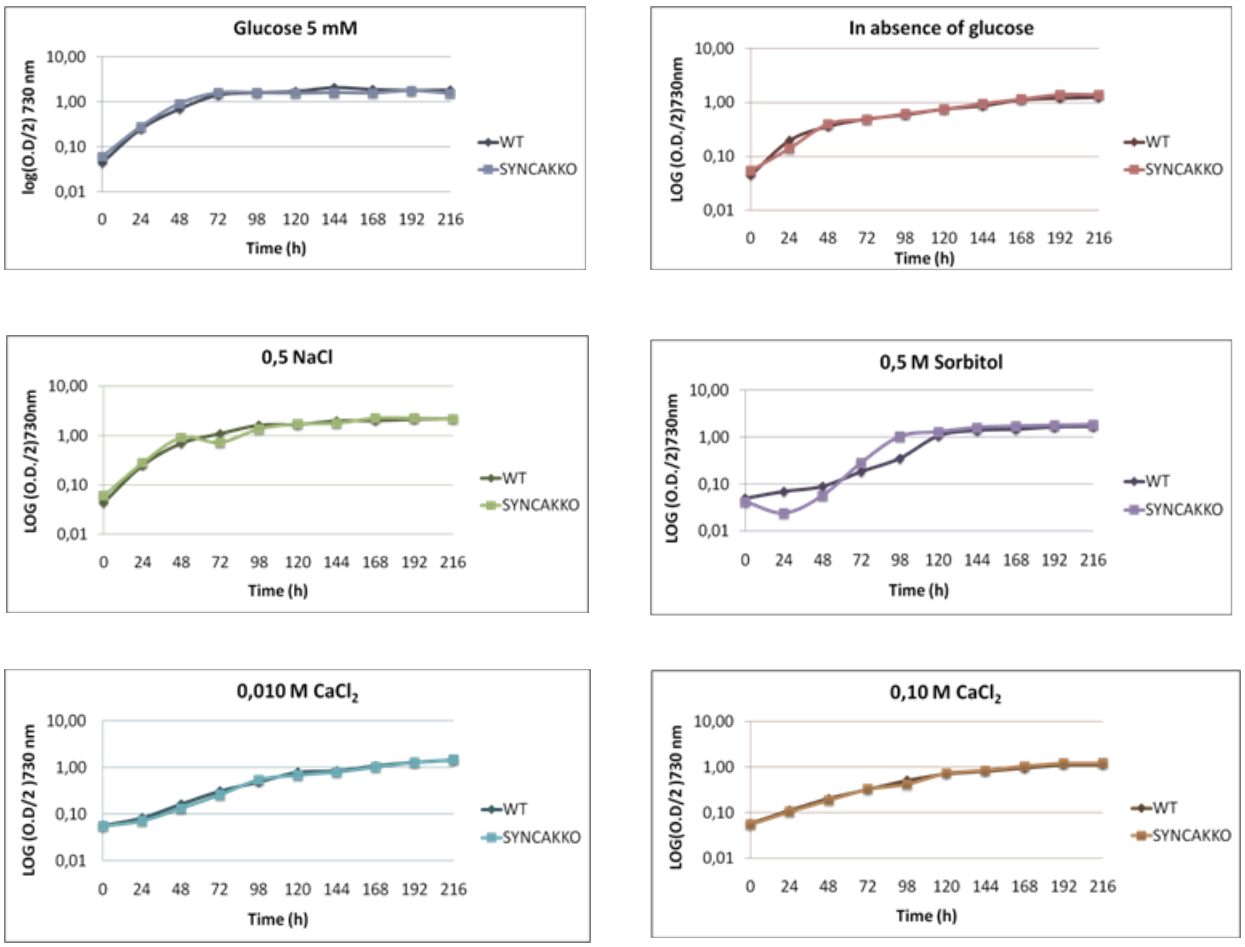

Figure 6:. Growth profiles of *Synechocystis* wild type and KO mutant. Growth of wild-type (WT) and mutant (**SynCaKKO)** cells on liquid BG11 medium with or without 5 mM glucose, or in BG11 medium supplemented with 5 mM glucose and 0,5 M sorbitol or 0,5 M NaCl or 0,010 M and 0,10 M $CaCl_2$. Curves shown are obtained from two independent experiments.

to determine the growth conditions under which a phenotype can be observed in the SynCaK-less organisms. This part of the work is still under way and hopefully will help to discover the role of SynCaK in cyanobacterial physiology. We intend to measure membrane potential of the PM in WT and mutant cells, as well as the internal potassium concentration. Furthermore, light and osmotic stress together will be applied as well as alkaline stress to uncover the role of SynCaK.

IV. MATERIALS AND METHODS

Strains and growth conditions

Strains cultured in BG-11 medium (Ono & Murata, 1982) supplemented with 20 mM TES-KOH (pH 8.2) (referred to as BG-11). The mutant strain grows in BG-11 added with 50 µg/ml kanamycin at 30°C under continuous illumination with rotary shaking.
The measurement of O.D. was performed using the plate reader Spectra Max 190 (Molecular Devices) at 730 mnm using 300 µl of the culture. For growth curves, the measurements were conducted every 24 hours (starting culture had an optical density of 0.1 (at 730 nm) for 9 days.

Determination of chlorophyll concentration and absorption spectra

Pigments were extracted with 100% (vol/vol) methanol (Lichtenthaler, 1987). The extracts were mixed, and the concentration of *chlorophyll a* was measured according to the method described by Mackinney (1941).

Determination of protein concentration

Total protein concentration was determined by the bicinchoninic acid (BCA) protein assay (Smith, 1989). We used the Sigma Bicinchoninic Acid Kit for Protein Determination.

Isolation of plasmamembrane, soluble and thylakoid membrane fractions from *Synechocystis*

Cyanobacteria cells were fractionated by performing a slight modification of the procedure described in Bolter *et al*., 1998 (see Zanetti *et al*., 2010).

SDS-polyacrylamid electrophoresis (SDS-PAGE) and Western-blotting

The electrophoretical separation of proteins in denaturing polyacrylamid gels was carried out according to the method of Laemmli (1970). For immunodetection, proteins were transferred onto a PVFD membrane. The membranes with bound proteins were first incubated for 1 h in blocking solution (10% skim milk powder in 100 mM Tris-HCl, pH 7.5, 150 mM NaCl) and then with primary antibody diluted (1: 2500) in blocking solution (without milk) for 2 hs at RT. Non-bound antiserum was removed from the membrane by wash buffer (100 mM Tris-HCl, pH 7.5, 150 mM NaCl, 0.1% Tween-20). HRP-conjugated goat anti-rabbit antibody was used as secondary antibody. Proteins were visualized with ECL Western Blot Detection Kit (Pierce). Anti-SynCaK antibody was produced against the synthetic peptide EQKVIERLADHYILC, corresponding to a specific sequence of SynCaK (Agrisera). For the competion assay, the α-SynCaK serum was pre-incubated for one hour at room temperature with 600 µM of the peptide used to immunize rabbits.

Construction of pSynCaK-EGFP vectors

The SynCaK gene was amplified by PCR from genomic DNA and cloned into pEGFP-N1 vector (Clontech). Primers were designed to introduce a HindIII site at the initiation codon and a BamHI site abolishing the stop codon, so that the gene could be expressed as fusions to the N-terminus of EGFP (SynCaK::EGFP). The HindIII-BamHI restriction fragment of PCR product was introduced into the pEGFP-N1 multiple cloning site, to give plasmid pSynCaK-EGFP. The single point mutation F68A was obtained by using the QuikChange Pulse protocol was applied and data analysis was performed using the Pclamp8 program set (Axon). The pipette resistance was 2-5 MegaOhm. Data were low

II Site Directed Mutagenesis Kit (Stratagene), to give plasmid pF68ASynCaK:EGFP. The recombinant construct obtained was verified by DNA sequencing. The wild-type and mutant fusion proteins SynCaK-EGFP were expressed in Chinese Hamster Ovary (CHO) cells and used in electrophysiological analysis, the mutant form being used as negative control.

CHO Cell culture and transfection

CHO cells were maintained at 37°C, 5% CO_2 in culture medium (DMEM, 10% fetal bovine serum, 1% penicillin/streptomycin and 1% non-essential amino acids). Cells were treated by standard trypsinization at 70-80% confluence. Culture medium was changed every 2 or 3 days to maintain good growth condition.
One day prior to transfection, the cells were trypsinized and counted; confluent layers of cells were grown on coverslips and were transiently transfected with Lipofectamine 2000 (Invitrogen) according to the manufacturer's instructions. Cells were transfected with 0,5 µg of DNA.

Confocal Microscopy

After transfection (48 hours), cells were incubated with FM® 4-64 dye (Invitrogen), a dye specific for plasmamembrane, and analyzed using a Leica LCS-SP2 system confocal microscopy (Leica Microsystems, Heidelberg, Germany). We prepared a working staining solution of 5 µg/mL dye in ice-cold HBSS (Invitrogen). The coverslip with the cells was washed once in HBSS and immersed in the ice-cold staining solution for 30 seconds. After removal from the staining solution, cells were then mounted on glass slides and observed with a laser-scanning confocal microscope. Fluorescence filters set was: excitation 488 and emission 520-660 nm. The images were analyzed using Leica LCS software (ImageJ).

Patch Clamp Analysis

Patch clamp experiments were performed in the whole-cell and inside-out patch configurations on control or transfected CHO cells. Bath solution: 150 mM Na-gluconate, 5 mM KCl, 2 mM $CaCl_2$, 10 mM Hepes, pH 7.2. Pipette solution: 150 mM K-gluconate, 10 mM EGTA, 1 mM $CaCl_2$, and 10 mM Hepes, pH 7.2. Transmembrane voltages were applied and currents were monitored using an EPC-7 amplifier (HEKA-List).

pass-filtered with an eight-pole Bessel filter with a cut-off frequency of 1 kHz and analyzed off-line.

Production of a ΔSynCaK *Synechocystis* mutant

Forward VC9FOR (5'-GGGCTGTCCATCGCTGTCGGGGT-3') and reverse CV10REV (5'-ACGCCCCCGGCCAGACCCTT-3') primers were used to generate a PCR product including the *sll0993* open reading frame. The MUT_FOR1 (5'-ACCATTTGAATTCGATATCCTCGTCGG-3') and MUT_REV4 (5'-CAACAAAGCATGCGATATCGTTTTGG-3') nested primers, introducing restriction sites (*EcoRI* and *EcoRV* MUT_FOR1; *SphI* and *EcoRV* MUT_REV4), were used with VC9/CV10 amplimer to generate a 2712 bp PCR product. This fragment was introduced in a TOPO TA vectors (Invitrogen) to give plasmid pSynCaK-topo1_4. In the new plasmid, the entire insert was completely sequenced to verify that no undesired mutation had been inserted by Taq polymerase (Finnzyme).

For the disruption of the SynCaK gene in *Synechocystis* PCC 6803, a mutagenic DNA fragment was assembled into pUC18 vector (Pharmacia). Three independent PCRs were performed: in the first two, parallel reaction plasmid pSynCaK-topo1_4 was used as template: primers MUT_FOR1 and MUT_REV2 (5'-GGATCCCATGGGGGACACCCATT-3') were used for the first PCR (PCR1, producing a 881 bp amplimer); primers MUT_FOR3 (5'-GAGGATCCCAATCCCATCCTAAAACC-3') and MUT_REV4 for the second PCR (PCR2, producing a 889 bp amplimer). In the third reaction the two partially overlapping 881 bp and 889 bp amplimers were used as template with primers MUT_REV2 and MUT_REV4, producing a final fragment containing a *BamHI* restriction site replacing the coding sequence *sll* 0993. This PCR product was cloned into the pUC18 vector (Pharmacia) by the mean of the EcoRI and SphI sites introduced at its boundaries.

A kanamycin-resistance cassette (kan^r), derived by *BamHI* digestion from plasmid pUC4K, was cloned into this site of the obtained plasmid. Lastly, the new plasmid was used to transform wild-type *Synechocystis* sp. PCC 6803 (Zang, Liu, Liu, Arunakumara, & Zhang, 2007). Transformants were selected by screening for antibiotic-resistance on BG-11 plates containing 10 µg/ml kanamicyn. After repeated subcloning, complete segregation of recombinant chromosomes in mutant strain was tested by PCR with primers: VC9FOR (5'-GGGCTGTCCATCGCTGTCGGGGT-3'), CV10REV (5'-ACGCCCCCGGCCAGACCCTT-3'), DISP2-rev (5'-ATAAATGGGCTCGCGATAATGTCGG-3') and DISP3-for (5'-CCGTCAAGTCAGCGTAATGCTCT GC-3').

V. REFERENCES

Bellamacina C.R. (1996). The nicotinamide dinucleotide binding motif: a comparison of nucleotide binding proteins. FASEB Journal. 10, pp. 1257-1269.

Derst, C., & Karschin, A. (1998). Review: Evolutionary link between prokaryotic and eukaryotic K+ channels. *The Journal of Experimental Biology, 201*(Pt 20), 2791-2799.

Durell, S. R., Hao, Y., Nakamura, T., Bakker, E. P., & Guy, H. R. (1999). Evolutionary relationship between K channels and symporters. *Biophysical Journal, 77*(2), 775-788.

Glatz, A., Vass, I., Los, D. A., & Vígh, L. (1999). The synechocystis model of stress: From molecular chaperones to membranes. *Plant Physiology and Biochemistry, 37*(1), 1-12.

Hille, B. (2001). Ion channels of excitable membranes.

Jiang, Y., Lee, A., Chen, J., Cadene, M., Chait, B. T., & MacKinnon, R. (2002). The open pore conformation of potassium channels. *Nature, 417*(6888), 523-526.

Kaneko, T., Sato, S., Kotani, H., Tanaka, A., Asamizu, E., Nakamura, Y., *et al*. (1996). Sequence analysis of the genome of the unicellular cyanobacterium synechocystis sp. strain PCC6803. II. sequence determination of the entire genome and assignment of potential protein-coding regions. *DNA Res, 3*(3), 109-36.

Laemmli, U. K. (1970). Cleavage of structural proteins during the assembly of the head of bacteriophage T4. *Nature, 227*(5259), 680-685.

Lichtenthaler H.K. (1987). Chlorophyll and carotenoids: Pigments of photosynthetic biomembranes. *Methods in Enzymology, 148*, 350-382.

Mackinney, G. (1941). Absorption of light by chlorophyll solutions. *Journal of Biological Chemistry, 140*(2), 315.

Ono, T. A., & Murata, N. (1982). Chilling-susceptibility of the blue-green alga anacystis nidulans: III. lipid phase of cytoplasmic membrane. *Plant Physiology, 69*(1), 125.

Parra-Lopez, C., Lin, R., Aspedon, A., & Groisman, E. (1994). A salmonella protein that is required for resistance to antimicrobial peptides and transport of potassium. *The EMBO Journal, 13*(17), 3964.

Smith, P. K. (1989). *Measurement of Protein using Bicinchoninic Acid,*

Williams, J. G. K. (1988). [85] construction of specific mutations in photosystem II photosynthetic reaction center by genetic engineering methods in synechocystis 6803. *Methods in Enzymology, 167*, 766-778.

Zanetti, M., Teardo, E., La Rocca, N., Zulkifli, L., Checchetto, V., Shijuku, T., *et al*. (2010). A novel potassium channel in photosynthetic cyanobacteria. *Plos One, 5*(4)

Zang, X., Liu, B., Liu, S., Arunakumara, K., & Zhang, X. (2007). Optimum conditions for transformation of synechocystis sp. PCC 6803. *The Journal of Microbiology* , 241-245.

Expression in *E.coli* of a putative calcium dependent potassium channel of the cyanobacterium *Synechocystis* sp. PCC6803

Vanessa Checchetto[a], Giorgio Mario Giacometti[a], Ildikò Szabò[a*] and Elisabetta Bergantino[a*]
[a]Department of Biology, University of Padova, Padova, Italy
[*]Corresponding authors. Tel. No +39 049 827 6342/6324; E-mail: elisabetta.bergantino@unipd.it (EB); ildi@civ.bio.unipd.it (IS)

Abstract— A calcium dependent potassium channel, coded by the ORF *sll* 0993 and named SynCaK, of *Synechocystis* sp. PCC 6803 was identified in the cyanobacterium proteome. Some features of this protein were analyzed by bioinformatic tools, showing that it displays sequence homology to the calcium dependent potassium channel from the archeon *Methanobacterium thermoautophicum* (Mthk), whose three-dimensional structure has been resolved (Jiang *et al*., 2002). To gain information about SynCaK activity, we plan to over-express the protein in *E. coli*. Indeed, recombinant channel proteins are often studied by electrophysiological techniques after incorporating them into an artificial bilayer system. The protein of cyanobacterial origin, however, resulted to be toxic in the chosen heterologous system. In the present work, we show that toxicity of the recombinant protein was mostly due to its channel activity. In fact, the use of a typical inhibitor of potassium channel, such as barium chloride, during expression could improve *E. coli* growth and yield of protein. (Work is in progress).

I. INTRODUCTION

Cyanobacteria are one of the oldest form of life on Earth. Some reports indicate that the time of appearance and evolution of cyanobacteria is thought to be closer to 2.7 billion years ago (Buick, 1992; Brasier *et al*., 2002). They are unicellular organisms, considered the ancestors of chloroplasts of higher plants. Today cyanobacteria grow in different environments, such as sluggish water, moist soil and wet rocks.

In particular, our attention is focused on *Synechocystis* sp. PCC 6803 strain. This cyanobacterium was isolated from a fresh water lake and is actually considered a model cyanobacterium. This organism displays various advantages for research, particularly in the field of photosynthesis. It can grow in a wide range of conditions, such as in the absence of photosynthetic activity when provided with a source of "fixable" carbon (e.g. glucose). Moreover, its entire genome sequence is available since 1996 (Kaneko *et al*., 1996) and it is handly for genetic manipulation, as it is easily transformable and prone to site-specific recombination. These properties together with its metabolic flexibility have allowed to use *Synechocystis* in the study of various processes dealing with the physiology of cyanobacteria, but also with that of other photosynthetic organisms, from algae to plants.

Ion channels selective for potassium are membrane proteins able to transport K^+ ions across biological membranes. In literature, various articles describe structure and activity of potassium channels in prokaryotes, animals and higher plants . However, the understanding of the mechanisms of ion transport is very limited in cyanobacteria, in fact the only cyanobacterial ion channels characterized up to now are the prokaryotic glutamate receptor GluR0 (Chen *et al.*, 1999), the ligand-gated channel GLIC (Bocquet *et al.*, 2007) and the voltage-gated SynK (Zanetti *et al*., 2010).

By homology search using the highly conserved selectivity filter amino acid sequence (T-X-G-[Y-E]-G-[D-F]-) as a query sequence, we identified in the genome of *Synechocystis* sp. PCC 6803 the sequence coding for a putative calcium dependent potassium channel (sll0993). The translated protein, that was named SynCaK, is predicted to harbour two membrane spanning segments, a recognizable K^+ channel signature sequence and a regulatory sequence for K^+ conductance (RCK).

The study of potassium channels is of great importance in cyanobacteria: it is thought that they can regulate the light phase of photosynthesis. In fact during photosynthesis, in chloroplasts of higher plants, a flow of potassium from the lumen to the stroma is required for counterbalance the entry of H^+ in lumen, while there is the formation of a H^+ gradient (not correlated with the formation of an electrical potential transmembrane) across the thylacoidal membrane. The transport of K^+ would electrically compensate the transport of protons from the stroma to the lumen, allowing acidification of the internal space and the concomitant alkalinization of the esternal space of thylakoids.

Protein reconstitution into artificial lipid bilayers represents a successful method for evaluating functional properties of protein channels. To this aim, we decide to start a protocol of over-expression of our candidate channel in the bacterial *E. coli* system.

II. RESULTS AND DISCUSSION

Heterologous protein expression in bacteria, preventing difficulties of purifying proteins with low yields from native tissue or organism, generally allows to obtain the great amount of polypeptides necessary to biochemical and functional characterization of gene products. The Gram-negative bacterium *E. coli* remains the easiest choice for recombinant protein expression and, obviously, the best one to produce protein from other bacterial species. Its widespread use is due to the ability to grow rapidly at high density in economical media, to the extensive knowledge of his genetic mechanisms and to the availability of a large number of cloning vectors and mutant strains.
A possible limit to the expression of procariotic proteins in *E. coli* can be its capability to afford, together with the metabolic load imposed by the process, the presence of huge quantities of the unfolded exogenous protein into the cytoplasm. Moreover, if the folded protein retains its functional properties, the physiology of the *E. coli* cell may be somehow affected.
Our aim was to obtain an adequate amount of purified SynCaK protein to perform electrophysiological experiments using artificial bilayer systems. Hence the *sll*0993 ORF was cloned in the inducible expression vector pET-28a. The system, based on T7 RNA polymerase, is known for the maintaining of genes that are very toxic to *E. coli*, assuring very low basal expression of target products and high levels of expression upon induction. Cloning was performed so that to direct the synthesis of a fusion protein with an His-tag at his C-terminus, a modification that would have allowed a simple and effective purification by affinity chromatography. As host for the expression we chose the *E. coli* strain CD41-DE3 (kind gift from Prof. Walker, University of Cambridge, UK), considered more tolerable and efficient than others for the expression membrane proteins.
Preliminary experiments performed in standard conditions (37°C, induction by 0,7 mM IPTG) were not satisfactory: growth of cells was clearly slown down when expression was turned on by the inducer, while no new band could be observed in SDS-PAGE of total extracts from induced cells. Very similar results were obtained by lowering growth temperature to 30°C, a condition often used to limit the synthesis, while favouring correct folding, of complex and/or toxic recombinant proteins (data not shown). We reasoned that the recombinant channel could interfere with the growth of *E. coli*. In fact once correctly synthesized, (even partially) folded and inserted into the membrane, it possibly destabilized the normal homeostasis of cells.
Therefore we planned to try SynCaK expression in the presence of $BaCl_2$, a classic inhibitor of potassium channels, to limit the eventual damage due to membrane protein toxicity. This measure had been already used by the group of Prof. Mackinnon, who succeeded in determining the X-ray structure of the recombinant voltage-gated potassium channel of *Methanobacterium thermoautophicum* produced in *E. coli* (Jiang *et al*., 2002).
First of all, we verified if $BaCl_2$ itself affected the growth of our strains. Curves were registered in the presence and absence of the inhibitor without the addition of the inducer IPTG at two different temperature, 30 and 37°C (Figure 1). The presence of the inhibitor was shown not to hamper cell growth rate, since measured O.D values were comparable with those of the control cultures (transformed cells with empty or recombinant plasmid). This result underlines that $BaCl_2$ has not significant effects in the normal *E. coli* homeostasis and on the survival of cells. Neither the combination of the two parameters growth temperature and presence of inhibitor did affect the growth.
We then proceeded to the expression of the SynCaK protein, by culturing non induced strains up to an O.D.=1 before induction with IPTG (0.7 mM). Again, cell growth was monitored by measuring the optical density. As shown in Figure 2, growth of control and SynCaK expressing cultures, were comparable until almost 1 hour after induction, while visibly differentiated later on. Both strains actively expressing the SynCaK protein changed their rate of growth. In particular, in the absence of $BaCl_2$ cell replication seemed completely hampered; in the presence of the specific inhibitor of channel activity, growth was maintained even though at a slower rate than the control. Comparable results were obtained for cultures grown at 30 and 37°C.
We infer that the toxicity of the protein in *E. coli* is mostly due to its residual channel activity, which is very likely detrimental to bacterial homeostasis, rather than to its over expression and/or to its unfavorable physical and chemical characteristics. We can therefore conclude that the *Synechocystis* protein is correctly translated and (at least partially) inserted into the membrane of the bacterial host, were it functions as a channel. Work is in progress to verify this conclusion: growth experiments will be repeated in *E. coli* strains expressing mutant forms of the channel devoid of functional activity. Vectors for the expression of a channel with a short deletion or a single point mutation, both located in

the highly conserved selectivity filter amino acid sequence, are under construction.
We finally verified identity and specifity of the recombinant (r) protein by Western-blotting with two different, specific polyclonal antibodies: α-His tag and α-SynCaK. The r-SynCaK was correctly expressed even though at a lower level than expected (not shown). We nevertheless started its purification by sonication and following fractionation of the obtained cellular suspension in supernatant and pellet. Aliquots of these fractions were loaded on SDS-PAGE and immunodetected after blotting, showing that no sufficient solubilization of the protein had been obtained (Figure 3). This work is in progress too, starting from the seeking for and the setting of a good purification protocol, with the aim of obtaining the channel in its functional form.

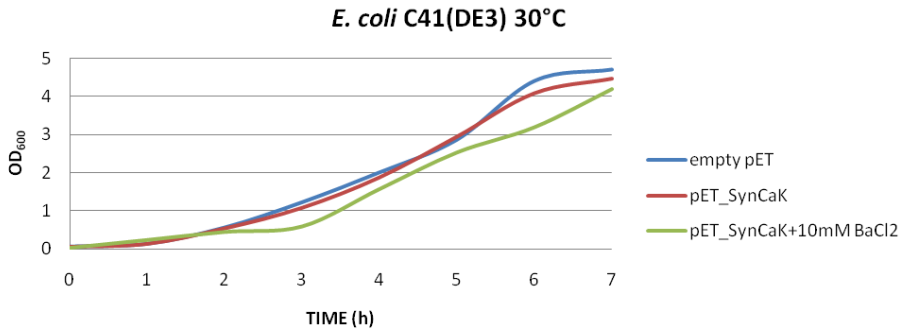

Figure 1: C41(DE3) GROWTH CURVES. Curves obtained by measuring the optical density at 600 nm. The cells were grown at at 30°C. The bacteria were transformed with the empty plasmid (BLUE), the construct containing the *sll 0993* sequence and grown in the presence (GREEN) and in the absence of $BaCl_2$ (RED). Comparable curves were drawn at the growth temperature of 37°C.

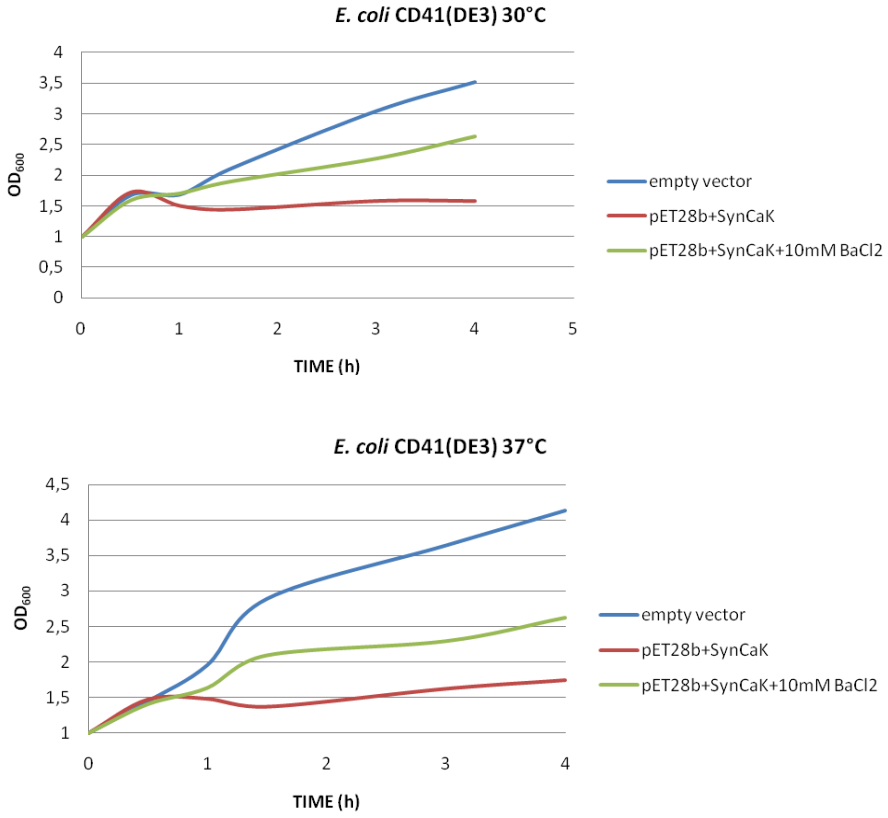

Figure 2: CD41(DE3) EXPRESSION CURVES. Induction of expression at T= 0 with 0.7 mM IPTG. Growth temperature: 37 C (down) and 30°C (bottom). BLUE LINE: control strain, RED LINE: strain transformed with plasmid pET28-SynCaK, grown without inhibitor; GREEN LINE: transformed strain, grown with $BaCl_2$.

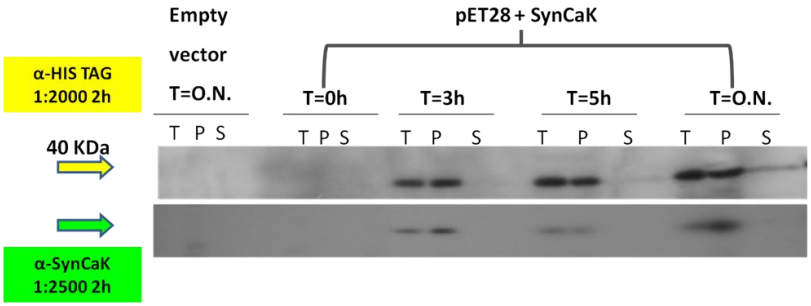

Figure 3: WESTERN BLOT OF PROTEIN EXPRESSED IN pET28-SynCaK TRANSFORMED CD41(DE3) CELLS. Induction at T= 0 with 0.7 mM IPTG. PVDF membrane decorated with α-His tag and α-SynCaK diluited as indicated. Control cells were transformed using the empty pET28a vector. T= whole cells, P= pellet and S= supernatant fractons.

III. MATERIALS AND METHODS

SynCaK gene was amplified by PCR and cloned into pEGFP-N1 vector (Clontech). This construct was used as template in two separate PCRs (30 cycles at 94°C, 20 sec; 64°C, 20 sec; 68°C, 1 min) with primers C-G_FOR (5'-ATTAATTGTGGGCCCGATGGGG-3') and pEGFP_Crick (5'-GTCCTGCTGGAGTTCGTG-3'), or pEGFP_Watson (5'-CGTCGCCGTCCAGCTCGACCAG-3') and C-G_REV (5'-CCCCATCGGGCCCACAATTAAT-3'), and high fidelity polymerase (Finnzyme). A following overlapping PCR (30 cycles at 94°C, 20 sec; 73°C, 20 sec; 68°C, 1 min) was performed using VC7 (5'-CGAGCTCAAGCCCATGGGATTGG-3', inserting a *NcoI* site) and CV8 (5'-GACCGGTGGCTCGAGATGGTTTTT -3', inserting a *XhoI* site) and both previous amplimers as template.

The PCR product and the expression plasmid pET28a(+) were digested with NcoI and XhoI, and ligated with T4 ligase. The resulting clone pET28a(+)-SynCaK was subjected to DNA sequencing and espressed in C41(DE3) cells (Miroux and Walker, 1996).

For protein expression, 1 ml pre-culture from one freshly transformed colony was grown overnight and used to inoculate 25 ml LB medium containing 50 µg/ml kanamycin at 37°C. Culture was grown under continuous shaking to A_{600}=1, expression was induced by 0.7 mM IPTG, then culture was devided and further grown at at two different temperatures, 37°C or 30°C for 24 h.

Aliquots of cells equal to A_{600}=1 were harvested at different times for each culture. Samples were centrifuged at 14,000xg for 3 minutes, recovered pellets were solubilized in Laemmli loading buffer (Laemmli, 1970).

Yield of expression was evaluated by Western blot using specific antibodies: anti-His-tag (SIGMA) and anti-SynCaK protein, produced against the oligopeptide EQVIERLADHYILC (purchased by Agrisera).

IV. REFERENCES

Brasier, M.D., Green, O.R., Jephcoat, A.P., Kleppe, A.K., Van Kranendonk, M.J., Lindsay, J.F., Steele, A., Grassineau, N. V.(2002) Questioning the evidence for Earth's oldest fossils, *Nature*, 247, 76-81.

Buick, R. (1991) Microfossil recognition in Archean rocks: An appraisal of spheroids and filaments from a 3500 M.Y. old chert-barite unit at North Pole, Western Australia, *Palaios* 5, 441-459.

Bocquet N., Prado de Carvalho L., Cartaud J., Neyton J., Le Poupon C., Taly A., Grutter T., Changeux J. P. & Corringer P. J. (2007). A prokaryotic proton-gated ion channel from the nicotinic acetylcholine receptor family 2, *Nature*. 445: 116-119.

Chen G-Q, Ciu C, Mayer M-L, Gouaux E (1999) Functional characterization of a potassium-selective prokaryotic glutamate receptor. Nature, 402: 817-821.

Jiang, Y., Lee, A., Chen, J., Cadene, M., Chait, B. T., & MacKinnon, R. (2002). The open pore conformation of potassium channels. Nature, 417(6888), 523-526.

Kaneko, T., Sato, S., Kotani, H., Tanaka, A., Asamizu, E., Nakamura, Y., et al. (1996). Sequence analysis of the genome of the unicellular cyanobacterium synechocystis sp. strain PCC6803. II. sequence determination of

the entire genome and assignment of potential protein-coding regions. DNA Res, 3(3), 109-36.

Laemmli (1970), Cleavage of structural proteins during the assembly of the head of bacteriophage T4. Nature 227, 680-685.

Miroux B. and Walker J.E. (1996) Over-production of Proteins in Escherichia coli: Mutant Hosts that Allow Synthesis of some Membrane Proteins and Globular Proteins at High Levels. J. Mol. Biol. (1996) 260, 289–298

Zanetti, M., Teardo, E., La Rocca, N., Zulkifli, L., Checchetto, V., Shijuku, T., et al. (2010). A novel potassium channel in photosynthetic cyanobacteria. Plos One, 5(4)

~ CHAPTER 3 ~

Plasma membrane aquaporin AqpZ is involved in cell volume regulation and sensitivity to osmotic stress in *Synechocystis* sp. PCC 6803

Masaro Akai[1], Kiyoshi Onai[2], Megumi Morishita[2], Yoshinori Yukutake[3,4], Hiroyuki Mino[5], Toshiaki Shijuku[1], Hideyuki Matsumoto[6], Hisataka Maruyama[6], Fumihito Arai[6], Vanessa Checchetto[7], Ildikò, Szabò[7], Hiroshi Miyake[8], Shigeru Itoh[5], Makoto Suematsu[4], Akihiro Hazama[9], Masato Yasui[3], Masahiro Ishiura[2], Nobuyuki Uozumi[1*]

[1] Department of Biomolecular Engineering, Graduate School of Engineering, Tohoku University Aobayama 6-6-07, Sendai 980-8579, Japan,
[2] Center for Gene Research, Nagoya University, Nagoya 464-8602, Japan,
[3] Department of Pharmacology and Neuroscience, School of Medicine, Keio University, Shinanomachi, Shinjyuku-ku, Tokyo 160-8582, Japan
[4] Department of Biochemistry and Integrative Medical Biology, School of Medicine, Keio University, Shinanomachi, Shinjyuku-ku, Tokyo 160-8582, Japan,
[5] School of Material Science (Physics), Graduate School of Science, Nagoya University, Furo-cho, Chikusa-ku, Nagoya 464-8602, Japan,
[6] Department of Bioengineering and Robotics, Graduate School of Engineering, Tohoku University, Aobayama 6-6-01, Sendai 980-8579, Japan,
[7] Department of Biology, University of Padova, Padova 35121, Italy,
[8] Graduate School of Bioagricultural Sciences, Nagoya University, Chikusa, Nagoya 464-8601, Japan,
[9] Department of Physiology, School of Medicine, Fukushima Medical University, Fukushima, 960-1295, Japan

Abstract— Aquaporins have been recognized as the primary water transport system in living cells since their first identification in red blood cells. The genome of the moderately halotolerant cyanobacterium, *Synechocystis* sp. strain PCC 6803 contains a single aquaporin gene, *aqpZ*. Here, we have studied the function of AqpZ and its physiological role in *Synechocystis*. The expression level of AqpZ was regulated by the circadian clock, and the peak of the AqpZ coordinated with the cell expansion in night. Oocytes expressing AqpZ exhibited significantly higher osmotic water permeability. AqpZ activity was insensitive to mercury in *Xenopus* oocytes and in *Synechocystis*. AqpZ was localized to the plasma membrane by immunoblotting after membrane fractionation as well as by immunogold labeling followed by electron microscopy. Stopped-flow light-scattering spectrophotometry showed that addition of sorbitol and NaCl decreased the cell volume of the *Synechocystis* Δ*aqpZ* strain more slowly than that of the wild type. When cells were exposed to hyperosmotic stress for an extended period of time both the wild type and mutant cells decreased in volume equally. The Δ*aqpZ* cells were more tolerant to hyperosmotic shock by sorbitol than the wild type. As consistent to this, recovery of oxygen evolution after a hyperosmotic shock with sorbitol was faster in the Δ*aqpZ* strain than in the wild type. Addition of NaCl has less effect on the growth rate and the oxygen evolution, compared with that of sorbitol. The amount of AqpZ protein remained unchanged by the addition of sorbitol, but decreased after addition of NaCl, indicating that the decrease of the AqpZ expression by high NaCl may help to protect water loss from cells. Our results show that *Synechocystis* AqpZ is directly involved in the control of cell volume through its function as a water transport system responding to osmolarity changes due to nonionic compounds, but not to salt stress due to NaCl.

I. INTRODUCTION

The photoautotrophic cyanobacterium *Synechocystis* sp. strain PCC 6803 (henceforth referred to as *Synechocystis*) is a useful model organism not only for the study of photosynthesis but also for understanding the process of osmoadaptation because this species belongs to the group of moderately halotolerant cyanobacteria (Rippka *et al.*, 1979). Cells have developed membrane transport systems to maintain cellular ion homeostasis and thereby secure their survival despite being exposed to frequent changes in the osmolarity of their environment. Sodium is an essential element for cell division, photosynthesis and pH regulation in cyanobacteria (Miller *et al.*, 1984; Zhao & Brand, 1988). *Synechocystis* contains several genes encoding Na^+/H^+ antiporters that mediate the exchange of Na^+ and H^+ across the plasma membrane and the thylakoid membrane.

These transporters supply or extrude not only Na^+ and H^+, but probably also K^+ (Tsunekawa *et al.*, 2009). The Ktr-type potassium transport system also contributes to protect cells from high salinity stress and high osmolarity (Berry *et al.*, 2003; Matsuda *et al.*, 2004). After an osmotic shock, a considerable amount of water immediately moves across the plasma membrane, mainly through water permeable channels called aquaporins. Water flux occurs simultaneously with the transport of ions across the membrane and the change in concentration of solutes synthesized de novo in the cells. *Synechocystis* accumulates the compatible solute glucosylglycerol to adjust its internal osmolarity in response to the external salt concentration or osmolarity change (Hagemann & Erdmann, 1994; Hagemann *et al.*, 1997; Hagemann *et al.*, 1997; Mikkat *et al.*, 1997; Reed & Stewart, 1985; Stirnberg *et al.*, 2007).

Since identification of the first aquaporin from red blood cells (Preston *et al.*, 1993), genes encoding aquaporins have been found in both prokaryotic and eukaryotic cells. In addition to water transport, it has been found

that aquaporins mediate the transport of other non-charged solutes, such as carbamides, polyols, purines, pyrimidines and glycerol (Maurel *et al.*, 1994; Tsukaguchi *et al.*, 1998). Moreover, some aquaporins were able to facilitate gas transport through biological membranes in heterologous expression systems (Jahn *et al.*, 2004; Nakhoul *et al.*, 1998).

The first aquaporin to be isolated from plant cells was the tonoplast intrinsic protein, γ-TIP (Maurel *et al.*, 1993). This finding indicated that aquaporins reside not only in the plasma membrane but also in endomembranes, presumably to coordinate water transport inside the cell. In *Synechocystis*, a single-copy gene encoding an aquaporin homolog, *aqpZ*, is present in the genome. The functional characteristics of AqpZ and its subcellular localization in *Synechocystis* have not been determined, although a list of genes induced by hyperosmotic stress in both the wild type (WT) and a Δ*aqpZ* strain based on microarray experiments has been published (Shapiguzov *et al.*, 2005).

Aquaporins belong to the major intrinsic protein (MIP) superfamily of membrane proteins (Pao *et al.*, 1991). All members of this group share a common six membrane spanning structure (Walz *et al.*, 1997). Some aquaporins are known to be inhibited by mercury (Maurel *et al.*, 1994; Preston *et al.*, 1993), and therefore mercurial sulfhydryl reagents has often been used to block aquaporin-mediated water transport. However, the sensitivity of AqpZ from *Synechocystis* to mercury has not been previously investigated.

Nicotiana tabacum aquaporin NtAQP1 has been localized to the chloroplast inner membrane as well as to the plasma membrane. It has been shown to mediate CO_2 transport across the membrane and to have an important function in photosynthesis (Uehlein *et al.*, 2003; Uehlein *et al.*, 2008). These findings are very interesting because chloroplasts in eukaryotes (algae and plants) likely evolved from an endosymbiotic relation with cyanobacteria (Cavalier-Smith, 2000). To understand the molecular function of *Synechocystis* AqpZ, we determined the membrane localization of the protein and characterized the function of AqpZ in mediating the response of the cell to changes in osmolarity, both in *Xenopus* oocytes as well as in *Synechocystis*.

II. RESULTS

Expression of AqpZ was controlled by the circadian clock in *Synechocystis*

Water transport across the membrane are likely to be dependent on the activities as diverse as cell division, respiration, and carbohydrate synthesis during light and dark cycles in cyanobacteria. Cells carrying a reporter construct consisting of the luciferase gene under control of the AqpZ promoter (P*aqpZ*::*luxAB*) were used to determine whether expression of *aqpZ* was regulated by the circadian clock, and whether the circadian rhythm was influenced by the aqpZ mutations. Luciferase activity was determined every hour under continuous light after *Synechocystis* cells were entrained by a 12-h dark period (Okamoto *et al.*, 2005; Okamoto *et al.*, 2005; Onai *et al.*, 2004) (Figure 1A). Cells expressing luciferase driven by the *dnaK* promoter were used as controls. The circadian period (wave length of the cosine curve) of the cells containing P_{dnaK}::*luxAB* was 22.2 h for the wild type and 22.5 h for the Δ*aqpZ* cells, which are very close to the standard circadian period (22.4 h) of *Synechocystis* (Kucho *et al.*, 2005) indicating that the pattern of the rhythm was not influenced by the mutation of the aqpZ gene. The peak of the expression of *aqpZ* for circadian time was at 15.3 for the wild type (CT15.3) and 15.5 for the Δ*aqpZ* cells CT15.5), corresponding to the early subjective night. The cell division rate reached at the highest level around the late of the day time to the early subjective night (Figure 1A), followed by the cell expansion in night. We also evaluated the expression profile of AqpZ proteins (Figure1B). The proteins level was high in night compared with the daytime, consistent to the expression of aqpZ shown in Figure 1A since the proteins expression comes after the transcription to some extent (Figure 1B). Taken together, we concluded that the synthesis of AqpZ apparently synchronized cell expansion in night after the cease of the division to mediate water flux across the membrane (Supplemental Figure 1).

AqpZ-mediated water transport was insensitive to inhibition by mercury in *Xenopus* oocytes.

In order to evaluate its water transport activity, *Synechocystis* AqpZ was expressed in *Xenopus* oocytes. Correct expression of wild-type AqpZ or a myc-tagged version in this system was confirmed by Western blot using either an antibody generated against *Synechocystis* AqpZ (see Methods) or an anti-myc epitope antibody. Both proteins, wild-type AqpZ and myc-tagged AqpZ, were detected in protein extracts of oocytes expressing the respective protein. Myc-tagged *C. elegans* aquaporin (myc-Y69) was used as a positive control (Figure 2A). The specificity of the anti-AqpZ antibody was also confirmed in this experiment. Confocal microscopy of immunolabeled oocytes showed that AqpZ was localized to the oocyte plasma membrane (Figure 2B).

Oocytes expressing either wild-type AqpZ or the myc-tagged version exhibited a significant increase in osmotic water permeability (P_f) when compared with water-injected cells (Figure 2C and D).

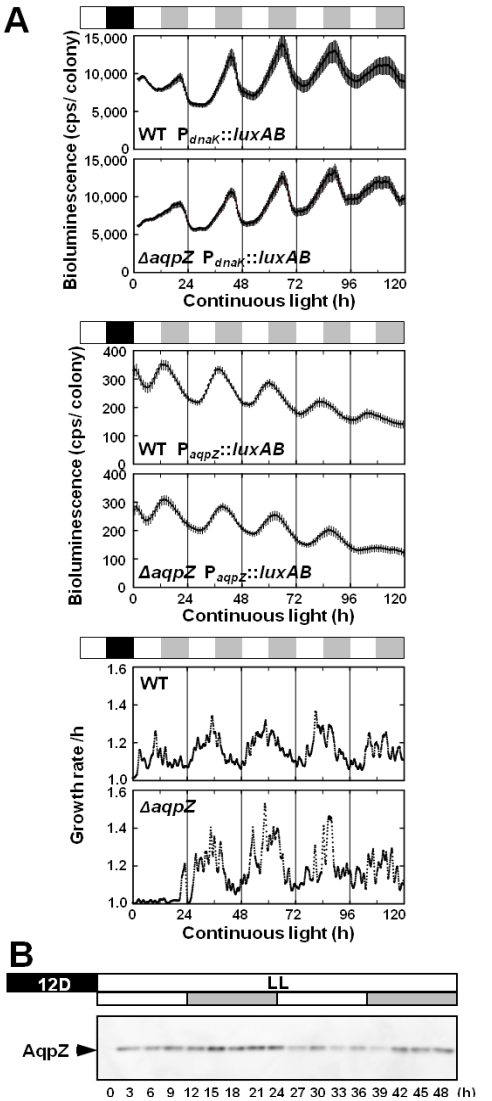

Figure 1. Circadian expression of *aqpZ* in *Synechocystis*.(A) *Synechocystis* cells containing a luciferase reporter gene under control of the *aqpZ* promoter (P*aqpZ*::*luxAB*) were entrained by a 12-h dark period and then shifted to continuous light. The P*dnaK*::*luxAB* reporter strain was used as positive and negative control, respectively. The time scale represents the actual time after transfer to continuous light conditions. The bioluminescence was determined every hour. Each point indicates the average ± standard deviation from six replicates. The black box represents darkness for 12 h to synchronize the circadian clock. The white and gray boxes above the graphs represent subjective day and night, respectively. **(B)** Immunodetection of AqpZ proteins. The wild-type *Synechocystis* cells were withdrawn every three hours from the culture for 48 hours.

These indicated that *Synechocystis* AqpZ has functional water permeability. Addition of $HgCl_2$, a known inhibitor of some aquaporins, had no effect on the water permeability of *Synechocystis* AqpZ, whereas the human aquaporin hAQP1 was about 50 % inhibited under these conditions (Figure 2E) (Preston *et al.*, 1993). The protein kinase C (PKC) activator phorbol-12-myristate-13-acetate (PMA) increased the water permeability of soybean nodulin 26 expressed in oocytes (Guenther *et al.*, 2003). However, when PMA was applied to oocytes expressing AqpZ, the osmotic water permeability did not change compared to that of untreated oocytes (Figure 2E). There was also no change in water permeability when the cells were incubated at lower pH (pH 6, Figure 2E) (Tournaire-Roux *et al.*, 2003; Yasui *et al.*, 1984).

AqpZ is localized to the plasma membrane.

Fractions of plasma and thylakoid membranes were prepared by sucrose density gradient fractionation followed by aqueous polymer two-phase partitioning (Norling *et al.*, 1998; Tsunekawa *et al.*, 2009; Zhang *et al.*, 2004).
As shown in Figure 3A, a single protein band of the corresponding molecular mass (25.5 kDa) of AqpZ was detected by Western blot in the plasma membrane fraction, which was identified by the presence of the plasma membrane marker protein NrtA (Omata, 1995).
No AqpZ protein was detected in the thylakoid membrane fraction, which was identified by the presence of $NhdD_3$ and $NhdF_3$. In addition, the membrane localization of the AqpZ protein was determined by immunogold labeling followed by electron microscopy. A cross-section of wild type *Synechocystis* cells grown under non-stress conditions showed gold particles decorating the plasma membrane when the AqpZ antiserum was used (Figure 3B). A small amount of the label was found in other locations. Control experiments with the Δ*aqpZ* strain did not show any significant labeling (Supplemental Figure 2). These results indicate that AqpZ was primarily localized in the plasma membrane of *Synechocystis* (Figure 3B).

The Δ*aqpZ* strain displays slower shrinkage under high osmolarity conditions.

The volume loss of *Synechocystis* cells in response to high osmolarity was measured by stopped-flow light scattering spectrophotometry. Figure 4A and 4B show a representative time course of light scattering of *Synechocystis* wild type (WT) and the Δ*aqpZ* cells in response to 1 M sorbitol or 0.5 M NaCl in BG11 medium (1,236 mosM and 1,015 mosM, respectively) .In response to both treatments WT exhibited a rapid and strong increase in light scattering, indicating a decrease in cell size. The response in the Δ*aqpZ* cells was much slower (Figure 4A and 4B). Changes in light scattering

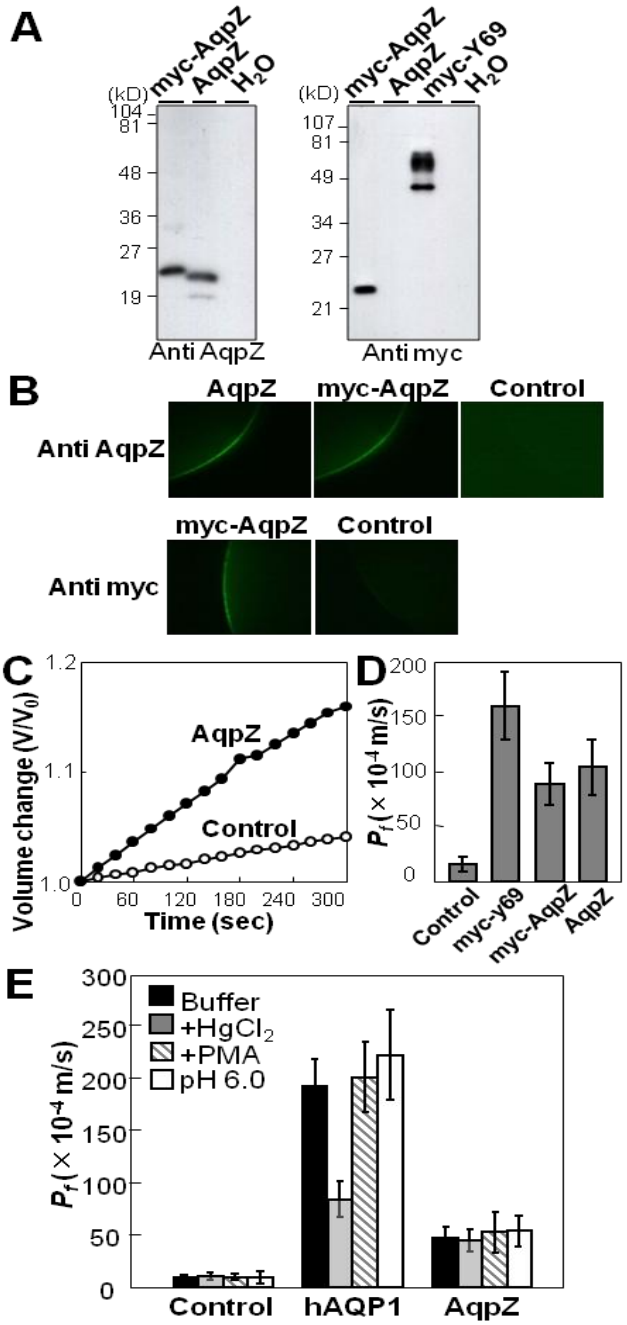

Figure 2. Expression of *Synechocystis* AqpZ in oocytes. (A) Immunoblotting of isolated membrane fractions from oocytes injected with water or expressing *Synechocystis* AqpZ, myc-AqpZ or *C. elegans* myc-Y69. Blots were probed with either anti-AqpZ (left panel) or anti-myc antibodies (right panel). **(B)** Confocal microscopy images of oocytes injected with water (control) or expressing *Synechocystis* AqpZ or myc-AqpZ. Oocytes were immunolabeled with anti-AqpZ antibodies (top row) or anti -myc antibodies (bottom row) followed by an Alexa Fluor 488 conjugated secondary antibody. **(C)** Time-dependent osmotic swelling of water-injected oocytes and oocytes expressing *Synechocystis* AqpZ. **(D)** Osmotic water permeability (P_f) of *Synechocystis* AqpZ, myc-AqpZ, or *C. elegans* myc-Y69 expressed in *Xenopus* oocytes. Osmotic-swelling assays were performed at 20°C (mean ± SD, n = 6 - 7). **(E)** Effects of mercury, the protein kinase C activator PMA and pH on the water permeability of AqpZ. hAOP1 is a mercury-sensitive human aquaporin that was used as control. $HgCl_2$ (0.3 mM) or PMA (10 μM) was added to the medium before start of the swelling assay**.**

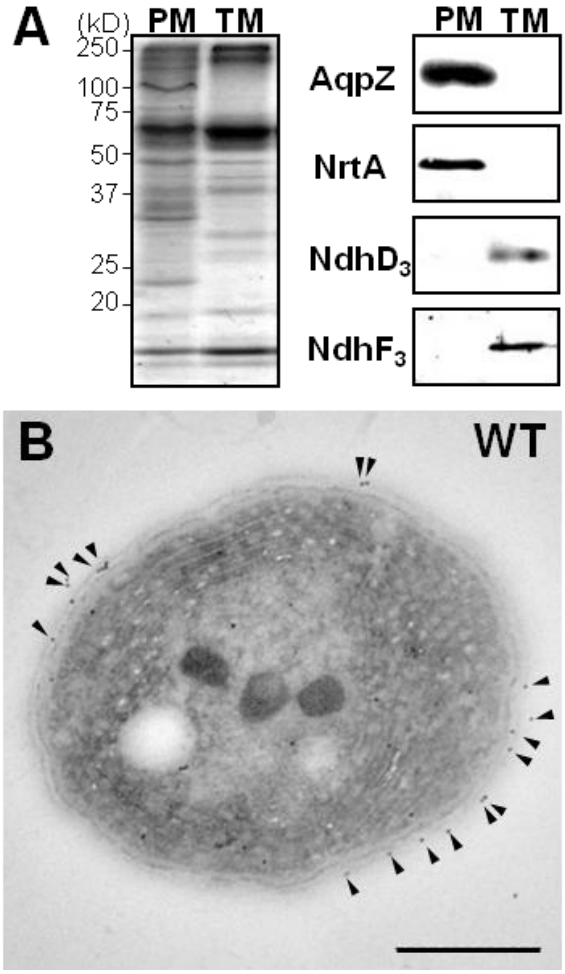

Figure 3. Disruption of *aqpZ* in *Synechocystis* and membrane localization of AqpZ. (A) Plasma membrane localization of AqpZ. Plasma membranes (PM) and thylakoid membranes (TM) were isolated by sucrose density fractionation followed by aqueous polymer two-phase partitioning. CBB staining (left panel) and immunoblotting (right panel) of the plasma membrane and the thylakoid membrane fractions from wild-type *Synechocystis*. NrtA (marker for the plasma membrane fraction) and $NdhD_3$ and $NdhF_3$ (markers for the thylakoid membrane fraction) were detected on Western blots using the corresponding antibodies. **(B)** Cross section of *Synechocystis* wild-type cell (left) and Δ*aqpZ* cell (right) immunolabeled using an anti-AqpZ antibody. AqpZ protein, indicated by the presence of gold particles (arrowheads in WT), was localized in the plasma membrane. Bars = 500 nm.

were also determined in response to treatments with increasing final osmolarities (0.25-1.0 M sorbitol and 0.25-1.0 M NaCl in BG11 solution) (Figure 4C and 4D) and the osmotic water permeability (P_f) was calculated. In these experiments the light scattering profiles and the values for P_f showed distinct differences between cells treated with sorbitol or NaCl (Figure 4A-4D). To exclude the possibility that the cellular response may have been influenced by ingredients of the BG11medium, the experiments were repeated with HEPES/MES buffer instead of BG11 (Figure 4E-4H). In the case of treatment with sorbitol there was not much difference between incubation in buffer or BG11 (Fig 4E and 4G). However, in case of treatment with NaCl, the P_f values of both wild-type and mutant cells were increased more than threefold by addition of 0.25 and 0.5 M NaCl in the buffer (Figure 4F and 4H) compared with results shown in Figure 4B and 4D. No increase in P_f value was seen with 1 M NaCl in buffer compared to 1 M NaCl in BG11, however, this may be because at 1 M NaCl cells may have reached the maximum rate of shrinkage. Overall the cells responded more strongly to NaCl in buffer than in BG11 medium. In addition, a delay in the start of the increase of light intensity scattering was detected upon NaCl addition in the Δ*aqpZ* cells (Figure 4F).

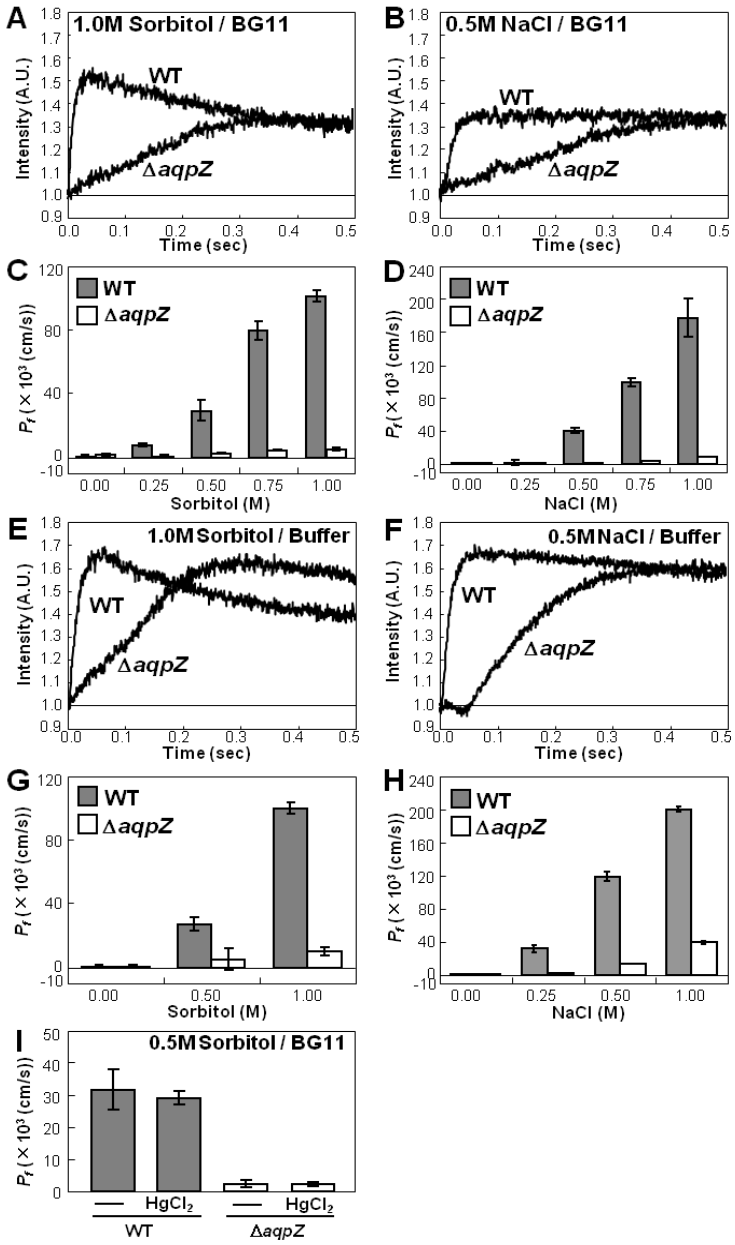

Figure 4. Characterization of AqpZ-mediated water permeability in *Synechocystis* cell subjected to hyperosmotic stress. **(A) and (B**) Time course of light scattering of *Synechocystis* wild-type (WT) and Δ*aqpZ* cells moved to BG11 medium containing 1.0 M sorbitol (A) or 0.5 M NaCl (B). **(C) and (D)** Osmotic water permeability (Pf) of WT and Δ*aqpZ* cells exposed to varying concentrations of sorbitol (C) or NaCl (D) in BG11 medium. **(E)-(H)** The same experiments as shown in (A)-(D) were repeated with cells incubated in 80 mM HEPES/MES (pH 8.0) instead of BG11. **(I)** Test of inhibition of water permeability by $HgCl_2$. *Synechocystis* cells (WT and Δ*aqpZ*) were pretreated with BG11 medium containing 300 μM $HgCl_2$ for 5 min before subjecting them to the hyperosmotic shock (BG11 containing 0.5 M sorbitol). Values are expressed as mean ± SD calculated for three independent experiments. A.U.: arbitrary unit.

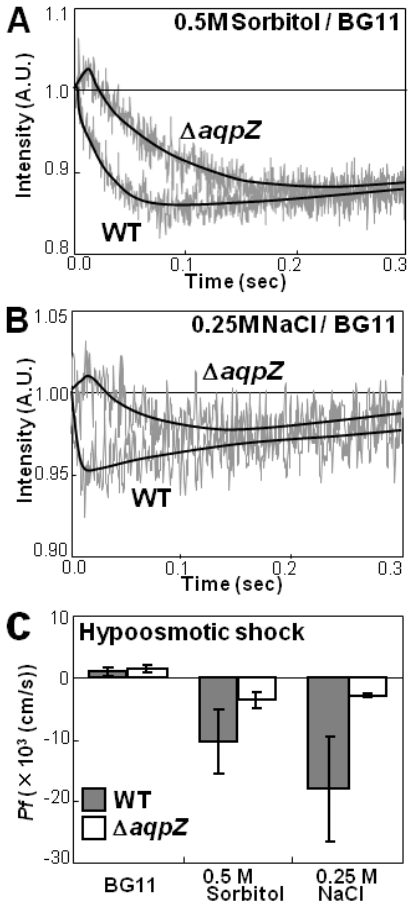

Figure 5. Effects of hypo-osmotic shock on *Synechocystis* wild type and Δ*aqpZ* cells. (A), (B) Representative time courses of light scattering of *Synechocystis* wild type and Δ*aqpZ* cells exposed to hypo-osmolar shock. Cells precultured for 2h in BG11 medium with 1 M sorbitol (A) or 0.5 M NaCl (B) were shifted to BG11 medium with 0.5M sorbitol (A) or 0.25 M NaCl (B). The calculated osmotic water permeability (P_f) is shown in (C). Values are expressed as mean ± SD calculated for three independent experiments.

As shown in Figure 2E, AqpZ expressed in *Xenopus* oocytes was insensitive to inhibition by mercury. We therefore tested whether this insensitivity to mercury could be reproduced in vivo (Figure 4I). When 300 μM $HgCl_2$ was applied to the cells in BG11 medium before performing the light scattering assay, no obvious decrease of water efflux as bserved in WT (Figure 4I). This insensitivity of AqpZ to $HgCl_2$ in vivo is consistent with the data in Figure 2E.

In addition, the cellular response to hypotonic stress was examined (Figure 5). For this *Synechocystis* wild-type and Δ*aqpZ* cells that had been pre-incubated in BG11 medium containing 1 M sorbitol or 0.5 M NaCl for 2 h were rapidly mixed with an equal volume of standard BG11medium to decrease the osmolarity and the change in light scattering was recorded. The size of the Δ*aqpZ* cells increased much more slowly compared to that of WT as indicated by the higher level of light scattering in the mutant (Figure 5C). These data demonstrate that AqpZ mediated water movement across the membrane in response to hypo- and hyperosmotic shock (Figure 4 and 5).

Comparison of oxygen-evolution between wild type and Δ*aqpZ* cells

We evaluated the effect of loss of *aqpZ* on photosynthetic activity by monitoring the oxygen evolution of the cells under different conditions (Figure 6). To examine the immediate effect of hyperosmotic shock on the oxygen evolution of wild type and Δ*aqpZ*, sorbitol or NaCl was directly added to BG11-suspended cells in a Clark type oxygen electrode cuvette (Figure 6A-D). The amount of oxygen evolution was similar in both Δ*aqpZ* and WT strains in standard medium (Figure 6A-D). When 0.5 M sorbitol or 0.5 M NaCl was added to the BG11 medium, the oxygen evolution rate of the Δ*aqpZ* cells was less inhibited than that of the WT (Figure 6B and 6D). Next, cells were incubated in BG11 liquid medium containing 0.5 M sorbitol or 0.5 M NaCl for 120 min (Figure 6E and 6F). The rate of oxygen evolution from both the wild type and the Δ*aqpZ* cells decreased to 40-50% of the initial level within 5 min. After reaching this lowest point, the recovery of the oxygen evolution rate of the Δ*aqpZ* strain was faster than that of the WT when cells were incubated with 0.5 M sorbitol (Figure 6E). When cells were incubated with NaCl the recovery rate of WT and the Δ*aqpZ* strain were similar (Figure 6F).

To assess the difference in the effect of high concentrations of sorbitol and NaCl, we examined the expression of AqpZ at the translational level (Figure 9). High concentration of sorbitol (0.5 M) had no effect on the amount of AqpZ protein in *Synechocystis*. In contrast, 4 h after addition of 0.5 M NaCl the amount of AqpZ protein had decreased by about 50 % (Figure 9C).

III. DISCUSSION

For moderately halotolerant cyanobacterium, *Synechocystis* sp. strain PCC 6803, water permeability across the membrane closely correlates with dynamic process of the physiological dairy responses and unexpected environmental changes. We show here that AqpZ functioned as a water permeable channel in the plasma membrane in *Synechocystis*, and circadian clock-mediated AqpZ expression levels showed diurnal and circadian oscillation (Figure 1). When Δ*aqpZ* cells were exposed to hyperosmotic or salt stress they

lost less water than the WT. This decrease in water loss coincided with an increase in tolerance to hyperosmotic stress (but not to salt stress) of the *ΔaqpZ* cells, demonstrated by increased growth rate (Figure 8) and oxygen evolution compared to the wild type (Figure 6). *Synechocystis* AqpZ participates in controlling the cell volume in response to osmolarity changes by nonionic compounds like sorbitol, but less in response to salt stress by NaCl.

The finding that AqpZ in *Synechocystis* is insensitive to mercury is significant, because mercurial sulfhydryl reagents often have been used to block aquaporins in living cells. Mercury-sensitive aquaporins like human AQP1 (hAQP1) and Arabidopsis γ–Tip (AtTIP1:1) contain cysteines, which are the targets of inhibition of water permeability by mercury (Daniels *et al.*, 1996; Maurel *et al.*, 1993).

Synechocystis AqpZ contains two cysteines, Cys 19 in the first transmembrane span and Cys 205 on the extracellular side (Supplemental Figure 2). Since no effect on AqpZ function was observed, it can be concluded that these two cysteins are not the target of inhibition of AqpZ activity by mercury (Figure 2E and 4I). The mercury compounds are not available for a specific blocker of water transport through AqpZ in *Synechocystis* sp. strain 6803, contrary to the case of *Synechococcus* sp. PCC 7942 (Allakhverdiev, *et al.*, 2000). According to the phylogenic tree, *Synechocystis* AqpZ appears to be most similar to *E. coli* AqpZ (Supplemental Figure 4B), and the aquaporins of both organisms have very short cytosolic N- and C-terminal domains (Supplemental Figure 4A). Like *Synechocystis* AqpZ, *E. coli* AqpZ is also insensitive to inhibition by mercury (Preston *et al.*, 1993).

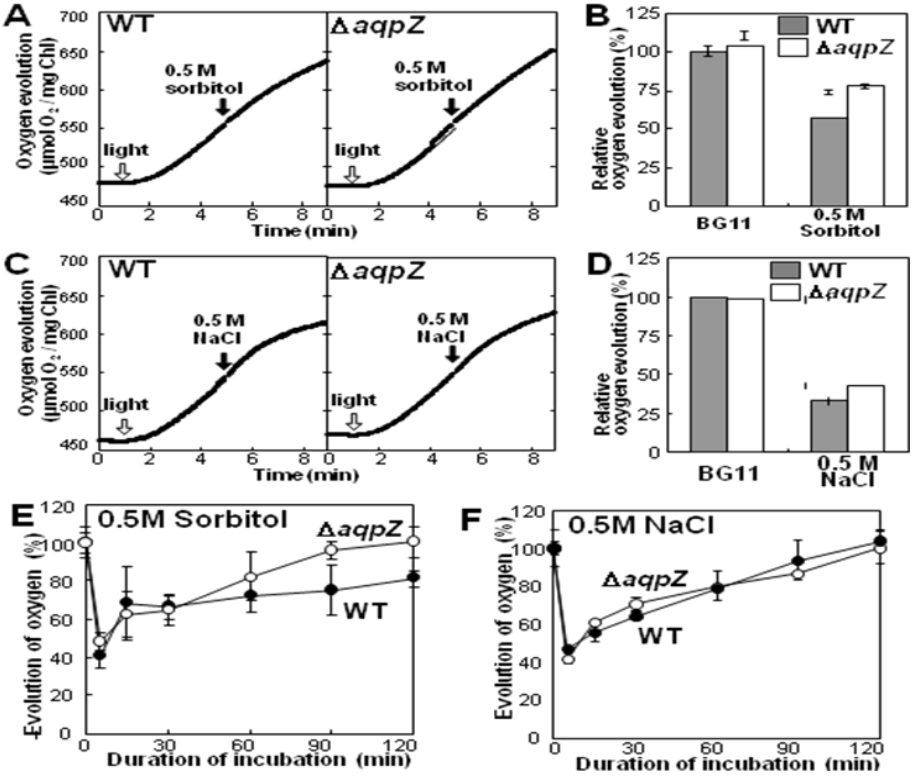

Figure 6. Photosynthetic oxygen-evolving activity in intact cells during incubation with sorbitol or NaCl. (A-D), The immediate effect of hyperosmotic shock on the oxygen evolution of wild type and Δ*aqpZ*. Oxygen evolution were monitored, and sorbitol (A) or NaCl (C) were directly added to BG11 suspended cells in Clark type oxygen electrode cuvette (B) and (D), Oxygen evolving activity were calculated from (A) and (C), respectively. White arrow: light was applied. Black arrow: hyperosmotic regent were applied. **(E)** and **(F)**, Oxygen evolution activity of cells incubated BG11 containing 0.5 M sorbitol or 0.5 M NaCl for a long time scale. Cells were incubated in the presence of 0.5 M sorbitol (E) or 0.5 M NaCl (F) at 25°C. At designated times, aliquots were withdrawn and whole chain mediated oxygen evolution was measured at 25°C after addition of 5 mM $NaHCO_3$. Each point and bar represents the average ± SE of results from four independent experiments.

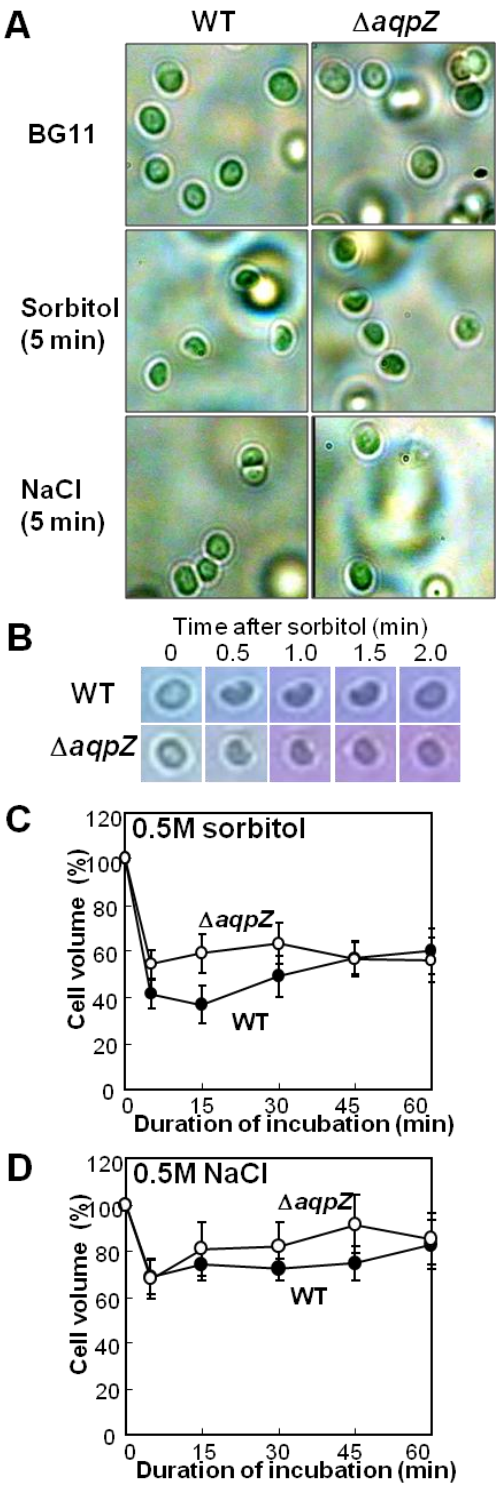

Figure 7. Changes in cell volume of *Synechocystis* wild type and Δ*aqpZ* by hyperosmotic shock. (A), Light microscopy photographs of *Synechocystis* WT and Δ*aqpZ* before and 5 min after application of osmotic stress by addition of 0.5 M sorbitol or 0.5 M NaCl. Shrunk or abnormal shaped cells were pointed out by black triangles. Bars, 3 μm. **(B)**, Trace of morphological change of the single cell of *Synechocystis* WT and Δ*aqpZ* after the addition of sorbitol or NaCl. **(C and D)**, The measurements of cell volume by ESR. Cells were treated with 0.5 M sorbitol (C) or 0.5 M NaCl (D) at time 0. At designated times, a portion of each cell suspension was withdrawn and the cell volume was determined from measurements of ESR. Each point and bar represents the average ± SE of results from four independent experiments.

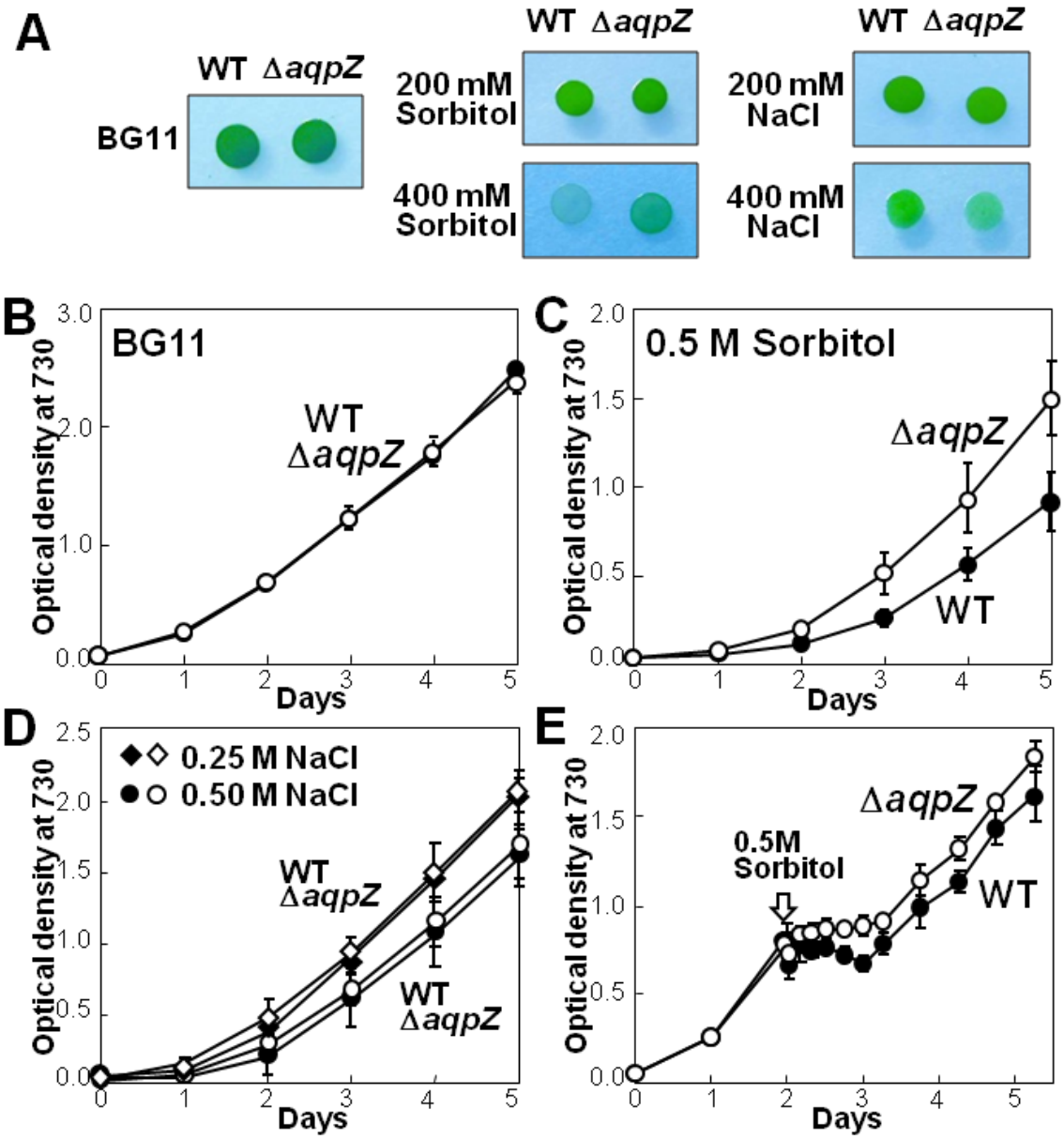

Figure 8. Growth profile of *Synechocystis* wild type and Δ*aqpZ*. (A) Growth of wild-type (WT) and Δ*aqpZ* cells on solid BG11 medium containing the indicated concentrations of NaCl or sorbitol. **(B)-(D)** Growth curves of WT (filled symbols) and Δ*aqpZ* (open symbols) cells growing in liquid culture. Cells were grown either in BG11 medium (B) or in BG11 medium supplemented with 0.5 M sorbitol (C) or 0.5 M NaCl (D). **(E)** Growth curves of WT and Δ*aqpZ* cells. Sorbitol (0.5 M) was added in the middle growth phase of the culture at 48 h.

The insensitivity of AqpZ to mercurialsulfhydryl reagents of *Synechocystis* and *E. coli* may provide preferential property to the bacteria, which usually habit in oxidative environment.

Many biological events depend on circadian control system in a wide range of living systems. Vasopressin is an antidiuretic hormone, which trigger the movement of Aquaporin 2 into the plasma membrane of the collecting duct epithelial cells to reabsorb water from the urine into the bloodstream. Recent study demonstrated that through the release of vasopressin was enhanced by an intrinsic biological clock during the sleep period when water intake is suppressed in the kidney in mammals (Trudel & Bourque, 2010). As consistent with this, the expression of *Synechocystis* AqpZ was regulated by the circadian clock (Figure 1), which consisted of endogenous oscillators composed by KaiA, KaiB and KaiC in cyanobacteria (Aoki & Onai, 2009; Ishiura *et*

al., 1998). This was confirmed by the experiment, where the pattern of the rhythm of *aqpZ* expression showed proportional relationship with the short circadian time in *Synechocysits* mutants containing point mutated *kaiC* (unpublished data). The dairy oscillation of AqpZ proteins coordinated with the cell growth circadian cycle (Figure 1). The peak of the expression of *aqpZ* for circadian time was corresponding to the early subjective night, which is consistent to the circadian profile of Na^+/H^+ antiport system, NhaS3 in *Synechocysits* (Tsunekawa *et al*., 2009) (Supplemental Figure 1). The increase of AqpZ in night mediates water uptake to support the cell expansion of daughter cells generated in day time,whereas the reduction of the *aqpZ* expression in day time at the dehydration circumstance helps preserve water content available for the photosynthesis.

An important finding of this study is that the loss of *aqpZ* produced tolerance to high osmolarity, which was shown by several different experimental approaches (Figure 6-8). On the other hand, hyperosmotic stress due to either non-ionic (sorbitol) or ionic solutes (NaCl) had different effects in *Synechocystis* (Figure 7 and 8) (Waditee *et al*., 2002). Hyper-accumulation of NaCl in the cells has been shown to inhibit photosystem I and II, leading to a decline in oxygen-evolution(Allakhverdiev *et al*., 2000). However, in case of NaCl stress, the difference in oxygen evolution rate between them (Figure 9) are not clear in our experiment conditions, whereas that was significant by addition of high sorbitol. NaCl produces both osmotic stress and ionic stress. It has been reported that *Synechocystis* allowed Na^+ influx and efflux across the plasma membrane and the thylakoid membrane via a Na^+ transport system, e.g. Na^+/H^+ antiporter to control the ionic homeostasis in cytosol (Mikkat *et al*., 1997; Tsunekawa *et al*., 2009).

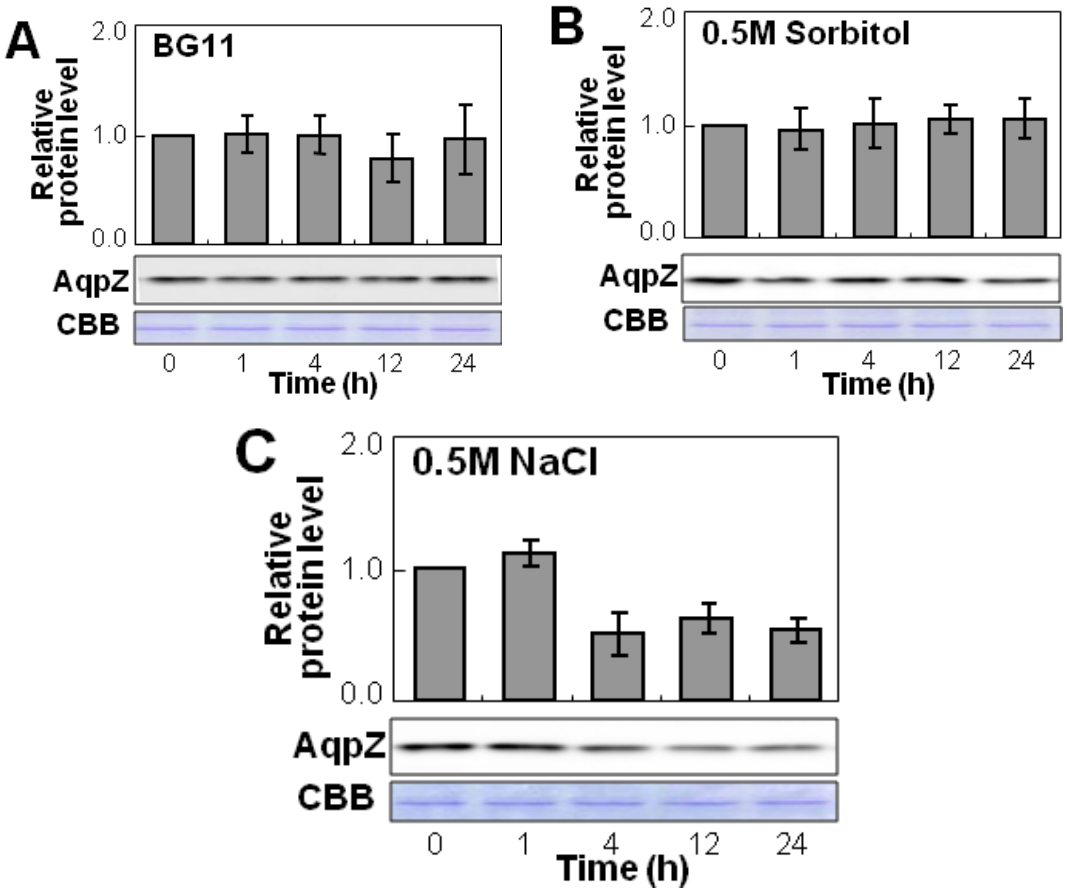

Figure 9. Expression of the AqpZ protein in *Synechocystis* cells after hyperosmotic shock. *Synechocystis* cells were treated with BG11 (A), supplemented with 0.5 M sorbitol (B) or 0.5 M NaCl (C). Cells samples taken from the cultures at the times indicated were subjected to western blot analysis using anti-AqpZ antibodies. Relative expression level of AqpZ protein was calculated by densitometric estimation in relation to the control in the absence of NaCl or sorbitol. Total protein (CBB) served as a loading control.

In addition to the Na^+ cycling system, NaCl also induces synthesis of the osmolyte glucosylglycerol in *Synechocystis* (Marin *et al.*,, 2006) It is reasonable that a reduction in the amount of AqpZ protein was observed during salt stress (Figure 9), which may help to protect the cell from water loss due to high external NaCl. The down-regulation of the aquaporin gene by high NaCl was consistent with previous results from DNA-microarray analysis in *Synechocystis* (Marin *et al.*, 2004). Similarly, in ice plant, the transcript levels of all three aquaporin genes (MipA, MipB and MipC) decreased initially during salt stress and later recovered to the pre-treatment level (Yamada *et al.*, 1995). As an initial response prior to the accumulation of osmoprotectants in the cytosol, the cells take up K^+ to restore the cell volume (Hagemann & Erdmann, 1994; Hagemann *et al.*, 1997; Hagemann *et al.*, 1997; Marin *et al.*, 2004; Shapiguzov *et al.*, 2005; Stirnberg *et al.*, 2007). Earlier studies identified the Ktr-type transporter, a Na^+ activated K^+ uptake system as responsible for this response (Berry *et al.*, 2003; Matsuda *et al.*, 2004). The loss of AqpZ prevented the cells from losing water and made the Δ*aqpZ* strain more tolerant to high osmolarity stress than the WT (Figure 6). These above adaptation mechanism to Na^+ are likely the reason why *Synechocystis* showed a relatively high tolerance to Na^+ toxicity (Figure 6-8).

In contrast to Na^+, sorbitol is probably not transported across the cellular membrane in *Synechococcus* sp. PCC 7942 (Allakhverdiev *et al.*, 2000), however, in one study a limited amount of sorbitol was taken up by the cell. Hyperosmotic shock due to sorbitol triggered strong deformation of the cell envelope in both WT and Δ*aqpZ*, this was not seen in cells subjected to hyperosmotic stress by NaCl (Figure 7). In *E. coli*, the large efflux of water driven by the osmotic gradient causes visible shrinkage of the cytoplasm, leading to a separation of the cytoplasmic membrane from the other components of the wall and consequently to the formation of plasmolysis spaces (Delamarche *et al.*, 1999). In *Synechocystis*, it is likely that physical force accompanied by the shrinkage of the intracellular space also affected adversely the function of the membrane proteins in plasma membrane and thylakoid membrane including photosynthetic electron transport system (Figure 7).

The difference in the rate of cellular shrinkage between the WT and the Δ*aqpZ* strain was small but detectable by microscopic observations and EPR measurements (Figure 7). This is different from an earlier study where almost no shrinkage of the Δ*aqpZ* strain was seen (Shapiguzov *et al.*, 2005). The fact that we observed shrinkage of the Δ*aqpZ* cells suggests that water can rapidly move through AqpZ (Figure 4 and Figure 5), and water can permeate across the plasma membrane through another, yet unknown water transport system different from AqpZ or that it moves by simple diffusion across the membrane.

Tobacco NtAQP1, which has been localized to the inner membrane of the chloroplast, mediated CO_2 transport (Uehlein *et al.*, 2003; Uehlein *et al.*, 2008). Reduction of NtAQP1 expression through RNA interference decreased CO_2 permeability of the membrane. In our study, *Synechocystis* WT or Δ*aqpZ* strain showed no difference in oxygen evolution when tested under non-stress conditions. In light of the generally accepted endosymbiont hypothesis, according to which chloroplasts originally arose from an internalized cyanobacterium (Cavalier-Smith, 2000), this study on AqpZ in *Synechocystis* will contribute to our understanding of chloroplast aquaporins in plant cells.

IV. MATERIALS AND METHODS

Plasmid construction

The *aqpZ* coding region of *Synechocystis slr2057* was amplified from genomic DNA by PCR using gene-specific primers (sense: 5'-CAGTAGATCTATGAAAAAGTACATTGCTG-3'; antisense: 5'-CAGTGCTAGCTCACTCTGCTTCGGGTTCG-3'). The resulting PCR product was cloned into the *Bgl*II and *Nhe*I sites of pXßG-ev1 (Preston, Carroll, Guggino, & Agre, 1992). To create myc-tagged AqpZ another set of primers (sense: 5'-CATGGAATTCCATGAAAAAGTACATTGCTG-3', antisense: 5'-CAGTGCTAGCTCACTCTGCTTCGGGTTCG-3') were used to amplify the coding region of aqpZ from genomic DNA by PCR, and the resulting PCR product was cloned into the *Eco*RI and *Nhe*I sites of pXβG-ev1, placing it in-frame with the N-terminal myc-tag contained in the vector. The correct frame was verified by sequencing. Myc-y69 (AQP-3) from *C. elegans* and the human aquaporin hAQP1 were used controls (Preston *et al.*, 1992).

Expression in *Xenopus* oocytes and measurement of water permeability.

Capped cRNAs were synthesized *in vitro* from *Xba*I-linearized pXβG-ev1 plasmids using mMESSAGE mMACHINE T3 kit (Ambion, Austin, TX). Defolliculated *X. laevis* oocytes were injected with 5 or 10 ng of cRNA or diethyl pyrocarbonate-treated water (Preston *et al.*, 1992; Uozumi, Gassmann, Cao, & Schroeder, 1995). Injected oocytes were incubated for 2-3 days at 18°C in 200 mosM modified Barth's solution (10 mM Tris-HCl (pH 7.6), 88 mM NaCl, 1 mM KCl, 2.4 mM $NaHCO_3$, 0.3 mM $Ca(NO_3)_2$, 0.4 mM $CaCl_2$,

0.8 mM $MgSO_4$). An oocyte swelling assay was used to determine the osmotic water permeability P_f (Preston *et al.*, 1992). Oocytes were transferred to modified Barth's solution diluted to 70 mosM with distilled water, and the time course of volume increase was monitored at room temperature by videomicroscopy with an on-line computer (Ma *et al.*, & Verkman, 1993). To test for inhibition of water permeability by Hg^{2+}, oocytes were incubated for 5 min in MBS containing 300 μM $HgCl_2$ before transferring them to the low osmolarity medium. To determine the effect of pH, oocytes were incubated for 1 min in 200 mosM modified Barth's solution (pH 7.5 adjusted with 5 mM HEPES or pH 6. 0 with 10 mM MES) before subjecting them to the swelling assay. The effect of the protein kinase C activator phorbol 12-myristate 13-acetate (PMA) was examined by incubating oocytes in MBS containing 10 μM PMA for 15 min prior to P_f measurements. The relative volume (V/V_0) was essentially calculated as described by (Preston *et al.*, 1992). The relative volume (V/V_0) was calculated from the area at the initial time (A_0) and after a time interval (At): $V/V\,0 = (At/A0)^{3/2}$. The coefficient of osmotic water permeability (P_f) was determined from the initial slope of the time course [$d(V/V_0)/dt$], initial oocyte volume ($V_0 = 9 \times 10^{-4}$ cm^3), initial oocyte surface area ($S = 0.045$ cm^2), and the molar volume of water ($V_w = 18$ cm^3/mol): $P_f = (V_0 \times d(V/V_0) / dt) / (S \times V_w \times (osM_{in} - osM_{out}))$

Oocyte immunofluorescence and confocal microscopy.

Oocytes were incubated in fixing solution (80 mM Pipes, pH 6.8, 5 mM EGTA, 1 mM $MgCl_2$, 3.7% formaldehyde, 0.2% Triton X-100) at room temperature for 4 h, transferred to methanol at -20°C for 24 h, equilibrated in PBS (3.2 mM Na_2HPO_4、0.5 mM KH_2PO_4、1.3 mM KCl、135 mM NaCl、pH 7.4) at room temperature for 2 h, incubated in PBS with 100 mM $NaBH_4$ at room temperature for 24 h, and bisected with a razor blade (Liu *et al.*, 2005). Fixed oocytes were blocked in PBS containing 2% BSA for 1 h at room temperature, and then incubated at 4°C with the anti-AqpZ antibody (see below) for 24 h followed by Alexa Fluor 488 goat anti-rabbit IgG in PBS containing 2% BSA for 24 h. Samples were mounted in Fluoromount-G (Southern Biotechnology Associates) and visualized with a PerkinElmer UltraView LCI confocal laser-scanning microscope.

Oocyte membrane extraction and immunoblotting.

For each sample ten oocytes were homogenized together by pipetting up and down in hypotonic lysis buffer (7.5 mM sodium phosphate/1 mM EDTA, pH 7.5) containing a protease inhibitor cocktail (Sigma–Aldrich) (Meetam *et al.*, 1999). The oocyte yolk was removed by discarding the pellet after a centrifugation at 735 x g and 4 °C for 10 min, and the supernatant was centrifuged at 200,000 x g, 4°C, for 1 h. The pellet containing the oocyte membrane fraction was solubilized with the buffer (50 mM Tris-HCl (pH 8.0), 50 mM NaCl, 50 mM EDTA-2Na, 10%(w/v) glycerol and 2% SDS). Total protein content was determined by the bicinchoninic acid assay BCA method (Pierce. Equal amounts of protein were separated by SDS-PAGE on a 12 % gel. Proteins were transferred to a polyvinylidene difluoride (PVDF) membrane, probed with either anti-AqpZ antibody (see below) or anti-myc antibody (Santa Cruz Biotechnology) followed by horseradish peroxidase-conjugated donkey anti-rabbit IgG (Amersham Pharmacia). The enhanced chemiluminescence detection system (Amersham Pharmacia) was used to visualize the immunoreactive proteins by exposure to x-ray films.

Bacterial strains and culture conditions.

The GT (glucose-tolerant) strain of *Synechocystis* sp. PCC 6803 and its derivatives was grown in BG11 medium (Stanier *et al.*, 1971) supplemented with 20 mM TES-KOH (pH 8.0) under continuous white light (50 μmol of photons /m^2 s; 400–700 nm) at 30 °C in air. For the construction of an *aqpZ* null-mutant, the *aqpZ* (*slr2057*) coding sequence from *Synechocystis* was amplified by PCR using specific primers (sense: 5'-GGATGGATTGGGACGACATG-3', antisense: 5'-GAATTACTTCGTCGGCATTT-3') and cloned into the *Hinc*II site of pUC119 (Takara). Part of the coding sequence of the *aqpZ* gene was replaced by insertion of a spectinomycin resistance (Sm^r) cassette into the *Eco*47III sites. The resulting construct was used to transform the GT strain. Colonies resistant to spectinomycin (20 μg/ml) were selected, and isolation of a single colony was repeated three times. The disruption of *aqpZ* was confirmed by PCR with specific primers and by immunoblot analysis with the anti-AqpZ antibody (see below).

Isolation of *Synechocystis* membranes

Thylakoid and plasma membrane fractions were prepared from *Synechocystis* cells as described previously (Norling *et al.*, 1998; Tsunekawa *et al.*, 2009). An anti-AqpZ antibody was raised against two synthetic peptides with the sequences NH_2-GSNPLATNGFGDHS-COOH and NH_2-VLEDLGRPEPEAE-COOH (Operon Biotechnologies, Japan). Polyclonal antibodies raised against the plasma membrane nitrate transporter NrtA (Omata, 1995), or against the thylakoid membrane proteins $NdhD_3$ and

$NdhF_3$(Ohkawa *et al.*, 2000; Zhang *et al.*, 2004) were used to identify the *Synechocystis* plasma membrane (PM), or thylakoid membrane (TM) fractions, respectively. Proteins were separated by SDS-PAGE on a 12.5% or 15% gel and then transferred to PVDF membranes. Membranes were incubated for 1 h with the primary antibody (1:2000 in blocking buffer), followed by incubation for 30 minutes with the secondary antibody (horseradish peroxidase-conjugated goat anti-rabbit IgG (Amersham Pharmacia, 1:1000) and subsequently developed by chemiluminescence detection (ECL, Amersham Pharmacia).

Immunolabeling and electron microscopy

Synechocystis cells grown to an OD_{730} of about 1.0 in BG11 medium were fixed with 50 mM phosphatase buffer containing 5% glutaraldehyde and 2% osmium tetroxide (pH 7.2). The samples were dehydrated through a graded acetone series and embedded in Spurr's resin and polymerized. Ultra-thin sections were first labeled with AqpZ antiserum (1:20) in Tris-buffered saline, and then with 12-nm colloidal gold particles coupled to goat anti-rabbit IgG. IgG was purified from the serum using the Melon^{TM} Gel IgG Spin Purification Kit (Pierce). The sections were stained with uranyl acetate followed by lead citrate solution and examined with a transmission electron microscope (H-7500, Hitachi).

Measurement of circadian rhythm of *aqpZ* promoter activity and change of cell volume in *Synechocystis*

A putative 371-bp *aqpZ* promoter sequence was fused to the bacterial luciferase gene set *lux*AB at the *Afl*II and *Nde*I sites of p68TS1ΩLuxAB(+)PLNK,and the construct was inserted into the TS1 region in *Synechocystis* chromosomal DNA (Kucho *et al.*, 2005). The selected cells were cultured in liquid BG11 medium at 30 °C under 34 μmol of white light illumination m^{-2} s^{-1} with bubbling of air and stirring. The optical density of the culture at 730 nm was maintained at ~0.35 by dilution with fresh BG11 medium. The culture was placed in darkness for 12 h to synchronize the circadian clock, and then kept under constant light conditions (Okamoto *et al.*, 2005; Okamoto, Onai, Furusawa *et al.*, 2005). The growth rate and bioluminescence from cells grown on the medium was measured by the continuous culture system as described previously (Matsuo *et al.*, 2008). Based on the optical density of cultures collected with an optical sensor every 5 min, growth rates were calculated. According to the data, fresh medium was replaced with the culture medium to keep the optical density constant. To monitor bioluminescence, aliquots of the culture were automatically sampled every 2 h, and subjected to bioluminescence measurements.

Stopped-flow spectrophotometry on *Synechocystis* cell suspensions

The water permeability of WT and Δ*aqpZ* strain was measured using a stopped-flow apparatus with a dead time of <3.95 ms (Unisoku, Hirakata, Japan) (Yukutake *et al.*, 2008). For the hyper-osmotic shocks, 100 μl of *Synechocystis* cells were rapidly mixed with an equal volume of high osmolarity medium at 30°C. The time course of changes in the 90° scattered light intensity was measured at 575 nm for 500 ms. For hypo-osmotic shocks, cells cultivated in BG11 medium were centrifuged and resuspended in BG11 medium containing 1 M sorbitol or 0.5 M NaCl for 2 h. To start the assay, the cell suspension (100 μl) was mixed in the stopped-flow device with an equal volume of H_2O. To test the effect of the incubation medium, 80 mM HEPES/MES buffer (pH 8.0) was used instead of BG11. Averaged data from multiple determinations were fitted to single or double exponential curves. The fitting parameters were then used to determine *Pf* by first applying the linear conversion from relative fluorescence into relative volume and then iteratively solving the *Pf* equation:
$P_f = (dV(t) / dt) / [(SAV) (MVW) (C_{in} - C_{out})]$ where P_f is the osmotic water permeability, $V(t)$ is the relative intracellular volume as a function of time, SAV is the cell surface area to volume ratio, MVW is the molar volume of water (18 cm^3/mol), and C_{in} and C_{out} are the initial concentrations of total solute inside and outside the cell, respectively (Zeidel *et al.*, 1992; Zeidel *et al.*, 1994) For the test of Hg^{2+} effects, *Synechocystis* cells were incubated for 5 min in BG11 containing 300 μM $HgCl_2$ before stopped-flow analysis.

Light microscopy.

An Eclipse E800 microscope (Nikon) equipped with a camera (KY-F1030; JVC) and the Diskus software package (Hilgers) was used for light microscopy. For cell size determination, pictures were analyzed using the ImageJ program. Beads of defined size (3.005 ± 0.027 μm) were used as standard for the measurements.

Measurement of cell volume by electron paramagnetic resonance

Synechocystis cell volume (cytoplasmic volume) was determined by electron paramagnetic resonance (EPR) spectrometry as described by Blumwald and and Shapiguzov (Blumwald *et al.*, 1983; Shapiguzov *et al.*, 2005). Cells were harvested and resuspended at 400 μg

chlorophyll ml $^{-1}$ in a solution containing 1.0 mM 2,2,6,6-tetramethyl-4-oxopiperidinooxy free radical (TEMPO), 20 mM $K_3[Fe(CN)_6]$ and 75 mM Na_2Mn-EDTA. TEMPO was used as spin probe. When oxidized by $Fe(CN)_6^{3-}$ TEMPO was able to penetrate the plasma membrane rapidly and reach an equilibrium throughout the cell suspension. The quenching agent Na_2Mn-EDTA, which cannot cross the plasma membrane, broadened the external spin-probe signal, and the remaining unbroadened spin signal was directly proportional to the cell volume. For the assay the cells were enclosed in a sealed-glass capillary in a final volume of 40 µL. EPR spectra were recorded at room temperature in an EPR spectrometer (model ESP 300E; Bruker) under the following conditions: 100 kHz field modulation at a microwave frequency of 11.72 GHz; a modulation amplitude of 0.4 mT; microwave power of 10 mW; a time constant of 80 ms; and a scan rate of 0.4 G s1 in dark.

Oxygen evolution measurements

Oxygen evolution of cells was measured in BG-11 medium with a Clark-type electrode at a chlorophyll concentration of 5 µg/ml. The medium was continuously stirred at 25 °C and illuminated with saturating actinic light (1000 µE /m^2 s). Whole-cell photosynthetic activity was measured as oxygen evolution supported by 5 mM $NaHCO_3$. Following methanol extraction, chlorophyll contents of individual samples were determined using a Hitachi U-2010 spectrophotometer (Porra *et al*., 1989).

Survival after drought stress

Synechocystis cells grown in BG11 medium were thoroughly washed and then resuspended with fresh BG11 medium. Cell suspensions were filtered onto filter discs (0.45-µm pore size, mixed cellulose ester; Millipore) by applying vacuum for 30 s. The filter discs containing the *Synechocystis* cells were allowed to dry out in air at 30 °C in the light (50 µmol of photons m^{-2} s^{-1}) for different lengths of time. At the indicated time, the *Synechocystis* cells on the filter discs were resuspended with fresh BG11 and plated on BG11 solid medium after appropriate dilutions. The colony forming units (CFU) were determined by counting colonies grown in BG11 solid medium.

Table 1 Characteristics of circadian parameters of the expression of *aqpZ* gene in *Synechocysitis*.

Strain	period (h)	phase (h)	hase f CT	amplitude		N 2)
WT P_{dnak}*::luxA*	22.2 ± (	20.0 ± 0.1	21.6 ± 0.1	1.44 0.09	±	3
Δ*aqpZ* P_{dnak}*::luxAB* 1)	22.5 ± 0.2	20.4 ± 0.2	21.8 ± 0.2	1.45 0.03	±	9
WT P_{aqpZ}*::luxAB*	22.9 ± 0.1	14.6 ± 0.2	15.3 ± 0.2	1.78 0.09	±	43
Δ*aqpZ* P_{aqpZ}*::luxAB*	23.4 ± 0.2	15.1 ± 0.2	15.5 ± 0.2	1.75 0.08	±	38

1) As control, the circadian parameters of the expression of *dnaK* were shown in this study {Matsuo, 2008 #1997}.
2) Phases were represented by circadian time (CT), which was calculated by dividing the phase value by the period length and multiplying by 24. In the cyanocbacteria, subjective day-time and night-time is CT 0-12 and CT 12-24 (CT 0 = CT 24), respectively.
3) Number of the experiments.

V. ACKNOWLEDGMENTS

We thank Tatsuo Omata (Nagoya University, Japan) for generously supplying anti-NrtA antibodies and Eva-Mari Aro (University of Turku, Finland) and Teruo Ogawa (Nagoya University, Japan) for generously providing antibodies against NdhD3 and NdhF3. This work was supported by grants-in-aid for scientific research (2008103, 22020002 and 22380056 to N.U.) from MEXT and JSPS.

VI. REFERENCES

Allakhverdiev, S. I., Sakamoto, A., Nishiyama, Y., Inaba, M., & Murata, N. (2000). Ionic and osmotic effects of NaCl-induced inactivation of photosystems I and II in synechococcus sp. *Plant Physiology, 123*(3), 1047.

Aoki, S., & Onai, K. (2009). Circadian clocks of synechocystis sp. strain PCC 6803, thermosynechococcus elongatus, prochlorococcus spp., trichodesmium spp. and other species. *Bacterial Circadian Programs*, , 259-282.

Berry, S., Esper, B., Karandashova, I., Teuber, M., Elanskaya, I., Rögner, M., *et al*. (2003). Potassium uptake in the unicellular cyanobacterium synechocystis sp. strain PCC 6803 mainly depends on a ktr-like system encoded by slr1509 (ntpJ). *FEBS Letters, 548*(1-3), 53-58.

Blumwald, E., Mehlhorn, R. J., & Packer, L. (1983). Studies of osmoregulation in salt adaptation of cyanobacteria with ESR spin-probe techniques. *Proceedings of the National Academy of Sciences of the United States of America, 80*(9), 2599.

Cavalier-Smith, T. (2000). Membrane heredity and early chloroplast evolution. *Trends in Plant Science*, *5*(4), 174-182.

Daniels, M. J., Chaumont, F., Mirkov, T. E., & Chrispeels, M. J. (1996). Characterization of a new vacuolar membrane aquaporin sensitive to mercury at a unique site. The Plant Cell Online, 8(4), 587.

Delamarche C., Thomas D., Rolland J.-P.,Froger A.,Gouranton J.,Svelto M., Agre P., Calamita G., (1999). Visualization of AqpZ-mediated water permeability in Escherichia coli by cryoelectron microscopy. J. Bacteriol. 181:4193-4197.

Guenther, J. F., Chanmanivone, N., Galetovic, M. P., Wallace, I. S., Cobb, J. A., & Roberts, D. M. (2003). Phosphorylation of soybean nodulin 26 on serine 262 enhances water permeability and is regulated developmentally and by osmotic signals. *The Plant Cell Online*, *15*(4), 981.

Hagemann, M., & Erdmann, N. (1994). Activation and pathway of glucosylglycerol synthesis in the cyanobacterium synechocystis sp. PCC 6803. *Microbiology*, *140*(6), 1427.

Hagemann, M., Richter, S., & Mikkat, S. (1997). The ggtA gene encodes a subunit of the transport system for the osmoprotective compound glucosylglycerol in synechocystis sp. strain PCC 6803. *Journal of Bacteriology*, *179*(3), 714.

Hagemann, M., Schoor, A., Jeanjean, R., Zuther, E., & Joset, F. (1997). The stpA gene form synechocystis sp. strain PCC 6803 encodes the glucosylglycerol-phosphate phosphatase involved in cyanobacterial osmotic response to salt shock. *Journal of Bacteriology*, *179*(5), 1727.

Ishiura, M., Kutsuna, S., Aoki, S., Iwasaki, H., Andersson, C. R., Tanabe, A., *et al*. (1998). Expression of a gene cluster kaiABC as a circadian feedback process in cyanobacteria. Science, 281(5382), 1519.

Liu, K.; Kozono, D.; Kato, Y.; Agre, P.; Hazama, A.; Yasui, M. (2005). Conversion of aquaporin 6 from an anion channel to a water-selective channel by a single amino acid substitution. Proc.Natl.Acad.Sci.U.S.A. 102 (6) 2192

Jahn, T. P., Møller, A. L. B., Zeuthen, T., Holm, L. M., Klærke, D. A., Mohsin, B., *et al*. (2004). Aquaporin homologues in plants and mammals transport ammonia. *FEBS Letters*, *574*(1-3), 31-36.

Kucho, K., Okamoto, K., Tsuchiya, Y., Nomura, S., Nango, M., Kanehisa, M., *et al*. (2005). Global analysis of circadian expression in the cyanobacterium synechocystis sp. strain PCC 6803. *Journal of Bacteriology*, *187*(6), 2190.

Ma, T. H., Frigeri, A., Skach, W., & Verkman, A. S. (1993). Cloning of a novel rat kidney cDNA homologous to CHIP28 and WCH-CD water channels. *Biochemical and Biophysical Research Communications*, *197*(2), 654-659.

Marin, K., Kanesaki, Y., Los, D. A., Murata, N., Suzuki, I., & Hagemann, M. (2004). Gene expression profiling reflects physiological processes in salt acclimation of synechocystis sp. strain PCC 6803. *Plant Physiology*, *136*(2), 3290.

Marin, K., Stirnberg, M., Eisenhut, M., Kramer, R., & Hagemann, M. (2006). Osmotic stress in synechocystis sp. PCC 6803: Low tolerance towards nonionic osmotic stress results from lacking activation of glucosylglycerol accumulation. *Microbiology*, *152*(7), 2023.

Matsuda, N., Kobayashi, H., Katoh, H., Ogawa, T., Futatsugi, L., Nakamura, T., *et al*. (2004). Na -dependent K uptake ktr system from the cyanobacterium synechocystis sp. PCC 6803 and its role in the early phases of cell adaptation to hyperosmotic shock. *Journal of Biological Chemistry*, *279*(52), 54952.

Matsuo, T., Okamoto, K., Onai, K., Niwa, Y., Shimogawara, K., & Ishiura, M. (2008). A systematic forward genetic analysis identified components of the chlamydomonas circadian system. *Genes & Development*, *22*(7), 918.

Maurel, C., Reizer, J., Schroeder, J. I., & Chrispeels, M. J. (1993). The vacuolar membrane protein gamma-TIP creates water specific channels in xenopus oocytes. *The EMBO Journal*, *12*(6), 2241.

Maurel, C., Reizer, J., Schroeder, J. I., Chrispeels, M. J., & Saier, M. H. (1994). Functional characterization of the escherichia coli glycerol facilitator, GlpF, in xenopus oocytes. *Journal of Biological Chemistry*, *269*(16), 11869.

Meetam, M., Keren, N., Ohad, I., & Pakrasi, H. B. (1999). The PsbY protein is not essential for oxygenic photosynthesis in the cyanobacterium synechocystis sp. PCC 6803. *Plant Physiology*, *121*(4), 1267.

Mikkat, S., Effmert, U., & Hagemann, M. (1997). Uptake and use of the osmoprotective compounds trehalose, glucosylglycerol, and sucrose by the cyanobacterium synechocystis sp. PCC6803. *Archives of Microbiology, 167*(2), 112-118.

Miller, A. G., Turpin, D. H., & Canvin, D. T. (1984). Na requirement for growth, photosynthesis, and pH regulation in the alkalotolerant cyanobacterium synechococcus leopoliensis. *Journal of Bacteriology, 159*(1), 100.

Nakhoul, N. L., Davis, B. A., Romero, M. F., & Boron, W. F. (1998). Effect of expressing the water channel aquaporin-1 on the CO2 permeability of xenopus oocytes. *American Journal of Physiology- Cell Physiology, 274*(2), C543.

Norling, B., Zak, E., Andersson, B., & Pakrasi, H. (1998). 2D-isolation of pure plasma and thylakoid membranes from the cyanobacterium synechocystis sp. PCC 6803. *FEBS Letters, 436*(2), 189-192.

Ohkawa, H., Price, G. D., Badger, M. R., & Ogawa, T. (2000). Mutation of ndh genes leads to inhibition of CO2 uptake rather than HCO3-uptake in synechocystis sp. strain PCC 6803. *Journal of Bacteriology, 182*(9), 2591.

Okamoto, K., Onai, K., Furusawa, T., & Ishiura, M. (2005). A portable integrated automatic apparatus for the real-time monitoring of bioluminescence in plants. *Plant, Cell & Environment, 28*(10), 1305-1315.

Okamoto, K., Onai, K., & Ishiura, M. (2005). RAP, an integrated program for monitoring bioluminescence and analyzing circadian rhythms in real time. *Analytical Biochemistry, 340*(2), 193-200.

Omata, T. (1995). Structure, function and regulation of the nitrate transport system of the cyanobacterium synechococcus sp. PCC7942. *Plant and Cell Physiology, 36*(2), 207.

Onai, K., Morishita, M., Itoh, S., Okamoto, K., & Ishiura, M. (2004). Circadian rhythms in the thermophilic cyanobacterium thermosynechococcus elongatus: Compensation of period length over a wide temperature range. *Journal of Bacteriology, 186*(15), 4972.

Pao, G. M., Wu, L. F., Johnson, K. D., Höfte, H., Chrispeels, M. J., Sweet, G., *et al.* (1991). Evolution of the MIP family of integral membrane transport proteins. *Molecular Microbiology, 5*(1), 33-37.

Porra, R. J., Thompson, W. A., & Kriedemann, P. E. (1989). Determination of accurate extinction coefficients and simultaneous equations for assaying chlorophylls a and b extracted with four different solvents: Verification of the concentration of chlorophyll standards by atomic absorption spectroscopy. *Biochimica Et Biophysica Acta (BBA)-Bioenergetics, 975*(3), 384-394.

Preston, G. M., Carroll, T. P., Guggino, W. B., & Agre, P. (1992). Appearance of water channels in xenopus oocytes expressing red cell CHIP28 protein. *Science, 256*(5055), 385.

Preston, G. M., Jung, J. S., Guggino, W. B., & Agre, P. (1993). The mercury-sensitive residue at cysteine 189 in the CHIP28 water channel. *Journal of Biological Chemistry, 268*(1), 17.

Reed, R. H., & Stewart, W. D. P. (1985). Osmotic adjustment and organic solute accumulation in unicellular cyanobacteria from freshwater and marine habitats. *Marine Biology, 88*(1), 1-9.

Rippka, R., Deruelles, J., Waterbury, J. B., Herdman, M., & Stanier, R. Y. (1979). Generic assignments, strain histories and properties of pure cultures of cyanobacteria. *Microbiology, 111*(1), 1.

Shapiguzov, A., Lyukevich, A. A., Allakhverdiev, S. I., Sergeyenko, T. V., Suzuki, I., Murata, N., *et al.* (2005). Osmotic shrinkage of cells of synechocystis sp. PCC 6803 by water efflux via aquaporins regulates osmostress-inducible gene expression. Microbiology, 151(2), 447.

Stanier, R. Y., R. Kunisawa, M. Mandel, and G. Cohen-Bazire. (1971). Purification and properties of unicellular blue-green algae (order Chroococcales). Bacteriol. Rev. 35:171-205

Stirnberg, M., Fulda, S., Huckauf, J., Hagemann, M., Krämer, R., & Marin, K. (2007). A membrane-bound FtsH protease is involved in osmoregulation in synechocystis sp. PCC 6803: The compatible solute synthesizing enzyme GgpS is one of the targets for proteolysis. *Molecular Microbiology, 63*(1), 86-102.

Tournaire-Roux, C., Sutka, M., Javot, H., Gout, E., Gerbeau, P., Luu, D. T., *et al.* (2003). Cytosolic pH regulates root water transport during anoxic stress through

gating of aquaporins. *Nature, 425*(6956), 393-397.

Trudel, E., & Bourque, C. W. (2010). Central clock excites vasopressin neurons by waking osmosensory afferents during late sleep. *Nature Neuroscience*,

Tsukaguchi, H., Shayakul, C., Berger, U. V., Mackenzie, B., Devidas, S., Guggino, W. B., *et al.* (1998). Molecular characterization of a broad selectivity neutral solute channel. *Journal of Biological Chemistry, 273*(38), 24737.

Tsunekawa, K., Shijuku, T., Hayashimoto, M., Kojima, Y., Onai, K., Morishita, M., *et al.* (2009). *Journal of Biological Chemistry, 284*(24), 16513.

Uehlein, N., Lovisolo, C., Siefritz, F., & Kaldenhoff, R. (2003). The tobacco aquaporin NtAQP1 is a membrane CO2 pore with physiological functions. *Nature, 425*(6959), 734-737.

Uehlein, N., Otto, B., Hanson, D. T., Fischer, M., McDowell, N., & Kaldenhoff, R. (2008). Function of nicotiana tabacum aquaporins as chloroplast gas pores challenges the concept of membrane CO2 permeability. *The Plant Cell Online, 20*(3), 648.

Uozumi, N., Gassmann, W., Cao, Y., & Schroeder, J. I. (1995). Identification of strong modifications in cation selectivity in an arabidopsis inward rectifying potassium channel by mutant selection in yeast. *Journal of Biological Chemistry, 270*(41), 24276.

Waditee, R., Hibino, T., Nakamura, T., Incharoensakdi, A., & Takabe, T. (2002). Overexpression of a na /H antiporter confers salt tolerance on a freshwater cyanobacterium, making it capable of growth in sea water. *Proceedings of the National Academy of Sciences of the United States of America, 99*(6), 4109.

Walz, T., Hirai, T., Murata, K., Heymann, J. B., Mitsuoka, K., Fujiyoshi, Y., *et al.* (1997). The three-dimensional structure of aquaporin-1. *Nature, 387*(6633), 624-627.

Yamada, S., Katsuhara, M., Kelly, W. B., Michalowski, C. B., & Bohnert, H. J. (1995). A family of transcripts encoding water channel proteins: Tissue-specific expression in the common ice plant. *The Plant Cell Online, 7*(8), 1129.

Yasui, M., Hazama², A., Kwon, T. H., Nielsen, S., Guggino, W. B., & Agre, P. (1984). Rapid gating and anion permeability of an intracellular aquaporin. *Heart Failure, 311*, 819-823.

Yukutake, Y., Tsuji, S., Hirano, Y., Adachi, T., Takahashi, T., Fujihara, K., *et al.* (2008). Mercury chloride decreases the water permeability of aquaporin-4-reconstituted proteoliposomes. *Biology of the Cell, 100*, 355-363.

Zeidel, M. L., Ambudkar, S. V., Smith, B. L., & Agre, P. (1992). Reconstitution of functional water channels in liposomes containing purified red cell CHIP28 protein. *Biochemistry, 31*(33), 7436-7440.

Zeidel, M. L., Nielsen, S., Smith, B. L., Ambudkar, S. V., Maunsbach, A. B., & Agre, P. (1994). Ultrastructure, pharmacologic inhibition, and transport selectivity of aquaporin channel-forming integral protein in proteoliposomes. *Biochemistry, 33*(6), 1606-1615.

Zhang, P., Battchikova, N., Jansen, T., Appel, J., Ogawa, T., & Aro, E. M. (2004). Expression and functional roles of the two distinct NDH-1 complexes and the carbon acquisition complex NdhD3/NdhF3/CupA/Sll1735 in synechocystis sp PCC 6803. *The Plant Cell Online, 16*(12), 3326.

Zhao, J., & Brand, J. J. (1988). Sequential effects of sodium depletion on photosystem II in synechocystis* 1. *Archives of Biochemistry and Biophysics, 264*(2), 657-664.

SUPPLEMENTAL FIGURE

Supplemental Figure 1

Pattern of the rhythm of *aqpZ* expression and *Synechocystis* cell division. The peak of circadian time of *aqpZ*, *nahS3* encoding Na^+/H^+ antiporters, *kaiA* and *dnaK* were indicated with red circles in the circadian time. The boxes show the averaged cell growth circadian cycle; cell division in the last day time, expansion of the cells during night, and generation of daughter cells in the late night and in the early day time.

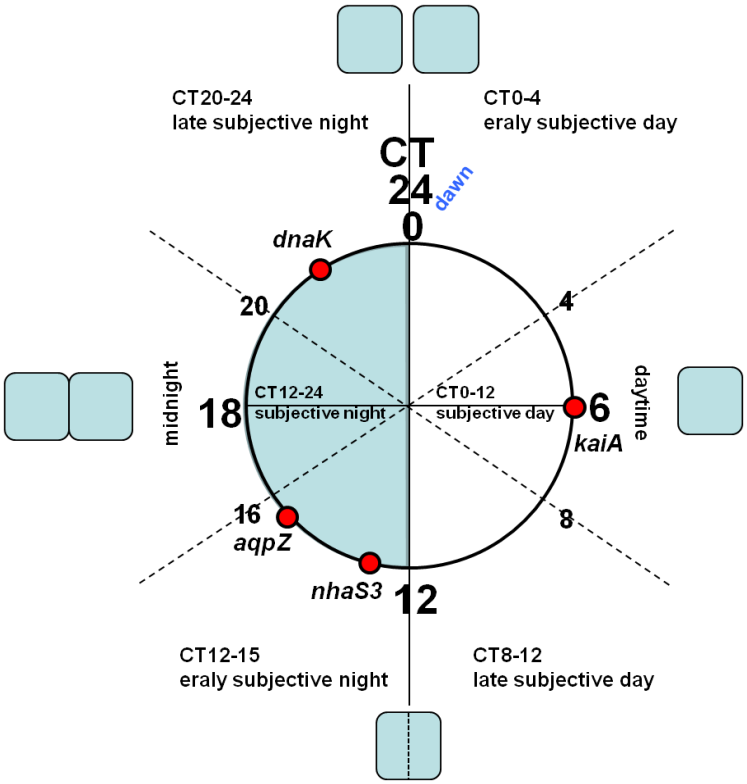

Supplemental Figure 2.

Disruption of *aqpZ* in *Synechocystis*. (A) The *aqpZ* gene (0.74 kb) was interrupted by insertion of a spectinomycin resistance (Sm^r) cassette (2.0 kb). The position and orientation of the specific primers for PCR are indicated by arrows (a, b), **(B)** Disruption of *aqpZ* in the insertion mutant (Δ*aqpZ*) was confirmed by PCR with the specific primers (a, b) indicated in (A). **(C)** Immunological detection of proteins isolated from wild-type or Δ*aqpZ* cells with anti-AqpZ antibodies. Note that AqpZ is absent from the sample from Δ*aqpZ* . Equal amount of protein (3 μg) of Δ*aqpZ* or WT were loaded in each lane. Total protein stained with Coumassie Brilliant Blue (CBB) is shown as loading control. **(**D**)** Cross section of *Synechocystis* Δ*aqpZ* cell immunolabeled using an anti-AqpZ antibody. AqpZ protein, indicated by the presence of gold particles, was not observed. Bars = 500 nm.

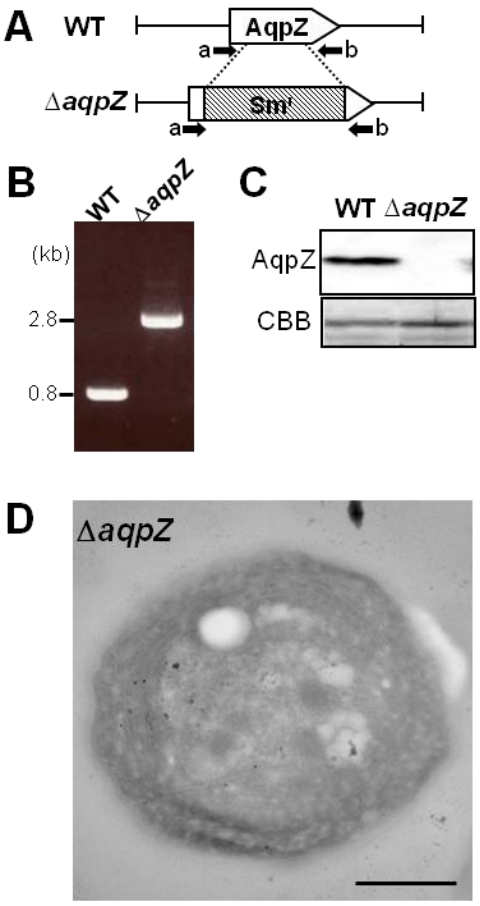

Supplemental Figure 3.
Hypotonic treatment and dehydration of *Synechocystis* wild type and Δ*aqpZ*.
(A) Prior to hypo-osmotic shock, the cells were incubated with BG11 medium containing the indicated concentrations of sorbitol and NaCl. Then, the cell suspension was mixed with the nine-fold volume of the standard BG11 (control) or in H_2O (osmotic downshift). After 1 hour, the cells were serially diluted, 5-µl spots were placed on BG11 plates and the plates were incubated at 30°C for 5 days. **(B)** Cells were filtered onto filter discs with help of vacuum. The filter discs containing the *Synechocystis* cells were allowed to desiccate in air at 30 °C for different lengths of time under illumination and the weight was determined. **(C)** Cells used in (B) were resuspended in liquid BG11 medium and plated onto BG11 plates. Cell forming units (CFU) were calculated from the number of colonies observed.

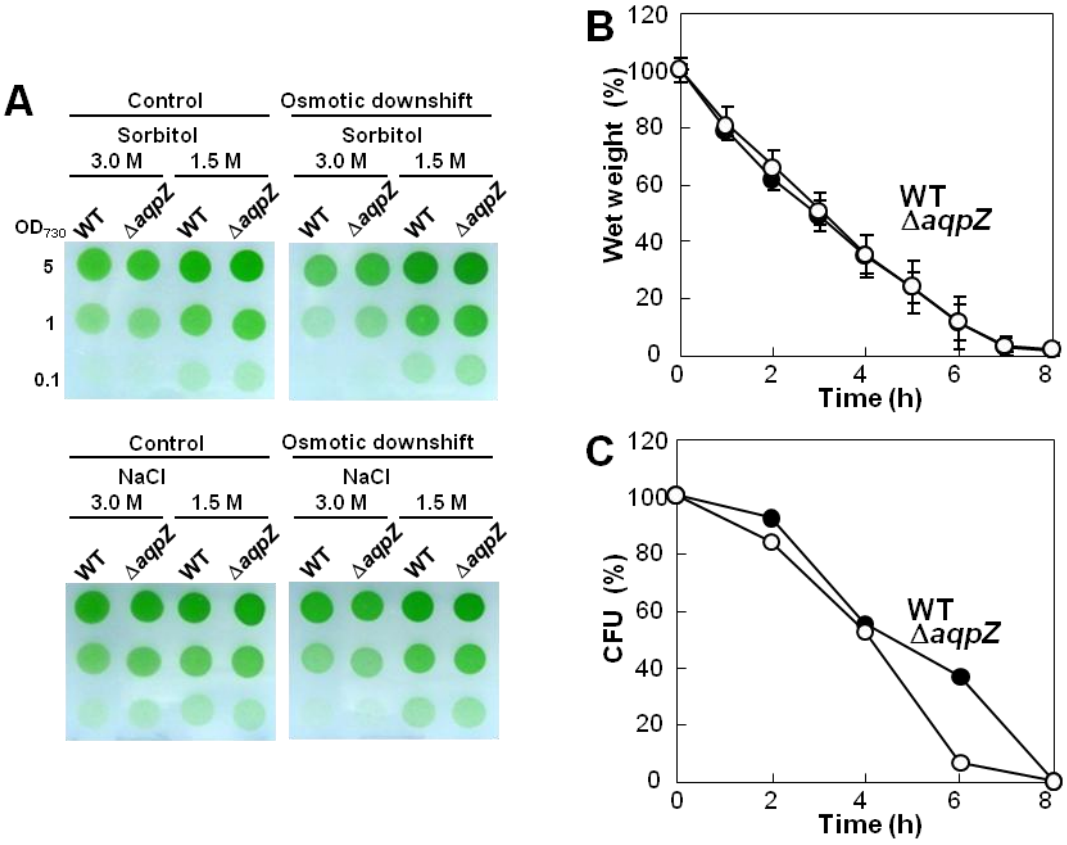

Supplemental Figure 4.

Comparative alignment and phylogeny of AqpZ.

(A) Deduced amino acid sequence of *Synechocystis* AqpZ aligned with aquaporins from *E. coli* (AqpZ) and human (AQP1). Cysteine residues are shaded with black. The box indicates the NPA motif of the aquaporin filter. The transmembrane domains, TM1-TM6, are indicated by lines above the alignment. Asterisks, colons, and periods indicate perfectly, highly, and moderately conserved amino acid sites, respectively.**(B)** Phylogenetic tree of representative members of the major intrinsic protein (MIP) family including water channels (aquaporins) and glycerol transporters (aquaglyceroporins) from various organisms including vertebrates, plants, and microorganisms. Sequences were extracted from the CyanoBase and GenBank and EMBL databases. *Synechocystis* sp. PCC 6803 Aquaporin Z "Synpcc6803 AqpZ" (accession no. slr2057), *Escherichia coli* Aquaporin Z "EcAqpZ" (AAC43518), *Escherichia coli* glycerol facilitator protein "EcGlpF" (NP_418362), *Archaeoglobus fulgidus* aquaporin "AfAqp" (NP_070255), human aquaporin-1 "hAQP1" (NP_000376), human aquaporin-3 "hAQP3" (NP_004916), *Methanosarcina barkeri* aquaporin homolog "MbAqp" (ZP_00077803), *Methanothermobacter marburgensis* aquaporin homolog "MmAqpM" (AB055880), rat aquaporin-4 "rAQP4" (NP_036957), *Arabidopsis thaliana* plasma membrane intrinsic protein "AtPIP1;1" (CAB71073), *Arabidopsis thaliana* tonoplast intrinsic protein "AtTIP1;1" (AAD31569), *Arabidopsis thaliana* nodulin-26-like protein "AtTIP1;1" (CAA16760), *Saccharomyces cerevisiae* aquaporin "ScAQY1" (AAC69713), *Saccharomyces cerevisiae* aquaporin "ScAQY2" (AAD25168), *Saccharomyces cerevisiae* aquaporin "ScFps1" (P23900), *Synechococcus elongatus* PCC 7942 *Synechococcus* membrane protein "Synpcc7942 SmpX" (D43774). Programs used were ClustalX (Thompson *et al.*, 1997) for alignments, and Treeview (Page, 1996) for graphical output. Asterisks indicate the number of times (50−69 % (*) or 70−100 % (**)) of 1,000 bootstraps that each branch topology was found during bootstrap analysis.

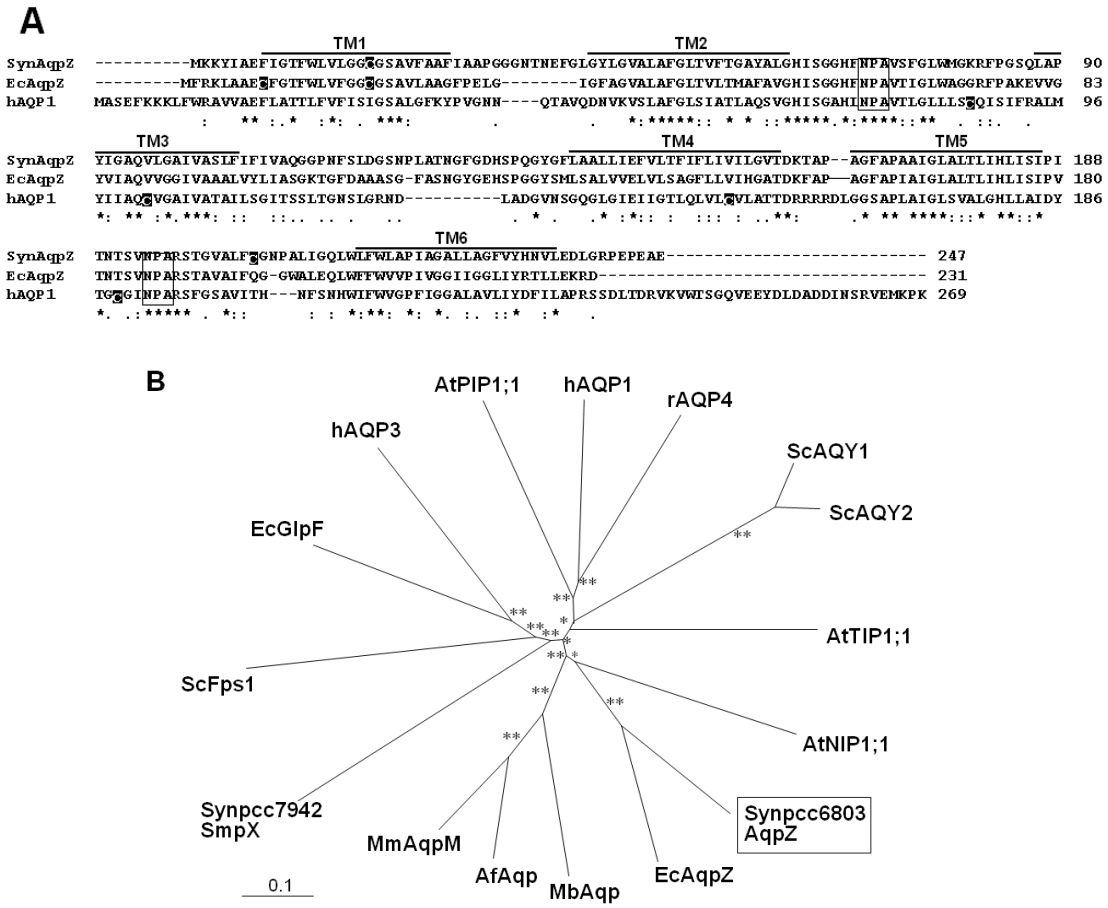

Original Paper

Cellular Physiology and Biochemistry

Cell Physiol Biochem 2010;26:975-982

Accepted: October 04, 2010

ATP-Sensitive Cation-channel in Wheat (*Triticum durum* Desf.): Identification and Characterization of a Plant Mitochondrial Channel by Patch-clamp

Umberto De Marchi[1,*], Vanessa Checchetto[2], Manuela Zanetti[2,°], Enrico Teardo[2], Mario Soccio[3], Elide Formentin[2], Giorgio Mario Giacometti[2], Donato Pastore[3], Mario Zoratti[1] and Ildikò Szabò[2]

[1]Department of Experimental Biomedical Sciences, CNR Institute of Neuroscience, University of Padova, [2]Department of Biology, University of Padova, [3]Department of Agricultural and Environmental Science, Chemistry and Plant Defence and BIOAGROMED Research Center, University of Foggia, *Present address: Department of Cell Physiology and Metabolism, University of Geneva, °Present address: Fondazione Bruno Kessler, Consiglio Nazionale delle Ricerche - Istituto di Biofisica, via alla Cascata 56/C, 38123 Povo

Key Words

Mitochondria • Patch clamp • ATP-sensitive cation channel • Plant

Abstract

Indirect evidence points to the presence of K^+ channels in plant mitochondria. In the present study, we report the results of the first patch clamp experiments on plant mitochondria. Single-channel recordings in 150 mM potassium gluconate have allowed the biophysical characterization of a channel with a conductance of 150 pS in the inner mitochondrial membrane of mitoplasts obtained from wheat (*Triticum durum* Desf.). The channel displayed sharp voltage sensitivity, permeability to potassium and cation selectivity. ATP in the mM concentration range completely abolished the activity. We discuss the possible molecular identity of the channel and its possible role in the defence mechanisms against oxidative stress in plants.

Copyright © 2010 S. Karger AG, Basel

Introduction

Potassium is the most abundant cation in plant cells, where it plays major roles in biochemical and biophysical processes [1]. A large number of K^+ channels and transporters have now been identified at the molecular level in this kingdom or are currently under investigation, demonstrating the complex nature of K^+ transport in plants. K^+ transport in plants is not restricted to the plasmamembrane, but like in animal systems, it takes place also in intracellular compartments and in particular in the bioenergetic organelles mitochondria [2-4] and chloroplasts [5].

In animal mitochondria five different K^+-selective channels have been identified and characterized, namely an ATP-sensitive potassium channel [6], two calcium-activated ones [7, 8], a voltage-gated channel [9] and a two-pore potassium channel [10]. These channels mediate the influx of potassium into the matrix according to the electrochemical gradient for this ion. The suggested physiological roles of these channels include regulation of mitochondrial matrix volume, respiration and membrane potential [11]. In addition, mitochondrial potassium channels seem to play an important role in protection against ischemic damage [12] and in regulation of apoptosis [13].

While much attention has been devoted to mitochondrial K^+ channels in animal systems, very few publications deal with plant mitochondrial K^+ channels.

KARGER

Fax +41 61 306 12 34
E-Mail karger@karger.ch
www.karger.com

© 2010 S. Karger AG, Basel
1015-8987/10/0266-0975$26.00/0

Accessible online at:
www.karger.com/cpb

Ildikò Szabò
Department of Biology University of Padova (Italy), E-Mail ildiko.szabò@unipd.it and Umberto De Marchi
Present address: Department of Cell Physiology and Metabolism
University of Geneva (Switzerland), E-Mail umberto.demarchi@unige.ch

We have previously described, using classical bioenergetics techniques, an ATP-inhibited mitochondrial K^+ uptake pathway in wheat and other species [2] and suggested that it could be involved in plant defence mechanisms against oxidative stress due to reactive oxygen species generation [14]. A similar, ATP-sensitive K^+ uptake system, which was however induced by Cyclosporine A, was also described [3]. Subsequently Ruy and colleagues [4] investigated an ATP-insensitive and highly active K^+ uptake pathway in potato (*Solanum tuberosum*), tomato (*Lycopersicon esculentum*) and maize (*Zea mays*) mitochondria by using similar methods. A fourth mitochondrial plant K^+ channel is the recently described calcium-activated mitoBK$_{Ca}$ from potato tuber mitochondria [15]. Activity of this channel was detected in a reconstituted system, using planar lipid bilayer techniques.

To directly identify plant K^+ channels in the native mitochondrial membrane, we took advantage of the patch clamp technique, applied for the first time to isolated plant mitochondria. We report here the identification and characterization by single channel recording of an ATP-sensitive cation channel in mitochondria isolated from wheat (*Triticum durum* Desf.).

Materials and Methods

Mitochondria isolation

Triticum durum Desf. seeds were germinated in the dark at 95% humidity and 25 °C for two days and only the etiolated seedlings (200 g) were used for further processes. Wheat mitochondria were then isolated by differential centrifugation, either by slight modification of a previously described procedure [2] or by the method described in Virolainen et al. [16]. Total extract was obtained by homogenizing the seedlings. The isolated mitochondria were assayed for membrane potential by using safranine or TMRE (not shown). Mitochondria thus obtained were further purified on a 28% Percoll and 0-10% Polyvinyl pyrrolidone gradient as described in [2, 16]. Rat liver mitochondria were isolated by conventional differential centrifugation procedures [for reference see 8]. Protein content in the mitochondrial suspension was determined using the BCA method.

Immunoblotting

Samples were dissolved in standard Laemmli sample buffer and loaded on SDS-PAGE. Proteins were then transferred to a PVDF (polyvinylidenfluoride) sheet. Primary antibodies used were as follows: Anti-cytochrome c was purchased from Sigma, anti-H^+-ATP-ase of the plasmamembrane was a kind gift of Prof. I. De Michelis, anti-P45 was a kind gift of Prof. N. Rolland, anti-BiP was generously provided by Prof. A. Vitale. Anti-Rubisco was produced in our laboratory. Secondary antibodies (Calbiochem) were horseradish peroxidase-conjugated and were used with enchanced chemiluminescence (ECL) detection (Pierce).

Patch-clamp of mitochondria

Experiments were carried out by modifying the procedures described in De Marchi et al. [17]. Mitochondria were added to the standard experimental medium (150 mM K-gluconate, 1 mM Pi, 20 mM HEPES, pH 7.4, containing either 2.5 mM or 0.5 mM or 0.1 mM $CaCl_2$; 1 ml) in the patch-clamp chamber at room temperature and allowed to swell spontaneously in a Ca^{2+}-dependent process presumably reflecting the occurrence of the mitochondrial permeability transition [18]. Alternatively, mitochondria were swollen in a KCl-based medium (the same composition as above with KCl instead of Kgluconate). The mitoplasts attached to the chamber bottom were washed with the experimental medium and seals were established under symmetrical ionic conditions. Seal configuration was mitochondrion-attached. Voltage was controlled manually via an Axopatch 200 unit. All data were filtered at 10 kHz and recorded on tape using a VR-10B (Instrutech) adaptor, and recovered later for off-line analysis. Axon pClamp 6.0 software was used for voltage control and data analysis. The voltages reported in this paper are those applied to the patch-clamp pipette interior. Current (cations) flowing from the pipette to the ground electrode was considered as positive and plotted upwards. For determination of the selectivity, the experimental medium was modified by employing symmetrical 150 mM KCl in place of K-gluconate. After initially recording with symmetrical salt conditions, bath [KCl] was increased by withdrawing an aliquot of the medium and adding back the same volume of a solution having identical composition except for a higher (2 M) [KCl]. For Na^+ versus K^+ selectivity, the standard experimental medium was replaced with an identical one containing Na-gluconate instead of K-gluconate. In all cases connection to the Ag/AgCl ground electrode was via a 1M KCl agar bridge. In pharmacological experiments small volumes of concentrated drug solution were added, and the bath contents were thoroughly mixed.

Results

Characterization of plant mitochondria preparation

Patch-clamp of plant mitochondria turned out to be technically much more difficult to perform than patch-clamp of mammalian mitochondria, possibly due to differences in lipid composition and to the small size of the swollen mitoplasts [16]. We tested mitochondria isolated from five different plant systems (carrot, *Arabidopsis,* cauliflower, rice and wheat) but the percentage of high-resistance seals between the patch-clamp pipette and mitochondrial inner membrane was extremely low in all cases. We modified pH, ionic strength, concentration of calcium and swelling protocol (osmotic

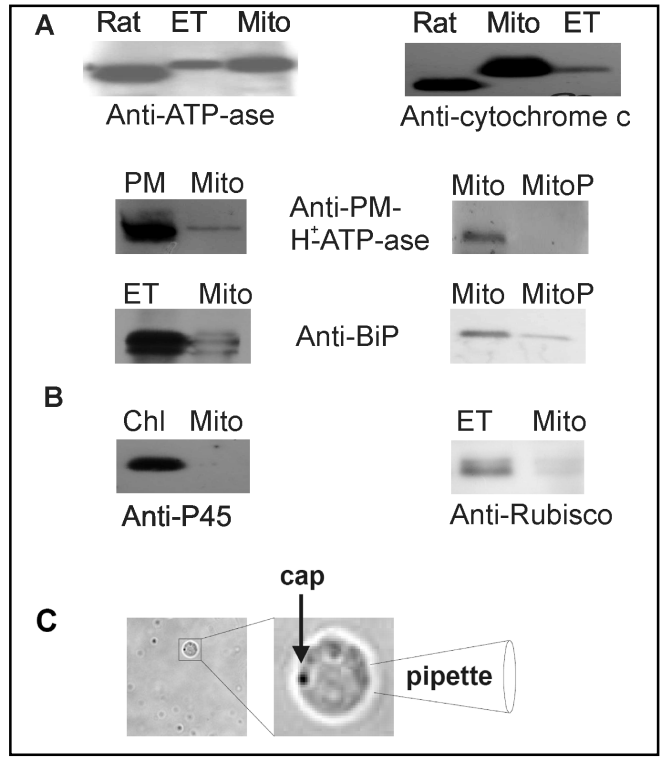

Fig. 1. Biochemical characterization of isolated mitochondria. A) Upper (top) three-lane panels: Western blots on isolated rat liver mitochondria, total wheat germ extract (ET) and wheat germ mitochondria (Mito) isolated according to the protocol described in [2]. 50 μg/lane of total proteins were loaded. Anti-ATP-ase of organelles recognizes an approx. 50 kDa band in rat mitochondria, and a 55 kDa band with the predicted MW in wheat germ. Anti-cytochrome c antibody reacts with 12 kDa and 14 kDa cytochrome c in rat and wheat, respectively. Please note the increase in the signal for both proteins in the mitochondrial fraction with respect to the total extract in wheat, indicating that our preparation was enriched in mitochondria. Lower left panels: Isolated mitochondria (Mito) are slightly contaminated by PM and ER as revealed by the presence of PM-H^+-ATP-ase and BiP. Isolated PM fraction and ET were loaded as controls. Lower right panels: The same antibodies were used for Percoll-purified mitochondria (MitoP). 50 and 75 μg/lane of total proteins were loaded for left and right panels, respectively. B) Isolated chloroplasts (Chl), mitochondria (Mito) and ET were loaded and developed with anti-P45, an inner chloroplast membrane marker and anti-Rubisco, a stromal enzyme responsible for carbon fixation. 50 μg/lane of total proteins were loaded. C) Phase contrast image of a typical wheat mitoplast with a schematic representation of the cell-attached configuration.

shock or Ca^{2+}/Pi, see Materials and Methods) to increase the percentage of successful seals, but to no avail. Despite the low percentage of successful trials (< 5% vs. ~ 50% in mammalian mitochondria) we were able to obtain single channel recordings. Wheat (*Triticum durum* Desf.) mitoplasts proved to be the best system.

To characterize the mitochondria from a biochemical point of view and for possible contaminations, we performed biochemical assays. Western blotting of wheat mitochondrial fractions confirmed the enrichment of typical mitochondrial marker cytochrome c and of the organellar ATP-ase β-subunit in purified mitochondria versus total extract, at equal protein quantities loaded on the SDS-PAGE. A very slight contamination by the plasmamembrane (PM) marker H^+-ATP-ase and the ER marker BiP can be observed in the isolated mitochondria (Fig. 1A). The PM contamination was completely abolished and the ER contamination greatly reduced when the mitochondria obtained by differential centrifugation were further purified on Percoll gradient (Fig. 1A). However, these Percoll-purified mitochondria did not form high-resistance seals in patch clamp experiments and this step greatly reduced the yield of the purification. We also verified whether the isolated mitochondria (not Percoll-purified) contained plastid contaminations: our preparation was free of Rubisco and of P45, marker proteins of the plastid stroma and inner membrane, respectively (Fig. 1B). These biochemical data indicated thus that the mitochondria used in our previous studies [2] and in the patch clamp experiments contain minor contaminations by ER and plasmamembrane but not by chloroplasts/plastids. A slight contamination by these membrane fractions is known to occur also in the case of mammalian mitochondria (due also to the presence of the so-called MAMs (mitochondria-associated membranes)), successfully used for patch clamp experiments.

For patch clamping, wheat germ mitoplasts (swollen mitochondria without outer membrane) were obtained either by inducing swelling in KCl medium or by presumably inducing the permeability transition as described in the experimental section. The resulting mitoplasts were morphologically undistinguishable from those of mammals under the microscope (see [7, 8, 19]), except for the fact that they were smaller, with an average diameter of 1-2 μmeter, in accordance with the observations of Virolainen et al [16]. Mitoplasts were easily recognizable due to their size, round shape and the presence of a "cap region". (Fig.1C).

Electrophysiological characterization of the wheat germ mitochondrial ATP-sensitive cation channel activity

To focus on potassium channels, patch-clamp recordings were obtained in K-gluconate medium.

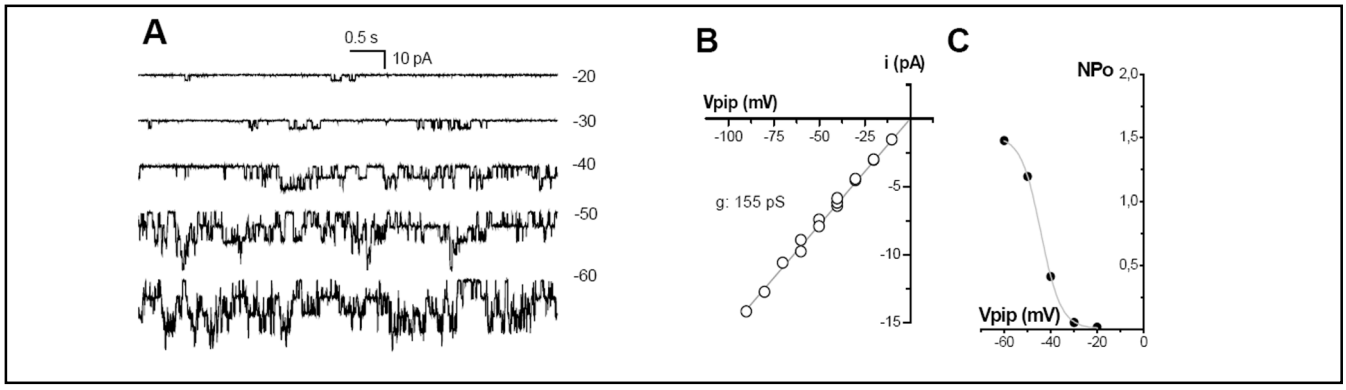

Fig. 2. Biophysical properties of the plant ATP-sensitive mitochondrial channel. A) Single channel activity recorded at the indicated pipette potentials (right) from a representative experiment in symmetrical 150 mM K-gluconate. B) Single channel conductance. i-V plot of the plant ATP-sensitive mitochondrial channel amplitude versus voltage. Symmetrical 150 mM K-gluconate medium. Data are representative of results from five independent experiments. C) Voltage-dependence. An experiment representative of results from ten experiments. N: number of active plant ATP-sensitive mitochondrial cation channels in the membrane patch; Po: open probability of each channel.

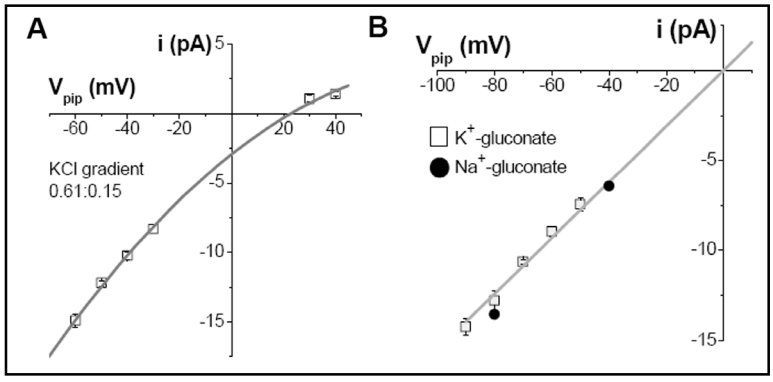

Fig. 3. The ATP-sensitive mitochondrial channel is cation-selective. (A) K^+/Cl^- selectivity. Single channel i–V plot from an experiment in a 610 (bath) versus 150 (pipette) mM KCl gradient. The line drawn is the exponential best fit of the data points, giving a reversal potential of +23 mV. Data are representative of similar experiments (n=4). (B) K^+/Na^+ selectivity. i–V plots of single-channel current values in symmetrical 150 mM K-gluconate medium (white squares) and in 150 mM K-gluconate (pipette) versus 150 mM Na-gluconate (bath) (black circles).

Gluconate is a large anion which does not permeate through most chloride channels. In a part of the experiments the mitoplast membrane patches did not exhibit channel activity, indicating a relatively low density of potassium channels in this system. However, a K^+-permeable channel with characteristic behavior could be clearly identified in 21 seals out of 69 seals established on wheat mitoplasts. Fig. 2A shows a typical recording of this activity. Only one or at most a few channels were active in any given membrane patch. The characteristics and kinetic behavior of the channel seemed to be independent of the calcium concentration used in the experimental medium (not shown). Fig. 2B shows a plot of the current flowing through the wheat mitoplast K^+-permeable channel versus voltage. The current reported was determined by averaging individual measurements obtained at the various voltages. The channel displayed a conductance of 150-155 pS in the negative pipette voltage range, a strong voltage sensitivity and an open probability (Po) value approaching 0 at positive pipette potentials (i.e. negative, physiological matrix potential) (Fig. 2C), suggesting that the channel tends to be closed under physiological conditions.

In symmetrical 150 mM KCl this channel showed basically identical biophysical properties to those observed in K-gluconate (the same kinetics, ohmic behavior, V-dependence) (not shown). To determine its selectivity we first measured the reversal potential (E_{rev}) in a KCl gradient (Fig. 3A). Given the conventions and experimental conditions, negative currents at 0 mV applied voltage correspond to a net flow of K^+ ions into the pipette, i.e., to cation-selectivity of the channel, as expected. In the presence of a 4.07 fold [KCl] gradient (bath versus pipette) the reversal potential was about +23mV (see Fig. 3A), corresponding to a ratio of permeability coefficients P_K/P_{Cl}=5.5. Under these ionic conditions a reversal potential of +36 mV is predicted for a perfectly potassium selective channel. To check for selectivity between K^+ and sodium, we measured the conductance of the channel in standard experimental medium (containing 150 mM K-gluconate) and then after exchanging the bath medium with one containing Na-gluconate instead of K-gluconate

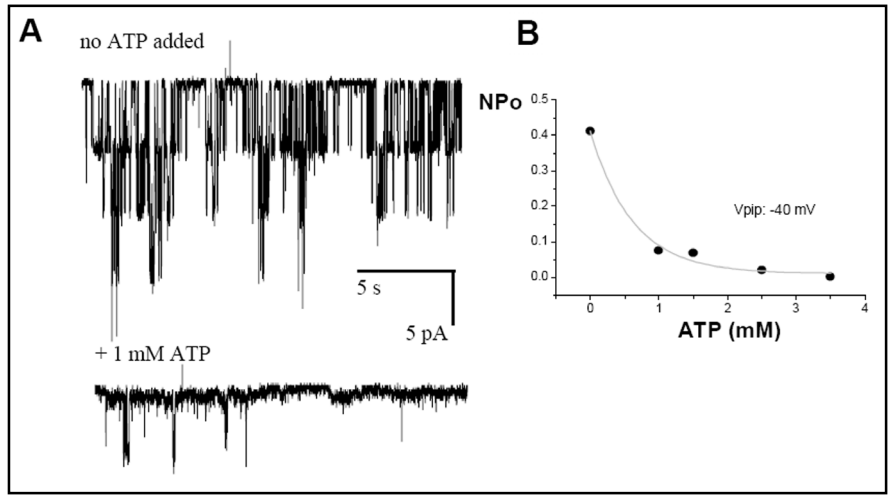

Fig. 4. ATP inhibits the mitochondrial 150 pS cation channel A) Representative current traces recorded in symmetrical K-gluconate, before and after addition of 1 mM ATP to the chamber. $V_{pipette}$: -40 mV. B) Probability of ATP-sensitive mitochondrial cation channels being open as a function of ATP concentration. N: number of active plant ATP-sensitive mitochondrial cation channels; Po: open probability of each channel. Po was calculated ad -40 mV. The solid line represents the best exponential fit of experimental data. The effect of ATP was observed in 3 experiments.

(Fig. 3B). The conductance did not change significantly, indicating a low selectivity for potassium toward sodium.

To check whether the channel described above might correspond to the ATP-sensitive potassium uptake system we have previously identified [2], we tested the effect of ATP. 1 mM ATP caused a significant reduction of the open probability of the channel (Fig. 4B) as observable also from the current traces before and after the addition of ATP (Fig. 4A). The activity was nearly completely abolished at higher concentrations of ATP (Fig. 4B).

Discussion

In the present paper, we describe for the first time the application of the patch clamp technique to mitochondria isolated from plants and present the characterization of the channel activity we observed most often (in 30% of the seals, indicating a relatively low density of the channel). The channel displays a conductance of 150 pS in 150 mM potassium, a strong voltage dependence and rectification, a relatively low selectivity for potassium over chloride and basically no selectivity for K^+ vs. Na^+. Importantly, channel activity is completely blocked by mM concentrations of ATP. This latter characteristic suggests that the channel activity we recorded by patch clamp might correspond to the potassium uptake system previously observed in the same system, i.e. in wheat germ mitochondria by classical bioenergetic approaches [2]. In that paper we reported that in addition to a potassium/proton antiporter, energized mitochondria accumulate potassium in an ATP and NADH-sensitive manner. Furthermore, we studied the effect of various classical potassium channel modulators and inhibitors of mammalian $mitoK_{ATP}$ and observed that magnesium (0.1 and 5 mM), TEA^+ (10 mM), calcium (1-3 μM), barium (1 mM) and aminopyridine (5 mM) did not have an inhibitory effect on the potassium uptake. In the absence of the determination of the channel's molecular identity, it is unclear whether the lack of effect of these inhibitors on the $mitoK_{ATP}$ activity have structural reasons. Unfortunately, the limited success rate of the patch clamp experiments did not allow us to perform a detailed pharmacological characterization of the observed activity preventing us to definitively identify the channel observed by patch-clamp with the activity we previously studied [2]. The technical difficulty to perform patch clamp experiments on plant mitoplasts is mainly due to their small size, but possibly also to the lipid composition of the inner membrane. In any case, the sensitivity to ATP points to the identification of the $mitoK_{ATP}$ channel by patch clamp.

The group of Vianello and colleagues have also reported the existence of a Cyclosporine A-induced, ATP-inhibited potassium channel in de-energized as well as in energized pea mitochondria [3]. They concluded that the channel is voltage-dependent, with a tendency to close at increasing $\Delta\Psi_m$ and that its inhibition by ATP is partially reversible by addition of GTP and diazoxide, openers of the $mitoK_{ATP}$ of mammalian mitochondria [20]. The channel we observe is clearly voltage-dependent and is open at positive matrix potential. However, in contrast to our findings described in this paper, both papers reported a selectivity for potassium over sodium in swelling and membrane potential measurement experiments. On the other hand, while swelling did not occur in sucrose medium, in sodium chloride swelling could be observed, although to a lower extent than in potassium chloride, suggesting that the plant $mitoK_{ATP}$ is not perfectly selective for potassium [20].

In addition to the mitoK$_{ATP}$, an ATP- and NADH-insensitive, highly active potassium uptake pathway has been identified in plant mitochondria [4]. Besides the ATP-sensitive channel, in patch-clamp experiments in a few cases we have observed channels with higher conductances, one resembling the mitochondrial megachannel [21] (not shown). It might *a priori* be possible that the same channel protein gives rise to ATP-dependent and ATP-insensitive activities, depending on the association or lack of regulatory subunits, which might dissociate depending on the isolation protocol used. Alternatively, the channel described by Ruy and colleagues [4] might correspond to the large-conductance calcium-activated channel that was recently observed by the group of Szewczyk [15]. Further work is required to test these hypotheses.

The question arises concerning the possible molecular identitiy of the channel we observed. The mammalian K$_{ATP}$ channel of the plasmamembrane is composed of the Kir6.1 or Kir6.2 inward rectifying potassium channel subunits and of a sulfonylurea receptor subunit (SUR 1, 2A, 2B). Whether the mammalian mitoK$_{ATP}$ has the same composition, is still under debate (for a recent discussion see, e.g., [11, 22]). In alternative to a Kir/SUR complex, mitoK$_{ATP}$ activity has been proposed to be due to a complex comprising a mitochondrial ABC transporter, the adenine nucleotide translocator, phosphate carrier, the ATP-ase and succinate dehydrogenase [23]. Interestingly, plant mitoK$_{ATP}$ appears to play a major role in the *in vitro* regulation of succinate dehydrogenase (SDH). Affourtit et al. [24] showed that SDH is inactivated by K^+ and reactivated by low concentrations of nucleotides acting from the intermembrane space, and hypothesized that these effects are mediated via plant mitoK$_{ATP}$.

In plants, only one Kir-like channel exists, the single pore potassium channel AtKCO3 (in *Arabidopsis*), belonging to the TPK (two-pore potassium channel) family. AtKCO3 however does not show any sequence homology with Kir6.1 and Kir6.2. Furthermore, Kir6.1 and Kir6.2 do not display any homology to any channel protein in *Arabidopsis*. For AtKCO3 a mitochondrial targeting is predicted, although with low probability, and according only to some localization prediction algorithms. It must be mentioned however, that numerous KCO two-pore K^+ channels (TPK) have a predicted localization in chloroplasts but have been shown nonetheless to be located in the vacuolar membrane [25]. Thus, such predictions must be considered with caution, and at the moment a localization of KCO3 in mitochondria *in vivo* cannot be excluded with certainty. The voltage dependence of the observed channel activity might be compatible with this channel being a member of the TPK family (TPK1 has been shown to behave as a voltage dependent channel). A variant of TPK1 in potato for example has a strong predicted localization in mitochondria. However, the high conductance, contrasting with that observed for TPK1 (22-45 pS) [26], and the high permeability to sodium argue against the proposal that the channel we observe might correspond to a TPK1-like channel. The channel activity of AtKCO3 is not known, preventing a comparison with the mitoplast channel.

The strong voltage-dependence of the channel activity we observe points to the possibility that it might be a *shaker*-like channel. In *Arabidopsis* there are nine *shaker*-like channels identified and none of them (except AtKC1, a regulatory silent subunit) shows a strong prediction for mitochondrial localization. On the other hand, AKT1 or an AKT1-like channel is predicted to be located in mitochondria in several other plant species, including barley, grape, rice and wheat (*Triticum aestivum*). In wheat root an AKT1-like channel, which has a strong prediction for mitochondrial targeting, has been cloned (Q9M671) [27]. The conductances (25 pS for OsAKT1 in 100/150 mM KCl [28]) and permeabilities to sodium of AKT1 from rice (strong mitochondrial targeting predicted) and of the wheat mitoplast channel are very different, and argue against an identification. It should be mentioned however that *shaker*-like channels may have a different conductance in the presence or absence of their regulatory β-subunits (e.g. [29]). A regulatory β-subunit has been identified by proteomics in rice mitochondria, although the channel associated with it is not known [30]. Thus, it cannot be excluded that the activity we observe is due to a *shaker*-like channel with altered characteristics due to the lack of β-subunit, or, alternatively, to the presence of another regulatory protein. Indeed, in the mammalian system the participation of SUR in mitoK$_{ATP}$ formation has been proposed. Interestingly, SUR1 (AAC36724) and SUR2A (NP_005682.2) subunits both show a high degree of sequence homology with several members of the multidrug-resistance protein family in *Arabidopsis*, including the ABC transporters of mitochondrion (AtATM1-3) (32% identity and 53% positivity over 1381 aminoacids (BLASTP algorithm) between SUR1 and AtMRP1). While AtATM1-3 proteins are implicated in iron homeostasis [31], AtMRP5 has been proposed to regulate a potassium channel activity [32]. Thus, one possibility is that an ABC-transporter protein associates with e.g. AtKCO3 or AKT1-like subunits to give rise to the ATP-dependent channel activity we observe.

Both the high conductance and the poor selectivity

for potassium over sodium are characteristic instead of the very heterogeneous non-selective cation channels (NSCC). Furthermore, some members of this family do not respond to classical inhibitors like TEA^+, a characteristic also of the K^+ uptake system we studied in wheat germ mitochondria [2]. Some members have also been reported to function as voltage-sensitive and ATP-inhibited channels [33]. In plants there are numerous genes encoding for members of the cyclic-nucleotide-gated (CNG) and ionotropic glutamate receptor (iGLR) family which may *a priori* give rise to NSCC activity [33]. AtCNGC13, 16 and 18, as well as GLR3.3 and 3.5 have strong targeting sequence for mitochondria, but their activity at single channel level has not been observed to our knowledge, preventing thus a possible identification of these gene products with the channel we observe.

The activation of a K_{ATP} in mammalian system is known to regulate matrix volume, decrease mitochondrial membrane potential and prevent mitochondrial ROS formation. In plants it is well known that cellular reactive oxygen species (ROS) production can be increased as a result of plant exposure to various environmental factors inducing oxidative stress; mitochondria, in particular, were reported to show increased ROS generation under drought and salt stress [14 and refs therein]. In durum wheat, $mitoK_{ATP}$ is activated by ROS [2]; the activated $mitoK_{ATP}$ may cooperate with a very active K^+/H^+ antiporter, thus generating a K^+ cycle able to completely uncouple mitochondria and dampen ROS generation [2, 34]. Therefore we suggested that the channel may act against the oxidative stress occurring when plants are exposed to environmental stresses [2]. Consistently, we observed a 400% increase in $mitoK_{ATP}$ activity in mitochondria from water stress-adapted potato cell and in mitochondria from osmotic and salt stressed durum wheat seedlings with respect to control condition. At the same time, a decrease of about 60% of mitochondrial ROS generation occurred [14, 34 and refs therein]. Under severe salt stress a strong decrease (about -70%) of ATP synthesis is also observable [35], that might result in a reduced inhibition of the channel (since $mitoK_{ATP}$ shows low affinity towards ATP). In fact, we measured a K_i equal to about 0.3 mM ATP by using an indirect method [2] and, similarly, an IC_{50} of 0.5 mM ATP by using patch-clamp experiments (this paper). In contrast, the mammalian counterpart is strongly inhibited by very low ATP concentration ($K_{0.5}$=22-40 μM), suggesting that in mammals ATP can hardly modulate the degree of channel opening *in vivo* [36].

Recently, we have reported that activation of $mitoK_{ATP}$ may also depend on the increase of mitochondrial free fatty acids and acyl-CoA aesthers occurring under hyperosmotic stress [37] and that a plant inner membrane anion channel (PIMAC) may work in coordination with $mitoK_{ATP}$ under de-energized conditions [38]. Interestingly, activation of plant $mitoK_{ATP}$ was generally observed alongside with uncoupling protein, but not with alternative oxidase [34, 37 and refs therein]. For detailed reviews on the physiological roles of different plant $mitoK_{ATP}$ see also [39] and [40].

In summary, the present work identifies for the first time an ATP-sensitive cation channel activity in native mitochondrial inner membrane in plants, namely in wheat. Further work is needed to understand the molecular identity of the channel in order to fully prove in the future its physiological role in intact plants by using genetic tools.

Acknowledgements

This work was supported by the projects MIUR 'AGROGEN' to D. Pastore and by Progetto di Ateneo 2008 and Progetto di Ricerca Nazionale (PRIN) to I. Szabò. The authors are grateful to Dr. Daniela Trono for initial help with the preparation of mitochondria. We are grateful to Prof. F. Lo Schiavo, P. Costantini and A. Moroni for useful discussions.

References

1 Szczerba MW, Britto DT, Kronzucker HJ: K+ transport in plants: Physiology and molecular biology. J Plant Physiol 2009;166:447-466.

2 Pastore D, Stoppelli MC, Di Fonzo N, Passarella S: The existence of the K+ channel in plant mitochondria. J Biol Chem 1999;274:26683-26690.

3 Petrussa E, Casolo V, Braidot E, Chiandussi E, Macri F, Vianello A: Cyclosporin A induces the opening of a potassium-selective channel in higher plant mitochondria. J Bioenerg Biomembr 2001;33:107–117.

4 Ruy F, Vercesi A-E, Andrade P-B, Bianconi M-L, Chaimovich H, Kowaltowski A-J: A highly active ATP-insensitive K+ import pathway in plant mitochondria. J Bioenerg Biomembr 2004;36:195-202.

5 Neuhaus H-E, Wagner R: Solute pores, ion channels, and metabolite transporters in the outer and inner envelope membranes of higher plant plastids. Biochim Biophys Acta 2000;1465: 307-323.
6 Inoue I, Nagase H, Kishi K, Higuti T: ATP-sensitive K+ channel in the mitochondrial inner membrane. Nature 1991;352:244-247.
7 Siemen D, Loupatatzis C, Borecky J, Gulbins E, Lang F: Ca2+-activated K+ channel of the BK-type in the inner mitochondrial membrane of a human glioma cell line. Biochem Biophys Res Commun 1999;257:549-554.
8 De Marchi U, Sassi N, Fioretti B, Catacuzzeno L, Cereghetti GM, Szabò I, Zoratti M: Intermediate conductance Ca2+-activated potassium channel (KCa3.1) in the inner mitochondrial membrane of human colon cancer cells. Cell Calcium 2009;45:509-516.
9 Szabò I, Bock J, Jekle A, Soddemann M, Adams C, Lang F, Zoratti M, Gulbins E: A novel potassium channel in lymphocyte mitochondria. J Biol Chem 2005;280:12790-12798.
10 Rusznak Z, Bakondi G, Kosztka L, Pocsai K, Dienes B, Fodor J, Telek A, Gonczi M, Szucs G, Csernoch L: Mitochondrial expression of the two-pore domain task-3 channels in malignantly transformed and non-malignant human cells. Virchows Arch 2008;452:415-426.
11 Szewczyk A, Jarmuszkiewicz W, Kunz W-S: Mitochondrial potassium channels. IUBMB Life 2009;61:134-143.
12 Xu W, Liu Y, Wang S, McDonald T, Van Eyk J-E, Sidor A, O'Rourke B: Cytoprotective role of Ca2+- activated K+ channels in the cardiac inner mitochondrial membrane. Science 2002;298:1029-1033.
13 Szabò I, Bock J, Grassme H, Soddemann M, Wilker B, Lang F, Zoratti M, Gulbins E: Mitochondrial potassium channel Kv1.3 mediates Bax-induced apoptosis in lymphocytes. Proc Natl Acad Sci U S A 2008;105:14861-14866.
14 Trono D, Flagella Z, Laus M-N, Di Fonzo N, Pastore D: The uncoupling protein and the potassium channel are activated by hyperosmotic stress in mitochondria from durum wheat seedlings. Plant Cell and Environment 2004; 27, 437-448.
15 Koszela-Piotrowska I, Matkovic K, Szewczyk A, Jarmuszkiewicz W: A large-conductance calcium-activated potassium channel in potato (Solanum tuberosum) tuber mitochondria. Biochem J 2009;424:307-316.
16 Virolainen E, Blokhina O, Fagerstedt K: Ca2+-induced High Amplitude Swelling and Cytochrome Release From Wheat (Triticum aestivum L.) Mitochondria Under Anoxic Stress. Annals of Botany 2002;90: 509-516.
17 De Marchi U, Basso E, Szabò I, Zoratti M: Electrophysiological characterization of the cyclophilin D-deleted mitochondrial permeability transition pore. Mol Membr Biol 2006;23:521-530.
18 Fortes F, Castilho R-F, Catisti R, Carnieri E-G, Vercesi AE: Ca2+ induces a cyclosporin A-insensitive permeability transition pore in isolated potato tuber mitochondria mediated by reactive oxygen species. J Bioenerg Biomembr 2001;33:43-51.
19 De Marchi U, Szabò I, Cereghetti G-M, Hoxha P, Craigen W-J, Zoratti M: A maxi-chloride channel in the inner membrane of mammalian mitochondria. Biochim Biophys Acta 2008;1777:1438-1448.
20 Chiandussi E, Petrussa E, Macri F, Vianello A: (2002) Modulation of a plant mitochondrial K+ATP channel and its involvement in cytochrome c release. J Bioenerg Biomembr 2002;34:177–184.
21 Zoratti M, De Marchi U, Biasutto L, Szabò I: Electrophysiology clarifies the megariddles ofthe mitochondrial permeability transition pore. FEBS Lett. 2010;584:1997-2004.
22 Zoratti M, De Marchi U, Gulbins E, Szabò I: Novel channels of the inner mitochondrial membrane. Biochimica et Biophysica Acta. 2009; 1787: 351–363]
23 Ardehali H, O'Rourke B: Mitochondrial K(ATP) channels in cell survival and death. J Mol Cell Cardiol 2005;39:7-16.
24 Affourtit C, Krab K, Leach G-R, Whitehouse D-G, Moore A-L: New insights into the regulation of plant succinate dehydrogenase on the role of the protonmotive force. J Biol Chem 2001;276:32567–32574.
25 Voelker C, Schmidt D, Mueller-Roeber B, Czempinski K: Members of the Arabidopsis AtTPK/KCO family form homomeric vacuolar channels in planta. Plant J 2006;48:296-306.
26 Gobert A, Isayenkov S, Voelker C, Czempinski K, Maathuis FJ: The two-pore channel TPK1 gene encodes the vacuolar K+ conductance and plays a role in K+ homeostasis. Proc Natl Acad Sci U S A. 2007;104:10726-10731.
27 Buschmann PH, Vaidyanathan R, Gassmann W, Schroeder JI: Enhancement of Na+ uptake currents, time-dependent inward-rectifying K+ channel currents, and K+ channel transcripts by K+ starvation in wheat root cells. Plant Physiol 2000;122:1387-1397.
28 Fuchs I, Stolzle S, Ivashikina N, Hedrich R: Rice K+ uptake channel OsAKT1 is sensitive to salt stress Planta 2005;221:212–221.
29 Spencer RH, Sokolov Y, Li H, Takenaka B, Milici AJ, Aiyar J, Nguyen A, Park H, Jap BK, Hall JE, Gutman GA, Chandy KG: Purification, visualization, and biophysical characterization of Kv1.3 tetramers. J Biol Chem 1997;272:2389-2395.
30 Tanaka N, Fujita M, Handa H, Murayama S, Uemura M, Kawamura Y et al: Proteomics of the rice cell: systematic identification of the protein populations in subcellular compartments. Mol. Genet. and Genomics. 2004; 271: 566-576.
31 Chen S, Sanchez-Fernandez R, Lyver E-R, Dancis A, Rea P-A: Functional Characterization of AtATM1, AtATM2, and AtATM3, a Subfamily of Arabidopsis Half-molecule ATP-binding Cassette Transporters Implicated in Iron Homeostasis J Biol Chem 2007;282:21561–21571.
32 Lee E-K, Kwon M, Ko J-H, Yi H, Hwang M-G, Chang S, Cho M-H: Binding of Sulfonylurea by AtMRP5, an Arabidopsis Multidrug Resistance-Related Protein That Functions in Salt Tolerance1. Plant Physiology 2004;134:528–538.
33 Demidchik V, Davenport R-J, Tester M: Nonselective cation channels in plants. Annu Rev Plant Biol 2002;53:67–107.
34 Pastore D, Trono D, Laus M-N, Di Fonzo N, Flagella Z: Possible plant mitochondria involvement in cell adaptation to drought stress. A case study: durum wheat mitochondria. J. Exp. Bot. 2007; 58:195-210.
35 Flagella Z, Trono D, Pompa M, Di Fonzo N, Pastore D: Seawater stress applied at germination affects mitochondrial function in durum wheat (Triticum durum) early seedlings. Funct. Plant Biol., 2006; 33:357-366.
36 Garlid K-D, Paucek P: Mitochondrial potassium transport: the K+ cycle. Biochim. Biophys. Acta, 2003; 1606:23-41.
37 Laus M-N, Soccio M, Trono D-M Liberatore M-T, Pastore D: Activation of the plant mitochondrial potassium channel by free fatty acids and acyl-CoA esters: a possible defence mechanism in the response to hyperosmotic stress. J. Exp. Bot. 2010; in press.
38 Laus M-N, Soccio M, Trono D, Cattivelli L, Pastore D: Plant inner membrane anion channel (PIMAC) function in plant mitochondria. Plant Cell Physiol 2008;49:1039–1055.
39 Jarmuszkiewicz W, Matkovic K, Koszela-Piotrowska I: Potassium channels in the mitochondria of unicellular eukaryotes and plants. FEBS Lett 2010;584:2057-2062.
40 Blokhina O, Fagerstedt K-V: Reactive oxygen species and nitric oxide in plant mitochondria: origin and redundant regulatory systems. Physiologia Plantarum 2010;138:447–462.